INSTRUMENTING GAIT IN NEUROLOGICAL DISORDERS: MULTI-MODAL APPROACHES USING WEARABLES

Yunus Celik

BEng, MSc.

Thesis submitted in partial fulfilment of the requirements for the award (Doctor of Philosophy) of the University of Northumbria at Newcastle.

Computer and Information Sciences

Submitted June 2023

Abstract

Gait - how someone walks - is considered the 'sixth vital sign' of health. This is because poor gait is associated with low life satisfaction, an increased risk of falls and severe injuries. In Europe, people over the age of 65 make up more than 19% of the population, a figure projected to rise significantly in the future. Accordingly, the frequency of age associated conditions such as neurological disorders (Parkinson's Disease or Stroke) also rise with the prevalence of neurological gait disorders increasing from 10% (60–69 years) to 60% in those > 80 years. Increased life expectancy, coupled with a growing prevalence of neurological disorders means more people will be coping with mobility loss. Therefore, understanding and evaluating impaired gait becomes essential for promoting healthy aging, managing neurological conditions, and/or improving the overall well-being of individuals. Although there are various reference technologies used in the gait analysis, the focus of this thesis is on wearable sensors (e.g., inertial measurement units, IMUs) due to numerous advantages including affordability, accessibility, and ease of use in clinical settings and beyond.

This thesis initially presents a thorough literature review, exploring the development and progression of gait assessment techniques, technologies, and methods as well as limitations in the previous gait studies. It then focuses on contemporary techniques such as the use of artificial intelligence (AI) for human activity recognition (HAR) and edge computing for remote gait analysis to gain the necessary knowledge improve the limitations. Through a series of original research investigations, this thesis 1) investigates the consistencies of two different IMU algorithms during walks in different environments in a pilot study. This study reveals the differences and inconsistencies in the extracted temporal parameters; however, the underlying reasons cannot be fully understood due to the limitations of unimodal temporal parameters. Afterwards, the thesis 2) focuses on developing a framework through a multi-layer data fusion technique for multimodal gait analysis to go beyond the limitations of the unimodal approach. The study results show that there are differences in all gait characteristics, not only temporal parameters, during indoor and outdoor walking in healthy participants and a small group of stroke survivors. This highlights the significance of conducting gait studies in various environments with extended data collection, to gain deeper insights into the impacts of habitual environments. Nonetheless, data collection outside of clinical settings results in a substantial volume of unlabelled data.

Data labelling, such as identifying walking bouts in a continuous wearable data stream, is essential for automatically labelling walking periods, thereby reducing the time required for offline processing. To achieve an effective data labelling, this thesis 3) develops an AI model that fuses the features of IMU and electromyography (EMG) data. In the case of limited datasets of neurological conditions, as mobility loss is a significant barrier in creating rich and diverse datasets to perform effective model training, this thesis also produce a data augmentation framework. The outcomes of HAR studies performed in this thesis show that IMU and EMG data fusion at the feature level can provide highly accurate activity classification, and data augmentation improves the performance of the AI model in limited neurological datasets. Finally, this thesis focuses on remote gait analysis due to the time-consuming and labour-intensive offline data processing. To mitigate this limitation, this thesis 4) presents a prototype edge device that can perform both real-time HAR and parameter extraction (e.g., step and stride times) without a need for data post-processing. Validation studies show that the developed device can accurately perform remote gait analysis in clinics and beyond. The comprehensive conclusions drawn from this thesis demonstrate that contemporary techniques significantly ameliorate the prevailing limitations in the domain of gait analysis. Utilising advanced methodologies, this thesis successfully addresses previous constraints, paving the way for more automated and comprehensive gait analysis.

Table of Contents

Table of Figures

Table of Tables

Appendix Table of Figures

Appendix Table of Tables

Abbreviations

Abbreviations	Meanings
°	Degrees
3D	Three dimensional
Abbreviation	Meaning
accx	Acceleration in x axis
accy	Acceleration in y axis
accz	Acceleration in z axis
AD	Alzheimer Disease
ADL	Activities of daily living
AI	Artificial intelligence
AUC	Area under the curve
aV	Vertical acceleration
CNN	Convolutional neural networks
CNS	Central nervous system
CoM	Centre of mass
CoP	Centre of pressure
COVID-19	Coronavirus disease
CWT	Continuous wavelets transform
DL	Deep learning
DS	Dataset
DWT	Discrete wavelets transform
ECG	Electrocardiography
EMG	Electromyography
FC	Final contact when the toe leaves the ground
FoG	Freezing of gait
FP	Force plate
fs	Frequency
g	Gravity
GRF	Ground reaction force
gyrox	Angular velocity in x axis
gyroy	Angular velocity in y axis
gyroz	Angular velocity in z axis
HAR	Human activity recognition
HP	Healthy participant
HS	Healthy subject
Hz	Hertz
IC	Initial contact when the heel first touches the ground
IMU	Inertial measurement unit
IMUs	Inertial measurement units
IoT	Internet of Things
kNN	k nearest neighbour
L5	Fifth lumbar vertebrae
LF	Left foot

LE	Linear envelope
LSTM	Long short-term memory
m/s2	Meters per second squared
mA	Milliampere
MIMUs	Magneto inertial measurement units
MAPE	Mean absolute percentage error
MEA	Mean absolute error
ML	Machine learning
mTBI	Mild Traumatic brain injury
MUAP	Motor unit action potential
mV	milli Volts
NN	Neural networks
OA	Older adults
PD	Parkinson's Disease
PoI	Point of inquiry
RF	Random forest
RF	Right foot
sEMG	Surface electromyography
SENIAM	Surface Electromyography for the Non-Invasive Assessment of Muscles
SNR	Signal to noise ratio
SS	Stroke survivor
SVM	1. Signal vector magnitude, 2. Support vector machine
TBI	Traumatic brain injury
UPDRS	Unified Parkinson's Disease Rating Scale
YA	Young adults
σ	Standard deviation
x	Mean

List of publications in thesis chapters (full list of publications & outputs please see Appendix 1)

Title: Gait analysis in neurological populations: Progression in the use of wearables
Authors: Yunus Celik, Sam Stuart, Wai Lok Woo, Alan Godfrey
Publication Type: Journal Article
Publication Date: January 2021
Published in: Medical Engineering and Physics
URL: https://doi.org/10.1016/j.medengphy.2020.11.005

Title: Wearable Inertial Gait Algorithms: Impact of Wear Location and Environment in Healthy and Parkinson's Populations
Authors: Yunus Celik, Sam Stuart, Wai Lok Woo, Alan Godfrey
Publication Type: Journal Article
Publication Date: September 2021
Published in: Sensors
URL: https://doi.org/10.3390/s21196476

Title: Sensor Integration for Gait Analysis
Authors: Yunus Celik, Rodrigo Vitório, Dylan Powell, Jason Moore, Fraser Young, Graham Coulby, James Tung, Mina Nouredanesh, Robert Ellis, Elena S Izmailova, Sam Stuart, Alan Godfrey
Publication Type: Book Chapter
Publication Date: March 2023
Published in: Encyclopaedia of Sensors and Biosensors
URL: https://doi.org/10.1016/B978-0-12-822548-6.00139-4

Title: Multi-modal gait: A wearable, algorithm and data fusion approach for clinical and free-living assessment
Authors: Yunus Celik, Sam Stuart, Wai Lok Woo, Ervin Sejdic, Alan Godfrey
Publication Type: Journal Article
Publication Date: February 2022
Published in: Information Fusion
URL: https://doi.org/10.1016/j.inffus.2021.09.016

Title: Exploring human activity recognition using feature level fusion of inertial and electromyography data
Authors: Yunus Celik, Sam Stuart, Wai Lok Woo, Liam T Pearson, Alan Godfrey
Publication Type: Conference Paper
Publication Date: July 2022
Published in: IEEE-EMBC22
URL: https://doi.org/10.1109/EMBC48229.2022.9870909

Title: Improving Inertial Sensor-Based Activity Recognition in Neurological Populations
Authors: Yunus Celik, M. Fatih Aslan, Kadir Sabanci, Sam Stuart, Wai Lok Woo, Alan Godfrey
Publication Type: Journal Article
Publication Date: September 2021
Published in: Sensors
URL: https://doi.org/10.3390/s22249891

Title: Gait on the edge: A proposed wearable for continuous real-time analysis beyond the lab
Authors: Yunus Celik, Jason Moore, Mahmut Durgun, Sam Stuart, Wai Lok Woo, Alan Godfrey
Publication Type: Journal Article
Under review in Computer Methods and Programs in Biomedicine

Impact of COVID-19

The COVID-19 pandemic (Mar 2020 – Feb 2022) presented unprecedented challenges to the initiation and progress of my doctoral research (Oct 2019 – Jun 2023). Given the unanticipated impact of the pandemic, the transition to a virtual working environment was significantly difficult. Adapting to this new mode of operation was a struggle, affecting my productivity and motivation due to the uncertainties and constraints imposed by the lockdown measures. Moreover, the limitations imposed on the utilization of university resources and laboratory facilities hindered the timely progress of my project.

One of the major limitations I encountered during the pandemic related to primary data collection. As my research involved the gathering of quantitative data from individuals with neurological conditions, who were categorized as vulnerable, my work was limited. The restrictions and safety concerns prevented me from accessing the laboratory and recruiting participants. Despite having obtained ethical approval, the inability to engage in data collection significantly impeded the advancement of my research. Accordingly, I drew upon existing datasets (via collaboration) to ensure some of my research activities were maintained. Upon the immediate easing of COVID-19 restrictions, I continued to encounter difficulties in recruiting participants, particularly among older adults with PD and stroke survivors who displayed hesitancy due to the prevailing infection rates in the region.

Funding declaration

During my PhD project, I was fortunate to secure funding from the Ministry of Turkish National Education. This financial support played a crucial role in facilitating my research activities and covering my daily expenses. I successfully applied for the Northumbria University PhD student conference grant, which granted me the opportunity to have my conference fees covered for the prestigious 42nd and 43rd IEEE International Engineering in Medicine and Biology Conferences (EMBC20-EMBC21). Presentations were performed remotely due to the pandemic. After the pandemic, I had the privilege of being awarded a travel grant by the Ministry of Turkish National Education. That grant enabled me to attend the 44th IEEE International Engineering in Medicine and Biology Conference (EMBC22) held in Glasgow, 2022. Furthermore, I received another travel grant from the European Society for Movement Analysis in Adults and Children conference (ESMAC22). That grant allowed me to present a poster at the conference held in Dublin, Ireland, in 2022. Additionally, I was honoured to be awarded the Wingate Foundation's Medical Research Travel Grant, £1000. This grant will provide financial assistance for my visit to a research lab at Trinity College Dublin, Ireland, scheduled for summer 2023.

Acknowledgements

First and foremost, I would like to express my deepest appreciation to the Ministry of Turkish National Education for providing the funding opportunity that enabled me to undertake my studies during my doctoral education. Additionally, I would like to thank Department of Computer and Information Sciences at the University of Northumbria Newcastle for providing the opportunity to undertake this research training.

I am indebted to my team of academic supervisors, Dr Alan Godfrey, Dr Sam Stuart, and Prof. Wai Lok Woo, for their unwavering support throughout my research journey.

Special thanks go to my principal supervisor, Dr Alan Godfrey, whose exceptional supervision, mentorship, and unwavering support were instrumental in every step of my PhD journey. Dr Godfrey's guidance not only shaped and directed my research work but also played a significant role in my personal growth and development. His commitment to providing exceptional continuing professional development and guidance towards the path of academia has taught me how to become an effective researcher and supervisor in academia. I am truly grateful for his expertise, dedication, and encouragement throughout the entire process.

I would also like to thank Dr Edmond Ho and Prof Nauman Aslam from the academic team for guiding me through project approvals and annual progressions, as well as providing invaluable feedback at each stage of my Ph.D.

My heartfelt gratitude goes to my esteemed colleagues, Dr Dylan Powell, Dr Graham Coulby, Mr. Liam T Pearson, Mrs. Julia Das, Mr. Jason Moore, Mr. Fraser Young, and my office friend Mr. Conor Wall, for their help and support over the last few years.

I am immensely grateful to all the participants who willingly contributed to this work. Their voluntary participation and support were indispensable in making this PhD study possible.

Last but certainly not least, I would like to express my sincerest gratitude to my parents. This journey has been challenging to navigate, but their patience, understanding, guidance, and support have been truly appreciated and have played a paramount role in the completion of my studies.

Thank you all.

Declaration

I hereby declare that the work presented in this thesis has not been submitted for any other degree or professional qualification, and that it is the result of my own independent work. I also confirm that this work fully acknowledges opinions, ideas, and contributions from the work of others.

Approval has been sought and granted by the Northumbria University Ethics Committee on [June 2021] reference number 23946.

I declare that the Word Count of this Thesis is 54034 words.

Mr Yunus Celik

09/06/2023

Foreword: Thesis overview

Given the escalating prevalence of neurological disorders and an ageing population, the need for effective, affordable, and accessible methods to analyse gait disorders is more urgent than ever. This PhD has broad implications for public health, particularly in mitigating the impacts of mobility loss on individuals' lives. By improving our understanding of gait abnormalities and offering a means to effectively monitor them using wearable technologies, this research supports the development of preventative and rehabilitative strategies. Additionally, it empowers individuals with neurological disorders to manage their conditions in a more informed and autonomous way. Furthermore, the application of this research in clinical settings can help healthcare professionals to provide more personalized and effective care. By innovating in this crucial field, the research brings us one step closer to improving the quality of life for those affected by neurological disorders and fostering healthier ageing populations.

Chapter 1

This opening chapter provides a succinct background and highlights several Points of Interest (PoIs) that were identified based on existing limitations in the field. Additionally, this chapter outlines the research aims, objectives, hypotheses, and the potential contributions to knowledge.

Chapter 2

Provides an overview of the evolutionary progression of gait analysis techniques, discussing various technologies and their advantages and challenges. Wearable sensors are highlighted for their portability and suitability for free-living gait analysis. The chapter also explores algorithms for gait analysis using wearable sensors, addressing challenges in sensor wear location and algorithm selection.

Chapter 3

A wide range of inertial measurement unit (IMU) algorithms have been validated for the computation of spatiotemporal parameters using various wear locations. However, inconsistencies may arise due to variations in methodology, wear location selection, walking environments, and cohorts. Consequently, Chapter 3 presents a comparative analysis conducted to examine the extent of consistency between two distinct algorithms and how it varies across different gait outcomes.

Chapter 4

In this chapter, applications of data fusion techniques, data mining, and AI application such as HAR and IoT to enhance the performance and usability of wearable algorithms for gait analysis were explored.

Chapter 5

Recap and reflection of chapters 2 to 4, to take note of the acquired knowledge of how digital technologies could be used to address research questions. From here, I springboard into multimodal gait analysis methodologies for free living gait analysis.

Chapter 6

This chapter aims to introduce the methodologies developed using the technologies and methodologies learnt in the previous sections. The chapter begins by showcasing various validated algorithms that effectively extract multimodal gait characteristics encompassing spatiotemporal measurements, joint kinematics, and muscle activation patterns. A key challenge that arises, leading to increased post-processing time, is the labelling of free-living data. This issue is identified and acknowledged within the chapter, highlighting the need for innovative approaches to address it. Subsequently, I present two distinct methodologies that incorporate HAR techniques for automated multimodal gait analysis. The first methodology focuses on the fusion of inertial and EMG data at the fusion level, aiming to enhance the accuracy and effectiveness of HAR. By combining data from multiple sensors, a more comprehensive and reliable representation of the individual’s gait patterns can be achieved. The second methodology addresses the limitations of existing HAR datasets specifically tailored to individuals with neurological conditions. Recognizing the scarcity of such datasets, this methodology proposes strategies to overcome this challenge and develop robust HAR models that cater to the unique needs and characteristics of this population.

Chapter 7

I present the outcomes of a series of experimental studies that were conducted based on the methodologies introduced in Chapter 6. This section provides a detailed analysis of the results obtained from these studies, offering insights into the reliability and accuracy of the proposed methodologies. Through discussions, the strengths and limitations of the developed approaches are evaluated, aiming to provide a comprehensive understanding of their performance. Furthermore, this chapter sheds light on the limitations inherent in the current work, identifying areas where improvements can be made in future research endeavours. These limitations are critically examined, emphasizing the need for further advancements to enhance the efficacy and applicability of the proposed methodologies.

Chapter 8

In this chapter, I provide a reflective analysis of the methods I have developed and presented in Chapter 6. By critically assessing these methodologies, I aim to gain deeper insights into their effectiveness, limitations, and potential areas for improvement. This reflection serves as a valuable exercise to refine and enhance the proposed approaches. Following my reflection, I shift focus towards exploring potential research directions and underscore the utilisation of edge computing technology in the analysis of gait among individuals with neurological conditions. This research exploration seeks to leverage the capabilities of edge computing to overcome challenges and enhance the efficiency and accuracy of remote gait analysis.

Chapter 9

Here, I introduce a state-of-the-art remote gait analysis device that leverages advanced edge computing technology. I provide a comprehensive overview of the hardware and software components incorporated into the design. Furthermore, I present detailed experimental results obtained from validation studies conducted to assess the device's performance and accuracy.

Chapter 10

Presents a comprehensive discussion of my PoIs and the findings derived from my research. This chapter serves as a platform to detail the conclusions drawn from testing my hypothesis and developing an automated multimodal gait analysis approach. Within this chapter, I provide an in-depth analysis of the outcomes and implications of my research endeavours. I highlight the key insights gained from the testing and implementation of the proposed methodologies, emphasizing their contributions to the field of gait analysis. Moreover, I aim to investigate the wider impact of the developed automated multimodal gait analysis tool. This speculation explores potential implications and future possibilities resulting from the integration of this tool within clinical practice, research domains, and broader societal contexts.

Chapter 1 Introduction

1.1. Introduction

Gait analysis refers to the systematic evaluation of a person's walking pattern and it provides valuable information about mobility, functional abilities, and potential abnormalities or impairments. Gait analysis plays a crucial role in healthcare, particularly in the context of the aging population, the increasing prevalence of neurological disorders, and the overall enhancement of quality of life[1, 2]. Gait abnormalities not only affect physical function but also have psychological implications. Because impaired gait can limit individuals' ability to engage in social activities, participate in hobbies, and maintain independence[3].

As societies undergo demographic shifts and advancements in medical care, understanding and evaluating gait patterns becomes essential for promoting healthy aging, managing neurological conditions, and improving the overall well-being of individuals. This chapter initiates the thesis by shedding light on the encountered challenges in wearable sensor-based gait analysis, presented in Chapter 2. This thesis will employ multiple points of inquiry (PoIs) to present a comprehensive understanding of the challenges and potential solutions.

1.2. Defining points of inquiry (PoIs)

In Chapter 2, I identified the limitations and the knowledge gaps in the field of wearable sensor-based gait analysis in neurological PD population and stroke survivors. Subsequently, a set of research questions, denoted as PoIs, were formulated to further investigate how the limitations can be mitigated. The methods devised in this thesis for neurological gait analysis primarily rely on data collected from subjects with Parkinson's disease (PD) and stroke survivors. These specific groups were chosen due to their significant prevalence within neurological conditions[4]. In experimental studies, healthy young adults and older adults were also included as a control group for comparative analysis and reference.

1.2.1. PoI 1: How consistent are the existing IMU algorithms for detecting initial contact (IC) and final contact (FC) moments considering sensor wear location, target cohort, and walking environments?

A plethora of IMU-based gait analysis algorithms were developed and validated for healthy and neurological cohorts (PD and stroke survivors) against various reference technologies (Chapter 2-Section 1.5). Although comparative assessment studies[5-7] were performed for various sensor locations, and algorithms on different cohorts to point out the most robust and accurate algorithms, these studies were limited to controlled clinical conditions. The level of consistency between algorithms in terms of detecting IC and FC points considering walking environments (indoor, and outdoor) was not fully investigated. PoI 1 is designed to investigate the level of consistency between the produced temporal parameters using different sensor locations and algorithms during treadmill, indoor and outdoor walking. The answer to this question aims to inform future studies in terms of how consistent and reliable these algorithms are based on sensor wear location, target cohort, and walking environment.

1.2.2. PoI 2: Could multimodal gait analysis overcome the limitations of unimodal, and how can it be achieved?

Unimodal gait analysis focuses on the assessment of gait using a single modality/measurement technique (e.g., spatiotemporal or kinematics). To date, a plethora of gait studies has been conducted based on unimodal gait characteristics due to the technical limitation in combining multiple reference technologies and wearable sensors[8]. Consequently, various gait models were developed to provide easy interpretation of gait parameters that rely on unimodal parameters only using a single wearable sensor[9, 10]. Although those models provide valuable insights into specific aspects of gait, they have limitations in capturing a comprehensive picture of an individual’s gait characteristics.

Multimodal gait analysis involves the integration of multiple modalities(e.g., spatiotemporal, kinematic, kinetic, muscle activation) using data fusion or sensor fusion techniques and multiple sensor units[11]. It combines information from different sources such as wearable sensors, force plates, and electromyography [12]. By combining data from various modalities, multimodal gait analysis offers a more comprehensive and accurate assessment of gait patterns, capturing a broader range of gait parameters and providing a more detailed analysis of gait abnormalities and characteristics. PoI 2 was designed to investigate the multimodal approach using advanced sensor and data fusion techniques in healthy adults and stroke survivors.

1.2.3. PoI 3: How could wearable inertial sensor based HAR assist extended periods of gait analysis studies in free living?

Wearable inertial devices offer a paradigm shift in gait assessment, extending the analysis from clinical environments to unrestricted free-living settings. In clinical settings, the labelling (e.g., segmenting walking bouts from a continuous data stream) of wearable sensor datasets is typically accomplished manually due to the controlled conditions characterized by

well-defined periods of walking with precise time stamps [2, 13]. Nevertheless, when transitioning to free living contexts for extended periods (e.g., 7 days), the datasets encompass substantial amounts of unlabelled data[14]. To address this challenge, artificial intelligence (AI) techniques, particularly deep learning (DL) methodologies, have emerged as essential tools for automatically identifying daily and habitual activities, thereby mitigating the need for labour-intensive manual segmentation and data labelling processes[15]. PoI3 aims to reveal how wearable sensor based HAR methodologies can be utilised to perform automatic labelling of activities in healthy, PD and stroke cohorts.

Existing human activity recognition (HAR) models exhibit exceptional accuracy and sensitivity in identifying daily activities performed by individuals without gait impairments[16, 17]. However, it is widely acknowledged that impaired gait differs from healthy gait, and the captured inertial and electromyography (EMG) signals are influenced by the characteristics of the specific population being studied[5, 7]. Literature also indicates that HAR models trained using data exclusively from healthy participants experience significant declines in accuracy when tasked with classifying activities performed by individuals with neurological conditions[18, 19]. Consequently, there is a pressing need to develop population-specific artificial intelligence (AI) models capable of accurately and sensitively recognizing daily activities among neurological populations. Achieving this objective requires the creation of comprehensive and diverse datasets for each neurological population that exhibits similar gait deficits. However, this endeavour poses challenges for neurological populations, as participants often encounter difficulties in performing certain daily activities due to limited mobility and pain (e.g., ascending stairs)[20]. I hypothesise that the utilisation of data augmentation techniques can mitigate these challenges by augmenting the dataset size through well-established augmentation methodologies and increasing the performance of deep learning models.

1.2.4. PoI 4: How Edge computing technology can improve time-consuming offline processing of collected gait data?

Previous studies that seek to examine gait in ecologically valid environments preferred data collection for multiple days (e.g., 2-7) or more [21-23]. Conventionally, wearable data has been locally stored on the device for subsequent post-processing. However, this storage approach requires significant local memory/storage capabilities, potentially impacting the device's size and portability. An alternative approach involves transferring inertial data to a base station in real-time during the data collection phase. Nonetheless, streaming data at high sampling frequencies entails substantial bandwidth requirements, introducing challenges such as data loss, latency, privacy concerns, and increased power consumption[24]. One possible solution to overcome the bandwidth challenges is to increase the processing power of the wearable device and perform calculations and assessments on the hardware itself, known as edge computing, detailed in Chapter 4.

Edge computing involves the decentralized distribution of computing power from the cloud or central computer to the edge of the network, where data is directly collected and processed in close proximity to the sensor unit. Edge computing approach alleviates the need for extensive memory space to store raw data locally. Moreover, it enables faster and more efficient data processing, while simultaneously reducing latency and bandwidth requirements. Previously, this approach has been employed for real-time gait phase detection using wearables and it has shown promise [25]. As a result, I hypothesise that conducting HAR and gait analysis on the device while data is being collected could significantly reduce post-processing time and facilitate real-time gait analysis (PoI4). This objective of remote monitoring can be achieved by utilizing modern devices such as microcontrollers and advanced communication protocols like the Internet of Things (IoT).

1.3. Defining a research hypothesis

I propose that exploration and a better understanding of PoIs are necessary to achieve a low-cost instrumented gait analysis tool that can provide insight into various aspects of impaired gait and the discovery of underlying reasons in clinics and beyond. Consequently, these PoIs form the foundation of my central hypothesis for my thesis:

"The use of wearable sensing technology in conjunction with advanced computing techniques may enable highly affordable, accessible, comprehensive, and objective multimodal gait analysis tools for clinical and free-living gait assessment"

1.4. Contribution to knowledge

This research aims to contribute to the existing literature by addressing a number of specific knowledge gaps related to wearable sensor-based gait analysis. The main contribution will be on developing a more comprehensive gait analysis tool using a multimodal approach to go beyond the limitations of a unimodal approach in both clinical and beyond. The secondary contributions include revealing the environmental effects on all gait characteristics and the use of HAR to

automate walking bout segmentation in prolonged recordings. The final contribution comes from a developed novel edge device to promote remote gait analysis in clinics and beyond with low cost and low computational costs. Contributions will enhance the assessment and monitoring of impaired gait, bridging the gap between supervised and unsupervised assessment.

1.5. Aims and objectives

To develop and conduct a wearable sensor-driven multimodal gait analysis for stroke survivors and individuals with Parkinson's Disease, in both clinical settings and beyond, to deliver meaningful insights that guide clinical decisions. Additionally, this work aims to automate data processing by leveraging modern AI methodologies and IoT infrastructures, fostering remote patient monitoring.

Therefore, the primary objectives for this PhD are to:

1. Conduct narrative literature review to explore the development and progression of gait assessment techniques, technologies, and methods as well as what technical opportunities/challenges must be overcome.
2. Conduct a detailed examination of contemporary computing methodologies to improve the limitations of current gait analysis.
3. Perform a two-phased multidisciplinary study with the Faculty of Health and Life Science in this experimental project by recruiting participants with PD and stroke survivors. Whilst, the former experiment, including IMU and EMG measurements, will be supervised in a clinic/laboratory condition with a physiotherapist, the latter experiment will be unsupervised in a free-living environment with data recording for later analysis.
4. Investigate how the collected multisensory data can be turned into actionable information to develop a multimodal gait analysis.
5. Utilise AI models to develop effective HAR models to automate data labelling and propose solution to limited neurological dataset problem.
6. Develop a novel edge device to promote remote monitoring to improve unsupervised assessment.
7. Engage with clinic partners to interpret study outcomes and disseminate findings of this PhD programme for clinical use.

1.6. Conclusion

In this chapter, a series of research questions are formulated by providing the rationales. These research questions are used to structure the research hypothesis. Moreover, the section on 'contribution to knowledge' is elucidated to spotlight the significance of this thesis within the realm of clinical gait analysis. Finally, aims and objectives are detailed to address each research question separately.

In the next chapter, a comprehensive examination of the technologies and methodologies employed in gait analysis will be presented. Through an extensive literature review, significant insights into the constraints and areas lacking in instrumented gait analysis will be uncovered.

Chapter 2 Instrumenting gait

This chapter primarily uses text from my previously published online articles to fit the context and narrative of this thesis. The review article "*Gait analysis in neurological populations: Progression in the use of wearables"*, was published in the **Medical Engineering & Physics** in **2021.**

URL: https://doi.org/10.1016/j.medengphy.2020.11.005

Additionally, some of the text included in this chapter appears as a book chapter (Sensor Integration for Gait Analysis) in the **Encyclopaedia of Sensors and Biosensors** published by **Elsevier** in 2023. Permission is granted to freely use the whole chapter with the declaration of authorisation included in Appendix 10.

(URL: https://doi.org/10.1016/B978-0-12-822548-6.00139-4)

2.1. Introduction

This chapter aims to offer a thorough literature review, exploring the development and progression of gait assessment techniques, technologies, and methods. By critically analysing existing literature, this review aims to present a comprehensive understanding of the current state of knowledge in the field. Furthermore, it will identify any gaps or limitations within the field, providing a foundation for the subsequent stages of the thesis. Then, this chapter will transition towards formulating the primary research questions through several Points of Inquiry (PoI) and hypotheses that will guide the research conducted within this thesis. These questions and hypotheses will be specifically tailored to address the identified knowledge gaps and limitations, ensuring a focused and targeted approach to the research.

The chapter begins by exploring the various methods used in the past, including observation and rating scales, as well as the utilisation of wearable sensors and laboratory technologies (Section 2.2). Moving forward, Section 2.3 presents a thorough examination of current clinical outcomes and gait models. Additionally, Section 2.4 offers a detailed analysis of commercially available wearable technologies, highlighting their technical capabilities and their application in gait assessment studies for different neurological conditions. In Section 2.5, an overview of existing inertial-based algorithms is provided, along with a concise guide summarizing the outcomes of previous neurological gait assessment studies. Section 2.6 presents the findings of wearable sensor-based gait studies conducted across various neurological populations. Subsequently, Section 2.7 focus on the potential of wearable technology in gait assessment, considering the limitations and gaps in the existing literature. That section also explores possibilities for future research, providing a foundation for further investigation and development in the use of wearables for gait assessment in neurological populations.

2.2. Background

Gait, the way a person walks, is one of the prominent functional activities that is needed to perform daily life routines [11] and maintain wellbeing [26]. Gait abnormalities due to underlying aetiology are among the most consistent predictors for falls [27] and abnormal gait can cause other severe consequences such as reduced life satisfaction and limited mobility [28]. Impaired gait is present in almost all neurodegenerative diseases. More than two-thirds of those admitted to the hospital frequently suffer from a neurological condition that leads to a fall, where 85% of those patients were previously undiagnosed [29, 30].

The prevalence of neurological gait disorders increases from 10% (60-69 years) to 60% in those >80 years, where sensory ataxia and parkinsonism are the most prevalent disorders [4]. Generally, patients with neurological conditions show similar gait abnormalities, such as reduced gait speed, reduced step length and poor postural balance – suggesting common mechanisms that still need to be unravelled [31]. However, there are also subtle but characteristically nuanced patterns between different neurological conditions. Typical gait for ataxia includes hard foot strike on each step and staggering gait patterns [32, 33], while slow movement (hypokinesia) and loss of movement (akinesia) are common symptoms of Parkinson's disease (PD) [34, 35]. Post-stroke hemiplegia causes severe disruption to gait, e.g. initially, 50% of the patients are unable to walk [36, 37] and for those who can, asymmetrical gait is common with a large variance in step length and step time [38, 39]. Other neurological disorders exist such as Multiple Sclerosis (MS), a progressive and demyelinating disease of the central nervous system (CNS) that exhibits significant reductions in walking speed and step length due to deficiencies associated with ataxia, muscular weakness, spasticity and general fatigue [40, 41]; Progressive Supranuclear Palsy (PSP) is an uncommon degenerative neurological disorder resulting in decreased cadence and stride length and increased step with [42]. As each neurological condition seems to present nuanced gait characteristics, robust exploration of underlying impaired gait mechanisms and accurate measurement may play a vital role in targeted physical and/or pharmaceutical intervention. In this sense, impaired gait is assessed typically with traditional approaches (e.g., clinical rating scales) but more frequently with modern digital approaches.

Traditionally, patient assessment methods in supervised clinical settings have been widely performed by visual observation from a trained physiotherapist [43] utilising subjective rating scales, which rely on clinician expertise. The latter include but are not limited to all or sections of the Unified Parkinson Disease Rating Scale (UPDRS) [44]; Scale for the Rating and Assessment of Ataxia (SARA) [45]; the Canadian Neurological Stroke Scale (CNSS) [46]; Alzheimer's Disease Assessment Scale (ADAS) [47]; or Expanded Disability Status Scale (EDSS) [48]; High-level Mobility Assessment Tool (HiMAT) [49]; Dynamic Gait Index [50]. However, there is ample evidence to suggest that clinical assessment scales may not be sensitive to disease severity and cannot evaluate specific characteristics [33, 43, 51, 52]. For example, shuffling gait in PD is difficult to assess from observation and subjective rating scores between patients lack clarity for robust comparison [51]. Consequently, the inability to collect standardised gait parameters from clinical rating

scales under observation may limit understanding of underlying disease mechanisms which restricts robust monitoring of disease progression and tailored interventions [52].

Instrumentation of gait using different digital-based technologies provides information that is not possible to detect from clinical observation alone. The use of those devices in conjunction with clinical judgment, provides new insight into the dysfunction causing an individual's symptoms by providing objective digital gait characteristics [53]. These devices can be classified based on data collection protocols as non-wearable and wearable sensors where each has its advantages and disadvantages [54]. Motion analysis systems, instrumented walkway systems and force plates/platforms have been pioneering non-wearable systems that are considered to be "gold/reference standard" for capturing kinetic, kinematic and spatiotemporal gait characteristics with reasonable to excellent accuracies [54, 55]. However, those technologies conform to a "one-size-fits-all" approach, meaning they do not apply to individual phenotypes or a particular condition, further limiting their use [51, 52, 54]. Additionally, those costly non-wearable systems require the use of controlled research facilities and trained staff, which provide a snapshot assessment in optimal testing conditions within a predefined capture volume, e.g., the length of an instrumented walkway. To overcome limitations of gait assessment in a controlled environment with limited time, home motion systems (e.g. Microsoft Kinect) that include cameras, infrared and radar-based devices have been used [56, 57]. Yet, when considering user feedback, security, and limited data capture due to the field of vision, these devices have limited use [58, 59].

Wearable technologies such as magnetic (e.g., magnetometers) and inertial measurement sensors (e.g., accelerometers and gyroscopes) and force sensors (e.g., insole foot pressure) have opened data capture opportunities that overcome limitations of non-wearable devices (e.g., continuous monitoring beyond the clinic). Magneto-inertial measurement units (MIMUs) have been used to reliably quantify the rate and intensity of movement by attaching to an anatomical segment (e.g. leg, arm) to extract kinematic, temporal and spatial gait characteristics [60]. Alternatively, wearable foot pressure sensors (e.g. insole) have also been used to gather continuous kinetic gait characteristics (e.g. ground reaction forces, moments) [61, 62]. Wearable sensors enable gait assessment in a range of testing locations but of recent interest is during daily, free-living environments such as the home and in the community. In contrast to laboratory-based assessment, free-living gait assessment can provide continuous monitoring in real-life (habitual) settings where natural dual-tasking or social interactions occur, which may provide new insights into neurological gait disorders [63].

To date, a plethora of digital gait outcomes has been extracted from various technologies and interpreted using different gait models and algorithms. This scoping narrative review aims to provide a comprehensive roadmap for the future development of neurological gait assessment by shedding light on limitations and knowledge gaps in existing methodologies and technologies, particularly wearable sensors.

2.3. Understanding gait: Clinical-based outcomes and conceptual models

Gait can be described as a cyclic pattern of body movements which advances an individual's position. Consequently, studying discrete gait cycles can provide nuanced and even personalised assessments. To analyse the gait cycle in detail, it is split into distinct periods [64] where gait characteristics such as kinematic (e.g. hip, knee, ankle joints), kinetic (e.g. force, momentum) and muscle activation (e.g. force, onset – offset) occur with alterations during the gait cycle that can be extracted for sub-phase analysis [65].

2.3.1. Gait outcomes

2.3.1.1. Kinematic

The study of kinematics starts with the reconstruction of a body as a multi-segment system using various technologies (e.g., motion analysis systems, inertial sensors). Digitally constructed body segments provide insightful knowledge about joint movements (e.g. joint angular velocity and acceleration) in 3D [53]. These 3D joint movements include rotations, flexions, extensions, abductions and adductions [66]. Typically, basic movements involved in human gait are (1) flexion and extension of the hip, knee, and ankle joints and front part of the foot; (2) abduction and adduction of the hip joint and (3) rotation of the hip and knee joints [67]. Furthermore, movements of the centre of mass (CoM) of each body segment impact overall body CoM, which is found critical for balance and energy expenditure [68].

2.3.1.2. Kinetic

Kinetic information consists of a set of insightful measures from force and momentum perspectives [69]. One useful kinetic outcome is ground reaction force (GRF), typically measured with force plates, instrumented treadmills or wearable pressure sensors (e.g. insole) during the stance phase (foot is in contact with the ground) [70]. GRF may be distinctive in patients with a neurological condition, e.g. PD patients who experience shuffling walking may experience decreases in progression force and the second peak of vertical force[71]. Other useful kinetic outcomes include centre of pressure (COP), highly useful for postural balance assessment and plantar pressure distribution of the foot, which contributes to understanding foot contact with the ground (force per unit area) [72-74]. The latter may help differentiate patients who demonstrate neurological gait patterns since neurological groups typically touch the ground with the entire foot unlike healthy comparisons [75]. The integration of kinetic (GRF, COP) and joint kinematics allows us to calculate joint moments, which is helpful to understand how external forces (e.g. GRF) interact with internal forces (e.g. muscle) to stabilize the joints [53].

2.3.1.3. Muscle activation

Normal gait relies on selective timing and intensity of responsible muscles at each joint [75]. Thus, investigation of the phasic contribution of muscles in a gait cycle is important [76, 77]. Highly informative muscle-related outcomes (e.g. muscle onset and offset times, muscle synergies) have been used to investigate when the muscle fires, how muscle forces change and what muscle synergies are responsible for walking [78]. Onset and offset times of muscle activations show the duration of active muscles during gait and are useful to diagnose abnormality in muscle coordination or altered muscle activity during freezing episodes in PD [79]. Additionally, motor unit action potentials (MUAP) provide insightful knowledge for the diagnosis of neuromuscular disorders since a raw muscle signal consists of super positioned MUAPs [80]. Amplitude, duration and number of phases are factors that characterise MUAP [81], where increased MUAP amplitude is associated with loss of muscle fibres [79]. Identification of muscle synergies during gait shows the coordinated recruitment of a group of muscles and helps to understand how the CNS regulates these muscle synergies during walking [78]. Synergy vectors from healthy subjects can be compared with a group that suffers from a neurological condition using statistical correlation methods (e.g. Pearson correlation) to monitor similarities and alterations [82].

2.3.1.4. Temporal and spatial outcomes

Temporal and spatial features are a common set of gait parameters since these are essential for the identification of more pragmatic gait characteristics. Typically, extraction of temporal and spatial outcomes starts with the identification of heel strike/initial contact (IC) and toe-off/final contact (FC) within the gait cycle. A gait cycle can be described with swing and stance phases, which comprise approximately 38% and 62 % of the gait cycle for healthy adults, respectively [83]. Swing phase duration (i.e. swing time) is a temporal/timed measure when the foot under consideration is not in contact with the ground, which changes to stance phase duration (i.e. stance time) when the same foot contacts the ground [84]. Useful outcomes stemming from those timed durations include single-limb support and double-limb support, which have been useful to examine knee joint impairments [85] and balance control during gait [86], respectively. Spatial measures (e.g. stride length, step length) have been used to identify small steps and shuffles of impaired gait [51] while the more technically challenging outcome of step width (from wearables) is associated with the base of support and postural balance [51]. Mathematical approaches for the estimation of temporal and spatial outcomes using wearables are explored in section 2.5.1.

2.3.1.5. Frequency and time-frequency outcomes

Typically, frequency domain analysis of acceleration signals allows investigation of how the signal's energy is distributed over a range of frequencies. Time-frequency domain analysis can answer the question of when (in time) a particular frequency component occurs. Frequency-based measures are a valid and sensitive estimator of stride-to-stride variability that can be used to assess neurological conditions [87]. For instance; width and dominant frequency in acceleration epochs were linked to the variability of the gait domain where dominant frequency reflects average step time while the width is associated with the variability of the acceleration signal [88]. Furthermore, the bandwidth and energy concentration of an acceleration signal in the Medio-lateral direction have been used to discriminate impaired gait. For example; PD patients can be discriminated from healthy subjects (HS) as the former has larger bandwidth and lower energy

concentrations [89]. Clinically, frequency and time-frequency outcomes are novel for use in neurological gait assessment compared to temporal and spatial outcomes where interpretation of the former remains subject to further investigation to inform pragmatic insights into neurological gait.

2.3.2. Conceptual models

Due to the redundancy of parameters and covariance amongst characteristics, conceptual gait models and classification approaches based on different technologies are proposed for ease of interpretation. Here is a non-exhaustive description of each stemming from creation in non-wearable to wearables.

1. Lord et al. developed a model consisting of 16 gait characteristics across 5 domains utilising non-wearable (instrumented walkway) outcomes and factor analysis with healthy older adults (69.5 years). The developed model is composed of (i) *pace* (e.g. step velocity), (ii) *rhythm* (e.g. step time), (iii) *variability* (e.g. step velocity variability), (iv) *asymmetry* (e.g. step-swing time asymmetry) and *postural control* (e.g. step width) [9]. The model was validated using a multimethod approach that included the replication of previous work [90].
2. Hollman et al. proposed a gait model that consists of 23 gait parameters extracted from non-wearable (instrumented walkway) data for healthy adults (>70 years). This model also consists of 5 domains: (i) *rhythm* utilises temporal parameters such as cadence and stride time; (ii) *phase* consists of swing, stance, single and double support with % gait cycle (GC); (iii) *variability* includes numerous parameters such as variability of stride length and stride speed; (iv) *pace* includes gait speed and; (v) *base of support* consist of step width and step width standard deviation [10].
3. Sejdic et al. studied 17 parameters of healthy adults (65 years) and PD group (>65 years) using a motion capture system and a single wearable attached to the lower back in clinical conditions. The extracted parameters are based on 5 different features; (i) *stride interval features* (e.g. gait speed), (ii) *statistical features* (e.g. standard deviation, skewness), (iii) *information-theoretic features* (e.g. entropy rate), (iv) *frequency features* (e.g. peak frequency, spectral frequency) and (v) *time-frequency features* (e.g. wavelet entropy) [89].
4. Morris et al. proposed a new model adapted from the previous model (Lord et al.) for use with wearable data from older adults (mean age 69 years) and those with PD (mean age 72.3) during free living, which resulted in 14 gait characteristics across 4 domain [91]. The model defines (i) *pace* (e.g., step velocity, step length), (ii) *rhythm* (e.g., step, stance, swing time), (iii) *variability* (e.g., variance of step, stance, swing time), *asymmetry* (e.g., asymmetry of step, swing, stance time).
5. Morris et al. upgraded previously proposed models by combining pace and turning gait characteristics in the same domain using six inertial sensors for a PD group (mean age 67.6). The developed model contains gait and balance components; each has four different domains. Gait model; (i) *pace & turning* (e.g., gait speed, stride length), (ii) *rhythm* (e.g., stride time, stance time), (iii) *trunk* (e.g., trunk coronal /sagittal/ transverse range of motion) and (iv) *variability* (e.g., standard deviation of stride length and stride time). Balance model: (i) *area & jerk* (e.g. sway area, JERK and Root Mean Square (RMS) in AP, ML directions), (ii) *velocity* (e.g. velocity in AP and ML directions) (iii) *frequency ML* (e.g. frequency in ML direction) and (iv) *frequency AP* (e.g. frequency in AP direction) [92].
6. Horak et al. proposed a model based on the outcomes of the instrumented stand and walk test of healthy adults (mean age 66.6 years) and PD patients (mean age 66.4) using six wearables. Here, the postural balance domain (e.g., sway parameters) is more dominant compared to the previous models. The proposed model consists 6 domains with 30 measures; (i) *sway area* (e.g. mean distance, CoM range), (ii) *sway frequency* (e.g. mean frequency, jerk (the rate of change of acceleration)), (iii) *gait speed* (e.g. stride velocity, step length), (iv) *gait trunk* (e.g. peak trunk velocity), (v) *gait timing* (e.g. cadence) and (vi) *arm asymmetry* (e.g. arm asymmetry velocity) [93].
7. Weiss et al. suggested a model heavily depends on frequency domain outcomes of healthy adults (>50 years) and a PD group (>50 years) during an uncontrolled (e.g., free-living) environment using a single wearable attached to the lower back. In the validation study, (i) *temporal measure*; average stride time and (ii) *frequency measures*; stride time variability, dominant frequency (Hz), amplitude, width and slope were examined[87].
8. Stuart et al. proposed a gait model for chronic mild traumatic brain injury (mTBI) (mean age 39.56) using five wearables. The proposed method consists of 13 gait characteristics and four domains; (i) *variability* (e.g. standard deviation of double support time, stride length), (ii*) rhythm* (e.g. stride time, single support time), (iii) *pace* (e.g. gait speed, foot strike angle) and (iv) *turning* (e.g. turn duration and turn velocity) [94].

These models show how complex instrumented gait assessment is, with numerous characteristics spread across different domains. Inconsistencies between studies result in reduced clarity and confusion where some gait characteristics are evidenced in different domains due to e.g., wearable placement and calculation of the same type of outcome.

2.4. Instrumenting gait

2.4.1. Reference standard technologies

Acquisition of quantitative information about the mechanics of the musculoskeletal system while executing motor tasks is a crucial phase of human movement analysis [95]. The following technologies are usually described as reference standards when compared to wearable technologies.

Motion capture systems (also known as `mocap/mo-cap`): Motion capture systems can be classified as marker-based and marker-less systems. The former system uses retro-reflective markers along with a video-based optoelectronic system and various models (e.g., the Newington model) to calculate the displacement of attached markers. Limitations such as the need for additional hardware (e.g., reflective markers, `mocap` suit) and time-consuming setup preparation drove researchers into developing more practical marker-less systems, where conventional cameras are used together with various three-dimensional human models. The positioning performance of a common motion analysis system (Vicon Motion Systems Ltd, Oxford, UK) was studied. The accuracy of displacements with certain errors for dynamic and static experiments was investigated and favourable results were reported [96]. Motion analysis systems have been used successfully to obtain kinematic data in terms of a joint (e.g. hip, knee, ankle) excursion and spatiotemporal parameters (e.g. step time and velocity) [97]. In-depth details on these systems are provided elsewhere [98, 99] but although they offer higher accuracies compared to other well know reference standards, their high costs and need for large space prohibit their use by researchers and clinicians.

Force platform technology (also known as force plates, FPs): Measure GRF, moments and COP using pressure sensors and load cells. FPs have been widely used to understand how movement is produced and maintained [100] but are limited to single-foot strikes due to their small dimensions. Alternatively, instrumented treadmills or pressure mats/walkways (using an array of pressure sensors) can detect repeated footfalls. Performance assessment of instrumented treadmills for measurement of kinematic gait characteristics was studied as a result of a comparison with a video-based system and results suggested that instrumented walkways provide comparable results for temporal parameters and further investigation is needed to evaluate the fidelity of its spatial performance [101]. Moreover, although instrumented walkway systems are widely accepted as the gold/reference standard, they are not without error[102]. In the validity studies, various technologies (e.g. clinical stride analyser) were used for validation of instrumented walkway systems and 0.51 cm and 0.67 cm mean absolute errors were reported for step length and stride length, respectively [55, 103].

2.4.2. Wearables for gait assessment

Wearables comprise a range of sensing technologies but the most popular comprise inertial-based devices where the proposed use of acceleration signals for human movement date from the 1970s [104]. Developments in micro-electromechanical systems (MEMS) and the rise of validation studies have enabled inertial-based wearable technologies to replace the perceived reference standards by providing equally or more useful information with many advantages (e.g. high accessibility, low cost, use beyond the lab) [72]. Yet, other wearable devices involving force sensing technology remain useful, but the creation of miniature data capture platforms has enabled new sensing capabilities. Examples of some commercially available wearables with numerous sensing capabilities are provided in Table 1.

2.4.2.1. Magneto-inertial measurement units (MIMUs)

MIMUs comprise magnetometers, accelerometers, and gyroscopes, which are capable of capturing data across a spectrum of sensing properties (e.g., flux, velocity, acceleration, orientation, gravitational forces). Accelerometers are perhaps the most popular gait assessment sensor, which can measure 3D linear accelerations and has been used to detect initial-final contact (IC-FC) events to quantify temporal and spatial outcomes. Gyroscopes with their capability of measuring 3D angular velocities aid the detection of body/segment rotation (e.g., turns). Magnetometers are often used to increase the sensing capabilities of accelerometers and gyroscopes [105] with sensor fusion techniques due to their capacity of measuring the direction, strength, and change of a magnetic field at a specific location [106]. Although accelerometers and gyroscopes could be used in isolation for gait assessment, a combination of these sensors together with magnetometers and additional features (e.g. wireless data transmission) produce a highly efficient system for reconstruction and analysis of in vivo locomotor system kinematics during gait [60]. Several reasons can be listed for the preference of MIMUs in human

movement analysis. Firstly, accelerometers and gyroscopes are self-contained during operation and can be used to collect quantitative motion data regardless of time and environment, and the ubiquitous presence of a magnetic field on earth makes it possible to use magnetometers in most locations [107]. Secondly, commercially available MIMUs are small, lightweight, and with additional hardware (e.g. Bluetooth, Wi-Fi, SD card), can gain useful features such as wireless data transmission or internal memory recording – facilitating easy data collection without affecting the natural movement of individuals [66].

2.4.2.2. Accelerometers

According to Newton's second law, an object with a constant mass (kg) accelerates (m/s^2) in proportion to the sum of applied net force (N). Accelerometers are developed from this principle using different approaches (e.g., piezoelectric, thermal, and capacitive). Accelerometers are highly configurable devices where their bandwidth or frequency response can be set through coupling filter capacitors. This is an important aspect of accurate sensing as bandwidth must include the frequency or vibration of the motion of interest. Range ($g = 9.81$ m/s^2) and sampling frequency (f_s, Hertz, Hz) are additional parameters of interest that need to be selected considering the type of activity to be measured [108].

The dynamic range of an accelerometer is ± maximum amplitude that can be measured before distorting the output signal during data collection. Low-intensity movement (e.g., postural balance) is assessed more sensitively with lower *g* values. Alternatively, high insensitive movements (e.g., gait) are accurately assessed with higher *g* values to capture high amplitude (range) movement without distorting or clipping. Most accelerometer-based wearables have selectable ranges; however, the optimal range depends on both the type of movement and the body part making the movement. For example, 3D linear accelerations recorded at joints ranges from 3.0 to 12.0*g*, while lower back vertical acceleration and horizontal acceleration range from -0.3 to 0.8*g* and from -0.3 to 0.4*g*, respectively [109]. Thus, accelerometers must be capable of measuring accelerations up to ±12*g* regardless of attachment location but with enough resolution to capture subtle (low *g*) movement [8, 110, 111]. Additionally, f_s needs to be set considering the type of movement to be measured but must also be considered for pragmatic reasons, high sampling rates negatively impact battery life [112]. Antonsson and Mann reported that during barefoot walking, 99% of the acceleration signal contained a frequency below 15Hz [113]. Similarly, Aminian et al. found that there was no significant acceleration frequency component above 16Hz at the lower back or the heel during treadmill walking [114]. Sun and Hill also found that the major energy band for daily activities (e.g. walking) ranges from 0.3 to 3.5 Hz [115]. Considering the findings of previous studies, Bouten et al. concluded that in order to assess daily physical activity accelerometers must be able to measure frequencies up to 20Hz [111]. Combining this knowledge with Nyquist theorem ($f_s > 2f_{max}$) where f_{max} is the max frequency component, preferred sampling frequencies ranged from 22–320 Hz [116], 50–1000 Hz [8] and 32–128 Hz [110] in previous gait studies where it seems 100 Hz is optimal, to capture adverse events during daily living, e.g. falls. An in-depth description of accelerometer use in generic human movement analysis is found elsewhere [1, 117, 118] and details on post-processing methodologies can be found in [118].

2.4.2.3. Gyroscopes

Gyroscopes measure angular velocity (°/s) and are the next most widely used inertial sensor after accelerometers [119]. During deployment, scale factor stability, representing the sensitivity of the optical gyroscope, must be considered. A minimum scale factor stability leads to small sensor errors and can be expressed by angle random walk (ARW) = R / [60sqrt(B)], where R and B represent resolution and bandwidth, respectively [120, 121]. A combination of a tri-axial accelerometer and tri-axial gyroscope can deliver relative heading/direction, but the output drifts overtime.

2.4.2.4. Magnetometers

Magnetometers measure the direction, strength and change of a magnetic field (Gauss) at a specific location. Specifically, magnetometers are sensitive to Earth's magnetic field and can be used to correct drift or for the detection of rotations in a known direction [106]. In the absence of magnetometers, 6 axes (accelerometer and gyroscope each in three axes) deliver relative heading, but with drift. Supplementing with magnetometers can solve drift by providing (absolute heading) a global reference point of the Earth's magnetic field [122]. However, magnetometers can be affected by localised magnetic fields, which may vary in uncontrolled environments (e.g., free-living). Given the popularity of accelerometer and gyroscope-based devices, the remainder of this text will focus on those only with IMUs.

2.4.2.5. Pressure (force sensors)

Pressure and force sensors (e.g. insole) are the cornerstone of gait analysis and are typically used to measure kinetic ground reaction forces (GRFs), and temporal and spatial outcomes [123, 124]. These sensors transform the pressure information into digital current or voltage data. Capacitive, piezoelectric and piezo-resistive types are the most commonly used underfoot sensors [54]. Estimation of GRF can be explained by Newton's third law; the plantar surface produces a vertical force in the direction of the ground, and in response, another force in the opposite direction with the same intensity is generated [125]. Alternatively, gait events initial-final contact (IC-FC) can be detected using pressure sensor data, and then spatiotemporal measures can be calculated from detected IC-FC in conjunction with simple mathematical equations. Recently developed foot pressure sensors provide plantar pressure profiles with visual feedback (e.g. pressure sensor map) [126].

2.4.3. Electromyography (EMG)

EMG sensors record myoelectric signals (i.e., motor neurons) using different electrode types (i.e., needle or surface). Needle (fine wire) electrodes are inserted into the muscle to detect neuromuscular abnormalities, while surface electrodes are used to record muscle activities by placement on the skin. Although the former provides more reliable outcomes, the invasive nature limits its use. Surface EMG electrodes (sEMG, which have wireless options) offer more pragmatic opportunities with a non-invasive setup to record muscle activities in clinical and/or free-living environments [127].

Myoelectric signals are generally at the millivolt (mV) level and range from 10–1,000 Hz. For example; a muscle contraction can generate signals around 10Hz as a result of tissue displacement and whereas ground impact during walking produces 25–30 Hz signals [75]. As the EMG signal has low signal reception, it is more susceptible to unwanted signals (i.e., noise) mostly derived from tissue motion and neighbour motors. However, these noises are detected and eliminated at certain levels during signal acquisition and post-processing. During signal acquisition, unwanted electronic signals including common mode signal, which is a noise that flows in the same direction in a pair of lines (e.g. two surface electrodes), can be eliminated using differential amplifiers or instrumentation amplifiers (IA), which has large common mode rejection ratio (CMRR) [75, 128]. For post-processing noise reduction, digital low pass, high pass or band pass filters are used considering the sEMG frequency spectrum [129]. After noise reduction, various signal processing techniques are used to process EMG signals and ease the interpretations. Rectification is the most common approach that turns EMG signals into single polarity. Once the EMG signal is rectified, further processing such as Root Mean Square (RMS), eq. 1 and thresholds can be applied to extract information regarding muscle activation amplitude and onset, offset timings.

$$\mathrm{RMS} = \sqrt{\frac{1}{N}\sum_{k=1}^{N}\left[x_k\right]^2} \quad k = 1, 2, \ldots\ldots\ldots, N \tag{1}$$

In gait assessment, EMG carries valuable information about motion as walking relies on selective timing and intensity of responsible muscles at each joint[75]. Gait relies on harmonised action of 28 main muscles to manage the trunks and limbs[130]. For example, the Biceps femoris and Rectus femoris muscle groups are involved in knee flexion and extension movements, respectively. Similarly, tibialis anterior and gastrocnemius are responsible for ankle dorsiflexion and plantarflexion, respectively[131]. In many neurological disorders, natural walking patterns can be disrupted, for example, persons after stroke[132], Parkinson's disease[133] or head trauma[134] experience disrupted muscle function at many levels. Instrumented gait aims to provide clinically useful information about different aspects of gait including gait kinetic characteristics. Kinetic analysis is particularly important as it provides information regarding how a movement is produced and maintained[1]. Movement kinetics involve external forces such as ground reaction forces (GRF), and internal forces produced by muscle mass. EMG measurement complements instrumented gait by providing information about internal force (e.g. muscle characteristics) and contributes to outlining the functional cause of a gait abnormality [135]. Early gait studies were limited in terms of including muscle activation characteristics during dynamic movements due to the lack of appropriate technologies. Recent advances in Microelectromechanical systems (MEMS) and wireless communication protocols have enabled the use of EMG and inertial sensors in a single wireless device without a need for external synchronisation. In this sense, the EMG signal is processed to provide comprehensive muscle characteristics in a gait cycle and its subphase, Figure 1. Electromyographic profiles were found also useful to investigate simple and complex activity recognition[136] and better understand falls[137], and freezing of gait (FoG), an abnormal gait pattern commonly observed in Parkinson's disease [138].

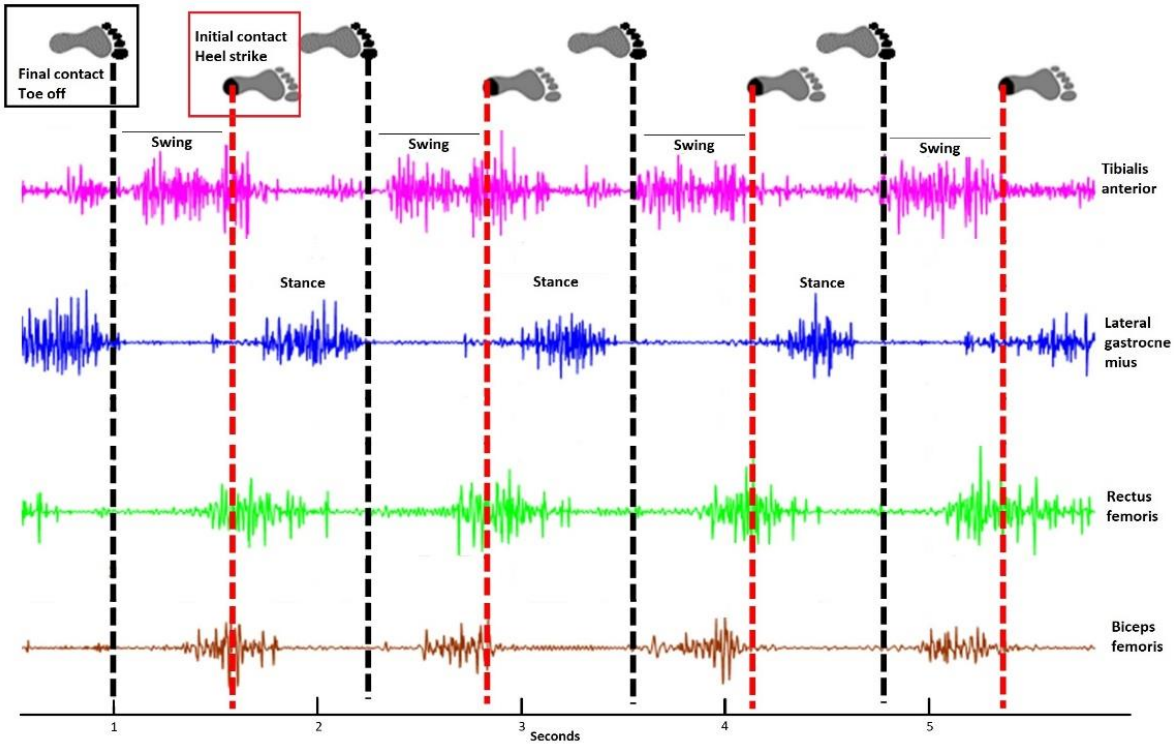

Figure 1. Raw EMG data of four different muscle groups during ground-level walking

Large inter-individual differences in EMG timing and intensity among participants can be observed as muscle activation signals are sensitive to age, Body Mass Index (BMI), and lifestyle[139]. Additionally, each gait cycle is different from the other, suggesting gait is characterized by high intra-subject variability. This variability can further increase in neurological cohorts[140, 141]. Therefore, EMG needs to be recorded for a longer time (at least 3-5 min), rather than a few gait cycles[135]. Comparing EMG activity in the same muscle on different clinic visits or with different individuals requires a normalisation[142]. Although maximum voluntary isometric contraction (MVIC) is a highly reliable method to normalize EMG data, performing MVIC tests on people with neurological conditions may not be appropriate or possible in some cases. Therefore, most neurological gait studies use peak or mean activation levels for normalisation[143]. Also, there are other factors that need to be considered during EMG measurement and signal processing to produce comparable results in gait studies. Scientific recommendations by the International Society of Electromyography and Kinesiology (ISEK) and Surface EMG for Non-Invasive Assessment of Muscles (SENIAM) project suggest the use of band pass filters with 10Hz low cut-off and 500Hz high cut of frequencies to reduce aliasing (noise) effect when using an sEMG with a sampling frequency of 1kHz [79]. The major disadvantage of sEMG is cross talk, an incident that can be expressed as recording activities of neighbour muscles other than the muscle of interest. Muscle cross-talk is more likely to occur in sEMG, but use of spatial filters based algorithm helps to reduce interferences [144].

Table 1. Examples of some wearable devices

Company	**Shimmer**		**Axivity**		**McRoberts**	**BTS Bio Engineering**	**Mc10**	**xSens**	**Micro Sensors. Big Ideas®**	**Delsys**	**Noraxon**
Product examples	*Shimmer3 IMU*	*Shimmer3 EMG*	*AX3*	*AX6*	*Move Monitor*	*G-WALK*	*BioStamp RC*	*MTw Awinda*	*Inertia-Link®*	*Trigno Avanti*	*Ultium EMG*
Size and weight (grams, g)	24.276 cm^3 23.6g	27.3 cm^3 31.0g	5.6 cm^3 11.0g	5.6 cm^3 11.0g	70.7 cm^3 55.0g	50.4 cm^3 37.0g	10.1 cm^3 7.0g	18.33 cm^3 16.0g	61.9 cm^3 39.0g	12.987 cm3 14.0g	14.95 cm^3 14.0g
Sensing capabilities	ACC. GYRO. MAG. PRES. TEMP.	ACC. GYRO. MAG. PRES. EMG ECG	ACC. TEMP. LIGHT	ACC. GYRO. TEMP. LIGHT	ACC. MAG. BAR. TEMP.	ACC. GYRO. MAG.	ACC. GYRO. EMG.	ACC. GYRO. MAG. BAR.	ACC. GYRO.	ACC. GYRO. MAG. EMG.	ACC. GYRO. MAG. EMG.
Range of ACC. (g)	± 2,4,8,16	± 2,4,8,16	± 2,4,8,16	± 2,4,8,16	± 2,4,8	± 2,4,8,16	± 16	± 16	± 2,5,10	± 2,4,8,16	± 16
Range of GYRO. (°/s)	± 250,500,1000,2000	± 250,500,1000,2000	×	± 125,250,500,1000,2000	×	± 250,500,1000,2000	± 2000	± 2000	± 75,150,300,600,1200	± 250,500,1000,2000	± 2000
MAG. (Gauss)	± 49.1	± 1.3-8.1	×	×	± 10.0	± 12.0	×	± 1.9	×	± 49.0	± 48.0
f_s (Hz) ACC.	10.24-1024	512	12.5-3200	12.5-1600	50-200	4-1000	15.6-250	20-120	1-250	24 – 473	4000
Memory	≤32 GB	≤32 GB	512 MB	1024 MB	1024 MB	256 MB	32 MB	×	×	×	2 GB
Battery life	≤69 hours @256 Hz	N/A	≤14 days @100 Hz	≤7 days @100 Hz	≤14 days	8 hours	3 days	6 hours	N/A	8 hours	8 hours
Each sensor #axes	3	3	3	3	3	3	3	3	3	3	3
Wireless data transfer	×	✓	×	×	×	✓	✓	✓	✓	✓	✓

ACC.: Accelerometer, GYRO.: Gyroscope, MAG.: Magnetometer, PRES.: Pressure, TEMP.: Temperature, BAR.: Barometer, EMG: Electromyography

2.4.4. Validity

The validity (and reliability) of wearables for robust gait analysis of neurological conditions is crucial for clinic and free-living assessment and is of great importance as the field matures. Recently developed expert opinion has a 3-way framework defined by (1*) verification*, (2) *analytical verification* and (3) *clinical validation* (V3) for biometric monitoring technologies [145]. According to the framework, *verification* entails systematic evaluation of sample-level sensor outputs considering patient safety using various methods such as bench testing prior to patient use. The *analytical validation* stage translates the evaluation procedure for sensors from the bench to patient use. This stage mostly investigates how well the data processing algorithms convert sample-level sensor measurements into physiological metrics and requires collaborative work between the engineering/computing team responsible for developing the sensor/wearable technology and the clinical team. *Analytical validation* requires a well-defined data collection protocol including the following information: type of system (e.g., inertial sensors used), the way the sensors are attached (e.g., orientation and exact location) together with study population details. Finally, *clinical validation* evaluates whether the sensor acceptably identifies or measures clinically meaningful outcomes in a stated context of use, conducted by clinical teams who investigated accuracy, precision, and reliability within a specific patient population.

Often *verification* is a technical process that is not conducted in the literature. One example of bench testing for IMU sensor assessment in gait includes the use of a pendulum to assess an accelerometer for its suitability to measure dynamic acceleration compared to an electronic goniometer [146]. Instead, various gold/reference standard technologies are used to conduct wearable *analytical* and *clinical validation* studies [147-151] in tandem, with no clear distinction between those processes. For these combined *analytical* and *clinical validations*, wearable outcomes and gold/reference standard systems are compared [152, 153] while the cohorts wear the IMU-based technology (for the first time), perhaps limiting insights to IMU or algorithm deficiencies for that group. Although each system (IMU, 3D motion and walkway) measure different components, systematic errors will always remain in practice [154]. Therefore, validation should be performed in a step-by-step approach where discrepancies and agreements should be investigated and reported, taking an acceptable rate of errors into consideration between V3 processes.

2.4.5. Wearable placement

2.4.5.1. IMU

Typically, IMU wearables are fixed on the skin with a strap or double-sided tape. Although this method of attachment provides a wide range of informative parameters with a certain accuracy, this might create problems like relative movement (e.g. linear, angular) between IMU wearables and underlying bones due to soft tissue artefacts, and displacement of the fixation clothes or strap [155]. Relative motion based on problems during data collection may cause a discrepancy, which can affect the accuracy and robustness of a developed algorithm. Therefore, attaching an IMU, considering the location of the soft tissues may provide more stable and reliable signal acquisition.

IMU locations have crucial impacts on algorithms (e.g., use of thresholds) since the characteristics of acceleration and angular velocity differ from one location to another. Moreover, the location of the IMU has a direct effect on the extracted parameters/outcomes. An extensive investigation of the effect of IMU locations on the extraction of different parameters for a neurological condition is presented elsewhere [156]. To date, the most preferred sensor locations for gait assessment are the lower back (3rd to 5th lumbar vertebrae, L3-L5) or feet/foot. In many circumstances, whole-body movement analysis with a single device is necessary; thus, IMU location as close as possible to the CoM (i.e. L5) is preferred [1, 157]. Various sensors and their locations for gait analysis in different pathologies are presented in Figure 2.

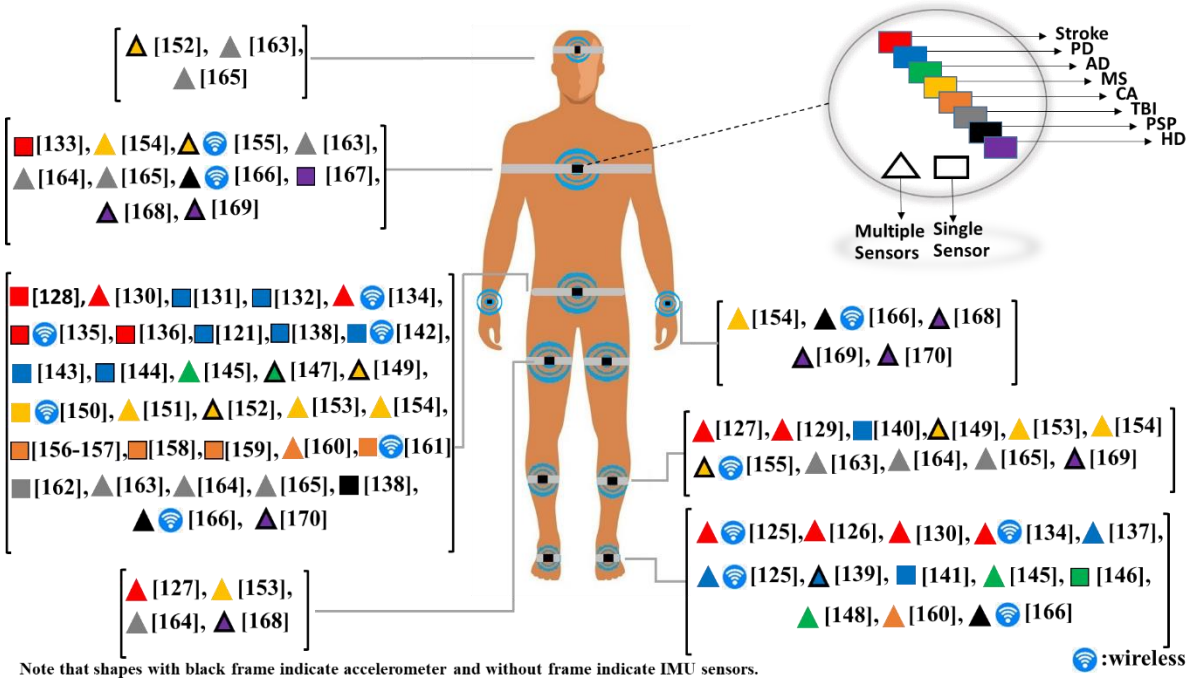

Figure 2. Previously preferred sensor configurations and locations for different pathologies (PD: Parkinson's disease, AD: Alzheimer's Disease, MS: Multiple Sclerosis, CA: Cerebellar Ataxia, TBI: Traumatic Brain Injury, PSP: Progressive Supranuclear Palsy, HD: Huntington's Disease)

2.4.5.2. EMG

Large discrepancies were observed in the previous EMG-based studies in terms of electrode placement protocols. Mainly, targeted muscle groups and the use of various types of surface electrodes such as different sizes and shapes limit the standardization of EMG. To overcome these discrepancies and to offer guidance to the field, an atlas of muscle intervention zone [204] and SENIAM [205] were introduced. In those guides, electrode placement protocols typically include the identification of electrode types such as shape and material, skin preparation, the position of the patient, electrode location and fixation [206]. Further guides for sEMG placement can be found in [207, 208] but of note is that soft tissue or inappropriate muscle selection during sEMG measurement limits the collection of meaningful data.

sEMG attached to lower limb muscle can provide reliable muscle activity and muscle force information for gait assessment of neurological conditions [209] where muscle activities of 28 major muscles controlling each lower limb can be readily identified [75]. In general, lower leg and foot muscles that are ideal for sensor placement include gastrocnemius medialis-lateralis, soleus, tibialis anterior, and peroneus longus-brevis, with reference electrode location for sEMG at the ankle [206]. Following SENIAM recommendations, tibialis anterior, lateral gastrocnemius and rectus femoris muscles have been selected to collect EMG parameters (amplitude, variability) for gait assessment of PD [210]. However, I observed discrepancies in the muscle groups selected, probably due to the study of different neurological conditions. In the literature, few studies have taken into account the recommendation in the atlas guides during sEMG measurement. I found tibialis anterior and lateral gastrocnemius muscle groups [211] and rectus femoris, biceps femoris, tibialis anterior and gastrocnemius medialis [212] were selected to investigate muscle activities in healthy and pathologic groups. Figure 3 presents the electrode locations for different patient groups.

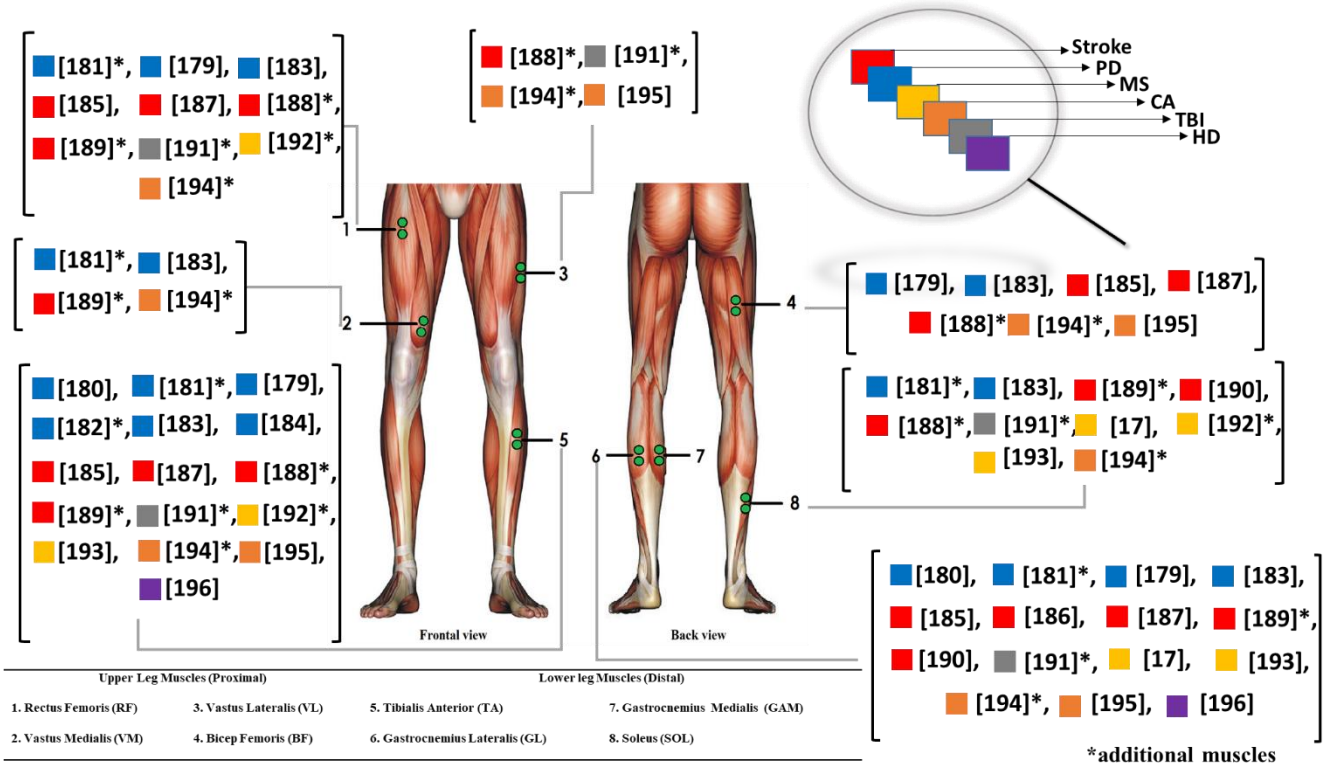

Figure 3.Previously preferred electrode locations for different pathologies (PD: Parkinson's disease, MS: Multiple Sclerosis, CA: Cerebellar Ataxia, TBI: Traumatic Brain Injury, HD: Huntington's Disease)

2.5. Gait algorithms

2.5.1. Inertial algorithms

Robust detection of IC and FC within an IMU signal draws upon timing sequences and mathematical formulae (Appendix 3) once regions of interest from IMU signals are identified. Some methods for defining and examining those regions have been presented previously [213, 214]. Here, I include more recent algorithms:

1. (Lower trunk based) McCamley et al. proposed an algorithm based on several different signal-processing techniques. Initially, vertical acceleration was pre-processed through Continuous Wavelet Transform (CWT) with Gaussian wavelet function, then IC events were detected as the times of the minima of the processed signal while FC events were detected as times of the maxima of the signal obtained after a further CWT differentiation [6].
2. (Lower trunk based) Zijlstra and Hof, proposed two different methods (zero-crossing and peak detection) that use the acceleration signal in the AP direction to detect the foot contact moment. After low pass filtering the forward acceleration signal with (4^{th} Butterworth 20 and 2 Hz cut-off frequencies), (1) the switch from positive to negative was taken as IC. In a refinement of this method, the peak forward acceleration was taken as the instant of Ics. [215].
3. (Lower trunk based) A paper by Gonzalez et al. reported a comprehensive algorithm that uses filtered (11^{th} order, finite impulse response filter) acceleration in the AP direction. In the algorithm, enclosed areas by positive values of the filtered signal, preceding every zero-crossing detected was approximately calculated. Then, the calculated areas were compared to the given threshold rates. When the calculated area is above the threshold rate, a search window together with a set of rules is used to locate the peak (local maxima) associated with the IC event. Once the IC event is detected, incoming samples are processed searching for the first local minimum that identifies the FC event [216].
4. (Lower trunk based) Shin and Park suggested a step duration estimation algorithm that uses a tri-axis acceleration norm. Sliding window summing (SWS) was used to reduce the noise in the acceleration norm signal. As the SWS

signal was sensitive to gravity, the acceleration differential technique was also used to eliminate the effect of gravity. Then, the obtained signals were processed to identify zero-crossing moments that are associated with periodic steps [217].

5. (Lower trunk based) Köse et al. proposed a wavelet-based approach that uses Daubechies wavelet due to the similarity of IMU signals during gait. First, accelerometer signals were decomposed in an approximation curve and ten levels of detail. Then, thresholds were applied, and signals were reconstructed using only the first three detail levels. In the following step, IC and FC were detected in the region of interest considering maximum and minimum points in different directions of accelerometer signals based on visual investigation [218].
6. (Lower trunk based) Yoneyama et al. proposed an extensive self-adaptive algorithm to detect the stride events and active rhythm blocks from an accelerometer signal attached to the lower back. The proposed algorithm consists of different analytical tools such as normalized cross-correlation, anisotropy, and biphasicity score, to process the 3-D acceleration signal and track long-term gait monitoring. The algorithm aims to detect correct gait peaks [165].
7. (Lower trunk based) Bugané et al. proposed an algorithm to estimate spatiotemporal parameters using filtered (Butterworth low pass filter, 2 Hz cut-off frequency) anteroposterior acceleration signals. From the typical acceleration curve with two positive and one negative peak, the second positive peak was taken as the instant of IC. To discriminate automatically between the left and right steps, the medial-lateral acceleration was analysed. Assuming the sensor was very close to the centre of mass (L5), acceleration to the left was taken as that during the right leg support phase and vice versa [219].
8. (Shank based) Trojaniello et al. proposed a gait event detection algorithm based on two MIMUs attached above the ankles. In the proposed algorithm, the first trusted swing phase time interval (T_{SW}) was defined with thresholds and a set of rules applied to angular velocity in the sagittal plane. Then, Ics and FCs were searched in a time interval (T_{IC} and T_{FC}) which were considerably reduced by considering the estimated T_{SW}. IC was identified as the minimum value of the ML angular velocity occurring before the instant of maximum AP acceleration in the reduced time interval (T_{IC}). The FC was identified as the instant of minimum AP acceleration in the T_{FC}, since it is expected to occur at the time of a sudden motion of the shank preceding the instant of the last maximum AP acceleration value in T_{FC} [220].
9. (Shank based) Salarian et al. developed an algorithm to estimate gait events (IC and FC) using a gyroscope signal attached to shanks. First, the mid-swing area (t_{ms}) was detected by applying a threshold (50 °/s), and then local minima of shank angular velocity (IC) were searched in the interval of t_{ms} [t_{ms}-1.5s- t_{ms}+1.5s]. In the following stage, the signal was low pass filtered with 30 Hz cut-off frequency and local minima with amplitude less than -20 °/s were searched to detect FC [221].
10. (Shank based) Aminian et al. proposed an algorithm to estimate initial-final contact (IC-FC) events based on the shank angular velocity. First, wavelet decomposition (Fifth order Coiflet with ten scales) was used to split the signal into low and high-frequency components. Then, the approximation approach was used to separate IC components and FC components. Global maximum values (mid-swing) were detected as a reference to detect IC and FC. In the following stage, IC- FC were detected by finding local minima inside pre-determined time intervals [222].
11. (Shank based) Catalfamo et al. developed an algorithm to detect IC-FC events from shank angular velocity. The determination of IC and FC events is based on the detection of two negative peaks in the shank angular velocity signal. The algorithm searches for the swing phase of the cycle which is detected when the gyroscope signal exceeds a threshold for another time threshold (40 ms). The first negative minimum after the swing is defined as IC. Then, the FC event is estimated after defining a waiting time and a set of rules [223].
12. (Shank based) Lee et al. suggested a novel algorithm to estimate hemiparetic and normal gait parameters after the detection of initial contacts (Ics) using 3 axis accelerometer. First, raw acceleration signals were filtered with Finite Impulse Response (FIR) bandpass filter and Least Square Acceleration (LSA) filter, respectively. Then, the highest peak points and lowest valley points were detected from Anteroposterior, Medio lateral and Vertical accelerations. Finally, estimated step detection points were extracted after applying a set of conditions to the extracted the highest and lowest point of all axes [153].
13. (Shank based) Khandelwal and Wickstrom proposed a novel algorithm that efficiently identifies gait events from accelerometer signals using continuous wavelet transform (CWT). The ‘symlet-4’ (sym4) mother wavelet was chosen with 40-80 scale rates. Then, a rough envelope (RE) was obtained for both IC and FC events. K means

clustering algorithm was used to differentiate IC (higher cluster) and FC (lower cluster) regions. Finally, IC and FC events were searched in relevant regions after the elimination of noisy IC-FC events [224].

14. (Foot based) Barth et al. developed a stride segmentation algorithm based on the subsequent dynamic time-wrapping technique. The developed algorithm uses a gyroscope signal in the vertical axis from an IMU attached to the foot to search similar points to the template. FC was detected with zero crossing while IC was detected by searching the minima between the steepest negative slope and steepest positive slope. The mid stance was also detected considering the lowest energy point in all axes of the gyroscope signal [225].
15. (Foot based) Chang et al. presented a gait phase detection algorithm that uses the tri-axis angular velocity of wearables attached to feet. First, signal vector magnitude (SVMag) was calculated from gyroscope data. Then, the slope of the SVMag and a sample timer were used to detect FC. The slopes of SVMag that are higher than the predefined threshold rate is considered FC moments. In the meantime, another threshold was used for a timer to extract true FC events by avoiding the influence of the user's unconscious foot trembles and walking friction. Once, FCs were detected, each local maximum (peaks) within the interval of each of two successive FC points were defined as IC events [158].
16. (Foot based) Hsu et al. proposed a partially similar algorithm to Chang et al. using SVMag approaches for foot-mounted inertial sensors. Initially, the SVMag of the accelerometer and gyroscope signals were calculated. A windowing technique that segments SVMag signals into windows was used, and then the variances of acceleration and angular velocity for each window were calculated. In the following step, the start flag was set, and the signals were scanned window by window. Then, starting points of the stride (IC) were detected when the variance of both acceleration and angular velocity of a window is higher than the predetermined two different threshold values (one for acceleration and one for angular velocity). Ending points of stride (FC) was calculated with a similar approach but different thresholds [178].
17. (Foot based) Stamatakis et al. proposed an algorithm based on an accelerometer attached to a foot. First, the accelerometer signal was high pass filtered with 10 Hz cut-off frequency, then peaks that represent Ics were detected as heel strike results in a high amplitude and frequency peak in the x-axis of the acceleration signal [172].
18. (Foot based) Chung et al. developed an algorithm that uses an acceleration signal of foot mounted sensor to detect starting and ending points of strides (also known as IC-FC events). First, the signal vector magnitude (SVMag) of the 3D acceleration signal was calculated and then segmented into 3 sample window sizes. IC contact was detected by finding the first sample point after the variance of the SVMag window surpass the pre-determined threshold. Equally, once the variance of the SVMag is found lower than the threshold, the first sample data was accepted as FC [179].
19. (Foot and shank based) Jasiewicz et al. developed three different algorithms using foot linear accelerations, foot sagittal angular velocity and shank sagittal angular velocity to identify IC-FC events in individuals with spinal cord injuries. (1) IC-FC detection using foot linear accelerations; FC was identified by searching for a peak in forward-directed acceleration, within the FC search window located 250 ms before and 50 ms after each peak of ankle plantar flexion. To identify IC events, the algorithm searched for a vertically directed acceleration peak within the IC search window 100 ms before and 100 ms after peak ankle dorsiflexion. (2) IC-FC detection using foot sagittal angular velocities; To identify FC using foot angular velocity data, the algorithm searched for the first maximum in angular velocity in the FC window defined earlier. IC was identified as the velocity zero-crossing point in the IC window defined above. (3) IC-FC detection using shank sagittal angular velocities; The algorithm evaluates rapid changes in timing characteristics and selects the two minima on either side of a peak in velocity. The first minimum was associated with FC and the second minimum with IC [226].

I found few studies that robustly investigated and compared these gait algorithms, especially in clinical cohorts. Of those retrieved within the literature, one performed a comparative evaluation for the accuracy of three methods (presented above *1-3*) using a single inertial sensor mounted on the lower back [6]. In a similar study, sensitivity and robustness together with the accuracy of five different algorithms (*1-5*) for the estimation of gait temporal parameters were studied using a single inertial sensor mounted on the lower trunk [5]. The findings of the study suggested that the accuracy in estimating step and stride duration for all methods was acceptable for clinical use but *1* was optimal. Moreover, the same study also investigated the robustness of the IMU positioning of three algorithms (*1-2* and *4*) for four different locations around the lower trunk, and algorithms *1* and *4* were reported as highly robust.

2.5.2. EMG algorithms

Often, EMG sensors are used with additional systems since the identification of the gait cycle is challenging from EMG signals alone [133, 138, 227]. Some recent EMG-based gait assessment studies, together with various technologies are presented in Table 2. When EMG signals arising from gait have been correctly identified, they have been used in conjunction with different signal analysis techniques (e.g., Fourier transform) or artificial intelligence techniques (e.g., fuzzy logic) to develop advanced EMG detection and analysis. These signal-processing techniques and algorithms facilitate the differentiation of neurological gait from healthy gait but also contribute to monitoring specific gait abnormalities [80]. The following are current approaches to analyse EMG data:

1. The linear envelope of an EMG signal is an easy-to-interpret representation of the raw signal as it gives an indication of the overall level of activity in a particular muscle at any time. Typically, the envelope of the raw EMG signal is extracted by means of a technique based on a full-wave rectifier followed by an integrator (smoothing filter) or RMS operation. D'Alessio et al. proposed an alternative method that improves the drawbacks of the traditional approaches by using an adaptive iterative procedure which automatically sets and dynamically changes the length of the smoothing filter [228].
2. Figueroa et al. used a Kalman filter and an unbiased finite impulse response (UFIR) filter to extract EMG envelopes and remove some artefacts with maximum accuracy [229].
3. Micera et al. presented the characteristics of novel statistical algorithms and traditional approaches for the detection of muscle activation intervals (on-set and off-set timings). Single and double threshold methods which compare EMG signal with predetermined thresholds are the most intuitive method for investigation of onset-off set durations of muscle contraction activity, studied in [230].
4. A paper by Otter et al. used a clustering algorithm to find similarities between EMG amplitude data points and grouped these data points according to their similarities to detect muscle activity/inactivity durations. The primary reason for using k-means is that it does not require a priori thresholds[132]
5. Ren et al. developed an algorithm based on single-channel EMG recording for the extraction of MUAPs. First, noises were removed through wavelet filtering and thresholds were estimated with wavelet transform. Then, MUAPs were extracted based on amplitude single threshold filtering. Finally, MUAPs were classified to detect active segments [231]. More algorithms are available for EMG decomposition into MUAPs [79, 80].
6. Linear decomposition of multi-source EMG signal is another investigation method that helps to monitor the alterations in EMG characteristics of patients with gait disorders [232]. In this sense, the muscle synergy approach has been widely used with a number of linear decomposition algorithms (e.g. principal component analysis (PCA), non-negative matrix factorization (NNMF)) to understand the physiologic aspects of gait disorders [79].
7. Frequency and time-frequency analysis of EMG data can be used to distinguish specific gait abnormalities by providing useful outcomes such as median power frequency (MdPF) and instantaneous mean frequency (IMNF) using signal processing techniques (e.g., fast Fourier transform (FFT), wavelet transform). The FFT technique was used to compute power spectra, which are found distinctive in certain neurological conditions [79]. While IMNF which is the average frequency of power density spectrum of a signal found discriminative factor between affected and unaffected sides of stroke patients [233]
8. Power spectral density (PSD) provides useful information to understand which frequencies contain the signal's power and can be distinctive for some patient groups (e.g. PD) [234]. Go et al. computed the PDS using FFT (Welch method 50% overlap) and also calculated MdPF and total power of low frequencies to investigate the differences between muscle characteristics of dystonic and non-dystonic patient groups [235].
9. In recent years, the classification of EMG signals has been the interest of many researchers. Different type of classifiers (e.g. ANN) has been used with a wide range of sEMG features (e.g. integrated EMG, mean absolute value, RMS) as detailed in a review [236].

Table 2.EMG approaches for gait assessment in some neurological disorders

Neurological Condition	Ref.	Device	f_s	Muscle of interest	Used together with to identify gait	Groups	# subject – (mean age)
PD	[237]	Delsys Trigno (Delsys Inc., Boston, MA)	4,000 Hz	TA-GL-GAM	Motion Analysis – (Vicon Nexus, Oxford, UK) Instrumented treadmill (Bertec Corporation, Columbus, OH)	PD HS	5-(57) 5-(27.6)
	[133]	Konigsburg Instruments, Pasadena, CA	1,200 Hz	SOL- GAM-VM-RF-TA-GM-SM	Motion Analysis- (Vicon Nexus, Oxford, UK)	PD HS	15-(66.6) 14-(66.2)
	[212]	TeleMyo 900, Noraxon USA, Inc.	1,000 Hz	RF-BF-TA-GAM	Motion Analysis -	Freezers Non-freezers	12-(69.1) 14-(66.1)
	[138]	K-Laboratory EMG system; The Netherlands	2,500 Hz	TA-GS	Motion Analysis- (Vicon Nexus, Oxford, UK)	Freezers	11-(64.8)
	[227]	EMG preamplifier SX230, Biometrics Ltd., Gwent, UK	1,000 Hz	RF-VM-TA-BF-GL-SOL	Motion Analysis- (Vicon Nexus, Oxford, UK)	PD	9-(76.6)
	[238]	TMSi Mobita, The Netherlands	2,000 Hz	TA	Foot switch – EEG (TMSi Mobita, The Netherlands)	PD HS	20-(67.4) 24-(65.1)
Stroke	[239]	MediTrace ECG 1801 Pellet	2,400 Hz	BF-RF-GAM-TA	Motion Analysis- (PRIMAS™	Stroke	14-(54.7)
	[240]	(SATEM Mygotron, SATEM srl, Rome,Italy	-	GL	Motion Analysis- ELITE (BTS, Milan, Italy)	Stroke HS	10-(61.6) (62.6)
	[241]	Noraxon USA Inc., Scottsdale, Arizona, USA	1,000 Hz	TA-GAM-RF-BF-	Motion Analysis- (Vicon Nexus, Oxford, UK) force plates (Advanced Mechanical Technology Inc., Watertown, Massachusetts, USA)	Stroke HS	35-(61.04) 9-(61.0)
	[242]	Noraxon, Inc., Scottsdale, AZ, USA	2,520 Hz	TA-GS-SOL-RF-VL-BF	Motion Analysis- (Inc., Santa Rose, CA, USA)	Stroke	5-(51)
	[243]	MA-416-003 Motion Lab System Baton Rouge, LA	2,000 Hz	TA-SOL-GAM-VM-RF-LH-MH-GM	Force Plate- (Bertec Corporation, Columbus, OH)	Stroke HS	34-(61.6) 20-(56.1)
	[244]	Motion Lab Systems MA300-28, Baton Rouge LA	1,000 Hz	SOL-GAM	Motion Analysis- (VICON, Colorado, USA)	Stroke HS	24-(62.7) 17-(70.1)
Traumatic Brain Injury (TBI)	[134]	Delsys Trigno (Delsys Inc., Boston, MA)	1926 Hz	TA-GAM-SOL-VL-RF-MH	Accelerometer – (Trigno Delsys Inc., Boston, MA)	TBI HS	44-(53.4) 20-(25.3)
Multiple Sclerosis (MS)	[40]	Noraxon Telemyo 2400T EMG system Noraxon, Scotsdale, AZ	1,200 Hz	GAM-GL-SOL	Motion Analysis- (Vicon Nexus, Oxford, UK) Force Plate- Kistler Instruments AG, Winterthur, Switzerland)	MS HS	16-(42.01) 10-(37.21)
	[245]	Tyco Healthcare Nederland BV, Zaltbommel, the Netherlands)	1,000 Hz	HS-RF-TA-SOL-GS	Motion Analysis- (Basler Pilot piA640-210gc GigE, Basler AG, Ahrensburg, Germany) Force Plate- (AMTI, OR6-5-1000, Watertown, Massachusetts)	MS	81-(47.1)
	[246]	(EMG) system Cometa, Milano, Italy	1,000 Hz	TA-GL-SOL	Motion Analysis-(Vicon Nexus, Oxford, UK)	MS HS	30-(42.5) 15-(36.8)
Cerebellar Ataxias (CA)	[247]	FreeEMG 1000; BTS SpA, Milan, Italy	1,000 Hz	GM-RF-VL-VM-SM-BF-TA-GAM-GL-SOL-PL- TFL	Motion Analysis- (SMART-D System; BTS, Italy, Milan)	CA HS	23-(50.0) 23-(48.4)
	[248]	EMG; FreeEMG300 System, BTS	1,000 Hz	VL-BF-TA-GAM	Motion analysis – (SMART-DX 500 System, BTS, Milan, Italy)	CA HS	13-(50.2) 13-(50.2)
Huntington Disease (HD)	[249]	Micromed Brain Quick-(Mogliano Veneto, Italy)	256 Hz	TA-GL	EEG- (Micromed Brain Quick, Mogliano Veneto, Italy)	HD HS	24-(48.13) 14-(48.8)

Semimembranosus (SM), gluteus medius (GM), peroneus longus (PL), gastrocnemius (GS), lateral hamstring (LH), medial hamstring (MH), hamstring muscle (HS), tensor fasciae latae (TFL),

2.6. Wearables in neurological conditions

Impaired gait and poor postural balance emerge with the development of a neurological condition and both are challenging to recover despite rehabilitation programs [250]. Therefore, accurate identification of these neurological conditions and understanding of the underlying pathology may contribute to better and more targeted treatment. Those at risk may display a minimal number of abnormal gait and postural balance deficits from the early stages of a disease. Individual signs are never pathognomonic for any specific disorder but rather come with an associated differential diagnosis [251]. However, some neurological gait studies report some unique gait deficits, linked to different regions of the brain which are susceptible to various conditions. Here, I present reported characteristics of gait together with technologies and techniques used for instrumentation in groups stratified by generic neurological conditions. Investigation of temporal and spatial measures using wearable devices in gait assessment of different pathologies are presented in Table 3.

2.6.1. Stroke

About half of post-stroke sufferers clearly present motor impairments such as synkinesis, abnormal muscle tone, and orthopaedic deformations [38]. More than half of stroke victims walk with hemiplegic gait, which is characterized by the change in the temporal and spatial outcomes, e.g. decreased stance phase and prolonged swing phase of the paretic side [76]. In addition, a significant decrease in the stride time and cadence is most likely to be observed in post-stroke groups [158, 252]. A foot-mounted IMU (±8g, 100Hz) was used to obtain gait characteristics, where increased stride time and decreased stride length and velocity were reported [158]. Elsewhere [241], as a result of an investigation of the muscle activity for both stroke and healthy subjects, the number of bursts in the tibialis anterior (TA) during the swing phase was found significantly lower in asymmetric stroke patients. Descriptive EMG measures and altered muscle activation patterns (AMAP), were compared for post-stroke hemiparetic gait and healthy controls to identify the alterations in the EMG gait patterns of the stroke population. Results indicated that significant numbers of stroke survivors experienced altered muscle activation patterns in some muscle groups (soleus, tibialis anterior, and medial gastrocnemius) in terms of amplitude and onset timing [243].

2.6.2. Traumatic Brain Injury (TBI)

Gait disorders following TBI (resulting from e.g. blow to the head) are often severe and complex, varying considerably between people [253]. Some TBI sufferers experience severe gait disruption and poor postural balance while others experience relatively mild difficulties. The gait quality of patients with severe TBI was investigated using five IMUs (128Hz) and found a reduced stride frequency, along with an increased stride duration for TBI groups [198]. Free-living mobility of mild TBI patients has been investigated with a single IMU (128 Hz, waist) and descriptors of ambulation (e.g., the number of bouts per hour, total steps per day) as well as turning parameters (e.g., a number of turns, velocity) was studied. Results have suggested that people with chronic mild TBI made larger turns, had longer turning durations together with slower average and peak velocities [195]. Abnormal muscle activation patterns have also been investigated with chronic gait deficits after TBI, where participants who experienced TBI exhibited characteristics changes in the temporal coordination of select lower extremity muscles, which may have an impact on impaired walking during challenging tasks (e.g. dual tasking) [134].

2.6.3. Hypoxic-Ischemic brain injury (HIBI)

HIBI mostly occurs as a result of cardiac arrest or respiratory failure and deprivation of adequate oxygen supply, which may result in death or long-term impaired gait [254]. As in many neurological conditions, HIBI patients often show different movement disorders like chorea and dystonia with reduced walking speed and cadence [255]. Although individuals after HIBI rarely experience freezing of gait (FOG), 3D motion analysis and force plate-based study results showed that HIBI sufferers with FOG have reduced velocity, stride length and increased double support time compared to those without FOG episodes in the HIBI group [256]. To the authors' knowledge, no gait assessment studies have investigated the gait characteristics of HIBI using wearables (see Appendix 3).

2.6.4. Parkinson's Disease (PD)

A neurodegenerative disease with resting tremor, bradykinesia and rigidity manifestations is one of the most common neurological conditions [257] and with significant developments in the use of wearables to assess PD gait. Reduced walking speed, shortened stride length and increased stride variability are quantified in the early stages [35]. Although swing and stance times are sensitive to age and severity of the disease, both are found lower in PD compared to controls [154]. Another manifestation observed in PD is freezing of gait (FOG), which frequently causes falls [258]. Free-living PD gait has been examined with the use of a single wearable (lower back) for extended periods (e.g. 7-days) to examine ambulation (e.g. volume, pattern, variability) as well as temporal and spatial gait where the latter was shown to be different to controlled lab conditions [21-23]. Elsewhere, an algorithm that sensitively and automatically distinguishes PD patients from healthy controls was developed using extracted EMG features and support vector machine (SVM) classification [237]. It is reported in an EMG-based gait assessment study that PD groups exhibit decreased neuromuscular complexity during gait and muscle activation profiles also undergo changes compared to controls [133].

2.6.5. Progressive supranuclear palsy (PSP)

PSP is characterized by poor balance, frontal dysfunction and rapid disease progression. Even though it is challenging to discriminate from PD groups in its early stages, diagnosis may be possible with the study of distinctive spatiotemporal gait parameters. In addition, FOG was reported as an indicator in the early stages, and its presence might improve the clinical diagnosis of PSP condition [259]. A single IMU (250 Hz, lower back) based study reported that PSP survivors experienced lower vertical displacement and higher acceleration than those with PD group in the same cadence. [171]. A walkway-based gait study findings suggested that, despite similar disease durations, increased step width and double support were found slightly higher in PSP groups than in PD groups and always higher than in healthy controls [42]. Although some studies investigated spatiotemporal gait characteristics of those with PDP, studies related to muscle characteristics of PDP gait are very limited.

2.6.6. Cervical dystonia (CD)

CD is a neurological movement disorder in the neck muscles. The condition is associated with involuntary muscle contractions that result in an impaired posture with twisting movements [260]. People with phasic CD experience poor postural control and impaired mobility, especially during walking and turning [261]. Contrary to the majority of neurological conditions, those with CD have increased step length compared to controls as well as displaying increased step time and double support time as reported in a walkway-based gait assessment study [262]. To the authors' knowledge, no gait assessment studies have investigated the gait characteristics of CD patients using wearables (Appendix 3).

2.6.7. Huntington's disease (HD)

An autosomal dominant inherited condition, HD has a different set of movement disorders like chorea, dystonia and bradykinesia. Gait disturbance, unpredictable accelerations and decelerations in gait speed, can be seen from the early stage [263]. In an IMU (250 Hz, upper sternum) based study, spatial gait characteristics and postural balance were investigated for healthy controls, pre-manifest HD and manifest HD groups. Results showed a considerable decrease in speed, and step-stride lengths together with increased step-time asymmetry in the pathologic groups. [200]. Furthermore, changes in motor activity during walking with dual tasking conditions were investigated using EMG and electroencephalogram (EEG). The study findings reported that for those with HD, associations with cognitive tests produced only a slight and not relevant deterioration of motor speed and muscle recruitment, whereas some modulation of EEG beta-band activity was observed during dual tasking [249].

2.6.8. Dementia: Alzheimer's disease (AD)

Dementia disease subtypes have been investigated with a single accelerometer (±8g, 100 Hz, lower back) [264]. AD is the most common subtype and damages the stability and symmetry of people's gait explicitly. Reduced stride length and cadence are preliminary deficits observed from the beginning of AD [97, 265]. Increased stride time, stance time and swing time and double support time measures are more likely to be seen in AD groups [178, 266]. IMUs (±4g, 100 Hz, feet and waist) were used to detect gait abnormalities and postural balance of those with AD group and controls during single and

dual tasking. Findings showed that those with AD have slower gait speed and lower stride length, whereas balance task findings reported that those with AD experienced a significantly larger average sway speed in Medio-lateral (ML) direction compared to controls [178]. There have been increasing reports of non-cognitive symptoms (e.g. loss of motor function) associated with AD; thus a review investigated links between motor function and preclinical AD [267]. Findings suggested that the change in BMI, and lower levels of function (muscle strength) together with both a lower level and more rapid rate of motor decline may be an early cognitive sign of AD.

2.6.9. Multiple Sclerosis (MS)

MS is commonly known for ataxia and weakness impairments [40]. Significant reductions have been reported in step length and velocity with the use of a single IMU [183]. Alternatively, two wireless IMUs (102.4 Hz, each shank) compared early MS patients to controls during a Timed-Up-and-Go (TUG) test. Classification with 53 extracted mobility parameters showed that those with early-stage MS could be distinguished with 96.90% accuracy [268]. Free-living physical activity of patients with MS was monitored with wearables, reporting that the least disabled MS patients performed significantly higher step numbers than those with severe MS [269]. Ankle mobility was investigated for MS patients using EMG sensors (with a motion analysis system) and study findings suggested that a decline in ankle push-off may be the common factor to induce limited walking ability in MS groups [245]. In [40], muscle activities in plantarflexion muscle groups were investigated for those with MS patients and controls, where results suggested that plantarflexion muscle groups in those with MS demonstrated an increased EMG amplitude.

2.6.10. Cerebellar Ataxias (CA)

Cerebellar Ataxias (CA) are a series of gait disorders as a result of impaired cerebellum and associated mechanisms, and gait disturbance was found to be one of the most pronounced and disabling symptoms for the disease [270]. An IMU (±10g, 20 Hz, lower back) showed decreased gait velocity, cadence and step length [189, 190]. Another study investigated the time-varying multi-muscle co-activation function (TMCf) in the lower limbs and concluded that global co-activation was significantly increased in patients with CA compared to controls [247]. In a similar EMG-based study, significantly higher mean co-activity index values were found in specific muscle groups (VL-BF-TA-GAM, Figure 3) during almost all gait phases in the CA groups compared to healthy controls [248].

Table 3.Wearables in neurological gait assessment with increased (↑) or decreased (↓) spatiotemporal outcomes for that groups

Neurological Condition	Ref.	Device – g-*fs*	Algorithms used. (Section 2.5.1.)	Group	# subject - (Age)	VEL	CAD	SPL	SDL	SPT	SDT	Additional findings
CA	[190]	ACC ± 10 20 Hz	-	HS	56- (57.2)	↑	↑	↑	-	-	-	-
				CA	51- (60.3)	↓	↓	↓	-	-	-	
	[189]	ACC ± 10 20 Hz	-	HS	57- (56.7)	↑	↑	↑	-	-	-	Decreased step regularity is observed in CA patients.
				CA	61- (61.1)	↓	↓	↓	-	-	-	
PD	[51]	IMU ± 6 51.2 Hz	Gait cycle algorithm-14 Spatial algorithm 1	HS	101- (41-84)	↑	↑	↑	↑	-	↓	Increased stance phase and reduced swing phase are found in PD.
				PD	190- (36-85)	↓	↓	↓	↓	-	↑	
	[158]	IMU ± 8 100 Hz	Gait cycle algorithm-15	HS	15- (68.47)	↑	↑	-	↑	-	X	Reduced swing time, non-significant difference for stance time in both group
				PD	5- (76.20)	↓	↓	-	↓	-	X	
	[154]	ACC ± 8 50-100 Hz	Gait cycle algorithm 1 Spatial algorithm 3	HS	30- (66.6)	↑	-	↑	-	↓	-	Reduced stance and swing time, increased stance and swing time asymmetry in PD group.
				PD	30- (66.9)	↓	-	↓	-	↑	-	
	[172]	ACC ± 10 100 Hz	Gait cycle algorithm-17	HS	-	↑	-	-	↑	↓	↓	Decreased step frequency, single support time and increased double support time in PD group.
				PD	-	↓	-	-	↓	↑	↑	
	[171]	ACC N/A 100 Hz	-	HS	24- (73.7)	↑	↑	↑	-	↓	-	Increased double support and step time variability in PD group.
				PD	124- (68.4)	↓	↓	↓	-	↑	-	
	[220]	MIMU ± 6 128 Hz	Gait cycle algorithm 8 Spatial algorithm 2	HS	10- (69.7)	↑	-	-	↑	↓	↓	Increased stance time in PD group
				PD	10- (73.8)	↓	-	-	↓	↑	↑	
HD	[200]	ACC ± 2.5-10 250 Hz	Gait cycle algorithm 2 Spatial algorithm 3	HS	10- (56.45)	↑	↑	↑	↑	↓	-	Increased step time asymmetry observed in manifest HD group.
				HD	14- (51.83)	↓	↓	↓	↓	↑	-	
	[220]	MIMU ± 6 128 Hz	Gait cycle algorithm 8 Spatial algorithm 2	HS	10- (69.7)	↑	-	-	↑	↓	↓	Increased stance and swing time in HD group
				HD	10- (50.3)	↓	-	-	↓	↑	↑	
PSP	[171]	ACC N/A 100 Hz	-	HS	24- (73.7)	↑	↑	↑	-	↓	-	No significant difference in double support. Increased step time variability in PSP.
				PSP	20- (71.8)	↓	↓	↓	-	↑	-	
Stroke	[158]	IMU ± 8	Gait cycle algorithm-15	HS	15- (68.47)	↑	↑	-	↑	-	↓	

Neurological Condition	Ref.	Device – g-*fs*	Algorithms used. (Section 2.5.1.)	Group	# subject - (Age)	VEL	CAD	SPL	SDL	SPT	SDT	Additional findings
		100 Hz		Stroke	4-(51.50)	↓	↓	-	↓	-	↑	Increased stance and swing time in stroke group
	[220]	MIMU ± 6 128 Hz	Gait cycle algorithm 8 Spatial algorithm 2	HS	10-(69.7)	↑	-	-	↑	↓	↓	Increased stance and swing time in stroke group
				Stroke	10-(58.6)	↓	-	-	↓	↑	↑	
Stroke-Paretic-non paretic	[159]	IMU 100 Hz	-	Non paretic	25-(66.6)	↓	↓		↓		↑	Reduced double support phase in paretic side.
				Paretic		↑	↑		↑		↓	
AD	[178]	IMU ± 4 100 Hz	Gait cycle algorithm-16	HS	50-(59.86)	↑	↑	-	↑	↓	↓	Increased stance and swing time in AD.
				AD	21-(61.48)	↓	↓	-	↓	↑	↑	
	[179]	IMU ± 2 100 Hz	Gait cycle algorithm-18	HS	3-(69.0)	↑	↑	-	↑	↓	-	Reduced mean stride frequency and increased stance phase in AD.
				AD	9-(71.0)	↓	↓	-	↓	↑	-	
MS	[182]	IMU 50 Hz	Gait cycle algorithm-12	HS	15-(57.9)	-	↑	-	-	↓	↓	-
				MS	45-(58.2)	-	↓	-	-	↑	↑	
	[183]	IMU N/A	-	HS	47-(39.4)	↑	↑	-	↑	↓	-	Minor differences for stance and swing phases (% of the GC), and increased double support time was reported for MS group.
				MS	105-(42.2)	↓	↓	-	↓	↑	-	

HS: Healthy subject, X: the same value, (-): not available, g=force, Fs= sampling frequency, VEL: velocity, CAD: cadence, SPL: step length SDL: stride length, SPT: step time, SDT: stride time

2.7. Discussion

To date, a large number of signal-based parameters have been quantified using various technologies and used along with different gait models to better understand impaired gait due to one or more neurological conditions [10, 91, 93]. Existing gait models may be limited as some originated from non-wearable technology-based temporal and spatial outcomes, later adapted for wearable purposes. Current models also fail to include kinematic, kinetic or muscle activation characteristics, which could prove beneficial. Furthermore, proposed models are developed for a particular neurological condition, meaning they may not translate to other pathological cohorts. Thus, developing a model based on more gait characteristics for use in specific pathologies may contribute to a better understanding and assessment of impaired gait.

Wearable IMU-based temporal and spatial outcomes are presented extensively in the literature, but novel frequency and time-frequency outcomes are becoming more evident and may provide further insights into free-living gait assessment. Alternatively, the use of EMG for muscle characteristics of impaired gait has been studied for some neurological conditions (e.g., PD, MS) and distinctive muscle-related parameters have been reported [40, 134, 271, 272]. However, the number of gait studies, which investigate muscle activities in other pathologies is limited. Moreover, it was found that there is a large variance in the methodology of sEMG use such as placement protocols. Although there are guidelines for the use of sEMG [204, 205], few studies are adhering to these recommendations.

In favour of wearable sensing technologies, gait assessments of pathologies have been moving away from clinics to free-living environments. Free-living gait assessment contributes to the existing knowledge because it reflects real-life settings such as environmental factors and natural dual tasking. Although the majority of gait abnormalities have been studied in the clinical environment, very few neurological conditions and very small populations were studied during free living. Instrumented gait is predominately investigated in PD and trends to monitor during free-living show large discrepancies in temporal and spatial outcomes between lab and free-living assessment [21-23]. However, the number of evidential studies to investigate whether there are large variances between lab and free-living assessments for other neurological conditions (e.g., Stroke, MS, AD) is very limited. Next, I discuss potential limitations, and future directions in wearable-based gait assessments, including inertial algorithms, multiple sensor fusion and free-living gait assessment.

2.7.1. Wearable signal processing – future directions

Use of wearable, primarily IMUs, have been validated and used in gait assessment of various neurological conditions (e.g. PD [154, 174], stroke [159, 168], AD [178, 179], MS [187, 273], CA [191, 192], HD [200, 201]). A plethora of inertial gait algorithms was used in these studies. The abundance of inertial algorithms is possibly due to the redundancy of preferred experimental protocols in methodology (e.g., statistical, mathematical) and data capture (e.g., sensor placement). However, both the lack of standardisation and the fact that these inertial-based algorithms were developed for a particular pathology are some limitations in the field. Although a comparative assessment study was performed for 5 different inertial algorithms to estimate gait temporal parameters using a single IMU (on L5) within three different pathologic groups (stroke, PD and HD) [7], the most appropriate algorithm for each pathology or for pathologies that experience similar deficits is still unclear. Due to these inconsistencies, developing conclusive interpretations of existing evidence based on wearables remains limited. Perhaps, a manual like sEMG guides can be developed for IMUs data capture and methodology to standardise use of wearable sensors in gait assessment of different pathologies. Furthermore, wearable validation studies should adopt the V3 approach[145] of clearly presenting verification (bench testing), analytical validation (efficiency and accuracy of sample-level sensor measurements into physiological metrics) and clinical validation (acceptably identifying or measuring clinically meaningful outcomes in a stated context of use with a predefined disease/condition) approaches within standalone or within a series of research output/papers.

2.7.1.1. Data synchronisation & fusion

Multiple sensors are used commonly in gait assessment of neurological conditions. Depending on the application (e.g. joint kinematics, muscle characteristics) a number of IMUs, pressure, EMG sensors and clinical-based technologies have been used collectively [64, 274]. Although, some studies use multiple IMUs for kinetic gait analysis [148, 275] and lab-based systems along with EMG [134, 238, 241, 271] for muscle activation analysis,

the number of studies that use multiple wearable sensors e.g. IMU and EMG are very limited. It is believed that this limitation is because of the incapability of technical devices. Previously, commercially available devices were not capable of capturing multiple gait characteristics (e.g., spatiotemporal and muscle activation) simultaneously, while multiple device configurations bring complexities such as data synchronisation and sensor data fusion.

Synchronisation of sampling frequencies (i.e., interpolation) has the utmost importance to achieve an accurate assessment. Using multiple devices with different sampling frequencies results in data loss or drift error and may not reflect simultaneous information. Utilising time stamps on devices to be synced provides convenience without the need for additional ports. With the recent advancements in wearables, commercially available sensors (e.g., *BioStamp RC*, *Shimmer3 EMG, Trigno Avanti* and *Ultium EMG*) can provide inertial sensing and muscle activation signals simultaneously in a single device. It is believed that this convenience will initiate new studies to overcome the limitations of previous gait studies e.g., gait models based on spatiotemporal parameters/outcomes only. The second complexity of the use of multiple sensors (sources) is sensor data fusion (also known as multi-sensor data fusion), which is a process of integrating multiple data sources to produce more consistent and reliable output. The type of data fusion algorithm depends on the target application considering the required output, operational time, and battery life. To date, data fusion algorithms have been used in activity recognition [276, 277], fall detection[278, 279], gait analysis [280, 281] and biomechanical modelling [282, 283]. Further discussion on data fusion algorithms; signal level, feature level and decision level can be found in [284].

2.7.1.2. Walking environments (treadmills, indoor, outdoor)

Gait analysis in neurological populations is typically performed in controlled environments, where pathways (e.g., instrumented mats, treadmills) are usually level, clear, and mostly straight or circular. Variations in environments exist due to fundamental research questions e.g., foot clearance due to obstacle crossing. Within controlled environments, various gold standards technologies such as 3D motion capture, instrumented walkways and treadmills are commonly used. Although these technologies offer highly accurate data, they lack ecological validity as outcomes may not apply to more complex outdoor environments and different walking terrains [285]. For example, treadmills are classified as an external cue since these devices force participants to walk at the device's programmed speed and incline rather than participants' comfortable speed and patterns. Walking on a treadmill requires additional balancing abilities compared to walking on the ground. Additionally, treadmill bars may have an impact on patients' perception and proprioception during walking, limiting participants' natural gait [286]. Consequently, gait characteristics (e.g., muscle activation) recorded during treadmill walking differ from overground walking [287].

Indoor ground-level walking allows participants to perform their natural gait patterns, typically instrumented via gold standard technologies that provide highly accurate multimodal data (e.g., pressure sensing from an instrumented walkway, displacement from 3D motion capture or inertial from wearables), informing different aspects of impaired gait in neurological populations [237, 288]. To date, various gait models are used to ease the interpretation of gait characteristics (e.g., spatiotemporal parameters), developed and validated for indoor walking assessments with instrumented walkways [9] as well as outdoor with wearable IMUs [91]. However, there is a trend toward more outdoor gait assessment as indoor walking studies have limitations such as limited walking bouts in unnatural idealistic conditions.

Data collected in outdoor environments for extended periods (e.g., days, weeks) can potentially complement clinical assessments. Exploring neurological gait beyond the clinic enables clinicians to capture some rare incidents such as increased gait variability that may lead to a fall, which is not likely to naturally occur during clinical visits. Indeed, data collected outside of the clinic was found more informative than the data collected in the clinics in terms of predicting the risk of future falls [289]. Moreover, previous studies revealed differences in spatiotemporal, kinematics and muscle activation between indoor and outdoor walking [150, 290-292]. Complex walking terrains in outdoor environments are associated with differences between indoor and outdoor walking since gait adaptation strategies to maintain stability are found sensitive to walking terrain [293]. Other factors that could explain differences are alertness, motivation, stress, and the white coat effect. The latter relates to a participant being more self-conscious during an observational assessment by a healthcare professional within a clinic. Data collection in controlled environments under observation may capture a participant's best performance rather than their usual everyday performance/capability in the home and community. Although data captured outside of the clinics reflects more about real life e.g., with natural dual tasking (see next section), certain

limitations are reported [294]. Primarily, data interpretation of outdoor walking for extended periods is challenging due to the lack of appropriate gait models and contextual information for outdoor walking. In addition, robustness, and test-retest reliability of existing sensor algorithms needs to be established for outdoor walking environments. However, the lack of gold-standard systems in outdoor environments could limit the validation of sensor algorithms.

2.7.1.3. Data Reduction; activity and terrain detection

Although wearable technology makes it possible to collect data for an extended time in free-living conditions, a convincing data collection period has not yet been established [22]. In this sense, a greater number of gait assessment studies using wearables in free-living is required to establish satisfactory data collection periods for each pathology. Alternatively, continuous data recording, especially with high sampling frequencies may result in a vast amount of data that includes different daily dynamic gait activities (e.g., level walking, stair ascend) and static activities (e.g., sitting, lying). Therefore, it is essential to process the collected data to extract meaningful gait information for a more comprehensive assessment. Currently, activity recognition with IMUs has been a widely used approach to segment dynamic movements from static. However, there is a large discrepancy observed for the preferred sensor numbers and locations. Considering the comfort and long hours recording possibilities, a single sensor on the wrist [295], two inertial sensors attached to feet [281], a single accelerometer on the chest [296] and a single accelerometer at the level of the waist [297] seem preferred during free-living activity detection. However, considering neurological conditions, the attachment of a single sensor to the waist may be ideal for both activity recognition and extraction of gait measures (e.g., cadence, stride length).

A similar discrepancy is observed in preferred methodologies. Physical activities have been classified using IMUs with traditional (e.g., threshold based) [298], time-frequency (e.g. DWT) [296] and analytical (e.g. statistical schemes) [297] approaches. Although threshold-based and time-frequency algorithms provide high-accuracy data classification, the need for calibration limits these approaches. Moreover, pre-determined threshold rates may not translate between different neurological conditions. Conversely, supervised methods that include machine learning (ML) and neural networks (NN) have been preferred due to many advantages such as less sensitivity to sensor location and high accuracy results and ability to be trained. In previous studies, activity recognition with modern approaches typically consists of two different stages: (1) feature selection and (2) classification. In the former stage, appropriate time domain (e.g. mean, signal magnitude area, skewness, variation) and frequency domain (e.g. energy, entropy) features are extracted [295]. In the latter stage, extracted features are used in training and testing to cluster different physical activities. Supervised classification techniques; k- Nearest Neighbour (k-NN), support vector machines (SVM), Random Forest (RF) and unsupervised; k-Means, Gaussian mixture model (GMM) and Hidden Markov Model (HMM) are commonly used machine learning techniques [276, 277]. However, discrepancies in selected features and classification techniques and the scarcity of labelled data are impeding factors. Therefore, a deep long short-term memory (LSTM) neural network architecture together with the spectrogram-based feature extraction approach are alternatives used for activity recognition with inertial data [299, 300].

A better understanding of free-living gait may become more meaningful when we know on which surface (e.g., terrain) it is performed, Figure 4. It is reported that gait adaptation strategies to maintain stability are sensitive to different walking surfaces [293]. Older adults are known to be less sensitive to maintaining balance in the moment of trips and slips when walking on different terrains due to deterioration in their sensory, motor and cortical functions [301]. In previous studies, indoor-outdoor and hard-soft walking terrains (e.g. tiles, carpet, grass) were accurately classified using SVM and RF with acquired inertial data from the chest and lower back [302], and indoor walking terrains were investigated with an IMU attached to lower back [303]. Although only a few studies investigated gait on uneven terrain for neurological conditions using clinic-based technologies [304], wearable-based gait assessment for those populations on different terrains has not been fully investigated. Thus, it is believed that extracting specific periods of gait together with the walking terrain may be useful to better understand how neurological conditions adapt to walking on different terrains (multi-surface). Then, this insightful knowledge may contribute to the design of interventions (e.g., bespoke rehabilitation programs) for people with neurological conditions to improve impaired gait, poor postural balance and minimise falls.

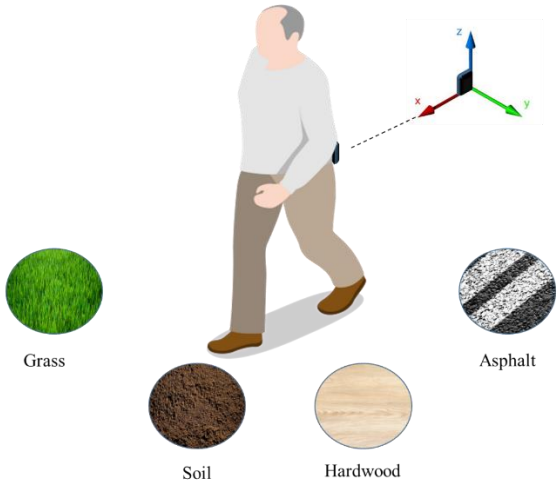

Figure 4. Walking on different terrains

2.8. Limitations and knowledge gap

1. Previously IMU based algorithms were validated for different sensor wear locations and cohorts to compute IC and FC moments. However, consistency/agreement levels between algorithms were not fully investigated considering sensor wear locations, target cohort or walking environment.
2. Current approaches utilise mostly unimodal/IMU from a single wearable only. Therefore, existing gait models were developed based on only unimodal characteristics to interpret gait. Multimodal gait analysis may potentially provide more comprehensive gait outcomes and can be used to improve the limitations of existing gait models. Nevertheless, the methodology for integrating multiple sensors or data sources is still not sufficiently advanced.
3. Clinical gait analysis is often performed in controlled lab environments and offers snapshot assessment. Moving beyond clinics using wearable sensors may potentially help collect gait outcomes for longer periods, but the obstacles associated with sensor technology and methodology have not yet been comprehensively explored.
4. Free-living gait analysis creates challenges such as a vast amount of unlabelled gait data. HAR methodologies may be used to automatically label the data collected in free-living environments.

2.9. Conclusion

In this chapter, a comprehensive examination of the technologies and methodologies employed in gait analysis is presented. The emphasis is primarily placed on the utilisation of wearable sensors, owing to their numerous benefits. Through an extensive literature review, significant limitations and knowledge gaps in instrumented gait analysis were uncovered. These identified shortcomings were subsequently utilised to develop the Points of Interest (PoI) presented in Chapter 1.

In the next chapter, an in-depth examination of the initial research question (PoI 1: "*How consistent are the existing IMU algorithms for detecting initial contact (IC) and final contact (FC) moments, considering factors such as sensor placement, cohort type, and walking conditions?")* will be investigated through a comprehensive comparative experimental study.

Chapter 3 Examining Agreement Levels in Inertial Gait Algorithms

This chapter uses text from my previously published online article to fit the context and narrative of this thesis. The open access journal article "*Wearable Inertial Gait Algorithms: Impact of Wear Location and Environment in Healthy and Parkinson's Populations"*, was published in the **Sensors** in **2021.**

(URL: https://doi.org/10.3390/s21196476)

3.1. Introduction

IMUs generate distinct acceleration and angular velocity signals (waveforms) depending on where they are placed on the body during walking [1]. Therefore, existing IMU methods to detect initial contact (IC) and final contact (FC) moments differ from each other in terms of the algorithms, digital filters and threshold values used. Moreover, systematic errors in these validated algorithms exist [305] and are sensitive to the target cohort as previous studies report that wearable IMUs attached to people with neurological conditions generate different acceleration and angular velocity signals than healthy controls[306]. This raises the question of what algorithms are the most accurate/consistent in terms of extracting spatiotemporal parameters in neurological conditions. Chapter 2.5 introduced some of these algorithms that were tailored to extract spatiotemporal parameters like step length and step time, considering the characteristics of the accelerometer or angular velocity signals. Consequently, inconsistencies in the extracted parameters were presented due to differences in signal type or the methodology employed, such as the use of digital low-pass filters[5, 7].

The purpose of this chapter is to conduct a comparative study that investigates the level of agreement between lower-back and shank sensor-based algorithms in adults and PD cohorts during walks in different walking environments. This will help to investigate PoI1. The objective of this chapter is to provide a guide for future studies and inform them about how cautious they should be when interpreting the temporal outcomes derived from these algorithms.

3.2. Background

Human gait is a complex cyclic pattern that relies on individuals′ kinetic, kinematic and muscle characteristics. Neurodegenerative disorders (e.g., PD) and other factors like age and lifestyle can alter an individual's gait pattern [307]. Typically, people with PD walk slowly with short fast shuffling steps [23, 91]. Additionally, those with PD may present with additional conditions due to poor gait such as pain arising from poor foot health and reduced quality of life [308] leading to increased depression scores [309]. Although most neurological conditions share similar gait deficits such as reduced gait speed and poor balance, there are also characteristically distinctive patterns (e.g., increased step time) that help differentiate particular neurological conditions [2]. Therefore, investigating discrete gait cycles may provide nuanced and even personalized assessments for those with gait disturbances.

Wearable IMUs are now commonly used for gait analysis due to their small form factor and long data recording possibilities, in indoor and outdoor environments [310, 311]. The vertical acceleration of the pelvis and sagittal plane angular velocity of the shins are commonly used inertial signals to detect initial contacts (ICs) and final contacts (FCs) within the gait cycle [150, 214, 305]. In general, methods to quantify ICs and FCs are dependent upon inertial signal quality as well as IMU location (e.g., lower-back, shin/shank, foot) and computational methodology (e.g., wavelet transform)[2, 150, 214, 305].

Research demonstrates that either linear acceleration or angular velocity sensors attached to various body locations/segments can be used to detect ICs-FCs as accurately as a reference system (e.g., footswitches, instrumented walkway) for both normal and pathological gait footfalls [216, 217, 219-221, 223, 224, 226, 312, 313]. However, the accuracy of the IMU algorithm also varies depending on the walking terrain (environment) and target population. Previous studies investigated the performance of IMU algorithms that provide accurate and repeatability valid ICs-FCs. For example, lower-back algorithms that use acceleration signals were compared in healthy [5, 6] and neurological populations during indoor walking [7]. Wrist, waist and shank accelerometer signal-based algorithms were compared during various walking settings (e.g., indoor, outdoor) in a healthy young population [314]. Performances of foot and shank angular velocity with foot acceleration signal-based algorithms were compared in spinal-cord injured individuals [226]. Other studies investigated optimal IMU locations (lower-back, shank, foot) and algorithms that provide accurate ICs-FCs moments for healthy young adults only [150, 214]. Each study reported various levels of accuracy, where inconsistencies could be associated with the fluctuations in performances of IMU algorithms e.g., better-detecting ICs than FCs [314] due to the higher variance of generated signals by each cohort during walking on different terrains [150].

Performances of lower-back IMU algorithms are typically poorer/lower in neurological cohorts compared to healthy cohorts, due to occasional failed detection of acceleration-based ICs-FCs [7]. This could be attributed to the development of the algorithms within controlled environments only [214]. Moreover, previous studies reported

certain differences between indoor and outdoor temporal parameters [21, 91, 315, 316] and this was associated with the fluctuation in performances of inertial algorithms along with many other factors such as the white coat effect [294]. Indeed, previous papers investigated and compared IMU algorithms based on sensor location and target signal used by using a reference system in healthy populations [150, 214, 305], but the margin of error between algorithms (or absolute agreement) has not been fully investigated in different groups and environment. Furthermore, the population size of validation and comparison studies was generally limited/low. Consequently, optimal algorithms, IMU locations for a specific cohort and environment to inform how cautious researchers should be while interpreting temporal parameters remain unclear.

This work aims to investigate the level of agreement between established lower-back and shank IMU algorithms in young adults (YA), older adults (OA) and PD cohorts during different walking protocols in various environments. I hypothesise that existing inertial algorithms may be sensitive to sensor wear location, target cohort and walking environments limiting the widespread use of wearable IMU algorithms during indoor and outdoor gait assessment. Discovering the effects of cohort and environment could help better understand the difference between indoor and outdoor walking. Unlike previous studies, this study directly investigates agreement between algorithms rather than agreement with a reference system in large healthy and PD populations. Accordingly, I aim to make a judgement about how confidently researchers can use one algorithm over the other. The results of this study will add to the current knowledge by providing details about how similar the results of two common IMU algorithms are in various environments. To the author′s knowledge, this is the first comparative study that investigates the level of agreement between lower-back and shank sensor-based algorithms on adults and PD along with a large YA population. The main contributions are to:

- Investigate agreement between algorithms across different groups (YA-OA-PD),
- Investigate the impact of the walking environment (treadmill-indoor-outdoor) on the agreement between algorithms,
- Provide recommendations when deciding on optimal IMU location and gait algorithms.

3.3. Materials and Methods

A total of 128 participants' gait data were analysed from previously created datasets. Public dataset 1 (DS1 http://gaitanalysis.th-brandenburg.de/ accessed 5 Oct 2020) contained 72 healthy young adults (YA) [317]. Additional dataset 2 (DS2) comprises 20 (age-matched) healthy older adults (OA) and 36 PD participants, a sample from a previous study [318]. See Table 4 for participant information and demographics and associated references for in-depth details Here, datasets are described briefly.

Table 4. Participant information/experimental protocols.

	DS1			DS2	
Environment	Treadmill	Indoor	Outdoor	Indoor	Indoor
Cohort-Number	(YA-16)	(YA-31)	(YA-25)	(OA-20)	(PD-36)
Male/Female (n)	10/6	22/9	16/9	10/10	18/18
Age(years) Mean ± SD	32.6 ± 11.9	26.6 ± 11.0	26.28 ± 12.2	69.76 ± 7.82	69.20 ± 6.64
Sampling Frequency	60 Hz	60 Hz	75–100 Hz	128 Hz	128 Hz
Disease Duration (years)	--	--	--	--	7.82 ± 5.62
UPDRS III	--	--	--	--	32.51 ± 4.12
NFOGQ	--	--	--	--	7.44 ± 8.62
LEDD	--	--	--	--	786.68 ± 416.88

OA: Older Adults, YA: Young Adults, PD: Parkinson's Disease, UPDRS: Unified Parkinson's Disease Rating Scale, NFOGQ: The New Freezing of Gait Questionnaire, LEDD: L-dopa equivalent daily dose.

3.4. Datasets

3.4.1. Datasets-1 (DS1)

Data capture took place in different countries (Austria, Finland, Kenya) and testing environments (treadmill, indoor and outdoor). All volunteers provided informed consent about the experiments, data storage and the future use of data before participating. Comprehensive information on protocols, data collection, etc., is provided elsewhere [317]. In short, each subject wore three IMUs (Xsens MTw, Enschede, Netherlands) on the right shank (SR), left shank (SL) and the lower back (fifth lumbar vertebrae, L5), Figure 5. a. Each synchronized Xsens IMU was configured for different protocols (acceleration ±16 g, angular velocity ±2000 deg/s and different sampling rates: 60 Hz, 75 Hz, 100 Hz) before data collection.

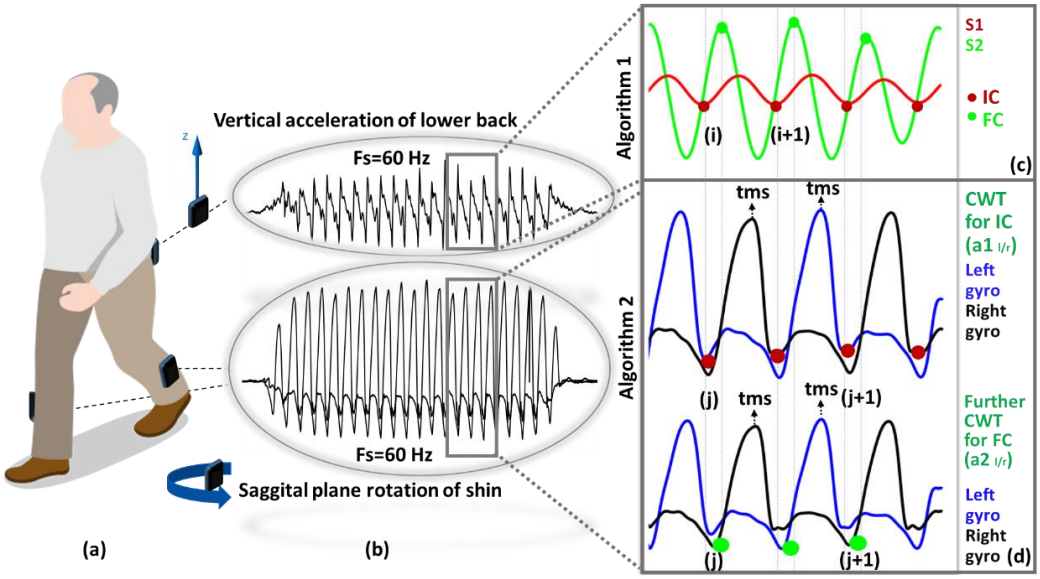

Figure 5.Data processing: (a) Sensor placement, (b) raw acceleration and rotation data of two different locations, (c) IC-FC detection with Algorithm 1 process, (d) IC-FC detection with Algorithm 2, ICss and FCs are represented with red and green dots, respectively.

During treadmill walking, participants were asked to walk between 7–9 mins. The speed was incremented every minute from 2–8 km/h with a step of 1 km/h. During repetitive indoor walking, participants walked 10–20 m four times at self-selected normal, slow, and fast speeds. The outdoor walking experiments consisted of two 40–80 m walks at a self-selected speed.

3.4.2. Datasets-2 (DS2)

Each subject wore three synchronized IMUs (Opal, V2 APDM Inc., Portland, OR, USA) located on the SR, SL and the L5 via a belt strap, Figure 5. a. Each recorded tri-axial acceleration (±2 g or 6 g, 128 Hz) and tri-axial angular velocity (±1500 degree/s). Gait assessment and instrumentation were carried out by a physiotherapist and trained researchers, respectively. Ethical consent was granted by the Oregon Health & Science University institutional review board (REF: 9903). All participants gave informed written consent before participating. Repetitive indoor/lab gait tasks included: walking back and forth over 10 m for 2 min at normal/self-selected speed.

3.4.3. Methodology

Two previously validated algorithms A1 and A2 [6, 222] were used for IC-FC detection. Both use a wavelet approach to process IMU signals but have fundamental differences such as signal (acceleration vs. angular velocity) and locations (waist vs. shank). Each anatomical segment of the human body has a characteristic movement pattern and thus produces distinct acceleration and angular velocity signals. Consequently, the selection of an appropriate mother wavelet is appropriate to best interpret and quantify characteristics from an IMU signal

produced by the movement of a particular body segment. Custom programs (MATLAB® 2019, MathWorks Inc., Natick, US) analysed raw (sample level) IMU data for ICs-FCs detection and temporal analysis.

3.4.3.1. Algorithm 1 (A1): Lower Back

A1 (see Appendix 4) uses the vertical acceleration signal generated with the movement of the hip during walking. First, the tri-axial accelerometer signals were transformed to the horizontal-vertical coordinate system from the sensor reference frame using an approximation algorithm [319] and low-pass filtered (4^{th} order Butterworth, cut-off frequency 20 Hz). Then, wavelet transform: (i) numerically integrated (cumtrapz) and then differentiated vertical acceleration using a first-order Gaussian (gaus1) continuous wavelet transform at scale 10 were used to detect the IC events (the local minima) (ii) further differentiated to find the FC events (local maxima), Figure 5.c.

3.4.3.2. Algorithm 2 (A2): Shanks (Right and Left)

A2 (see Appendix 4) uses the sagittal plane rotation of the shin during walking. First, wavelet decomposition 5^{th} order Coiflets (coif) at 10 scales split the angular velocity signal into low and high-frequency components. Then, drift and high-frequency movement artefacts were removed with an initial approximation. Afterwards, two new approximations (a1 and a2) were obtained to enhance the detection of IC/FC events. For each approximation, the time corresponding to the global maximum (tms, mid-swing) was detected. Finally, IC/FC events (negative peaks) were searched in predetermined intervals [a1: IC (tms + 0.25 s, tms + 2 s), a2: FC (tms – 2 s, tms – 0.05 s)], Figure 5. d.

3.4.3.3. Temporal Parameter and Statistical Calculations

From IC-FC moments, temporal gait characteristics were calculated. Among all temporal characteristics, only step time calculation requires both right and left foot ICs-FCs moments. Therefore, the right, and left foot's step times were calculated using time stamp information. Temporal calculation formulas are presented in Appendix Table 2 for the left side only as the same approach is used for the right side. Temporal characteristics of both sides are then used to calculate mean, variability, and asymmetry results.

Agreements between two algorithms on the temporal parameters were evaluated using Pearson's I, Spearman's (rho) and interclass correlation coefficients (ICC2,1) with upper and lower bounds and calculated using a two-factor mixed model to assess the level of absolute agreement (between A1 and A2) [320]. A coefficient value of ≤0.30 indicates no agreement, 0.31 to 0.50 reflects fair, 0.51 to 0.70 moderate, 0.71 to 0.90 substantial, and ≥0.91 indicates very good agreement [321, 322].

Graphical analysis was performed using Bland and Altman plots [323]. Absolute differences were calculated as AD =abs(A1-A2). All statistical analyses were performed using IBM® SPSS® Statistics 26.

3.5. Results

Generally, algorithms provided similar results for mean temporal characteristics but with small AD. A higher agreement was found on the mean compared to variability and asymmetry characteristics in all cohorts and environments.

3.5.1. A1 vs. A2: Treadmill

The agreement was substantial to very good for mean stride time, step time and stance time, shown in Table 5. The agreement was moderate for mean swing time. Agreement for stride and step times variability was substantial to very good but fair to moderate for stance time variability and poor for swing time variability. Asymmetry parameters did not show any significant correlation except for stride time (r-rho > 0.40, ICC2,1 > 0.50), shown in Table 5. There were small Ads for mean stride time (0.004 s), stance time (0.001 s), swing time (0.003 s) and step time (0.004 s). Comparing overall AD and correlation coefficients between stride-step parameters and stance-swing parameters revealed that the latter parameters experience larger AD and lower correlation coefficients. The AD of standard deviation in mean temporal parameters did not show any significant values.

Table 5.Extracted temporal parameters and agreements for treadmill walking.

		A1-Lower Back		A2-Shank		Pearson's R	Spearman's *Rho*	95% CI Bounds			
	Mean time (s)	*Average*	*SD*	*Average*	*SD*			*ICC2,1*	*lower*	*upper*	*p*
	Stride	1.156	0.065	1.152	0.054	0.965 **	0.988 **	**0.975**	0.929	0.991	0.000
	Stance	0.733	0.042	0.732	0.042	0.832 **	0.753 **	**0.914**	0.750	0.970	0.000
	Swing	0.423	0.023	0.420	0.033	0.537 *	0.547 *	**0.684**	0.073	0.890	0.019
	Step	0.578	0.033	0.578	0.027	0.907 **	0.865 **	**0.945**	0.841	0.981	0.000
	Variability Time (s)										
	Stride	0.068	0.029	0.075	0.028	0.918 **	0.956 **	**0.946**	0.814	0.982	0.000
(YA) Treadmill	Stance	0.045	0.018	0.084	0.021	0.630 **	0.632 **	0.441	−0,228	0.804	0.005
	Swing	0.026	0.010	0.027	0.006	0.116	−0.300	0.132	−1.666	0.704	0.398
	Step	0.036	0.014	0.040	0.017	0.885 **	0.886 **	**0.915**	0.735	0.971	0.000
DS1	**Asymmetry Time (s)**										
***n* = 16**	Stride	0.000	0.000	0.003	0.010	0.436	0.455	**0.564**	−0.150	0.847	0.049
	Stance	0.004	0.004	0.016	0.013	0.019	0.176	0.019	−0.633	0.552	0.476
	Swing	0.004	0.004	0.013	0.008	−0.050	0.037	−0.050	−0.698	0.408	0.563
	Step	0.005	0.005	0.019	0.009	−0.085	0.046	−0.069	−0.509	0.428	0.612

**. Correlation is significant at the 0.01 level (2-tailed). *. Correlation is significant at the 0.05 level (2-tailed).

3.5.2. A1 vs. A2: Indoor

Absolute agreements between temporal characteristics extracted using A1 and A2 during indoor walking varied for YA, OA and PD, shown in Table 6. The agreement was very good for YA, OA and PD mean stride and step times. There were substantial to very good (YA), and moderate to substantial (OA and PD) agreements for mean stance and swing times.

Agreements between A1 and A2 for variability and asymmetry temporal parameters were poor. There were small Ads in mean stride, stance, swing, and step times for YA (0.017 s, 0.029 s, 0.014 s, 0.010 s), OA (0.002 s, 0.009 s, 0.003 s, 0.009 s) and PD (0.015 s, 0.022 s, 0.004 s, 0.010 s), respectively. Absolute agreement for temporal characteristics during indoor walking was highest in YA and lowest in PD. Comparing overall AD and correlation coefficients between stride-step parameters and stance-swing parameters revealed larger differences and lower correlation coefficients in the latter.

Table 6.Extracted temporal parameters and agreements for indoor walking.

		A1-Lower back		A2-Shank		Pearson's R	Spearman's *Rho*	95% CI Bounds			
	Mean Time (s)	*Average*	*SD*	*Average*	*SD*			*ICC2,1*	*lower*	*upper*	*p*
	Stride	1.096	0.138	1.079	0.138	**0.982** **	**0.974** **	**0.987**	0.965	0.994	0.000
	Stance	0.692	0.084	0.663	0.092	**0.931** **	**0.892** **	**0.936**	0.716	0.974	0.000
	Swing	0.402	0.052	0.416	0.058	**0.863** **	**0.797** **	**0.909**	0.842	0.942	0.000
	Step	0.548	0.069	0.537	0.070	**0.989** **	**0.984** **	**0.989**	0.916	0.996	0.000
(YA) Indoor	**Variability Time (s)**										
	Stride	0.040	0.037	0.032	0.018	0.040	0.221 **	0.600	−0.176	0.251	0.294
	Stance	0.026	0.020	0.024	0.015	0.025	0.122 *	0.047	−0.204	0.246	0.343
DS1	Swing	0.019	0.020	0.032	0.011	0.054	0.301 **	0.070	−0.116	0.231	0.217
***n* = 31**	Step	0.024	0.021	0.023	0.016	−0.025	−0.016	−0.049	−0.325	0.169	0.656
	Asymmetry Time (s)										
	Stride	0.005	0.006	0.007	0.010	−0.034	0.000	−0.060	−0.338	0.159	0.690
	Stance	0.009	0.008	0.016	0.019	0.013	0.800	0.017	−0.214	0.207	0.437
	Swing	0.009	0.009	0.017	0.015	0.130 *	0.155 **	0.184	−0.011	0.344	0.025
	Step	0.011	0.010	0.032	0.036	0.081	0.097	0.062	−0.122	0.223	0.241
	Mean Time (s)										
	Stride	1.162	0.077	1.164	0.0866	**0.962** **	**0.974** **	**0.979**	0.947	0.992	**0.000**
	Stance	0.707	0.0404	0.716	0.0630	**0.816** **	**0.811** **	**0.851**	0.631	0.941	**0.000**
	Swing	0.447	0.05	0.444	0.0442	**0.699** **	**0.657** **	**0.824**	0.551	0.930	**0.000**
(OA) Indoor	Step	0.579	0.043	0.570	0.0452	**0.989** **	**0.991** **	**0.985**	0.766	0.996	**0.000**
	Variability Time (s)										
DS2	Stride	0.086	0.034	0.162	0.106	0.130	0.316	0.124	−0.639	0.603	0.356
***n* = 20**	Stance	0.041	0.008	0.151	0.108	−0.153	−0.041	−0.025	−0.494	0.428	0.542
	Swing	0.046	0.012	0.043	0.004	−0.109	−0.039	−0.155	−1.991	0.547	0.621
	Step	0.042	0.010	0.033	0.009	0.061	0.108	0.083	−0.609	0.561	0.396
	Asymmetry Time (s)										
	Stride	0.001	0.002	0.016	0.012	0.147	0.278	0.042	−0.319	0.441	0.418
	Stance	0.000	0.000	0.020	0.016	0.226	0.199	0.013	−0.338	0.406	0.475
	Swing	0.001	0.002	0.012	0.011	−0.028	−0.017	−0.011	−0.549	0.462	0.516
	Step	0.000	0.000	0.016	0.011	0.050	0.068	0.004	−0.177	0.308	0.488
	Mean Time (s)										
	Stride	1.168	0.096	1.183	0.106	**0.973** **	**0.960** **	**0.979**	0.940	0.991	**0.000**
	Stance	0.704	0.051	0.727	0.087	**0.804** **	**0.750** **	**0.806**	0.608	0.903	**0.000**
	Swing	0.458	0.052	0.454	0.052	**0.570** **	**0.545** **	**0.730**	0.469	0.863	**0.000**
(PD) Indoor	Step	0.584	0.049	0.574	0.049	**0.979** **	**0.949** **	**0.980**	0.849	0.993	**0.000**
	Variability Time (s)										
	Stride	0.083	0.044	0.237	0.161	0.033	0.082	0.018	−0.350	0.360	0.461
DS2	Stance	0.058	0.038	0.231	0.163	0.057	0.315	0.025	−0.295	0.343	0.441
***n* = 36**	Swing	0.054	0.023	0.045	0.007	0.316	0.361 *	0.284	−0.299	0.620	0.140

	Step	0.059	0.038	0.038	0.023	0.069	**0.525** **	0.097	0.528	0.499	**0.359**
	Asymmetry Time (s)										
	Stride	0.002	0.006	0.023	0.021	−0.161	0.136	−0.158	−0.699	0.777	0.760
	Stance	0.001	0.005	0.032	0.024	−0.165	−0.075	−0.062	−0.354	0.256	0.664
	Swing	0.002	0.003	0.026	0.018	−0.309	−0.211	−0.076	−0.343	0.236	0.723
	Step	0.002	0.005	0.033	0.026	−0.200	−0.021	−0.073	−0.391	0.262	0.682

**. Correlation is significant at the 0.01 level (2-tailed). *. Correlation is significant at the 0.05 level (2-tailed).

3.5.3. A1 vs. A2: Outdoor

The agreement was very good for mean stride, stance, and step times and substantial for mean swing time. The agreement between A1 and A2 for the variability of stride times was moderate and fair for stance times, Table 7. The remaining variability and asymmetry characteristics did not show any significant correlation. AD found 0.004 s, 0.001 s, 0.003 s, and 0.004 s for mean stride, stance, swing, and step times, respectively. Differences are larger and correlation coefficients are lower in mean stance-swing times compared to mean stride-step times during outdoor walking.

Table 7.Extracted temporal parameters and agreements for outdoor walking.

		A1-Lower Back		**A2-Shank**		**Pearson's R**	**Spearman's *Rho***	**95% CI Bounds**			
	Mean Time (s)	*Average*	*SD*	*Average*	*SD*			$ICC_{2,1}$	*lower*	*upper*	*p*
	Stride	1.084	0.152	1.084	0.153	**0.996** **	**0.997** **	**0.998**	0.997	0.998	**0.000**
	Stance	0.680	0.085	0.668	0.111	**0.924** **	**0.936** **	**0.940**	0.913	0.958	**0.000**
	Swing	0.403	0.068	0.416	0.055	**0.779** **	**0.835** **	**0.856**	0.790	0.900	**0.000**
	Step	0.541	0.076	0.539	0.076	**0.996** **	**0.993** **	**0.998**	0.997	0.999	**0.000**
	Variability Time (s)										
(YA) Outdoor	Stride	0.025	0.018	0.040	0.030	**0.563** **	0.434 **	**0.605**	0.314	0.757	**0.000**
	Stance	0.018	0.011	0.033	0.026	0.445 **	0.346 **	0.413	0.102	0.607	0.000
DS1	Swing	0.016	0.014	0.035	0.011	0.226 **	0.257 **	0.195	−0.123	0.436	0.004
	Step	0.017	0.011	0.025	0.018	0.044	0.025	0.068	−0.234	0.305	0.314
***n* = 25**	**Asymmetry Time (s)**										
	Stride	0.003	0.003	0.006	0.010	0.104	**0.202** *	0.109	−0.2013	0.350	0.234
	Stance	0.014	0.014	0.022	0.028	0.079	0.066	0.113	−0.210	0.353	0.226
	Swing	0.014	0.014	0.023	0.024	0.008	−0.026	0.013	−0.337	0.277	0.466
	Step	0.014	0.014	0.040	0.054	0.030	−0.013	0.025	−0.271	0.264	0.429

**. Correlation is significant at the 0.01 level (2-tailed). *. Correlation is significant at the 0.05 level (2-tailed).

3.6. Discussion

To the author's best knowledge, this is the first study to comprehensively investigate agreement levels between the lower back and shank IMU algorithms. This study aimed to reveal the suitability of lower back and shank inertial algorithms on various experimental walking protocols, with different cohorts and walking environments. The alterations in the performances of lower back and shank inertial algorithms in various cohorts, especially PD, have not been previously investigated. Moreover, the impacts of a treadmill, indoor and outdoor walking on the agreement of both algorithms have not been revealed. Therefore, the implications of this study will contribute to the current knowledge by providing information about the similarity of lower back and shank inertial algorithms under different conditions. The statistical results presented in this study will also shed light on future studies regarding how cautious researchers should be while interpreting results belonging to a particular environment (e.g., indoor-outdoor), cohort (e.g., PD) or temporal parameter (e.g., stance time).

Overall, location and algorithm pairs provided highly correlated mean temporal results for all cohorts during treadmill, indoor and outdoor walking. However, this is not true for variability and asymmetry characteristics. These findings attest to the common knowledge that variability and asymmetry values extracted from inertial algorithms differ across wear locations [324]. This could be associated with the fact that errors or systematic delays in ICs-FCs detection affect variability measures more than mean values [325]. My findings also suggest that the agreement between location/algorithm is sensitive to age, neurological condition, and walking environment. My results are deemed suitable for exploratory investigation as they are derived from previously validated algorithms.

3.6.1. Impact of Pathology and Age

The lowest agreement with the largest AD between algorithms was in PD compared to YA and OA during indoor walking for mean, variability, and asymmetry. A previous study reported global performances of lower back IMU algorithms decreased when applied to a neurological group [7], which supports my similar findings for lower agreement. Among the underlying reasons for this limitation, missing or detecting extra ICs-FCs is the most likely

cause [7]. Given gait abnormalities affect the movement patterns of hip and shank segments to cause disrupted inertial waveforms [2, 7], decreases in performance/agreement levels are likely. Furthermore, existing IC-FC algorithms were developed and validated for healthy populations only [9,23,32]. Disagreement was at its highest level for stance-swing time characteristics that rely on both ICs-FCs moments, aligning with previous findings [7] where A1 [6] returns greater (extra) FCs moments, thereby reducing accuracy and repeatability.
Age also affects algorithm accuracy for ICs-FCs. A study investigated age on mean, asymmetry and variability gait characteristics using chest and lower back algorithms and reported more accurate results for YA compared to OA [324]. Similarly, comparing mean temporal parameters of YA and OA during indoor walking in this study revealed agreement between algorithms is higher on YA than OA.

The above was further investigated with regression analysis, Figure 6. For example, more ordinated regression lines were present in OA than in PD. A higher agreement was observed in Bland-Altman plots where the difference axis experienced significantly lower values for OA than PD. Similarly, more ordinated regression lines were present in YA than in OA. A higher agreement was observed in Bland-Altman plots where the difference axis experienced lower values for YA than OA, Figure 6, Figure 7.

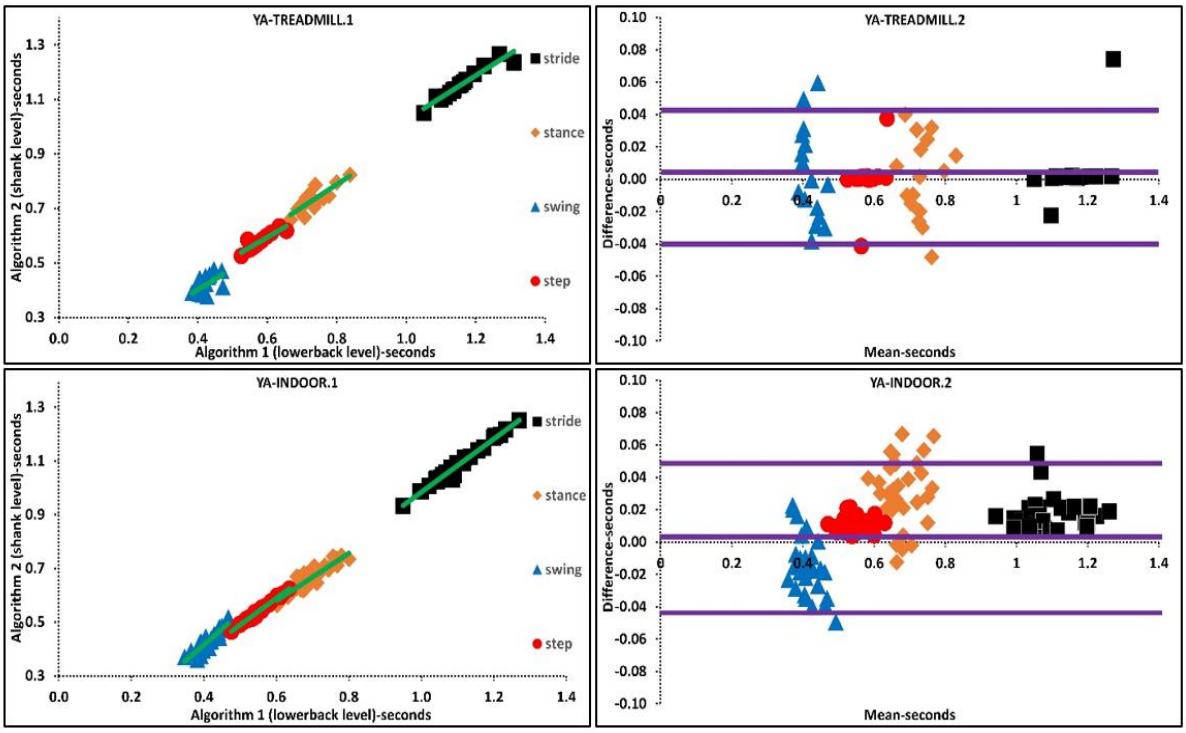

Figure 6.Scatter and Bland-Altman plots of algorithms 1 and 2 for investigating the agreements in older adults (OA) and PD populations by pooling all temporal parameters. OA1 and PD1 are scatter plots with regression lines (green), respectively. OA2 and PD2 are Bland-Altman plotting with mean, lower and upper bands (purple), respectively.

3.6.2. Impact of Environment

Various agreement levels were observed in mean, variability and asymmetry characteristics during treadmill, indoor and outdoor walking. Agreement in stride and step times is slightly higher during outdoor whereas agreement in stance and swing times is slightly higher during indoor walking. Studies have shown differences in characteristics between indoor and outdoor using IMU sensors [22, 326]. There are several factors that could explain the differences between extracted temporal parameters during treadmills, and indoor and outdoor walking. Primarily, treadmills are classed as an external cue; forcing the person to walk to the set speed of the device, rather than having the freedom to select their own walking pattern/style. Therefore, walking on a treadmill requires additional balance skills with respect to overground walking, and harnesses or treadmill bars have an impact on patients' perception and pro-prioception during walking [135]. Daily life and laboratory gait are also different, and this is associated with participants being more conscious of measurements being taken during laboratory walking compared to free-living, which reflects more about real-life e.g., with natural dual-tasking [326]. Another factor that could explain the difference between indoor and outdoor walking is the walking terrain used (e.g., carpet,

cobble) [2]. This was further studied and reported that gait adaptation strategies to maintain stability are sensitive to different walking surfaces, meaning different gait patterns are employed while walking on soft and hard terrains [293]. Given the fact that there are characteristic differences between the treadmill, and indoor and outdoor walking, a previous study hypothesized that the environment plays an important role in generating different walking signals, influencing the accuracy of ICs-FCs detection [150].

Based on the findings, I suggest that the instability of IMU algorithm performances could also be a prominent reason that accounts for differences between indoor and outdoor mean characteristics. Furthermore, the agreement between algorithms for the variability of temporal parameters during treadmill walking is higher than indoor/outdoor walking. A higher agreement between algorithms could be associated with the fact that the treadmill as an external cue reduces variability by means of controlling walking belt speed. These results are valid for different walking speeds since treadmill walking and indoor walking experiments were performed at various walking speeds. Regression and Bland-Altman plots belonging to various walking environments suggest that the difference between mean temporal parameters is lower during treadmill walking than during indoor-outdoor walking, Appendix 4.

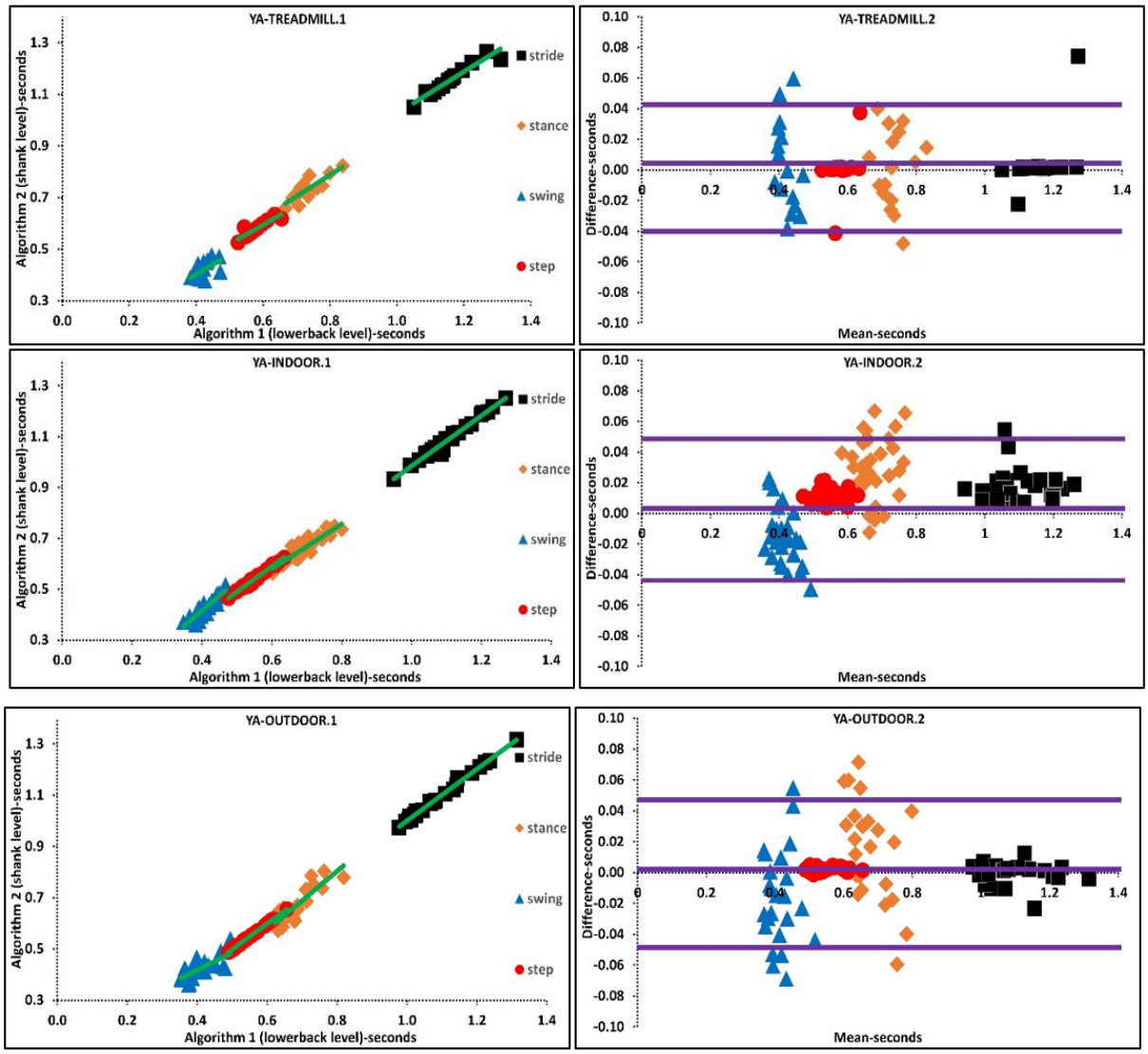

Figure 7.Scatter and Bland-Altman plots of algorithms 1 and 2 for investigating the agreements in various walking environments by pooling all temporal parameters. Treadmill.1, Indoor.1, Outdoor.1 are scatter plots with regression lines (green), respectively. Treadmill.2, Indoor.2, Outdoor.2 are Bland-Altman plotting with mean, lower and upper bands (purple), respectively.

3.6.3. Considerations: Sensor Location and Algorithms

Systematic delays, errors and inconsistencies in IC′s-FC′s detection are present even between two reference systems such as treadmill and motion analysis [305]. Therefore, it is crucial to investigate the level of error (agreement) between two or more IMU algorithms and minimize inconsistencies to achieve a reliable and robust methodology.

Using different IMU systems and processing methods are possible factors accounting for inconsistencies [150]. Previous studies investigated the listed factors and their impacts on the accuracy of the results on healthy subjects [150, 214, 305]. Here, I studied these factors in YA, OA and PD and merged them with previous findings to provide a guide for future studies.

- The first factor needing consideration for IMU gait algorithms is the preferred pre-processing and post-processing methodologies as it has an impact on the extracted mean, variability, and asymmetry of temporal characteristics. For example, using algorithms like A1 [6] requires strict filtering and may affect the variability of extracted characteristics as the signal is much smoother compared to less strict filters (e.g., A2).
- Sensor location and sensor signal are other important factors affecting accuracy. Research suggests the shank angular velocity signals provide more accurate and repeatable results for IC-FC detection compared to algorithms that use waist acceleration [214, 305]. However, this has not been fully investigated in neurological cohorts. Here I also found that correlation/agreement of lower back and shank algorithms change when applied in various walking environments and decrease when applied to those with PD.
- Although findings show that the threshold/rule-based inertial algorithms for ICs-FCs detection provide highly correlated mean results, the fact that performances are sensitive to target cohort and environment limits widespread use.

3.6.4. Limitations and Future Works

Despite the algorithms being previously validated against reference standards (e.g., instrumented walkways), it remains a limitation that I did not collect and compare reference data in this study. However, study results are deemed suitable as validated algorithms and high-grade wearable IMUs were used, showing good agreement with previous studies [125, 154, 169, 310, 311], and the purpose here is to compare between algorithms. However, systematic errors (e.g., delays) exist in the algorithms, 0.006 s and −0.029 s were reported for ICs and FCs, respectively in the lower back algorithm whereas 0.01 s in IC detection was reported for the shank-based algorithm [6, 222]. Systematic delays in ICs-FCs detection may increase in OA and PD populations due to the change in the acceleration and angular velocity of the hip and lower limb [7, 150]. Given the importance of accurate ICs-FCs detection in gait analysis, more reliable and robust algorithms are needed, especially for the gait assessment of neurological conditions. Moreover, wearable sensor-based gait assessment is shifting from supervised environments (e.g., lab) to unsupervised environments (e.g., free-living) because the latter enables habitual data capture [327]. Therefore, there is a need for validated inertial algorithms to be used in unsupervised environments, however, the absence of gold/reference standard systems to validate inertial algorithms in unsupervised environments brings new challenges as the field matures [294]. The severity of gait impairment has an impact on the waveform of acceleration and angular velocity signals [2]. Therefore, more advanced approaches (e.g., machine learning, deep learning) which already have shown promising results [328-330] should be adopted in neurological gait studies as they work independently from signal shape and thresholds. Furthermore, the use of a particular target signal e.g., vertical acceleration of the hip or sagittal plane angular velocity of the shin makes the orientation of the sensor crucial. In case of inaccurate sensor placement, the algorithms provide inaccurate results. Therefore, future studies also should aim to develop algorithms that work independently from sensor orientation.

3.7. Conclusions

Based on a comparative study conducted, this chapter reveals that the agreement levels of parameters extracted from various algorithms or sensor locations can vary across different cohorts and environments. The results also highlight that temporal characteristics such as stance and swing times exhibit lower levels of agreement compared to step and stride times. It was also shown that the agreement level is sensitive to the cohort as higher agreements

were obtained in healthy participants compared to PD. The discrepancy in the agreement between these parameters could be attributed to the fact that stance and swing times are calculated using both initial contact (IC) and final contact (FC) moments, whereas step and stride times are solely derived from IC moments. These findings answer the PoI1 by suggesting that researchers should be cautious when interpreting the stance and swing times derived from these algorithms on Parkinson's cohort and different walking environments.

In summary, Chapter 3 investigated common algorithms and sensor locations for extracting temporal characteristics (unimodal) of gait using single sensor units. However, the literature review conducted in Chapter 2 suggests that combining multiple sensor units can better inform gait studies by providing multimodal gait data (e.g., temporal and kinematics). This can be achieved through the utilisation of sensor data fusion (also known as multi-sensor data fusion) which is a process of integrating multiple data sources to produce more consistent and reliable output. In addition, using data mining and AI techniques can improve wearable sensor-based gait analysis. Chapter 2 provided a concise overview of some of these considerations. However, further investigation of these topics in greater depth is needed. Therefore, the next chapter (4) will investigate data/sensor fusion, AI, and data mining techniques. After, I will use the acquired knowledge to overcome challenges in Chapters 2 and 3.

Chapter 4 Considering Contemporary Approaches for Gait Analysis

This chapter uses text from my previously published online article to fit the context and narrative of this thesis. The article appears as a book chapter (Sensor Integration for Gait Analysis), appearing in the book **Encyclopaedia of Sensors and Biosensors** published by **Elsevier** in 2023. Permission is granted to freely use the whole chapter with declaration of authorisation included in Appendix 10.

(URL: https://doi.org/10.1016/B978-0-12-822548-6.00139-4)

Permission to reuse up to 8x 500-word excerpts of the published work was obtained from Elsevier on 26 May 2023 – License Number: 5556541043665. The declaration of authorisation is included in (Appendix 10).

Permission to reuse 1 figure of the published work was obtained from Elsevier on 26 May 2023 – License Number: 5556541290238. The declaration of authorisation is included in (Appendix 10).

4.1. Introduction

The literature review conducted in Chapter 2 suggests that the implementation of a multimodal/multi-sensor approach has the potential to enhance unimodal gait analysis. Furthermore, the utilisation of wearable sensors outside of laboratory settings holds promise for informing clinical gait analysis. Before attempting to utilise these methods and techniques in wearable sensor-based gait analysis, I need to further enhance my understanding of their application, as well as the associated considerations and limitations, thereby acquiring a higher level of expertise in this area. Therefore, this section will aim to study data fusion techniques with various frameworks to fuse different wearable sensor technologies. Moreover, the use of IoT in multimodal gait analysis and data mining techniques by various AI applications including HAR will be discovered and studied. The knowledge gained could be helpful to set a foundation before utilising these techniques and methods to address my PoI2 and PoI3.

4.2. Data fusion

Data fusion is the process of integrating multiple data sources to achieve new information or improved information that is not possible to obtain from a single data source alone. The combination of multiple data sources primarily aims to produce more reliable and desired physiologic and behavioural measures with less computational costs while reducing uncertainty [331]. The use of multiple sensor systems and data fusion ensures a higher signal-to-noise ratio (SNR), increased dimensionality of the measurement and increased sensing robustness [332]. In the case of gait analysis, data fusion is performed based on clinical needs. For example, researchers/clinicians aiming to investigate the change in muscle activation characteristics, heartbeat or respiratory system during gait are required to use multiple sensor configurations along with an appropriate data fusion algorithm. Investigating muscle activation characteristics in a gait cycle and its subphases (stance and swing) can provide clinically relevant information [132]. In such a scenario, an additional data source such as inertial signals can help identify stance and swing periods in accordance with specific EMG activity, as EMG data alone does not solely have sufficient information for detecting gait phases [290].

The data fusion approach can be very useful when a whole set of biometrics is needed [333]. For example, assessment of human walking along with the cardiovascular system and autonomic control systems can provide insightful information to better understand underlying deficits of neurological conditions. The development of such systems requires the fusion of multiple data sources including accelerometer, respiratory band, electrocardiogram (ECG), force sensor and electrodermal response sensors, Figure 8. Among neurological cohorts and elderlies, falls are common and have a negative impact on the cost of healthcare. Recent developments in data fusion techniques have triggered intensive research efforts toward the early detection of falls [334, 335]. Early fall detection systems were developed by fusing inertial (accelerometer and gyroscope) and ambient (infrared sensors, vibration, and pressure) sensors [336]. These efforts also have enabled monitoring of the changes in various sensor data before the fall event. This information could be useful when investigating the posture and motion of fallers in neurological groups.

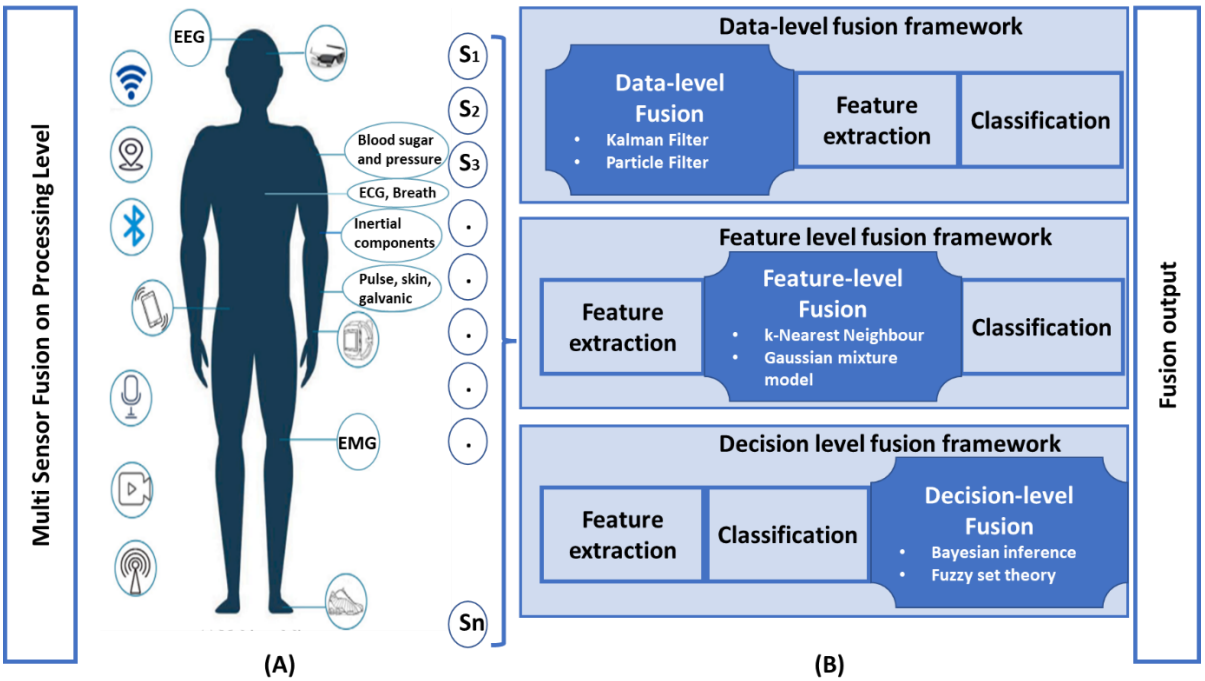

Figure 8. Multi-sensor fusion categories on processing level, figure modified from [331, 337] (A) Commonly used wearable/ambient sensors in gait assessment of neurological populations. (B) Sensor fusion frameworks and some of the common fusion algorithms

A variety of data fusion methods have been developed and adopted in the literature for wearable sensor-based gait assessment/health monitoring [284, 331, 337]. On the processing level, fusion from multiple sensor modalities can be done at data, feature, and decision levels, Figure 8. When the same type of sensor is present to measure the same physical phenomenon, raw signals collected from each sensor are typically fused via data-level fusion to produce the most accurate and reliable outcome. Data-level fusion is common in body sensor network (BSN) based neurological gait analysis studies, e.g., a combination of three axial acceleration and gyroscope or multi-channel EMG measurement of lower limbs [338]. Data-level fusion has been used for various purposes including data adaptation, parameter estimation and calibration [337]. Weighted averages, Kalman filter (KF), and Particle filtering (PF) are common data-level fusion approaches.

Alternatively, having heterogeneous sensors in BSN requires higher fusion levels (feature-level or decision-level) as outputs of two different sensor types cannot be fused directly. Feature level fusion is the process of combining extracted features from multiple data sources and is commonly used in classification (e.g., activity recognition) studies [339]. For example, features extracted from accelerometers are informative but limited due to their sensing capacity. Thus, combining accelerometers with gyroscopes provides additional insight into the rotational activities of the trunk or legs that cannot be (easily or accurately) measured via accelerometers only [17]. Although the aim of feature-level fusion is to provide a high dimensional feature vector, steps such as feature selection that extracts highly correlated features are needed along with domain knowledge[340]. Gaussian mixture model (GMM), k-Nearest Neighbour (k-NN), and Decision Trees (DT) are some of the widely preferred feature-level fusion algorithms. In addition, popular deep learning (DL) techniques such as convolutional neural networks (CNN) have been drawing the attention of researchers as feature extraction is performed without any domain knowledge. Decision-level fusion is the process of generating one final decision (hypothesis) from the produced decisions. Decision-level data fusion is performed after feature extraction and classification of each sensor in the corresponding sensor modalities. Common decision-level fusion algorithms are Bayesian inference and Fuzzy Logic (fuzzy set theory). Factors such as system accuracy, computational time, diversity of data available and power consumption are determinants when deciding on a fusion algorithm.

4.3. Data mining (big data and AI)

Typical approaches to gait analysis involve the use of sensing devices (e.g., IMU, EMG, smartphone), with the participant wearing the sensing modality over extended periods at up to 100Hz [2, 341-343]. Consequently,

the culmination of large-scale datasets has become prevalent, especially coinciding with the ubiquity of the IoT, commonly referred to within the 'Big Data' paradigm [344]. With the prevalence of big data in healthcare analytics, wider adoption of artificial intelligence (AI) is being deployed [345], providing a wider understanding of gait in varying conditions, pathologies and demographics. Generally, AI and big data rely on:

4.3.1. Sensing modality streaming to IoT device/edge device

Sensors used within healthcare monitoring typically rely on technologies such as Bluetooth to have the data streamed to either an edge computing device (Raspberry Pi, Smartphone) or more common networking technologies such as Wi-Fi on IoT enabled devices [346, 347]. Through the application of IoT enabled devices the need for physical wires is alleviated allowing the participants a greater and unobstructed range of movement.

4.3.2. Range of classifiers

Typically, within healthcare the AI methods employed are that of classifiers e.g., classifying a fall risk. A range of AI-based classifiers are available, each offering distinct advantages over others. For time series data such as polling data from an IMU sensor to classify fall risk [348], long short-term memory (LSTM) could be used. LSTMs are a type of recurrent neural network that retains information from previous examples when processing their output. Other types of less computationally complex classifiers exist such as support vector machines (SVM) and perform well on select tasks [349], which do not retain information from previous examples but provide much faster outputs while retaining a high degree of accuracy. There are too many different forms of AI-based classifiers to discuss in this paragraph however the choice of the classifier will always depend on the requirements of the task at hand e.g., does the algorithm need to run in real-time or, is accuracy more important than speed?

4.3.3. Outputs

Applications of big data and AI within healthcare are vast, with an accompanying range of outputs. For lots of AI-based health applications, typically the output is binary (detected, not detected) with a probability range of 0.0 and 1.0 (<0.5 not detected, >0.5 detected) [350]. The higher probabilities of course mean the stronger the risk of e.g., a fall to occur. Binary classification problems are not the only available type, classifiers with multiple possibilities are also prevalent i.e., classification of different respiratory diseases or balance abilities [351].

The use of AI and big data demonstrate utility for smarter gait assessment, especially remote. However, concerns of high dimensionality and heterogeneity of healthcare data (e.g., sensing modalities will have different outputs) [352] require verification and validation before an AI agent can be effectively used. In response, dimensionality reduction techniques can be employed, aiming to reduce the complexities within a dataset. For example, utilisation of an edge computing-based system could provide semi-frequent, local feature extraction [353], before transmission to a large-scale big data instance containing pre-processed, lower dimensionality data. Provision of pre-processed gait data into a concise dataset of features in a big data context could inform clinically relevant outcomes [354], but also provide computationally optimal execution to streamline the analysis, as seen in other big data-centric domains [355].

4.3.4. HAR using wearable technology and AI

Machine learning (ML) algorithms such as Support Vector Machine (SVM) or Decision Tree (DT), rely on manual feature extraction and selection that greatly impact HAR accuracy. Prior works have shown that designing hand-crafted features in a specific application requires human-based domain knowledge [356] and heuristically-defined features may perform well in recognizing one activity, but not others [357]. Furthermore, hand-crafted features may not be sensitive to targeted cohorts and environments [358] i.e., models developed with a set of features in a lab lose accuracy when applied in free living (beyond the lab) due to the diversity of user's habitual behaviour and complexity of activities and environments. Equally, human expertise may not always select the best features, which can decrease accuracy and make it necessary to apply additional feature selection methods to reduce dimensionality [17]. The use of ensemble classifiers has been recommended to increase classification accuracy [359, 360] but studies utilized complex methods that were computationally inefficient. To optimize performance, IMU-based HAR approaches have generally converged on DL [361]. DL algorithms are capable of generating complex and high-level features that well represent raw data and do not require expert knowledge for feature extraction and

selection [17, 362]. DL methods are considered state of art in computational processing [363] and have provided very accurate classification approaches [306, 364].

Common DL approaches include Convolutional Neural Networks (CNN) which can learn multiple layers of feature hierarchies to provide high accuracy for the recognition of repetitive activities with a long duration [361]. Compared to other AI methods, CNNs have a local dependency, an ability to identify correlation between close signals and scale invariance with an ability to work with different frequencies in time series data [364]. CNN models have been used with other AI methods such as Long-short-term memory (LSTM) recurrent neural networks to capture time dependencies on features extracted by convolution operations. This kind of combined architecture outperformed other studies that used the same HAR dataset [365]. Additionally, spectrogram-based feature extraction methods using Short-Time Fourier transform (STFT) from raw IMU data have been proposed through data augmentation with down sampling and shuffling techniques before classification with LSTM [299].

In both ML and DL models, the variety and size of data have the utmost importance to minimize overfitting. Failing to provide a diverse and large data set will cause training and validation errors. Data augmentation is a powerful method to solve training, validation errors, overfitting [366, 367] and data sparsity problems. Previously, a two-stage end-to-end CNN model was proposed along with an augmentation technique to enhance datasets by inserting data points via linear interpolation [368]. The results of the proposed methodology outperformed previous studies in terms of classifying activities in a dataset of healthy participants. Another study used two different time series data augmentation techniques to investigate the impact on accuracy and reported that the use of data augmentation significantly enhances recognition accuracy in three public datasets of healthy participants [369]. Alternatively, the Generative Adversarial Network (GAN) framework [370] was adopted to generate more data samples. Although GAN could improve the performance of classifiers with limited labelled data, weaknesses such as lack of explicit representation of the generator's distribution and the need for model synchronization were reported [371]. Synthetic Minority Over-sampling technique (SMOTE) is another technique that uses oversampling to generate more data samples [372] and achieves better classifier performances in ML classifiers (such as Naive Bayes) but has not been fully investigated in DL classifiers and HAR of neurological populations.

Interpretation of numeric IMU data as images has been implemented in very few HAR studies. In [373], IMU data was stacked row by row into an array (called a signal image) before a 2D Discrete Fourier transform (DFT) was applied to generate activity images which were then input to a CNN. Elsewhere, frequency (activity) images were created from the raw IMU signals by applying STFT [306] and Fast Fourier Transform (FFT) [374] before being used as input to a CNN. However, the referenced studies performed HAR using activity images (spectrum) rather than a direct representation of numerical sensor values. Although these studies produced accurate HAR, the images (spectrum) used do not fully represent raw sensor data. Using raw sensor data to create images where pixel brightness increases/decreases with the numerical value of the IMU is a novel and potentially more accurate alternative as it better represents raw (sample level) IMU data. Previously, images that were created with this approach provided very promising classification results of the survival status of the patient using a clinical record dataset [375].

4.3.4.1. Inertial sensor based HAR in neurologic populations

The use of inertial sensors in HAR eliminates immediate privacy, and security concerns and offers pragmatic data collection possibilities via various technologies such as commercially available devices, smartphones, and smartwatches. Despite providing unique opportunities, inertial sensor-based HAR also poses many challenges such as accurately recognizing the activity type from an unknown environment using an inertial signal [16]. Unlike camera-based HAR systems, inertial sensor-based HAR requires additional mechanisms such as video recording or scripted data collection protocol to label the data before training. Another challenge posed by inertial sensor based HAR is the requirement of wearing multiple sensors. Although multiple inertial sensors-based HAR have provided highly accurate activity classification [306], wearing multiple devices may cause discomfort while increasing computation and project costs. Accordingly, most studies utilize a single waist-mounted sensor [376].

Several publicly available benchmark datasets have been generated using a single sensor configuration to enable researchers to develop highly accurate HAR models [377, 378]. However, those datasets were produced from healthy people only [364]. The lack of HAR benchmarking datasets for neurological populations forces researchers to create local (project-specific) datasets. The creation of a local dataset that has diverse and sufficient data is challenging due to several reasons [371]. For example, researchers interested in HAR within neurological disorders may struggle with patient recruitment (due to a lack of clinical partners) or ensure the longevity of recording to

obtain sufficient data due to a lack of patient adherence. Additionally, data may be skewed as those with functional limitations may generally perform light activities only, such as level ground walking rather than stair ascent/descent or walking over uneven terrain due to fear of falling. These real-life implications result in datasets of SS [358, 379], PD [19] and people with spinal cord injury [380] that may not be rich and diverse enough to achieve very high HAR accuracies on new data.

Accurate HAR in neurological populations requires diverse data from multiple participants with a broad range of ages, fitness levels, disease duration, mood, and health conditions to ensure inter-subject and intrasubject variability have minimal impact on recognition accuracy [381]. For example, people with different stroke types (e.g., ischemic) and post-stroke recovery durations may show different levels of impaired mobility during stair ascending/descending. Increasing the size of the dataset may also contribute to minimizing the impact of subject variability in classification models.

4.4. Internet of Things

As described, instrumented gait assessment beyond the clinic has many challenges to overcome such as multimodal sensing (e.g., IMU + EMG) as well as robust interpretation of data while knowing/understanding the context of how and where people are walking. Yet, there is a desire to achieve robust gait assessment beyond the clinic and to enable a streamlined process of communication technologies that need investigating. The Internet of Things (IoT) is a term used to describe a rapidly growing infrastructure of interconnected, embedded devices that harness the power of the Internet to derive enhanced intelligence through intra-device communication and multimodal data analytics [382]. IoT is predominantly defined as a network of billions of globally interconnected physical devices [383, 384], but the term also encompasses virtual services and platforms [385]. Passive sensors and multimodal data analytics provide established methods for determining patient pathologies in clinical assessment. Due to the accessibility of IoT-based sensor technologies, IoT-enabled data collection methods have the potential to extend research beyond the clinic, to enable free-living assessment of patients in their habitual environments [353]. This has the potential to monitor patients as they perform everyday tasks to determine e.g., where functional limitations may exist.

Within the field of gait assessment, IoT presents many opportunities to address a recognised need for free-living assessment that exposes patients to habitual environments and everyday obstacles, without researcher supervision [316]. Increased accessibility and low costs mean that IoT devices can overcome the inhibiting factors that have made research in this area unfeasible [386]. Moreover, sensor technologies used by clinicians are becoming pervasive in everyday life, as these technologies are targeted to a consumer health market in the form of fashion items such as clothes and jewellery [387]. However, IoT devices are internet-enabled, communication technologies, so healthcare researchers face new challenges, due to the frequency of data that is required to assess underlying pathologies. Medical grade gait analysis sensors typically use tri-axial accelerometers with a capture frequency of 100Hz. Capturing data at this frequency can be challenging in an IoT context due to the bandwidth/costs required to transmit the large amount of data that is created.

One possible solution to overcome the bandwidth challenges is to increase the processing power of the wearable device and perform calculations and assessments on the hardware itself, known as edge computing. This is commonly used when computationally expensive tasks need to be done with minimal latency [388], but it can also be used to reduce the amount of data being transmitted. For example, instead of directly sending raw data from an IoT-enabled tri-axial accelerometer to an IoT service, data could be processed on the device itself, transmitting only key information e.g., when walking bouts stop and start or arising gait characteristics, Figure 9.

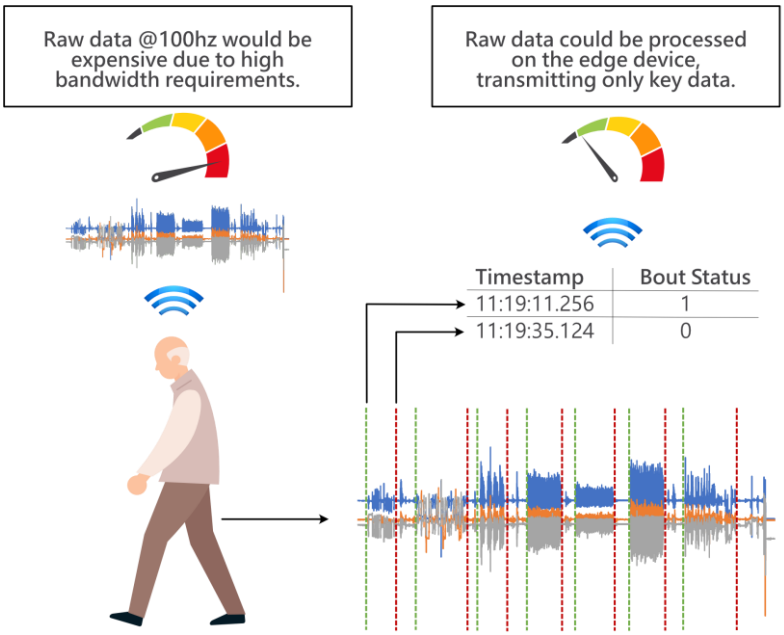

Figure 9. IoT on the Edge: Transmission of processed data to the cloud, to reduce bandwidth and costs.

Another solution to overcome bandwidth challenges would be to reduce the frequency of the data capture, depending on the pathologies under interrogation and outcomes being measured. Since the rate of human motion is considered to be in the range of 3-5hz, for measuring steps/walking bouts, it is possible to reduce the frequency down to around 10Hz [389]. However, Yang et al. [390] found that many gait features can be accurately assessed (with 90% accuracy) when a lower data capture frequency (between 10-50hz) is adopted. However, gait features captured at that range may be less sensitive (than those quantifiable at 100Hz data capture) and lack clinical utility.

While the current technological limitations of IoT feasibly prevent the transmission of raw gait data. There are approaches to overcome many of the challenges. If traditional approaches for data collection are augmented these approaches it could be possible to capture and store raw data locally on the device, while simultaneously transmitting low-frequency data/real-time event data.[391] Thus, if managed correctly, IoT has a lot of potentials to enable real-time assessment of free-living gait.

4.5. Conclusion

This chapter has been instrumental in enhancing my understanding of data fusion, data mining, and the utilization of IoT to address the limitations of clinical gait analysis. The section highlights the potential benefits of multi-sensor fusion at both the processing level and the feature level. By merging signals from various wearable sensors, processing level fusion can offer valuable insights. For example, inertial data collected can be used to segment individual gait cycles and monitor how joint kinematics and muscle activation change during a gait cycle (e.g., during stance and swing periods). Similarly, feature-level fusion can enhance human activity recognition (HAR) models by leveraging features extracted from both IMU and EMG sensors, thereby improving overall performance. Additionally, for time series data, such as polling data from an IMU sensor, classical machine learning methods like SVM and kNN can be employed due to their lower computational complexity compared to deep learning models such as LSTM. Furthermore, the integration of IoT technology can unlock opportunities for remote gait analysis. The next chapter will provide an overview of lessons learned to this point.

.

Chapter 5 Lessons Learned

5.1. Introduction

The purpose of this chapter is to determine how the PoI1 detailed in Chapter 1 have been addressed from preliminary investigations (Chapters 3) and how the remaining PoIs will be addressed in the following chapters. Here I outline the lessons learned as part of my research so far in this thesis and introduce the next stage of my research to provide a unique contribution to knowledge while examining my thesis statement/research hypothesis.

5.2. Lessons learned and the next stages of the thesis

There have been some important and practical findings gathered to this point to inform clinical and free-living gait analysis of people with neurological conditions. To this point, I have uncovered the need to do a wearable-based multimodal gait analysis for free-living assessment. I also performed preliminary work to explore the reliability of existing IC-FC moment detection algorithms considering the wearable location and walking environment. Although certain crucial PoIs remain unanswered, the existing findings have established a robust foundation and deeper understanding. These findings provide a stronger rationale for the second half of the thesis, where the objective is to address the remaining PoIs and further expand the knowledge in this field.

5.2.1. Addressing PoI1 and gaining a deeper knowledge of the foundation of remaining PoI

Chapter 2 introduces various algorithms for wearable IMU and EMG devices, considering the selection of sensor wear location. However, the optimal sensor placement, in terms of both accuracy and convenience, as well as the reliability of these algorithms, requires further investigation and assessment. Chapter 3 conducted a comparative study that investigates the level of agreement between two of the most common sensor locations/algorithms. The findings of the comparative study suggest the level of agreement between algorithms sensitive to the walking environment and target cohorts (lower agreement in the PD population compared to the healthy population). I also observed higher agreement in step and stride times compared to stance and swing times parameters.

In Chapter 3, a thorough examination was conducted on the application of sensor fusion as a potential solution to enhance wearable algorithms in terms of consistency, robustness, accuracy, and reliability. The investigation focused on different sensor fusion techniques, both at the processing and feature levels, with the aim of developing a comprehensive multimodal gait analysis tool capable of functioning not only in clinical settings but also in natural and complex environments. Furthermore, this chapter deepened the understanding of the significance and implementation of remote assessment through the utilisation of IoT technology in free-living environments.

5.2.2. Addressing PoI2 and PoI3

5.2.2.1. Fusing sensor data to achieve multimodal gait analysis (PoI2)

Chapter 4 introduced a range of frameworks essential for establishing a robust multimodal gait analysis tool. Among these frameworks, processing level fusion (multilayer sensor fusion) was highlighted due to its appropriateness to address PoI. The primary objective is to leverage data from multiple sensors and utilise validated unimodal algorithms to create a comprehensive tool capable of extracting simultaneous spatiotemporal, joint kinematic, and muscle activation parameters. This processing level fusion framework serves two key purposes: (1) improving the accuracy of joint kinematic estimation by effectively detecting sensor orientation using both accelerometer and gyroscope sensors, and (2) integrating various aspects of gait. In Chapter 6, a comprehensive overview of the complete data fusion algorithms, as well as algorithms specific to IMU and EMG, is presented to provide support for the development of the proposed multimodal gait analysis tool.

5.2.2.2. Employment of HAR for automatic segmentation of walking bouts in free-living (PoI3)

PoI3 emerged from the literature search conducted in Chapter 2, focusing on the need to adapt human activity recognition (HAR) techniques for the automatic labelling of free-living data to streamline gait analysis. This objective will be achieved by leveraging advanced AI methods to predict and segment walking bouts based on data collected from wearable sensor units. The chosen approach involves feature-level fusion of IMU and EMG data, accompanied by the utilization of Support Vector Machine (SVM) and k-Nearest Neighbours (kNN) algorithms. These machine learning methods were selected due to their demonstrated effectiveness and informative features identified in previous gait studies. By employing this approach, the main aim is to an achieve accurate and robust HAR model that can predict/segment gait bouts in data collected in free living. However, there are certain

challenges and limitations in HAR use in the dataset of neurological populations such as limited dataset. Literature also indicates that HAR models trained using data exclusively from healthy participants experience significant declines in accuracy when tasked with classifying activities performed by individuals with neurological conditions [18, 19]. Therefore, population-specific models (e.g., HAR model trained and tested on PD group only) are needed to classify the daily activities accurately and sensitively among neurological groups. The development of accurate population-specific AI models requires the availability of rich and diverse datasets, enabling high classification accuracies for activities of daily living. However, creating such datasets is inherently challenging for individuals with neurological conditions, as their impaired gait often prevents them from performing certain activities over extended periods. Consequently, the limited dataset size can lead to suboptimal AI model performance. To address this issue, an assertion is put forth, proposing the utilisation of advanced data augmentation techniques to artificially increase the size of training datasets. This augmentation approach is hypothesised to enhance the overall performance of AI models by providing additional variations and examples for training, compensating for the limitations in dataset size inherent to neurological populations.

Chapter 6 Exploring Multimodal Gait Analysis and HAR Methodologies in Neurological Conditions

This chapter uses text from my previously published online articles to fit the context and narrative of this thesis.

The first journal article "Multi-modal gait: A wearable, algorithm and data fusion approach for clinical and free-living assessment", was published in Information Fusion in 2021. (URL: https://doi.org/10.1016/j.inffus.2021.09.016).

The second publication appears as a conference paper "*Exploring human activity recognition using feature level fusion of inertial and electromyography data"*, which was published 44th Annual International Conference of the IEEE Engineering in Medicine & Biology Society (EMBC) in **2022.** *(URL: https://doi.org/10.1109/EMBC48229.2022.9870909)*.

The third journal article "*Improving Inertial Sensor-Based Activity Recognition in Neurological Populations"* was published in the **Sensors** in **2022.** *(URL:* https://doi.org/10.3390/s22249891*)*.

6.1. Introduction

In this chapter, I present three different methodologies and associated study protocols I developed during the implementation of my thesis. These were developed based on the identification of knowledge gaps from an extensive literature review (chapter 2) and acquired knowledge (chapter 4). Accordingly:

- Section 6.2 introduces a comprehensive framework for multimodal gait assessment, utilising data fusion techniques (methodology 1, M1).
- Section 6.3, I present a methodology to explore human activity recognition (HAR) by employing a feature-level fusion of inertial and electromyography data (methodology 2, M2).
- Section 6.4 presents a proposed solution to address the issue of limited datasets inherent to neurological conditions, with the aim of achieving accurate HAR outcomes (methodology 3, M3).

6.2. Methodology 1 (M1): Multimodal gait analysis with data fusion

6.2.1. Fusion fit for the wild

Fusion of multiple measurement resources presents a promising development for human movement studies such as increased activity recognition and more informed gait assessment [392, 393]. Previously, IMU sensor fusion with accelerometers and gyroscopes was adopted to produce more consistent and reliable outputs [280]. Typically, accelerometers produce useful but limited data such as static and dynamic characteristics but when fused with gyroscopes could deliver relative heading/direction. Sensor fusion often equated to bulky devices, but micro-electromechanical systems (MEMS) facilitated new synchronized/unsynchronized data collection possibilities with discrete wearable technologies. This has enabled more pragmatic multi-modal sensor fusion to provide real-world and clinically relevant information to increase the utility and accuracy of rehabilitation systems. For example, fusion approaches have seen acceleration signals fused with electrocardiography (ECG) signals to calculate energy expenditure [394] and EMG signals to monitor functional activities in stroke survivors [395]. However, studies generally rely on gait data gathered indoors within a controlled environment only.

Development of any multi-modal fusion approach needs to examine the methodology in laboratory and free-living based environments. This is important as previous research reported that gait adaptation techniques for maintaining stability are affected by walking terrain [293]. The impact of the environment has been investigated in uni-modal gait studies for neurological conditions, and significant spatiotemporal differences were revealed between indoor and outdoor/free-living environments [169, 316]. However, understanding potential reasons for poor mobility and falls is limited since additional gait characteristics (i.e., kinematic joint angles and muscle activation) were not previously included. Additionally, outdoor studies focused on activity recognition or activity level tracking rather than specific gait characteristics. For example, a study proposed an ECG, skin conductance, respiration and gait acceleration signals-based gait monitor system for habitual environments, but failed to include clinically relevant lower limb gait characteristics such as spatiotemporal, kinematic and muscle activation [333].

Therefore, the proposed novelty of this research is to investigate multi-modal gait characteristics in both clinical/lab and habitual environments by proposing a novel multi-layer fusion approach along with synchronized IMU and EMG. Although existing chosen wearable algorithms are individually validated for a single gait outcome, these algorithms have not been fused for the purposes outlined here. Multi-modal investigation of neurological gait with clinically relevant characteristics in natural habitats remains lacking, perhaps due to the shortage of developments in the field. Here, I utilise a multi-modal wearable to implement a novel fusion approach consisting of validated algorithms and synchronized sensor data for use in the lab/clinic and beyond such as outdoor level walking, incline walking, and stair ascent/descent. Preferred algorithms and locations were chosen based on their performances that were investigated in the literature [7, 150, 213, 214, 305] and as part of investigative developments conducted within this study. I hypothesise that the proposed work can better inform gait assessment through the adoption of a multi-layer fusion approach (wearables/sensors, algorithms and gait characteristics). Therefore, the main contributions of this chapter section are to:

i. develop a framework that fuses validated wearable-based gait algorithms for multi-modal gait assessment use in laboratory and free-living environments,
ii. examine implementation by investigating use on a cohort of healthy adults and,

iii. investigate use within a pilot study of SS to evidence clinical effectiveness for use beyond the clinic/lab, revealing the impact of different terrains and activities on spatiotemporal, kinematic and muscle activation,
iv. provide insight into limitations with existing algorithms.

The fusion methodology provided here will showcase how multi-modal gait assessment can be created which could enable clinicians to prepare more informed rehabilitation programs and measure their effectiveness. Section 6.2.2. summarises the experimental protocol including participant demographics, data collection protocol and performed gait tasks. Section 6.2.3. contains various algorithms adopted here and provides details about pre-processing, used signal, sensor orientation and multi-layer data fusion framework. Chapter 7 presents the results extracted from the framework, including indoor, and outdoor level walking multi-modal gait characteristics and impacts of changing environments for both healthy populations and stroke survivors. Experimental results of walking on the rocky surface, incline walking and stair ambulation are provided in Appendix 5.

6.2.2. Experimental protocol M1

6.2.2.1. Participants

Ten healthy participants (HP's) were recruited for the main study (28.4 ± 7.0yrs, 79.2 ± 14.4kg, 176.8 ± 8.4cm, 8M:2F) and three SS (72.3 ± 3.1yrs, 78.5 ± 12.1kg, 176 ± 8.2cm, 3M, right side mostly affected for all) for the clinical pilot. Assessment and instrumentation were carried out by a physiotherapist and trained researchers, respectively. Ethical consent was granted by the Northumbria University Research Ethics Committee (REF: 21603). All participants gave informed written consent before participating in this study. Testing took place at the Clinical Gait Laboratory, Coach Lane Campus, Northumbria University, Newcastle upon Tyne.

6.2.2.2. Data collection and gait tasks

Each participant wore four Shimmer3 EMG wearables (24.9cm^3, 31g) with straps on the lateral side of the thighs and shanks, approximately 7-8 cm above the ankle and knee joints, respectively, (Figure 10, S). Before data collection, wearables attached to the shank and thigh level were positioned in the same vertical line while the participant stood still to achieve a better knee flexion angle estimation. The wearable enables multi-modal capture of IMU and EMG data simultaneously. Inertial data is sampled at a rate of 100 Hz, while EMG data is sampled at 512 Hz, following device configuration (16-bit resolution, ±8g, ±500°/s) prior to data collection. Skin preparation for EMG electrode attachment was performed with alcohol swabs to achieve better skin-electrode contact. Disposable surface electrodes (circular – Ag/AgCI, silver/silver chloride) were placed bilaterally (inter-electrode spacing ≈30mm) on clean skin according to SENIAM recommendations and locations: rectus femoris (**RF**), biceps femoris (**BF**), tibialis anterior (**TA**) and gastrocnemius (**GS**), with a reference electrode on the ankle and knee. In each wearable (worn on the left and right legs), channel 1 (ch1) was assigned to TA and RF muscle groups for shank and thigh level sensors, respectively. Similarly, channel 2 (ch2) was assigned to GS and BF muscle groups for shank and thigh level sensors, respectively.

Each participant was instructed to walk over the ground for 2-minutes around a 20m circuit at their preferred self-selected walking speed inside the laboratory. Subsequently, participants walked outdoors with the same wearables. Outdoor walking consisted of a pre-defined route, including ground-level walking on different surfaces (e.g., asphalt, uneven rock, pavement) (Figure 10, F1-F2-F3), inclined walking (wheelchair ramp) (Figure 10, F4), ascending/descending stairs (Figure 10, F5-F6), with a physiotherapist and trained researcher. For safety, walking on an uneven rock surface and inclined walking on a wheelchair ramp were excluded from SS. Two-minute data recorded inside and outside (on asphalt and pavement) during level walking are presented here (additional walking surface data available online).

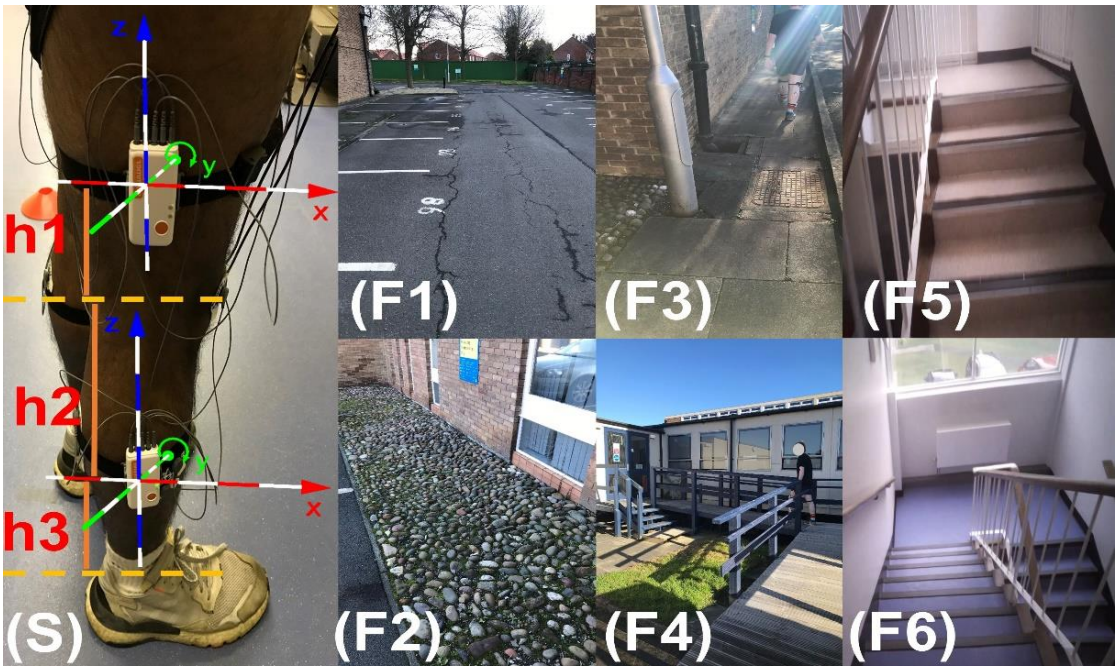

Figure 10. Sensor placement and physical tasks. (S) sensor placement illustration, (F1, F2 and F3) free-living walking on asphalt, uneven rock surface and pavement, (F4, F5 and F6) free-living incline walking, stair ascent and stair descent, respectively.

6.2.3. Approach M1

Here I present the proposed multi-layered fusion approach by combining validated algorithms, multi-modal sensors, and inertial and EMG data culminating in many gait characteristics. IMU and EMG data were transferred to a workstation (Windows 10) from the wearable via proprietary software (Consensys). Custom programs in MATLAB® (2019, Statistics and Machine Learning Toolbox, MathWorks, Inc., Natick, US) analysed raw (sample level) IMU and EMG data for spatiotemporal, kinematic and EMG analysis. Stride time was calculated as the average of left and right strides. All spatiotemporal gait characteristic results are presented similar to clinical domains of gait (pace, rhythm, variability and asymmetry) [91, 396].

Various validated algorithms (***A***) were selected to extract informative multi-model gait characteristics. Of critical importance within the suggested approach are initial contact (IC i.e., heel strike) and final contact (FC i.e., toe-off) times for the right and left foot derived from the shank-mounted wearables. IC and FC events help segment the gait cycle and denote specific regions of interest. Walking periods on different terrains and stair ambulation were manually segmented based on the pre-defined route and time stamps. Participants were asked to stand still for five seconds before and after each activity for more accurate manual segmentation. A general logical flow is presented in Figure 11 and broadly described as follows:

- IC and FC were extracted with two different algorithms. Ground level IC-FC times were detected with (algorithm) 1 (***A1)*** [222], whereas incline walking, stair ascent & descent IC-FC times were detected with ***A2*** [223, 397]. Only step time is calculated using the synchronised left and right shank IMU sensor timestamps. The remaining spatiotemporal parameters are calculated from the right shank sensor for the right side and the left shank sensor for the left side.
- Spatial characteristics (stride velocity and stride length) were estimated using ***A3*** [398] and IC-FC times of ***A1 and A2***, depending on activity (e.g. level walking or incline walking)
- Knee flexion angle and muscle activation for each stride were segmented considering the type of activity. For example, knee flexion angles during ground level and incline walking were estimated using ***A4*** [399] and ***A1***, while knee flexion angles for stair ascent & descent were estimated with ***A5*** [400] and ***A2***.
- Muscle activation (bursts) patterns were extracted using the k-means approach ***A6*** [239] together with ***A1*** (for ground-level walking and incline walking) and ***A2*** (for stair ascent & descent), Figure 11.

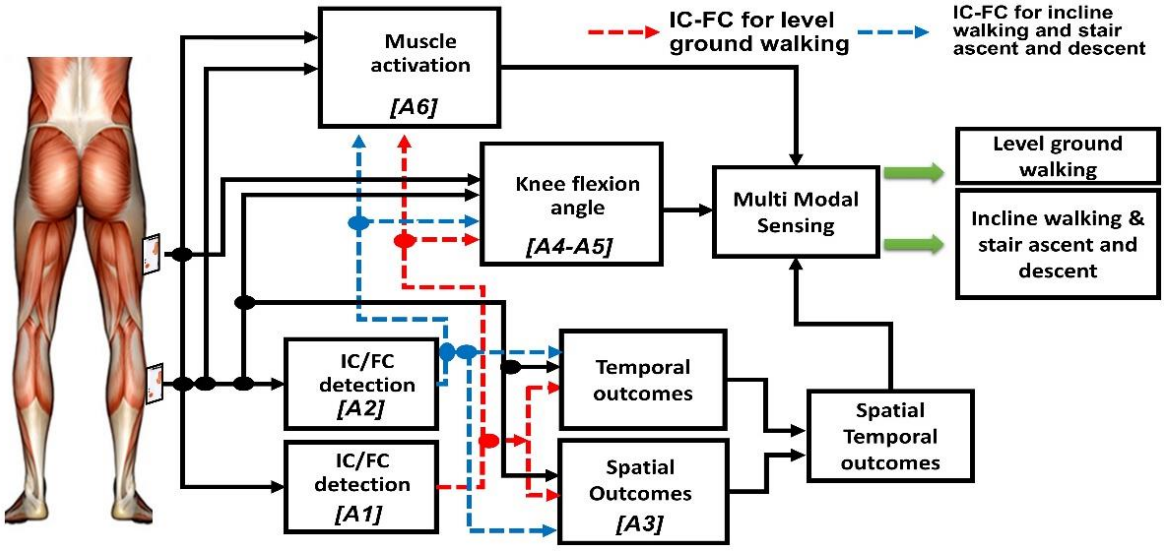

Figure 11.General flow chart (left to right) of the sensor and data fusion framework, A for the algorithm used. This details the fusion approach for the right leg only, the same is repeated for the left-mounted multi-modal wearables.

6.2.3.1. Data pre-processing

Appropriate filtering must be performed to ensure all sensor signals are physiologically related and not corrupted by noise [118]. For example, previous studies reported that during barefoot walking, 99% of the acceleration signal contained a frequency below 16 Hz [112, 114]. Thus higher frequencies are filtered out in the majority of the gait studies[117]. Here, various pre-processing algorithms (Table 8) were applied to raw sensor data depending on the parameter to be extracted as detailed in validation studies:

- IC-FC during level walking: a multi-resolution wavelet decomposition was applied on raw angular velocity signal (perpendicular to the sagittal plane), and drift and high-frequency artefacts were cancelled by obtaining an approximation, ***A1***. A digital filter (second-order Butterworth low pass filter with a cut-off frequency of 35Hz) was applied to the collected angular velocity signal to smooth the signal prior to detection of IC and FC during incline walking and stair ascending & descending, ***A2***.
- Spatial parameters: Accelerometer and gyroscope signals were filtered (first-order Butterworth low pass filter with a cut-off frequency of 5Hz) to cancel high-frequency components before the estimation of step velocity from shank mounted sensor. Additionally, the angular velocity signal was filtered (first-order Butterworth low pass filter with a cut-off frequency of 0.001Hz) to reduce integration drift, ***A3***.
- Knee joint flexion: A third-order Savitzky–Golay filter was applied to smooth the accelerometers and gyroscopes signals before the extraction of knee joint angles, ***A4***. Both physical sensors' signals attached to shanks and thighs were filtered (fourth-order Butterworth low pass filter with a cut-off frequency of 4 Hz) prior to the estimation of sensor orientation, consequently calculation of the joint angle in **A5**.
- EMG: A zero-lag fourth-order bandpass Butterworth filter with cut-off frequencies of 20Hz and 250Hz was applied to EMG data, followed by rectification, and a second zero-lag fourth-order Butterworth low-pass filtering at 6Hz, **A6**.

Table 8.Data pre-processing

Input:	*// upload Shank (S) and thigh (T) sensors, accelerometer (acc) and gyroscope(gyro) signals*
$Sacc_{x,y,z}(i)$; $Sgyro_{x,y,z}(i)$;	
$Tacc_{x,y,z}(i)$; $Tgyro_{x,y,z}(i)$;	*// upload EMG channels ($EMG_{ch1, ch2}$) of upper(thigh) and lower (shank) leg sensors*
$S,T_{EMG\text{-}ch1, ch2}$;	
Fs=512;	*// sampling frequency (Fs)*
Filtering:	
$Sgyro_y$=*wavedec*($Sgyro_y$) & *appcoef;*	*// wavelet decomposition and approximation (coif5)-A1*
$Sgyro_y$=*lpf* ($Sgyro_y$);	*// low pass filtering (lpf)-A2*
$Sacc_{x,z}$,$Sgyro_y$= *lpf,hpf* ($Sacc_{x,z}$,$Sgyro_y$);	*// low pass filtering (lpf)- high pass filtering (hpf)- A3*
$S,Tacc_{x,z}$,$S,Tgyro_y$= *sgf* ($S,Tacc_{x,z}$,$S,Tgyro_y$);	*// Savitzky–Golay filtering (sgf)-A4*
$S,Tgyro_y$=*lpf* ($S,Tgyro_y$);	*// low pass filtering (lpf)-A5*
$S,T\text{-}EMG_{ch1, ch2}$=*bpf,lpf*($S,T\text{-}EMG_{ch1,ch2}$);	*// band pass filtering (bpf)-A6*

6.2.3.2. Multi-modal wearable and data fusion methodology

Here, validated algorithms are fused i.e., implemented in a co-dependent arrangement to inform the identification and segmentation of the gait cycle during 2-minute indoor and outdoor walking. The fusion approach also utilises inertial data from different sensor locations (shank and thigh) to quantify kinematic data. Lastly, a range of inertial and EMG gait derived gait characteristics are presented in two different cohorts.

6.2.3.2.1. A1: IC and FC events during level walking

A previously validated algorithm was used to identify IC-FC times using shank-mounted sagittal plane IMU angular velocity [222]. In brief, wavelet decomposition (5th order coiflet, ten scales) was used to split the signal into low (approximation) and high frequency (details) components. Subsequently, drift and high-frequency movement artefacts were removed with an initial approximation. Then, two new approximations were obtained to enhance the detection of IC-FC events, respectively. For each approximation, the time corresponding to the global maximum (t_{ms} = time of mid-swing) of the signals were detected. Finally, IC-FC events (negative peaks) were searched (local minima) in predetermined intervals [IC (t_{ms}+0.25s, t_{ms}+2s), FC (t_{ms}-2s, t_{ms}-0.05s)].

A1: IC-FC detection and temporal gait characteristic estimation during level walking	
Input:	
$Sgyro_{y\text{-}r,l}(i)$;	// upload right and left shank angular velocities
$Fs=512$;	// sampling frequency (Fs)
Procedure:	
1. $a_{2,3}$=get two new approx.	
2. for i=1: N	// (1: N=sample number at the end of walking period), mid-swing (ms)
3. $msIC_{r,l}$=find global max points (a_2);	// reference points for detecting ICs
4. $msFC_{r,l}$=find global max points (a_3);	// reference points for detecting FCs
5. end for	
6. for i=1: numel(a2)	
7. $ICs\text{-}_{r,l}$=find local minima [msIC+0.25s, msIC+2s]	// saving initial contact times
8. end for	
9. for i=1: numel(a3)	// saving final contact times
10. $FCs\text{-}_{r,l}$ =find local minima [msFC-2s, msFC-0.05s]	
11. end for	// temporal parameter estimations
12. for i=1: numel(ICs+1)	
13. $stance(i)\text{-}_{r,l}$=FCs(i+1)-ICs(i);	
14. $swing(i)\text{-}_{r,l}$=ICs(i+1)-FCs(i+1);	
15. $stride(i)\text{-}_{r,l}$=ICs(i+1)-ICs(i);	
16. rstep(i)= rIC(i)-lIC(i)	// right/left step time are estimated using timestamp information of
17. lstep(i)= lIC(i+1)-rIC(i)	right/left IC-FC times
18. end for	
19. StepTimeVar=sqrt((var(rstep)+ var(lstep))/2);	
20. StepTimeAsym = abs(mean(lstep)–mean(rstep));	// variance calculation
Output: rIC, rFC, lIC, lFC;	// asymmetry calculation
stance times-$_{r,l}$;swing times-$_{r,l}$;stride times-$_{r,l}$;step times-$_{r,l}$;	

6.2.3.2.2. A2: IC and FC events during inclined walking and stair ascent or descent

Formento *et al*. validated an algorithm for IC-FC detection during inclined walking [223] and stair ascent or descent [397]. Similar to ***A1***, IC-FC events were estimated based on the detection of two negative peaks considering the swing period as a reference point in the shank angular velocity signal. In the ***A1***, IC-FC events were searched in predetermined intervals, whereas, in ***A2***, these events were detected based on a set of predetermined rules. Briefly, the algorithm begins with searching the swing phase of a gait cycle. When the gyroscope signal exceeds a predetermined threshold for at least 40 milliseconds, the algorithm considers the swing phase is detected. Then, the first negative minimum after swing phase is defined as IC. Around the time of IC, the gyroscope signal may present further negative peaks related to events during the loading response. In order to avoid false FC detection during that time, a "waiting time" was set during which there was no search for FC events. The waiting time was set to be 50% of the duration of the positive wave for the first step analysed and 50% of the last stance phase for the remaining steps. Once waiting time is over, FC is defined as the sample that represents a minimum negative peak in a window of 200ms, that is preceded by a decreasing (more negative angular velocity) trend in the signal and followed by an increasing (more positive voltage) trend.

A2: IC-FC detection and temporal gait characteristic estimation during incline walking and stair ascent or descent	
Input:	
$Sgyro_{y\text{-}r,l}(i)$;	*// upload right and left shank angular velocities*
Fs=512;	*// sampling frequency (Fs)*
Procedure:	
1. *for i=1: N*	
2. *ms=find global max points ($Sgyro_{y\text{-}r,l}$);*	*// (1: N= sample number at the end of walking period), mid-swing (ms)*
3. *end for*	*// reference points for detecting ICs and FCs*
4. *for i=1: numel(ms)*	
5. *$ICs_{r,l}$ =find local minima after [ms]*	
6. *set waiting time*	*// saving initial contact times*
7. *$FCs_{r,l}$ = find following local minima after waiting time*	
8. *end for*	*// saving final contact times*
9. *for i=1: numel(ICs+1)*	
10. *stance(i) $_{r,l}$ =FCs(i+1)-ICs(i);*	*// temporal parameter estimations*
11. *swing(i) $_{r,l}$ =ICs(i+1)-FCs(i+1);*	
12. *stride(i)-$_{r,l}$=ICs(i+1)-ICs(i);*	
13. *rstep(i)= rIC(i)-lIC(i)*	*// right/left step time are estimated using timestamp information of right/left IC-FC times*
14. *lstep(i)= lIC(i+1)-rIC(i)*	
15. *end for*	
Output: rIC, rFC, lIC, lFC;	
stance times-$_{r,l}$;swing times-$_{r,l}$;stride times-$_{r,l}$;step times-$_{r,l}$;	

6.2.3.3. A3: Spatial parameter extraction during ground level walking

A validated algorithm (***A3***) [398] was used to estimate spatial parameters (stride velocity) from shank mounted IMU. The algorithm is an improved and simplified version of [401], where both horizontal and vertical accelerations were considered. As only horizontal velocity and displacement are needed, acceleration and angular velocities in the sagittal plane (the plane of progression) were considered, vertical components were excluded.

First, gait cycles were segmented from mid-stance to mid-stance (unlike A1 and A2) based on the assumption that the velocity of the shank is zero in the moment of mid-stance, the moment when the shank is parallel to the direction of gravity. Then, the angular velocity signal was integrated to calculate Θ for each gait cycle, Eq. 2. Afterwards, horizontal acceleration components of the sensor's coordinate system were calculated for the global coordinate system using calculated Θ (Eq.3). Finally, horizontal velocity was computed with the integration of horizontal acceleration and corrected with the horizontal velocity component Eq. 4. Horizontal correction velocity (Vhor-correction) component was calculated considering the initial horizontal speed at the start of the stride and the distance (Figure 10, h3) between the ankle joint and shank wearables. Finally, the stride length is calculated by multiplication of corrected horizontal stride velocity and stride time (estimated spatial parameter) for each gait cycle, Eq. 5. Results of the developed algorithm suggest that the distance between the shank mounted wearable and the ankle (h3) has a negligible impact (± 2cm) on the accuracy of the measure [398]. Study findings also reported that the effects of numerical drifts are insignificant as integrations are performed for a short period of time - only gait cycle (max 1.4s).

$$\theta(t) = \int_{0}^{t_{end}} \omega_s(t)dt \tag{2}$$

$$a_{hor}(t) = \cos\theta(t)ax(t) - \sin\theta(t)az(t) \tag{3}$$

$$v_{hor}(t) = \int_{0}^{t_{end}} a_{hor}(t)dt + v_{hor-correction} \tag{4}$$

$$Stride\_length = v_{hor}\ x\ stride\_time \tag{5}$$

where, θ and ω_s are orientation angle and shank angular velocity, respectively. The a_{hor}, v_{hor} and t are horizontal acceleration, velocity, and the duration represents stance to stance period, respectively.

A3: Stride length and velocity estimation	
Input:	
$Sacc_{x,\ z\text{-}r,l}(i)$; $Sgyro_{y\text{-}r,l}(i)$;	*// upload right and left shank accelerations and angular velocities*
$Fs=512$;	*// sampling frequency (Fs)*
Procedure:	
1. *for i=1: numel(rIC-lIC)*	
2. *find mid-stance= max* ($Sgyro_{y\text{-}r,l}$ *(ICs* $_{r,l}(i)$*: FCs* $_{r,l}(i+1)$*))*	*// segmenting relevant signals from mid stance to mid stance for a stride using timestamp information of ICs and FCs*
3. $segmented\_\ Sacc_{x,\ z\text{-}r,l}(i)= Sacc_{x,z\text{-}r,l}$ *(mid-stance(i): mid-stance (i+1));*	
4. $segmened\_\ Sgyro_{y\text{-}r,l}(i)= Sgyro_{y\text{-}r,l}$ *(mid-stance(i): mid-stance (i+1));*	
5. *end for*	
6. $segmened\_\ Sgyro_{y\text{-}r,l}=deg2rad(segmened\_\ Sgyro_{y\text{-}r,l})$	*// convert angle from degrees to radians*
7. *theta (i)= integration of segmented_Sgyro* $_{y\text{-}r,l}(i)$;	*// calculation of the orientation of the sensor across a stride*
8. *costheta=cos(theta); sintheta=sin(theta);*	
9. *for i=1: numel(theta)*	
10. $ahor_{r,l}(i)=$ *costheta(i)* Sacc*$_x$*(i)- sintheta(i)* Sacc*$_z$*(i);*	*// estimation of horizontal acceleration in world coordinate system*
11. *end for*	
12. *vhor* $_{r,l}$*= integration of* $ahor_{r,l}+vhor_{correction}$	*//calculation of the velocity and displacement across a stride*
13. *Stride_length=mean(vhor)*stride_time*	
14. *Output:* $vhor_{r.l}$*; Stride_length* $_{r,l}$*;*	

6.2.3.4. Kinematic angles

6.2.3.4.1. A4: Knee angle estimation during level walking

Kinematic joint angles are typically calculated from the orientations of IMU wearables that are estimated either using gravitational acceleration or integrated angular velocity [400]. In the latter, an error (drift) may occur due to integration. One method to avoid integration drift is to use neural networks, which require training from sufficient data involving a large number of participants [275]. Kalman filtering is another approach, but three-dimensional orientation errors are reported [402]. However, in the former approach, it is possible to estimate the orientation of sensors by the gravitational acceleration in static states, but in dynamic states like gait, translational acceleration will be included.

Takeda et al. [399] developed an algorithm (a simplified version of [403]) considering measurements at the centre of a proposed link model. The developed algorithm estimates knee flexion angles for a dynamic state (level walking) after the elimination of translational acceleration. Here, [399] was replicated to estimate knee flexion angles. First, each stride was segmented from continuous walking using IC-FC estimations (A1). Then, segmented acceleration and angular velocity signals from each left and right thigh and shank were used to estimate knee flexion. For the purposes of this chapter section, angular velocity and the sensor distance from the knee were used to calculate the translational acceleration during gait, Eq6. The estimated translational acceleration was then subtracted from the measured acceleration data to obtain the gravitational acceleration. The gravitational acceleration provided the orientation angle of the segments and, consequently, the three-dimensional posture of lower limb segments, Eq. 7. Once the orientation of each segment was calculated, knee flexion was estimated by the difference between the angle of inclination of the shank and thigh, Eq. 8.

$$\ddot{r}_{KS} = \dot{\omega}_S \times r_{KS} + \omega_S \times (\omega_S \times r_{KS}) \quad , \quad \ddot{r}_{KT} = \dot{\omega}_T \times r_{KT} + \omega_T \times (\omega_T \times r_{KT}) \tag{6}$$

where $\ddot{r}_{KS}$ and $\ddot{r}_{KT}$ are calculated translational accelerations for the shank and thigh sensors, respectively. ω_S and ω_T are angular velocity signals of shank and thigh sensors, r_{KS} and r_{KT} are the distance of the attached sensors from the knee (Figure 10, h1-h2).

$$\theta_1 = \arctan(\left|O_T - \ddot{r}_{KT}\right|_x / \left|O_T - \ddot{r}_{KT}\right|_z) \qquad \theta_2 = \arctan(\left|O_S - \ddot{r}_{KS}\right|_x / \left|O_S - \ddot{r}_{KS}\right|_z) \tag{7}$$

$$\theta_{Flexion} = \theta_2 - \theta_1 \tag{8}$$

where O_S and O_T are raw acceleration outputs of sensors.

A4: Knee joint flexion-extension angle estimation	
Input:	
$Sacc_{x,\ z\text{-}r,l}(i)$; $Sgyro_{y\text{-}r,l}(i)$; $Tgyro_{y\text{-}r,l}(i)$; $Tacc_{x,\ z\text{-}r,l}(i)$;	*// upload right and left shank accelerations and angular velocities*
$Fs=512$;	*// sampling frequency (Fs)*
Procedure:	
1. *for i=1: numel(rIC-lIC)*	
2. *segmented_* $Sacc_{x,\ z\text{-}r,l}(i)$= $Sacc_{x,\ z\text{-}r,l}$ (ICs $_{r,l}(i)$: ICs $_{r,l}(i+1)$);	
3. *segmened_* $Sgyro_{y\text{-}r,l}(i)$= $Sgyro_{y\text{-}r,l}$ (ICs $_{r,l}(i)$: ICs $_{r,l}(i+1)$);	*// segmenting relevant signals for a stride using timestamp information of right and left ICs and FCs*
4. *segmented_* $Tacc_{x,\ z\text{-}r,l}(i)$= $Tacc_{x,\ z\text{-}r,l}$ (ICs $_{r,l}(i)$: ICs $_{r,l}(i+1)$);	
5. *segmened_* $Tgyro_{y\text{-}r,l}(i)$= $Tgyro_{y\text{-}r,l}$ (ICs $_{r,l}(i)$: ICs $_{r,l}(i+1)$);	
6. *end for*	
7. *segmened_* $S,Tgyro_{y\text{-}r,l}$=deg2rad(segmened_ $S,Tgyro_{y\text{-}r,l}$)	*// convert angle from degrees to radians*
8. $\ddot{r}_{KS}(i)$= diff (segmened_ $Sgyro_{y\text{-}r,l}$).r_{KS} + segmened_ $Sgyro_{y\text{-}r,l}$. (segmened_ $Sgyro_{y\text{-}r,l}$. r_{KS});	*// calculation of translational accelerations*
9. $\ddot{r}_{KT}(i)$= diff (segmened_ $Tgyro_{y\text{-}r,l}$).r_{TS} + segmened_ $Tgyro_{y\text{-}r,l}$. (segmened_ $Tgyro_{y\text{-}r,l}$. r_{KT});	
10. $theta_1$= atan((abs($Tacc_{\text{-}r,l}$ - $\ddot{r}_{KT}$))$_x$ / (abs($Tacc_{\text{-}r,l}$ - $\ddot{r}_{KT}$))$_z$);	*// estimation of orientation angle of shank and thigh sensors*
11. $theta_2$= atan((abs($Sacc_{\text{-}r,l}$ - $\ddot{r}_{KS}$))$_x$ / (abs($Sacc_{\text{-}r,l}$ - $\ddot{r}_{KS}$))$_z$);	
12. $theta_{F\text{-}E}$=$theta_2$-$theta_1$	
13. $theta_{F\text{-}E}$ = rad2deg($theta_{F\text{-}E}$)	*// calculation flexion extension angle*
Output: $theta_{F\text{-}E}$	*// convert angle from radians to degree*

6.2.3.4.2. Knee angle estimation during inclined walking, stair ascent and descent

Nestares and Callupe developed an algorithm based on orientations of shank and thigh level sensors to evaluate knee joint angle during level walking and stair ascent on HP and SS [404]. The study reported that shank and thigh level sensors' orientation could compute knee flexion angles with high accuracy during level walking and stair ambulation. The developed algorithm used a complementary filter to estimate sensor orientations. However, it was reported that the fusion coefficient of a complementary filter is too sensitive to be pragmatically used and thus requires additional operations [405]. An alternative and more practical way of estimating sensor orientation is integrating angular velocity as suggested by Tong *et al.* [400] (during level walking).

Here, a novel application of both algorithms was utilised for the purpose of this chapter section to achieve a practical knee flexion angle estimation algorithm during incline walking and stair ambulation. First, each stride was segmented from continuous walking using ICs and FCs (***A2)***. Then shank and thigh sensor angular velocities were integrated to estimate sensor orientation (inclination) across a stride, Eq. 9. Finally, the knee angle was calculated by subtracting the inclination (orientation angle) of the thigh from the inclination of the shank, Eq. 10 (similar to ***A4*** Eq.8).

$$\theta(t)_S = \int_0^{t_{end}} \omega_S(t)dt\ ,\ \theta(t)_T = \int_0^{t_{end}} \omega_T(t)dt \tag{9}$$

$$\theta_{F-E} = \theta_S - \theta_T \tag{10}$$

where ω_S , ω_T and t are angular velocities measured from shank and thigh sensors and gait cycle period (stride time), respectively.

A5: Knee joint flexion-extension angle estimation	
Input:	
$Sgyro_{y\text{-}r,l}(i)$; $Tgyro_{y\text{-}r,l}(i)$;	// upload right and left shank angular velocities
$Fs=512$;	// sampling frequency (Fs)
Procedure:	
1. for i=1: numel(rIC-lIC)	
2. segmened_ $Sgyro_{y\text{-}r,l}(i)$= $Sgyro_{y\text{-}r,l}$ ($ICs_{r,l}(i)$: $ICs_{r,l}(i+1)$);	// segmenting relevant signals for a stride using timestamp information of ICs and FCs
3. segmened_ $Tgyro_{y\text{-}r,l}(i)$= $Tgyro_{y\text{-}r,l}$ ($ICs_{r,l}(i)$: $ICs_{r,l}(i+1)$);	
4. end for	// convert angle from degrees to radians
5. segmened_ $S,Tgyro_{y\text{-}r,l}$ =deg2rad(segmened_ $S,Tgyro_{y\text{-}r,l}$)	// estimation of orientation angle of shank and thigh sensors
6. $theta_1(i)$= integration of segmented_$Tgyro_{y\text{-}r,l}(i)$;	
7. $theta_2(i)$= integration of segmented_$Sgyro_{y\text{-}r,l}(i)$;	// calculation flexion extension angle
8. $theta_{F\text{-}E}=theta_2-theta_1$	// convert angle from radians to degree
9. $theta_{F\text{-}E}$ = rad2deg($theta_{F\text{-}E}$)	
Output: $theta_{F\text{-}E}$	

6.2.3.5. A6: EMG muscle activity (burst) detection

Detection of muscle activity/inactivity and overall level of activity in a muscle at any time is relatively identifiable from the linear envelope of raw EMG signals. There are various methods to extract the linear envelope of EMG signal such as root mean square (RMS), mean of moving window, and use of a set of filters along with rectification [75, 79]. Once the linear envelope is extracted, muscle activity/inactivity can be detected via a predetermined threshold, manual observation, or clustering algorithms[142]. The latter finds resemblances between data points and groups these according to their similarities.

Here, the filters described in Section 6.2.3.1 (A6) and full-wave rectification were used to extract the linear envelope of the EMG signal, while k-means clustering was used to search muscle bursts (activity). The rationale for k-means is that it does not require an a priori setting of thresholds for each individual and has shown the ability to differentiate bursts, even when bursts are short or have spike-like characters [243]. Similar to [239], each data point in the EMG linear envelopes is clustered into subsets of data using k-means. Then, EMG signals are dichotomised into periods of activity and inactivity according to the amplitude of each data point. Here, the numbers of centroids (clusters), which influence sensitivity, were set to five after visual inspection for all EMG signals analysed. Muscle inactivity is identified for the lowest two clusters, whereas the remaining three clusters are accepted as muscle activity. All EMG values for each participant underwent time normalisation within the gait cycle and amplitude normalisation to the highest EMG value in the gait cycles.

A6 Muscle burst detection via k-means clustering	
Input:	//upload EMG channels ($EMG_{ch1,\ ch2}$) of upper(thigh) and lower leg (shank) sensors
$S,T\text{-}_{EMG\text{-}ch1,\ ch2}$;	
$Fs=512$;	// sampling frequency (Fs)
Procedure:	
1. for i=1: numel(rIC-lIC)	// segmenting relevant signals for a stride using timestamp information of ICs and FCs
2. segmened_ $S_{EMG\text{-}ch1,\ ch2\text{-}r,l}(i)$= $S_{EMG\text{-}ch1,\ ch2\text{-}r,l}$ ($ICs_{r,l}(i)$: $ICs_{r,l}(i+1)$);	
3. segmened_ $T_{EMG\text{-}ch1,\ ch2\text{-}r,l}(i)$= $T_{EMG\text{-}ch1,\ ch2;\text{-}r,l}$ ($ICs_{r,l}(i)$: $ICs_{r,l}(i+1)$);	// k-means clustering (# of cluster is five)
4. end for	// sort calculated mean value (descend)
5. [idx_segmened_$S_{EMG\text{-}ch1,ch2\text{-}r,l}$,mean_val]	
6. =kmeans (segmened_$S,T_{EMG\text{-}ch1,\ ch2\text{-}r,l}$,5);	
7. mean_val= sort(mean_val,'descend');	// find muscle activation if EMG envelope value is greater than lowest two mean values
8. for i=1: numel (segmened_ $S,T_{EMG\text{-}ch1,\ ch2\text{-}r,l}$)	
9. if segmened_$S,T_{EMG\text{-}ch1,\ ch2\text{-}r,l}(i)$<mean_val1(4)	
10. kmeans_$S,T_{EMG\text{-}ch1,\ ch2\text{-}r,l}(i)$=muscle_off;	
11. else	
12. kmeans_$S,T_{EMG\text{-}ch1,\ ch2\text{-}r,l}(i)$=muscle_on;	
13. end if	
14. end for	
Output: kmeans_$S,T_{EMG\text{-}ch1,\ ch2\text{-}r,l}$	

****

6.3. Methodology 2 (M2): Human activity recognition using feature level fusion of IMU and EMG data

6.3.1. Background M2

Here, I utilised handcrafted feature extraction (from domain knowledge) and supervised ML classification models. I hypothesise that knee flexion-extension waveform and sEMG linear envelope along with specific features such as integrated EMG belonging to four different lower limb muscles have discriminative and consistent characteristics to improve HAR when fused with inertial data. Accordingly, this chapter section aims to explore: (i) how feature-level fusion of sEMG and inertial data improve classification accuracies, (ii) the impact of post-processing on classification performance, and (iii) which lower limb muscles have the most discriminative and consistent information for HAR.

6.3.2. Approach M2

6.3.2.1. Data collection, protocol, and labelling

Ten healthy subjects (HS) (28.4±7.0yrs, 8M:2F) were recruited. Ethical consent was granted by the Northumbria University Research Ethics Committee (REF: 21603). Each participant wore two Shimmer3 EMG devices (24.9cm^3, 31g) with straps on the lateral side of the right thigh (TR) and shank (SR), Figure 12 (a).

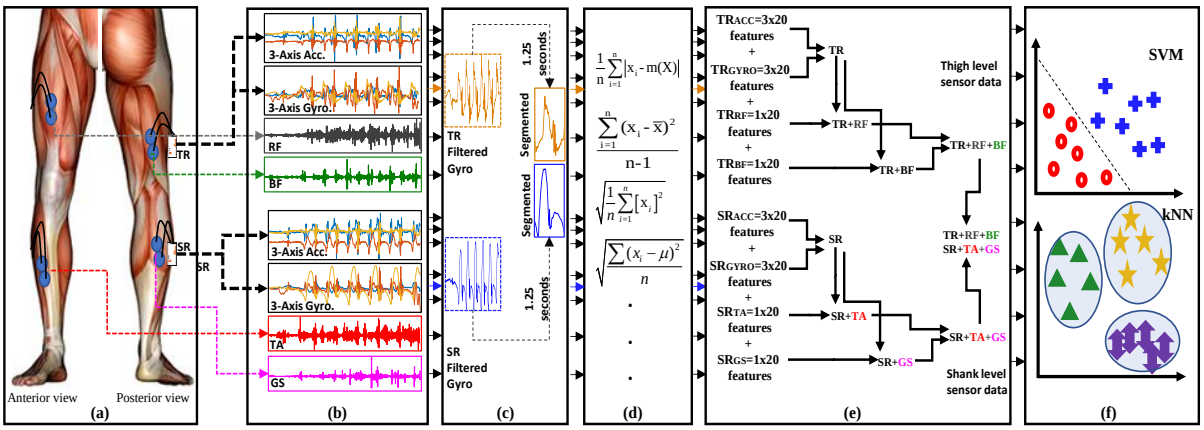

Figure 12.Classification procedure of activities using IMU and sEMG data (a) sensor placement, (b) acquisition of raw IMU and sEMG data, (c) signal post-processing and segmentation, (d) feature extraction, (e) feature level fusion, (f) state-of-the-art classification models.

The Shimmer3 consists of IMU (tri-axis accelerometer + tri-axis gyroscope) and 2-channel EMG, Figure 12 (b). Synchronised data were recorded at a sampling frequency of 512 Hz, and IMU was configured (16-bit resolution, ±8g, ±500 °/s) prior to data collection. Disposable sEMG electrodes (circular, Ag/AgCI: silver/silver chloride) were placed bilaterally (inter-electrode spacing ≈30mm) on clean skin (prepared with alcohol swabs) according to SENIAM recommendations and locations [406]: tibialis anterior (TA) and gastrocnemius (GS), rectus femoris (RF) and biceps femoris (BF), Figure 12 (a) with a reference electrode around the ankle.

Each participant was instructed to first stand (2min- eyes open), then walk for 2 min (110-130 strides) around a 20m circuit at their comfortable walking speed inside a lab. Participants then walked outdoors with the same wearables, navigating a pre-defined route including ground-level walking, stair ascent and descent (24 steps). As a result, there were imbalances in the dataset since time spent e.g., during ascending/descending stairs was shorter than walking and standing. Performing classification in an imbalanced dataset is biased in favour of the majority class. Here, accuracies of walking and standing activities are dominant. Although the synthetic minority oversampling technique (SMOTE) can generate synthetic samples for minority classes, SMOTE has a very limited impact on SVM classifiers [407]. Therefore, some walking and standing data were excluded to produce a balanced dataset.

Activity labelling in continuous data streams was done via the scripted experimental protocol and timestamp information. Custom programs in MATLAB® (2019, MathWorks, Inc., Natick, US) analysed raw (sample level) IMU and sEMG data for HAR of walking, standing, stair ascent and stair descent.

6.3.2.2. Feature extraction and post-processing

Raw IMU data are typically characterized by noise, making it difficult to be used directly in HAR models [408]. Consequently, a standardised approach of applying a low pass filter (4^{th} order Butterworth, cut-off frequencies 5Hz and 20Hz) was used for acceleration and gyroscope signals, respectively. sEMG signals were post-processed by a band-pass filter (zero-lag 4^{th} order Butterworth filter with cut-off frequencies of 20Hz and 250Hz) followed by rectification, and a second zero-lag 4^{th} order Butterworth low-pass filtering at 6Hz. That removes baseline drift often associated with movement artifact, perspiration, or any DC offset [409], Figure 12 (c). After post-processing, inertial and sEMG data streams for each activity were segmented into 1.25 seconds windows with 50% overlap using a sliding window. Overlap between two consecutive windows was adopted to eliminate information loss at window edges. The window size was selected to ensure fast feature extraction (small-size window) while covering sufficient information about activities. Specifically, the size was set to 1.25s to ensure each window covers at least one stance and swing period during dynamic activities, Figure 12 (c). A total of 252 (walking), 232 (standing), 206 (stair ascent) and 191 (stair descent) units of activity (occurrence) were obtained, after segmenting a continuous data stream. To investigate the impact of sEMG post-processing on classification performances, two different feature-level classifications were investigated. The first combined features of IMU data with features of band pass filtered sEMG. The second combined features of IMU data with features of linear envelope which is obtained by bandpass filtered and rectified sEMG following low pass filtering.

6.3.2.3. Features

Handcrafted features are independent variables that act as input for most classifiers. Typically, features are calculated from raw segmented data and designed for comparing and differentiating activities [408]. Here, I created a feature set based on the features previously found informative [409, 410] for inertial and sEMG data. Features are extracted for each acceleration and gyroscope axis, as well as sEMG channel, Figure 12 (d). Consequently, 60 (tri-axial × 20 features) features were extracted for one single accelerometer, 60 (tri-axial × 20 features) features for one gyroscope, 40 (2 channels × 20 features) features for sEMG, Figure 12 (e). One hybrid feature, the difference of SR and TR sensor orientation also known as knee flexion/extension angle, was extracted using [400] to improve classification accuracy as walking, stair ascent and descent have their own distinctive knee flexion angles [411]. The area under the curve also known as integrated EMG provide discriminative information for each muscle during various activities since previous studies highlighted different sEMG signal wave for different activities [412, 413]. In classification with sEMG linear envelope (sEMG-LE), zero crossing feature was excluded as the signal has single polarity.

The features used for classification were: 1. Maximum fractal length, 2. Variance, 3. Simple square integral, 4. Mean absolute value (MAV), 5. Log detector, 6. Average amplitude change, 7. Waveform length, 8. Root mean square, 9. Mean absolute deviation, 10. Interquartile range, 11. Skewness, 12. Kurtosis, 13. Coefficient of variation, 14. Standard deviation, 15. Variance, 16. Average energy, 17. Area under the curve (integrated EMG) 18. Modified MAV, 19. Slope sign change, 20. Zero crossing, and 21. Hybrid feature (orientation difference between SR and TR).

Features extracted from IMU and sEMG data were then input to two different supervised classification models (SVM and kNN), commonly used with labelled data, Figure 12 (f). These classifiers compared classification performances based on different feature-level fusions. SVM is a binary classifier searching for the separation between two classes after mapping data into a high-dimensional space. Alternatively, k-NN has a simple structure measuring the distance between unlabelled observations and training samples to perform classification [284]. No feature dimensionality reduction or feature selection processes were performed as the number of the initial set of features does not have computational cost (i.e., the training time for each <30s). k-fold cross-validation was used on the training and testing datasets. The *k* value was set to 5 which has empirically yielded a classification model accuracy estimate with low bias and a modest variance [408].

6.3.2.4. Analysis

Accuracy (ACC.%), sensitivity (SEN.), and specificity (SPE.) were used to evaluate model performance. Accuracy is a common metric, giving a general representation of a model's performance in a balanced dataset [408]. Sensitivity and specificity are produced from confusion matrices using the formula presented in [17].

****

6.4. Methodology 3 (M3): Improving inertial sensor-based activity recognition

6.4.1. Background M3

In this section, I propose a methodology to investigate how limited data can be better utilized to achieve accurate HAR/mobility classification in limited healthy, PD and SS population-specific models. To achieve my goal, I propose numerical-to-image conversion as the fundamental component of my proposed methodology. The use of data augmentation complements my framework by providing solutions to the limited dataset and overfitting problems. Finally, using transfer learning enable applications with small data to benefit from models that are more experienced and trained with big data. An investigation of the proposed method's performance was initially performed on two public datasets. Results were compared to the reference studies with and without data augmentation operations in the same datasets. Then, several pilot studies tested my numerical-to-image conversion approach along with a data augmentation technique on limited local datasets belonging to healthy, PD, and SS participants. Therefore, the contributions of this section are:

1. Developing a novel framework that converts inertial sensor time-series data into images (activity images).
2. Adopting established data augmentation techniques in image processing to artificially increase limited datasets for the purpose of better HAR in neurological populations (where access to data may be difficult).
3. Verifying the proposed approach in public datasets and conducting experimental pilot studies for a single sensor based HAR on limited HS, PD, and SS datasets.

6.4.2. Approach M3

The proposed methodology developed for better HAR of people with neurological conditions is presented in Figure 13. Three limited local datasets and two independent benchmarking public datasets were used to verify the proposed methodology. To replicate the pragmatic problems in this domain, the local dataset has a limited number of participants, data sparsity and class imbalance. In the proposed methodology, numerical inertial sensor data were first normalized and then converted into images (initial state). Then, established image augmentation techniques were adopted to artificially increase the number of images (enhanced state). Finally, generated images were fed into different CNN architectures. All steps are further detailed in this section.

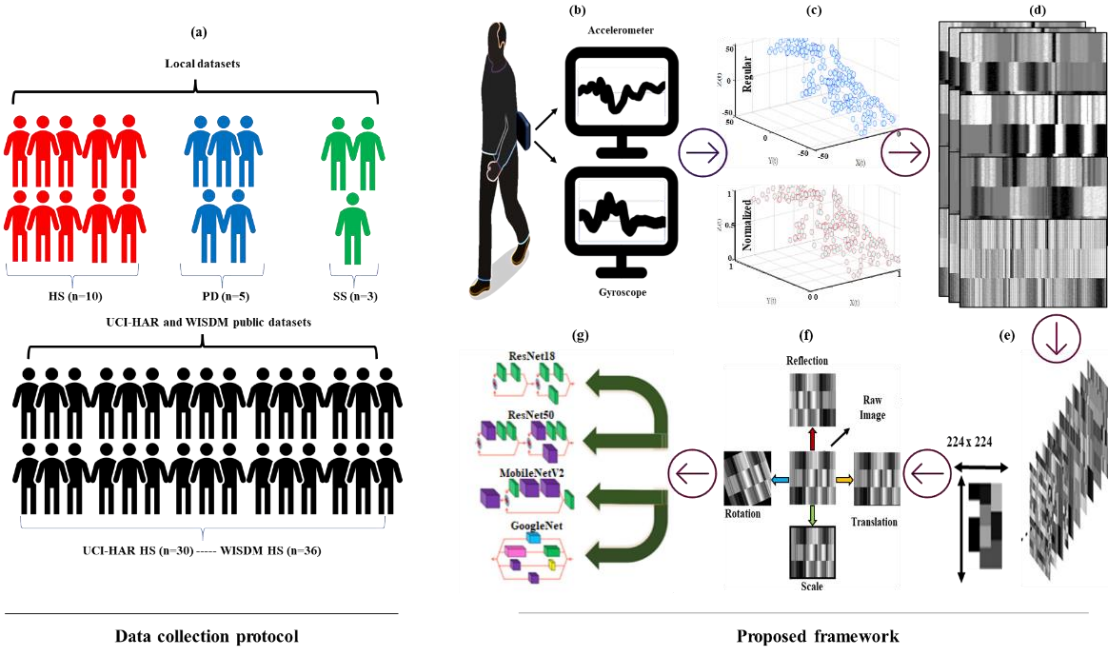

Figure 13.Data collection protocol and proposed framework: (a) Dataset illustration. Flow of the proposed HAR methodology with data augmentation and CNN architectures: (b) IMU data acquisition, (c) data normalization, (d) numerical to image conversion, (e) resizing, (f) data augmentation, (g) CNN classification.

6.4.2.1. Data normalization and numerical to image conversion (initial state)

Raw accelerometer and gyroscope signals experience different lower and upper limits, because of configuration (e.g., an accelerometer typically can collect data at the range of ±16 m/s2 whereas gyroscopes can sense up to ±2000°/sec). Normalizing features with different upper and lower limits is a commonly used pre-process in AI as extreme differences between different features may have a negative impact on the learning abilities [414]. In the normalization step, a feature scaling-based normalization method is preferred due to its convenience. Here, raw IMU data (x) is normalized ($\hat{x}$) considering max value (x_{max}) and min value (x_{min}), as depicted in Figure 13 4(c). As a result of normalization, the value in matrices ranges between 0 and 1 for both accelerometer and angular velocity, Eq.11.

$$\hat{x} = \frac{x - x_{min}}{x_{\max} - x_{min}} \tag{11}$$

After normalization, data were divided into sub-segments (windows) considering each sub-segment should contain sufficient characteristics that allow HAR to be successfully performed. A previous study [415] investigated windows size impact on HAR application and reported that the ideal size for fixed windows ranges between 2s and 5s considering a frequency of 20Hz to 50Hz. Therefore, each activity was divided into consecutive segments of fixed-length (≈2.5s windows) considering that at least two strides are needed to recognize walking and stair ambulation. IMUs typically sense tri-axial acceleration (a_x, a_y, a_z) and tri-axial angular velocity (w_x, w_y, w_z) in the t moment (Eq.12). Generally, popular CNN models are not suitable to use 1D datasets and require 2/3D images to feed input layers [416]. Therefore, many previous studies [365, 417, 418] extract IMU data features with 1D convolution layers and then evaluate those features with recurrent neural network-based methods. Here, I convert numerical IMU data to images to go beyond that limit, as shown in Figure 13 (d).

$$\mathbf{IMU}_t = \left[\mathbf{a}_{x_t}, \mathbf{a}_{y_t}, \mathbf{a}_{z_t}, \mathbf{w}_{x_t}, \mathbf{w}_{y_t}, \mathbf{w}_{z_t}\right] \tag{12}$$

Eq. 13 represent 2D data (also can be referred to as an image) created by vertical placement of accelerometer and gyroscope values recorded in 2.50s window/250 sample and 2.56s windows/128 sample for the local dataset and UCI HAR dataset, respectively. In WISDM dataset, only accelerometer values were placed in 2.50s window/50 sample. Unlike previous studies [306, 373, 374], this work ensures that each numerical IMU value corresponds to a specific pixel in an image. The normalized values in the matrices were multiplied by 255 to produce grey images with pixels ranging from 0 to 255. As a result, images whose brightness increases/decreases with the numerical value of the IMU are produced. However, image dimensions are not suitable to feed the input layer of CNN models since each CNN model's input layer accepts images with a size of 224×224 [416]. Therefore, resizing is applied by stretching row length to obtain a square matrix from these images Figure 13 (e).

$$\begin{bmatrix} \mathrm{IMU}_{\mathrm{acc}_x} \\ \mathrm{IMU}_{\mathrm{acc}_y} \\ \mathrm{IMU}_{\mathrm{acc}_z} \\ \mathrm{IMU}_{\mathrm{gyro}_x} \\ \mathrm{IMU}_{\mathrm{gyro}_y} \\ \mathrm{IMU}_{\mathrm{gyro}_z} \end{bmatrix} = \begin{bmatrix} \mathrm{a}_{x_t}, \mathrm{a}_{x_{t+1}}, \mathrm{a}_{x_{t+2}}, \ldots\ldots, \mathrm{a}_{x_{t+126/248}}, \mathrm{a}_{x_{t+127/249}} \\ \mathrm{a}_{y_t}, \mathrm{a}_{y_{t+1}}, \mathrm{a}_{y_{t+2}}, \ldots\ldots, \mathrm{a}_{y_{t+126/248}}, \mathrm{a}_{y_{t+127/249}} \\ \mathrm{a}_{z_t}, \mathrm{a}_{z_{t+1}}, \mathrm{a}_{z_{t+2}}, \ldots\ldots, \mathrm{a}_{z_{t+126/248}}, \mathrm{a}_{z_{t+127/249}} \\ \mathrm{w}_{x_t}, \mathrm{w}_{x_{t+1}}, \mathrm{w}_{x_{t+2}}, \ldots\ldots, \mathrm{w}_{x_{t+126/248}}, \mathrm{w}_{x_{t+127/249}} \\ \mathrm{w}_{y_t}, \mathrm{w}_{y_{t+1}}, \mathrm{w}_{y_{t+2}}, \ldots\ldots, \mathrm{w}_{y_{t+126/248}}, \mathrm{w}_{y_{t+127/249}} \\ \mathrm{w}_{z_t}, \mathrm{w}_{z_{t+1}}, \mathrm{w}_{z_{t+2}}, \ldots\ldots, \mathrm{w}_{z_{t+126/248}}, \mathrm{w}_{z_{t+127/249}} \end{bmatrix} \tag{13}$$

6.4.2.2. Data augmentation

Table 9 presents the number of occurrences along with class distribution in limited local datasets. To alleviate the problems related to small dataset size and prevent overfitting, data augmentation was applied to increase the number of generated images using established image processing techniques. In this sense, four different image position augmentation techniques (reflection, rotation, scale, and translation) were applied to each image to ensure data diversity and robust training, see Figure 13 (f). Reflection also known as symmetry is an image pre-processing operation that can occur in horizontal or vertical access. Rotation, scaling, and translation are other pre-processing operation that deal with spinning, resizing, and moving (right, left, up and down) in given upper and lower limits, respectively. The lower and upper limit values of rotation, translation (pixel) and scale are ±30°, ±10° and 0.9-1.1,

respectively, since these values have proved to be efficient [375]. Consequently, the size of the original dataset in the initial state was enhanced by adding 8 times more artificial data (4 different techniques with lower and upper limits). In this context, the number of occurrences for each class in the local datasets are increased, Table 10.

Table 9.Class distributions in local datasets (initial state)

Dataset	Walking	Ascent	Descent	Standing	Total
HS	50 (25)	50 (25)	49 (25)	50 (25)	199 (100)
PD	81 (29)	64 (23)	60 (21)	75 (27)	280 (100)
SS	49 (28)	18 (11)	31 (18)	75 (43)	173 (100)

Number of occurrences/images (% class distribution)

Table 10.Number of occurrences after data augmentation (enhanced state) in local dataset

Dataset	Walking	Ascent	Descent	Standing	Total
HS	450	450	441	450	1791
PD	729	576	540	675	2520
SS	441	162	279	675	1557

Number of occurrences/images (% class distribution)

6.4.2.3. HAR via CNN

Benchmarking analysis of various deep learning models was previously studied and performance indices such as accuracy, model complexity, memory usage, computing power and interference times were evaluated [416, 419]. I determined my priority performance indices as high accuracy rate, minimal computing power and short prediction time to achieve an effective HAR framework. Therefore, I chose four optimal pre-trained networks GoogleNet [420], ResNet18 [421], ResNet50 [421] and MobileNet-v2 [422, 423] in the Pareto frontier as these architectures satisfy my requirements. Each CNN architecture used in this chapter section differs from each other in layer, size and parameters, and is often preferred in benchmarking studies to evaluate CNN performances [424, 425], Table 11. MATLAB® (2021, MathWorks, Inc., Natick, US) software on a laptop with Intel Core i7-7700HG CPU (2.80 GHz), 16 GB RAM, NVIDIA GeForce GTX 1050 4 GB was used to perform CNN training and testing.

Residual network (ResNet) [421] was developed to improve unexpected low performances of deeper network architectures by adding a skip connection (shortcut) to convey information between layers and avoid the vanishing gradient problem [425]. There are different ResNet variants (18-layer 34-layer 50-layer 101-layer 152-layer) proposed considering the number of layer and output sizes, ResNet18 and ResNet50 were implemented here. MobileNet was employed as it has low computation and fast operation by using depth-wise separable convolutions to reduce number of parameters and computation time. Specifically, MobileNet-v2 [423] was implemented, which has 54-layers, distinguishing it from MobileNet in using inverted residual blocks with bottleneck properties. GoogleNet [420] is 22-layer deep (excluding pooling) model designed with computational efficiency and practicality. It uses the inception module to extract features more effectively using various filter sizes. And the computational load is reduced with a 1×1 convolution of the depth of the network. Minor adjustments such as the use of fine-tuning network were made to the existing architecture for the four-class classification problem in chapter section. In this context, a fully connected layer with four outputs and a classification layer was added to the existing structure, see Figure 13 (g).

Table 11.Properties of pre-trained CNN architectures

CNN architecture	Layer (Depth)	Size (Megabyte)	Parameters (Millions)	Input image size
ResNet18	18	44	11.7	224 × 224
ResNet50	50	96	25.6	224 × 224
MobileNetv2	54	13	3.5	224 × 224
GoogleNet	22	27	7	224 x 224

6.4.3. Datasets M3

6.4.3.1. Local datasets

Ten HS (28.4 ± 7.0yrs, 79.2 ± 14.4kg, 176.8 ± 8.4cm, 8 Male, M: 2 Female, F), five people with PD (61.5± 3.43yrs, 82.9 ± 10.3kg, 175.8 ± 4.6cm, 5M) and three SS (72.3 ± 3.1yrs, 78.5 ± 12.1kg, 176 ± 8.2cm, 3M) were recruited, as illustrated in Figure 13 (a). Each participant was instructed to stand for 2-minutes (eyes open and comfortable standing) then walk over level ground for 2-minutes around a 20m circuit at their self-selected walking speed inside the lab. Afterwards, participants ascended and descended stairs (15 steps) outside of the lab (in a generic university campus stair well).

Assessment and instrumentation were carried out by a physiotherapist and trained researcher, respectively. Ethical consent was granted by the Northumbria University Research Ethics Committee (REF: 21603). All participants gave informed written consent before participating in this study. Testing took place inside and outside of a gait laboratory/lab, Coach Lane Campus, Northumbria University, Newcastle upon Tyne.

Each participant wore a Shimmer3 IMU device (24.3cm3, 23.6g) on the 5th lumbar vertebrae (L5), as shown in Figure 13(b). IMU signals (tri-axial accelerometer and tri-axial gyroscope) were recorded at a sampling frequency of 100Hz and configured with 16-bit resolution (±8g, ±500°/s). IMU data were transferred to a workstation (Windows 10) from the IMU device via proprietary software (Consensys, Shimmer). Labelling of activities in a continuous data stream was done via a wearable camera for PD and SS, whereas a scripted experimental protocol was used for HS. All participants performed the same protocol. Inertial data streams for each activity were segmented into 2.5 seconds (s, 250 sample points) windows with 50% overlap using a sliding window.

6.4.3.2. UCI-HAR and WISDM independent benchmarking datasets

UCI-HAR dataset [378] was preferred to test the development methodology as it was created using the same data collection protocol as the local dataset. UCI-HAR dataset has accelerometer and gyroscope recording of 30 HS (19-48 years), collected by a device attached at waist level. The dataset was randomly portioned into training and testing. Data were recorded at a sampling frequency of 50Hz and segmented to fixed width sliding windows of 2.56s (128 sample points) with 50% overlap. WISDM dataset was created from 36 HS under controlled laboratory conditions. The dataset has tri-axial accelerometer readings only recorded at 20Hz. Accelerometer recordings were segmented to fixed width sliding windows of 2.50s with 50% overlap.

Table 12 presents activity classes along with class distributions in the benchmarking datasets. Skewed class distributions are present in the public datasets. This typically limits the learning/training process by causing class overlapping, small sample size or small disjuncts [426]. In addition, models trained with imbalanced datasets are often biased towards the majority class and therefore there is a greater misclassification rate for the minority class occurrences such as sitting and standing in WISDM dataset[427]. Furthermore, the most common evaluation metric, accuracy treats all classes as equally important which makes it inefficient [17]. To alleviate the limitations of imbalanced public datasets, I utilized 500 occurrences from each class for training in public datasets. In total, 3000 occurrences were utilized for each dataset and the train/test split ratio.

Table 12.Class distributions in benchmarking datasets (initial state)

Dataset		Walking	Ascent	Descent	Sitting	Standing	Laying	Jogging	Total
UCI-HAR	Original	1226 (17)	1073 (15)	986 (13)	1286 (17)	1374 (19)	1407 (19)	-	7352
	Utilized	500 (16.6)	500 (16.6)	500 (16.6)	500 (16.6)	500 (16.6)	500 (16.6)	-	3000
WISDM	Original	424,400 (38.6)	122,869 (11.2)	100,427 (9.1)	59,939 (5.5)	48,395 (4.4)	-	342,17 (31.2)	756,030
	Utilized	500 (16.6)	500 (16.6)	500 (16.6)	500 (16.6)	500 (16.6)	-	500 (16.6)	3000

Number of occurrences/images (% class distribution)

6.5. Conclusion

This chapter provides a comprehensive overview of my three proposed methodologies (M1 to M3) and study protocols employed, encompassing a cohort of healthy individuals, SS, and individuals with PD. The first methodology outlined in this chapter focuses on investigating PoI2. Subsequently, the second and third methodologies address PoI3 with a specific emphasis on human activity recognition (HAR) in PD group and stroke survivors. The next chapter will present the experimental results obtained from these published studies, offering further insights into the outcomes of the conducted research.

Chapter 7 Experimental results of methodologies 1 to 3

This chapter uses text from my previously published online articles to fit the context and narrative of this thesis.

The first journal article "Multi-modal gait: A wearable, algorithm and data fusion approach for clinical and free-living assessment", was published in the Information Fusion in 2021. (URL: https://doi.org/10.1016/j.inffus.2021.09.016).

The second publication appears as a conference paper "*Exploring human activity recognition using feature level fusion of inertial and electromyography data"*, was published 44th Annual International Conference of the IEEE Engineering in Medicine & Biology Society (EMBC) in **2022.** *(URL: https://doi.org/10.1109/EMBC48229.2022.9870909)*.

The third journal article "*Improving Inertial Sensor-Based Activity Recognition in Neurological Populations"* was published in the **Sensors** in **2022.** *(URL:* https://doi.org/10.3390/s22249891*)*.

7.1. Introduction

This chapter entails the presentation of the experimental results and discussions derived from the studies outlined in the previous chapter. Section 7.2 provides a detailed account of the outcomes of multimodal gait analysis, encompassing spatiotemporal, kinematic, and muscle activation parameters, obtained from both healthy individuals and stroke survivors in both indoor and outdoor environments. In Section 7.3, the effectiveness of feature-level fusion of IMU and EMG sensor data in enhancing the performance of classical machine learning models for the classification of basic daily activities is demonstrated. Finally, Section 7.4 presents the experimental findings pertaining to the improvements in deep learning model performance achieved through data augmentation techniques applied to public datasets as well as local datasets comprising healthy individuals, stroke survivors, and individuals with Parkinson's disease.

7.2. M1 results: Multimodal gait analysis with data fusion

This novel fusion approach quantifies and contrasts temporal, spatial, knee joint kinematics, and muscle activation characteristics in (i) HP's during 2min walks in a lab (indoor) vs 2min outdoor walking on level ground, and (ii) in a pilot study of SS walking for 2mins, indoor vs outdoor. Here, results are deemed suitable for exploratory investigation as they are derived from validated algorithms for use on level ground terrain. Similar modes of investigation have been conducted previously, examining unimodal, spatiotemporal gait between clinic/lab and habitual environments [316].

Outputs of the fusion approach can be classified as; spatiotemporal, knee joint flexion and muscle activation patterns. Muscle bursts timing and durations are presented throughout the gait cycles. Multi-model gait characteristics of the left side for one HP participant (#9) during outdoor level walking were not extracted due to wearable malfunction; therefore, only mean values for the right side were calculated. IC-FC events were not detected for the paretic side of one SS participant (#3) as algorithms (***A1-A2***) failed to detect peaks due to poor gait; therefore, only mean values for the non-paretic side were calculated.

7.2.1. Healthy participants-M1

7.2.1.1. Two-minute walks: Spatiotemporal, kinematics and EMG

There were differences in gait domains for spatiotemporal characteristics between indoor and outdoor walks, Table 13. Generally, participants walked with greater *pace* and *variability* but with decreased *rhythm* in outdoor compared to indoor level walking (stride length variability characteristic did not experience any changes between outdoor level walking and indoor). Among *asymmetry* characteristics, only stride length asymmetry was found higher during indoor level walking compared to outdoor. There were slightly increased mean knee flexion angles (~1°) and decreased variance and asymmetry in outdoor level walking compared to indoor, Table 13. Although there are large inter-individual differences among participants, common muscle burst timing and durations patterns can be extracted via EMG signals [239], where common muscle activity patterns were observed within a gait cycle. Regardless of indoor/outdoor, the prevalence of TA muscle activation had similar patterns with RF and BF, all active around the start and end of a gait cycle during level walking. TA was also found active at stance to swing transition period (around FC) and throughout the swing phase in some participants. BF muscle activation was observed at the end of a gait cycle around the time of the next IC. GS prevalence was observed mostly during the later stance phase before the FC moments for push-off of the foot, Figure 14.

Table 13.Multi-modal gait characteristics of healthy participants during 2-minute walks

		Indoor		*Outdoor*	
	# Mean of strides	*99.6*		*108.1*	
		Mean	*± SD*	*Mean*	*± SD*
SPATIOTEMPORAL	PACE				
	Mean Stride V. (m/s)	1.174	0.127	1.319	0.101
	Mean Stride L. (m)	1.332	0.147	1.415	0.142
	RHYTHM				
	Mean Stride Time (s)	1.136	0.082	1.074	0.060
	Mean Step Time (s)	0.566	0.037	0.534	0.032
	Mean Stance Time (s)	0.647	0.057	0.597	0.038
	Mean Swing Time (s)	0.489	0.039	0.476	0.034
	VARIABILITY				
	Stride V. Var (m/s)	0.105	0.024	0.125	0.023
	Stride L Var (m)	0.130	0.041	0.129	0.029
	Step Time Var (s)	0.034	0.020	0.039	0.013
	Stance Time Var (s)	0.014	0.010	0.050	0.012
	Swing Time Var (s)	0.018	0.011	0.043	0.004
	ASYMMETRY				
	Stride L. Asy (m)	0.086	0.062	0.104	0.068
	Step Time Asy (s)	0.033	0.006	0.025	0.022
	Stance Time Asy (s)	0.041	0.010	0.012	0.008
	Swing Time Asy (s)	0.044	0.007	0.011	0.007
KNEE JOINT KINEMATICS	Mean K.F.E angle	62.621°	4.229°	63.580°	5.220°
	Variability	5.1875°	1.217°	4.490°	1.239°
	Asymmetry	1.8117°	1.040°	1.593°	1.069°

Stride V = stride velocity, Stride L = stride length. Var = variability, Asy = symmetry
(K.F.E) knee flexion
Bold indicate greater mean values comparing indoor to outdoor.

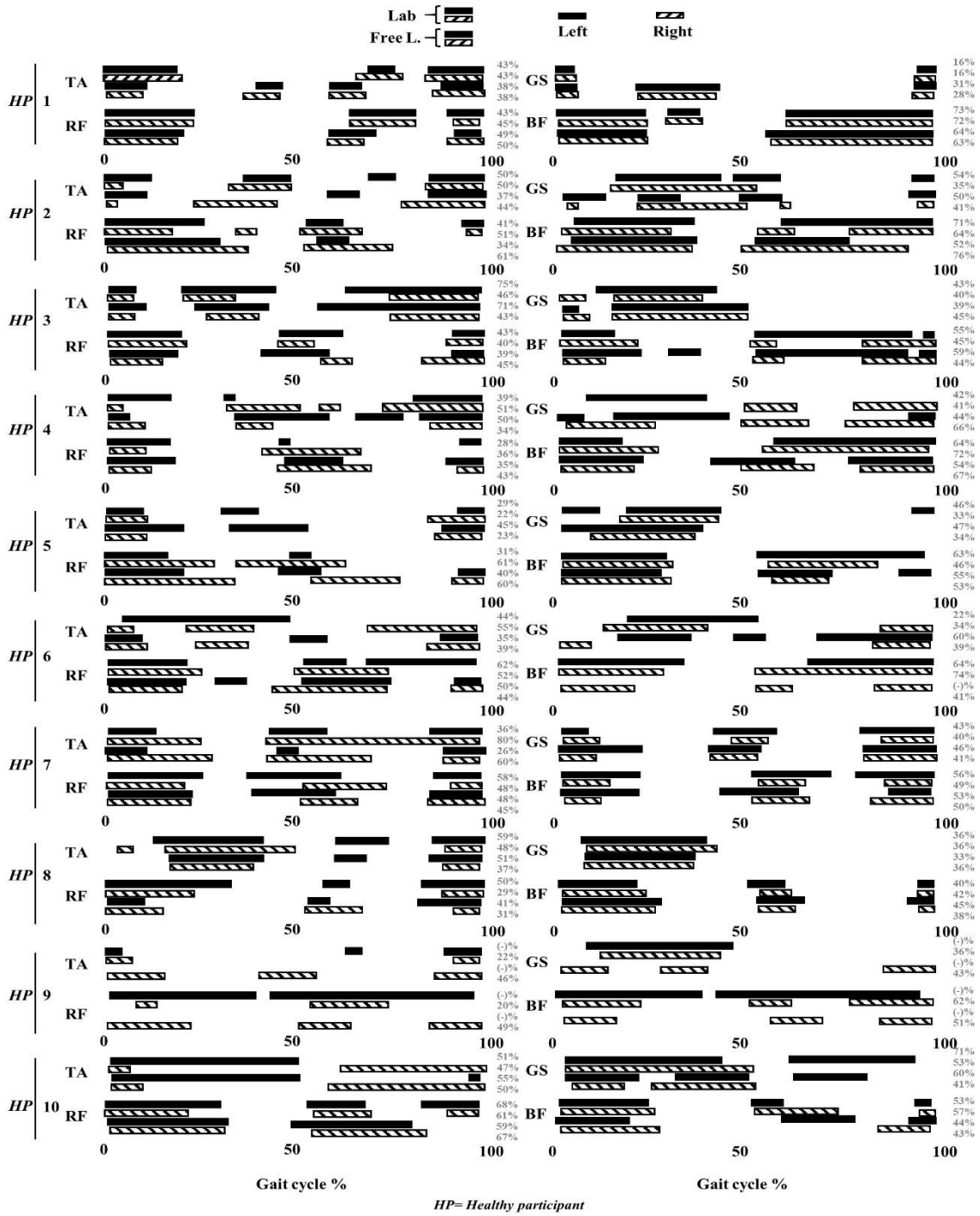

Figure 14.Muscle activity pattern healthy participants for indoor/outdoor ground-level walking

7.2.2. Pilot study: Multi-modal gait analysis in stroke survivors-M1

The process of extracting multi-modal gait during level walking is generally illustrated in Figure 15, highlighted here for those with stroke gait. The proposed sensor and data fusion tool provides multi-model gait characteristics during indoor and outdoor activities, but IC-FC times must be detectable initially.

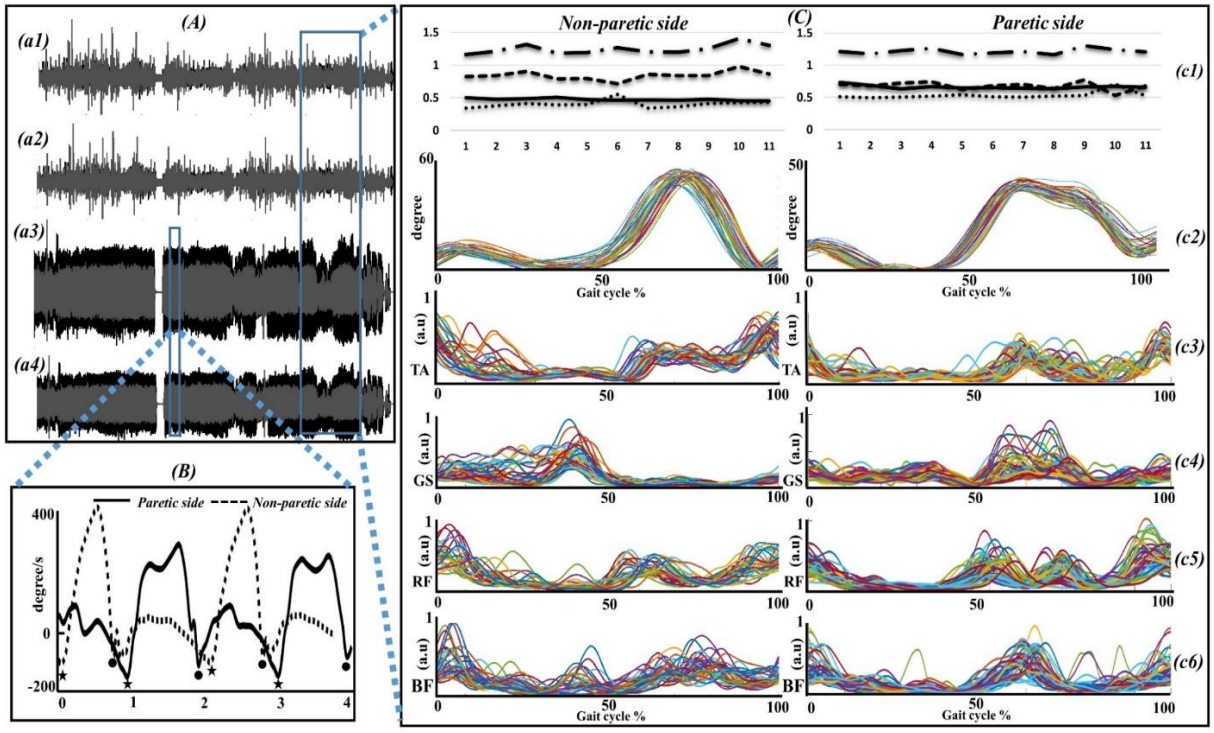

Figure 15.Level walking extracted parameters from the proposed tool. (A) Raw wearable IMU data for EMG (a1-a2) and angular velocity (a3-a4) – black represents shank mounted sensors – grey represents thigh mounted sensors, (B) Shank angular velocity of paretic and non-paretic sides: initial (dots) and final (stars) contact moments, (C) outcome of sensor fusion work for non-paretic and paretic sides: (c1) temporal characteristics where long dot dush, square dot, solid line and round dot represents (top-to-bottom) stride, stance, step and swing times respectively: (c2) estimated kinematic knee angles: (c3-c4-c5-c6) EMG activity for TA, GS, RF, and BF, respectively. a.u, Arbitrary unit-peak normalised EMG.

7.2.2.1. Two-minute walks: Spatiotemporal, kinematics, and EMG

Although SS presented similar shank angular velocity patterns with disturbances (e.g., oscillations) between paretic and non-paretic sides during ground-level walking, extracted indoor and outdoor temporal and spatial characteristics varied, Table 14.

SS walked with increased *pace* and decreased *rhythm* during outdoor level walking compared to indoor. Swing time asymmetry is the only *asymmetry* characteristic that was found to be higher during indoor compared to outdoor. Among *variability*, there was no difference in stride velocity, but stance time was lower during indoor level walking compared to outdoor. (Individual and left/right data available via Appendix 5).

Noticeable differences were observed for mean, variance and asymmetry of knee joining angles. Increased mean knee flexion angles (~4°) and decreased variability and asymmetry were found during outdoor walking, compared to indoor, Table 14. Muscle activity (bursts) during indoor and outdoor walking presented in Figure 16. TA, RF and BF muscle burst were detected around the starting and ending moments of gait cycles (around IC moments). GS muscle bursts most frequently observed in the stance phase in most SS.

Table 14.Multi-modal gait characteristics of stroke survivors during 2-minute walks

		Indoor		*Outdoor*	
	# Mean of strides	*93.6*		*109.33*	
		Mean	*±SD*	*Mean*	*±SD*
SPATIOTEMPORAL	PACE				
	Mean Stride V. (m/s)	1.021	0.049	1.067	0.119
	Mean Stride L. (m)	1.303	0.134	1.384	0.338
	RHYTHM				
	Mean Stride Time (s)	1.254	0.077	1.235	0.130
	Mean Step Time (s)	0.614	0.041	0.535	0.011
	Mean Stance Time (s)	0.770	0.085	0.748	0.142
	Mean Swing Time (s)	0.483	0.045	0.452	0.016
	VARIABILITY				
	Stride V. Var (m/s)	0.189	0.013	0.182	0.033
	Stride L Var (m)	0.275	0.046	0.224	0.052
	Step Time Var (s)	0.100	0.096	0.033	0.006
	Stance Time Var (s)	0.070	0.058	0.074	0.002
	Swing Time Var (s)	0.071	0.052	0.037	0.002
	ASYMMETRY				
	Stride L. Asy (m)	0.197	0.179	0.290	0.182
	Step Time Asy (s)	0.060	0.003	0.102	0.061
	Stance Time Asy (s)	0.063	0.001	0.088	0.046
	Swing Time Asy (s)	0.062	0.001	0.067	0.036
KNEE JOINT KINEMATICS	Mean K.F.E angle	48.120°	1.196°	52.096°	1.014°
	Variability	6.064°	0.188°	5.297°	0.660°
	Asymmetry	22.251°	4.506°	19.920°	6.821°

Stride V = stride velocity, Stride L = stride length. Var = variability, Asy = asymmetry
(K.F.E) knee flexion
Bold indicate greater mean values comparing indoor to outdoor

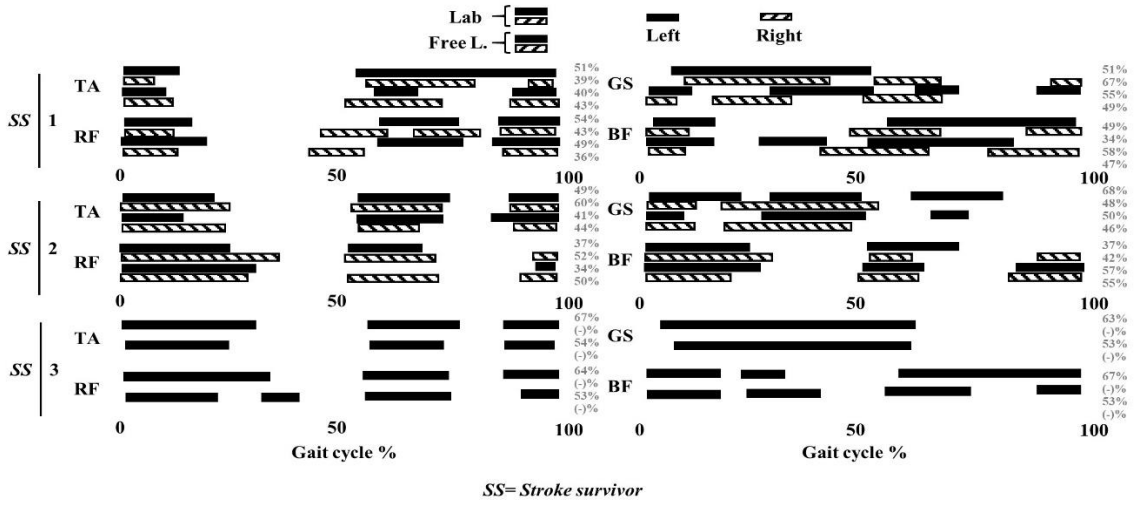

Figure 16.Muscle activity pattern stroke survivors for indoor vs. outdoor ground level walking. IC-FC moments were not able to detect for the paretic side of SS survivor (#3). Thus, only the left side muscle activity patterns are segmented only.

7.2.3. Impact of changing terrain-M1

The fusion approach can quantify multi-model gait characteristics on different terrains, but I present level ground data only. Multi-model gait characteristics and descriptions of HP's and SS during different indoor (e.g., stairs) and outdoor (e.g., cobbles) terrains are presented in Appendix 5 but mentioned briefly here.

- Spatiotemporal characteristics: Comparing spatiotemporal gait characteristics of HP and SS in four domains during indoor/outdoor walking activities revealed notable differences. Among all indoor/outdoor walking activities of HP, the highest *pace* along with the lowest *rhythm* and *asymmetry* were found during outdoor level walking. Also, spatial parameters experienced the highest values for the *variability* domain, whereas temporal parameters were found second highest in outdoor level walking after incline walking.

SS groups experienced slightly increased *pace* and increased *asymmetry* during outdoor walking compared to indoor.

- Knee joint kinematics: HP revealed that mean knee flexion angles did not experience significant change while indoor/outdoor ground-level walking and walking on a rock surface.

  SS group revealed a slightly increased knee flexion angle (~4°) during outdoor level walking compared to indoor level walking. When comparing the paretic side and non-paretic side knee flexion angles of each SS, higher differences observed, Figure 15.
- EMG, burst timing and durations during level walking: Prevalence of muscle burst and duration showed similar patterns between the right and left sides of lower limb muscles in most HP. Additionally, durations of muscle burst slightly decreased during outdoor level walking compared to indoor in most HP.

  The durations of muscle burst found slightly decreased during outdoor level walking compared to indoor in most SS.

7.2.4. Discussion M1: Multimodal gait analysis with data fusion

The methodologies provide a comprehensive range of lower limb gait characteristics (spatiotemporal, kinematics, and EMG) for use in different environments. The work presented here shows how algorithms developed in isolation can be successfully adapted and fused to create a more rounded/holistic gait assessment tool for use in the clinic/lab and beyond. The multi-modal fusion approach proposed here may better contribute to gait studies for clinical as well as habitual gait assessments, better informing rehabilitation programs that aim to regain community-based ambulatory mobility for those with neurological conditions such as stroke. Improved understanding of gait through my proposed multi-modal approach could lead to a better understanding of the effect of walking environment and how that contributes to the underlying mechanisms to reduce mobility and induce falls.

The proposed fusion methodology defined here consists of the detection of IC-FC contact moments along with timestamp information (using ***A1-A2*** algorithms and shank sensors data) by considering the type of activity (e.g., level walking or incline walking). That enables segmentation of gait cycles and sub-phases (stance and swing periods) as well as extraction of temporal parameters (e.g., step time). Then, gait cycles are segmented from mid-stance to mid-stance using the IC-FC information obtained from ***A1-A2***, and spatial characteristics (***A3*** and shank sensors data). Afterwards, knee joint flexion angles are estimated (***A4-A5*** and shank-thigh sensors data) by considering the type of activity (e.g., level walking or stair ambulation) for each gait cycle segmented. Finally, segmented gait cycles and corresponding timestamp information were used to segment EMG data belonging to four different lower limb muscles and muscle onset/offset timings (using ***A6***).

Previous studies have investigated gait during free-living to better understand the impacts of real-life settings such as environmental factors on gait [58, 269]. Most of these studies aim to extract clinically useful gait characteristics (spatiotemporal, kinematics) and are based on cameras and IMUs. However, camera-based systems are not pragmatically feasible due to several factors such as privacy, security and, limited data capture due to field of vision [2, 428]. Although existing inertial sensor-based studies use a more feasible data collection approach, most fail to include clinically useful gait characteristics such as lower limb kinematics [429]. Additionally, the number of those focusing on free-living gait analysis in neurological conditions (e.g. stroke) is very limited and provides uni-modal characteristics only [2]. Those who investigated a multi-sensor fusion approach, utilised wearable sensors attached to the right lower limb for use during indoor level walking only [430]. Although that study quantified kinetic characteristics with a pressure sensor, spatial characteristics were not included.

7.2.5. The multi-modal approach-M1

Multi-modal wearable sensor deployment is of growing interest during free-living activities. For instance, an approach to develop a vital sign monitoring system involving physiological components (e.g., respiratory band, electrocardiography) has been presented previously [333]. Another study used a similar approach where multiple sensors were fused to develop a body sensor network that can measure motor functions in children with spastic diplegia [431]. Multi-modal wearable sensor use is possible due to the miniaturisation of wearable technologies

and the increasing paradigm shift to monitoring people in their habitual environments. As gait is now classed as the sixth vital sign [432], it is important that multi-modal approaches are developed to capture gait in its entirety across more natural environments.

Most gait analysis studies have been conducted that do not immediately aim to make clinical decisions but to learn about a condition affecting a group of patients or the effect of an intervention [433]. Also, studies are based on a single sensor and provide either activity detection or informative gait outcomes. However, the next generation of wearables could be fused in a way that human activity assessment (i.e. activity detection and gait characteristics extraction) can be done using multiple sensor configurations [434]. Contemporary gait analysis requires evaluation of various aspects (e.g. kinematic, muscle) of the lower limb with a large number of outcomes [2]. Variances in gait are very subtle [392], and so the multi-modal gait approach enables granular capture of characteristics considering key digital biomarkers, i.e., clinically relevant gait characteristics. A study already reported that these variances/fluctuations in gait can be used to differentiate a particular neurological condition from healthy participants using gait data along with complexity measures [435]. Here, subtle differences were observed between indoor and outdoor level walking (as the differences between walking on various outdoor surfaces and stair ambulation) for HP and SS. This corroborates the benefit of using wearables for outdoor/habitual gait assessment as observed in another neurological cohort, albeit with a uni-modal device in Parkinson's disease [22]. The use of a multi-modal sensor and data fusion approach may provide more insights into the underlying neurological mechanisms due to, e.g., changing terrain.

Spatiotemporal outcomes have been widely used to reveal distinctive gait deficits and interpret impaired gait during indoor and outdoor assessments. Particularly for outdoor assessments, a previous study reported gait adaptation strategies to maintain stability are sensitive to different walking surfaces [293]. Thus, investigating the adaptation of *pace* on various surfaces may help better understand control of the sensory, motor and cortical functions that are critical to minimise trips, slips and falls [2]. Additionally, the proposed multi-modal sensor fusion approach efficiently computed spatiotemporal characteristics during indoor and outdoor gait for a more holistic gait assessment. Here, extracted spatiotemporal characteristics (e.g., indoor step, stance, swing times: 0.566s, 0.647s, 0.489s, respectively, outdoor step, stance, swing times: 0.534s, 0.597s, 0.476s, respectively) show good agreement with previous indoor level walking (0.534s, 0.668s, 0.401s) [436] and outdoor level walking (0.593s, 0.741s, 0.449s) studies [22] for HP. The small difference between the extracted temporal results perhaps is due to the difference between preferred experimental protocols, preferred sensor location, sensors, and algorithms. This is equally true for SS; indoor level walking (step, stance, swing times: 0.614s, 0.770s, 0.483s, respectively) and outdoor level walking (step, stance, swing times: 0.535s, 0.748s, 0.452s, respectively) findings of this study show good agreement with a previous study [169], where indoor level walking (step, stance, swing times: 0.6 s 0.743s 0.485, respectively) and outdoor level walking (step, stance, swing times: 0.613s, 0.764s, 0.474s) are reported. However, small differences (e.g., in stance-swing times <0.09s) were also observed in the stroke population due to referenced studies using a single IMU attached to the lower back compared to my approach of two IMU's attached to both shanks. Performance comparison of sensor locations and used methodology was further investigated[150, 305]. It was found that the shank-based methods provide more accurate temporal results compared to lower back based methods because the sensor is closer to IC-FC points of the foot. Moreover, reference studies used an algorithm based on acceleration signals whereas the proposed fusion approach used algorithms based on angular velocity for extracting spatiotemporal outcomes. The proposed multi-modal approach also attests to the existing knowledge that stroke survivors are high likely to experience decreased stance time and increased swing time in the paretic side, compared to non-paretic[437].

Many physical therapy techniques focus on the restoration of joint kinematics and hence promote the rehabilitation of functional activities [411]. Thus, kinematic joint characteristics are crucial as these characteristics provide additional insight into indoor/outdoor gait analysis. The prevalence of joint kinematic analysis in gait studies is low as kinematic characteristics require lab-based motion analysis systems that are complex and costly or goniometers, which brings synchronisation issues with other technologies [2]. Alternatively, a few gait studies estimate joint angles (e.g. knee flexion) during indoor and outdoor activities using wearable sensors [399, 403]. Findings of the proposed multi-modal sensor fusion tool (62.621°, 48.120° for indoor level walking of HP and SS, respectively) show good agreement with previous study findings based on indoor level walking (~60°, ~40°

for indoor level walking of HP and SS) [38, 438] and outdoor [439, 440] activities in terms of estimated knee joint angles. Additionally, stroke participants experience decreased knee flexion angles during indoor/outdoor level walking on the paretic side, compared to non-paretic as previously reported [438].

Muscle activation pattern analysis of one or more muscles, particularly when the examination is conducted together with additional gait characteristics such as kinematics (joint angles), provides better insight into the performance of muscles and their role in accomplishing a motor task [441]. Although other crucial parameters, such as walking velocity and age that affect muscle burst timing and durations exist [442], comprehensive knowledge of muscle activation and co-activation may contribute to the individualised bespoke rehabilitation programs[142]. The findings of the proposed multi-modal fusion tool attest to the common muscle activation patterns in terms of muscle burst timings and durations during indoor [132, 442] and outdoor activities [412, 441].

7.2.6. Implementation-M1

Importantly, extraction of multi-model gait characteristics starts with the detection of gait cycles, IC, and FC events. ***A1*** and ***A2*** were sufficient to estimate IC-FC moments during level walking (as well as incline walking and stair ambulation) for HP's and non-paretic sides of SS. However, failing to detect IC-FC events in the paretic side of SS, where significant foot clearance is lacking, negatively impacts the multi-model gait characteristics (primarily temporal) to be extracted. Alternatively, spatial characteristics successfully computed with ***A3*** for HP and non-paretic sides of SS, but similar problems occurred for the paretic sides of SS.

Sensor misplacement is also a consideration that needs to be considered during the implementation of this framework. It was previously reported that algorithms that use angular velocity for IC-FC detection (such as ***A1*** and ***A2***) are less sensitive to positioning compared to acceleration due to their measurement principle. ***A3*** and ***A5*** also stated that the sensor placement anywhere along the same plane on the anatomical segment (e.g., shank) gives almost identical signal output [213, 398, 400]. The proposed tool has potential use in free-living as it enables an extended period of data recording opportunities. Gyroscopes tend to consume up to several hundred milliamperes whereas accelerometers consume in the range of a few microamperes [213]. The use of additional hardware or sensing capabilities such as EMG can increase energy consumption significantly. Therefore, the energy consumption of the hardware (sensor) to be used should be taken into consideration. Here I use the Shimmer3 EMG sensor, which can be used in clinical studies as it provides reliable output for around 70 hours, depending on the activated sensing capabilities (e.g., sampling frequencies). Sensors that can collect data for a week or more are also available but there is a trade-off between e.g., data resolution, battery life and memory [2].

A review for sensor fusion use in orientation tracking found that advanced algorithms such as extended Kalman filter and complementary filter approaches should meet the need to perform offline calibration, vector selection technique for imperfect measurement rejection [443]. Although high accuracy and robust estimations were reported, these approaches are complex and require prior technical information regarding the IMUs to be used. Here, I proposed a less complex and more practical novel approach ***(A5)*** to estimate knee flexion angles during stair ambulation and incline walking by novel combination of two different validated algorithms [400, 404]. That approach allowed us to achieve a knee joint flexion angle approach that works during stair ambulation and without a need for prior configuration coefficients during orientation estimation.

EMG signals were segmented for each gait cycle using IC-FC timed events. Segmented raw EMG signals are difficult to interpret with a visual inspection alone [142]. Thus, processing raw EMG signals allow the extraction of clinically useful outcomes (e.g., muscle burst timing). Additionally, normalisation of EMG signals is crucial to make comparisons between muscles on different days or in different individuals during different walking tasks. Most studies time normalise EMG signal into gait cycles (%) or sub phases (stance %). However, the same standardisation is not common for amplitude normalisation. Peak activation level, mean activation level, maximum voluntary contraction and peak to peak maximum amplitude (M wave) normalisation approaches have been widely used [142]. Although there are standards for EMG data collection (SENIAM), EMG signal processing standards are needed to achieve a more consistent EMG-based gait assessment [2].

7.2.7. Limitations and future work-M1

Wearables offer high resolution data recording opportunities for extended periods. Continuous recording during free-living may result in a vast amount of unlabelled data that includes different daily dynamic gait activities (e.g., level walking, stair ambulation) and static activities (e.g., sitting, lying). Here, the proposed framework was used with manually segmented gait data (e.g., indoor level walking). However, manual segmentation of different activities before feeding into the proposed framework is a limitation to achieve a more automatic gait assessment tool. Therefore, automatic recognition of all activities (also known as human activity recognition, HAR) would provide a more pragmatic gait analysis tool, negating the time-consuming manual segmentation adopted here. Previous studies report that wearables can be deployed to recognise gait events with high accuracies using artificial intelligence approaches (e.g. machine learning, deep learning) [444, 445].

The time spent on sensor configuration and placement before data collection can be accepted as a limitation since it was approx. 50% of the total testing time for each participant. Here, the configuration of wearables and placement took 15-20 min for each participant. Much of the time (≈10 min) was spent on the placement of surface EMG electrodes and their connections with sensor units using wires. Technology is becoming more user friendly with wireless EMG sensors which could significantly decrease the setup time of wearables.

Successful implementation of the proposed multi-modal approach is significantly dependent on the correct detection of IC-FC times that is used to split gait into sub-phases and extract joint angles and muscle activities. As presented in (Figure 15, b), more oscillations were observed in paretic side angular velocity compared to the non-paretic side of a stroke survivor. These oscillations affect the accuracy of proposed algorithms (e.g. ***A1***) as these algorithms estimate IC-FC times by taking reference to a single positive peak (mid-swing) [162]. In the paretic side of SS (#3), more oscillations were observed in peaks during mid-swing, and negative peaks were not present for the detection of IC-FC moments. Therefore, the proposed algorithms (***A1*** and ***A2***) failed to detect IC-FC moments, and consequently, kinematic and muscle characteristics could not be extracted for the gait cycles.

Some algorithms presented here use a set of rules and thresholds. The use of threshold-based algorithms could be a limitation since time and frequency domain features of the wearable signals can be significantly affected by several factors such as weight, age, the severity of impaired gait and walking speed. Alternatively, previous studies suggested that although amplitudes of these peaks vary depending on different factors, IC-FC moments can always be localised once approximate locations are known in time and frequency domains [2, 222]. Therefore, appropriate signal processing approaches (e.g. advanced wavelet) and artificial intelligent (machine learning, deep learning) approaches should be used in future studies to overcome this limitation [446]. Equally, developing new algorithms by considering signal power and statistical features rather than wave shape could be a solution for the algorithms that rely on peak detection.

7.2.7.1. Factors influencing the accuracy of gait characteristics

Small errors and systematic delays (e.g. <0.009s) are present even in two different gold/reference standard systems [150]. Therefore, it is crucial to investigate and interpret the agreement levels between reference systems and wearable sensors with caution. Although most inertial signal-based validation studies reported very good agreements when compared to a gold standard system[222, 399], the developed algorithms were validated on healthy participants only during controlled environments. When these algorithms were adopted to use in a neurological population, it was observed that their accuracies decrease [7, 398]. The primary reason for the poor performances of the algorithms is that movement patterns of hip and lower-limb segments experience different acceleration and angular velocity compared to healthy participants[7]. The secondary reason is the effects of the walking environments. This was further investigated by Storm *et al.* who reported that shank sensor-based algorithms such as ***A1-A2*** perform better in outdoor walking in terms of detecting some temporal parameters (e.g., stance time) compared to indoor walking [150]. The other reasons that affect the accuracy of inertial signal-based gait outcomes are preferred sensor locations (e.g., shank, lower back) and used target signal (e.g., acceleration, angular velocity) in the experimental protocol. A previous study investigated the impact of both factors on the extracted parameters, and findings showed that shank level sensor angular velocity signals pair provide more

accurate and repeatable results than lower back sensor- acceleration signal algorithms for healthy participants[214].

My future work will aim to:

(i) investigate validity in a larger stroke cohort with the latest technology wearable sensors (e.g., wireless EMG),

(ii) integrate automated gait detection into a multi-modal fusion approach to achieve an automatic approach and,

(iii) investigate potential solutions for better detecting IC-FC moments in neurological conditions, particularly in severely disrupted gait.

****

7.3. M2 results: Human activity recognition using feature-level fusion of IMU and EMG data

This section presents the performances of SVM and kNN models for walking, standing, stair ascent and descent activities.

7.3.1. HAR with inertial data-M2

Table 15 shows the classification performances of the different classifiers for single and two sensor modalities that include inertial data only. SVM (ACC% = 91.4, 93.0, 95.5) had better classification than kNN (86.0, 87.2, 88.3) for SR, TR, and SR+TR, respectively. Multi-modal sensor configurations and data level fusion classified activities with higher ACC., SEN., and SPE. than the single sensor, where thigh-level wearable slightly outperformed the shank-level wearable for HAR.

7.3.2. HAR: Inertial and sEMG (filter and use of LE)-M2

After post-processing IMU and sEMG signals, data fusion is performed at the feature level to improve the classification. Table 16 presents the results of the different models trained with inertial and sEMG data. Here, sEMG signals were bandpass filtered and corresponding features were extracted. When classification is performed with only SR sensor data, the use of GS muscle data resulted in higher performances than TA.

Table 15.HAR with inertial data only

Case	SVM			kNN		
	ACC.	***SEN.***	***SPE.***	***ACC.***	***SEN.***	***SPE.***
SR	91.4	0.915	0.971	86.0	0.858	0.953
TR	93.0	0.930	0.976	87.2	0.871	0.957
SR+TR	95.5	0.955	0.985	88.3	0.879	0.961

SR shank right and TR: thigh right

Table 16.HAR with inertial data and sEMG data (Bandpass filtered)

Case	SVM			kNN		
	ACC.	***SEN.***	***SPE.***	***ACC.***	***SEN.***	***SPE.***
SR+TA	90.3	0.904	0.967	85.2	0.849	0.951
SR+GS	92.6	0.926	0.976	89.6	0.897	0.966
SR+TA+GS	91.8	0.918	0.973	89.1	0.889	0.964
TR+RF	93.5	0.935	0.978	88.0	0.879	0.960
TR+BF	94.4	0.944	0.981	88.9	0.885	0.963
TR+RF+BF	94.7	0.946	0.982	88.9	0.884	0.963
SR+TR+TA+RF	94.2	0.942	0.981	89.6	0.893	0.965
SR+TR+GS+BF	95.2	0.953	0.984	89.4	0.895	0.965
SR+TR+CASE*	95.6	0.956	0.985	90.7	0.904	0.969

SR: shank right, TR: thigh right, TA: Tibialis anterior, RF: Rectus femoris, GS: Gastrocnemius, BF: Biceps femoris.
*CASE=TA+GS+RF+BF

Table 17.HAR with inertial data and sEMG data (LE)

Case	SVM			kNN		
	ACC.	***SEN.***	***SPE.***	***ACC.***	***SEN.***	***SPE.***
SR+TA	95.3	0.953	0.985	90.8	0.908	0.970
SR+GS	94.7	0.947	0.982	89.1	0.890	0.964
SR+TA+GS	96.5	0.964	0.988	92.2	0.921	0.974
TR+RF	95.5	0.953	0.985	89.7	0.892	0.966
TR+BF	96.5	0.965	0.988	88.5	0.886	0.962
TR+RF+BF	98.1	0.980	0.994	92.2	0.917	0.974
SR+TR+TA+RF	97.2	0.971	0.991	92.6	0.923	0.976
SR+TR+GS+BF	97.5	0.974	0.992	92.6	0.922	0.976
SR+TR+CASE*	99.0	0.990	0.997	94.6	0.944	0.982

SR: shank right, TR: thigh right, TA: Tibialis anterior, RF: Rectus femoris, GS: Gastrocnemius, BF: Biceps femoris.
*CASE=TA+GS+RF+BF

For TR multimodal sensor data, use of BF had higher performance than RF. Additionally, thigh level inertial and sEMG better classified HAR than shank, Table 16. To investigate impact of post-processing on classification, LE was obtained from band-pass filtered sEMG data using rectification operation). Results of the two different HAR models based on sEMG-LE are shown in Table 17. Feature level classification with LE seems to provide a better overall classification compared to band-pass filtered sEMG (ACC., SEN., SPE.). Comparing Table 16 and Table 17, overall accuracy was improved by 3.11% in SVM models and 2.54% in kNN models. Figure 17 was created using confusion matrixes derived from a case (TA+GS+RF+BF) to display differences between performance for each activity. Here, HAR accuracy increased by 4.4%, 2.2%, 3.6%, 3.6%(SVM) and 3.4%, 6.9%, 1.7%, 3.9% (kNN) in stair ascent, stair descent, standing and walking, respectively.

7.3.3. M2 discussion: Human activity recognition using feature level fusion of IMU and EMG data

This chapter section investigated how sEMG data improves HAR and the importance of sEMG post-processing on classification performance. Preliminary results show use of multimodal data and feature level fusion improves HAR. This finding corroborates the existing knowledge that inertial sensor-based HAR can be further improved when fused with sEMG [447], especially in walking and stair ambulation related HAR [448]. Here, classification accuracy was increased by 3.5% for SVM and 6.3% for the kNN classifier after inertial features were fused with sEMG features. Findings also reveal how sEMG signal post-processing can impact the performance of the classifiers, where use of sEMG-LE results with higher overall performance than the use of band-pass filtered sEMG. Use of single polarity LE signal improved recognition of each activity Figure 17.

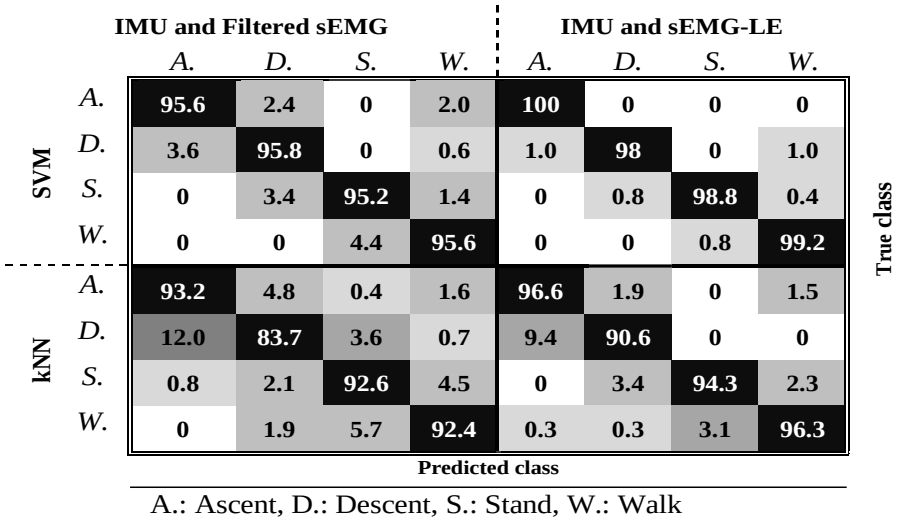

Figure 17.Confusion matrix (%) from feature level fusion classification, case (SR+ TR+ TA+ GS+ RF+ BF).

When sEMG-LE is used for training, posterior muscles GS+BF provided slightly higher classification performances than anterior TA+RF. Additionally, classification with features extracted from TR outperformed SR.

That could be useful when minimising sensing modalities in HAR systems as single or multiple sEMG configurations have been extensively studied. For example, only the gastrocnemius medial muscle [449], four lower limb muscles of one leg [339] and two legs [450] muscle activation data were utilised. I also found SVM outperformed kNN for HAR, similar to [136, 284].

Performing a direct comparison to another study would not be appropriate since I created a unique dataset for the purpose of this study. Similar to [451], significant improvement in the recognition of stair ambulation can be achieved when IMU data is fused with EMG. Several factors could contribute to this including the extracted features. Instead of extracting a single wearable dependent feature [136, 408], I extracted an orientation feature knee flexion/extension [452] that improved classification. This was motivated from [411] that reported knee flexion/extension angles and wave shapes during walking, stair ascent and descent are unique to those activities. Another factor to explain classifier improvement is the use of agonist and antagonist muscle pairs that are responsible for the activity (e.g. knee flexion/extension during walking) [413]. There was a study limitation, datasets were created from healthy subjects in a controlled environment and with a scripted protocol. Equally, I did not assess my approach for identifying separate tasks as the focus here were all activity tasks. A future study will include neurological cohorts, HAR for mobility specific tasks as well as application on independent datasets to examine wider performance.

****

7.4. M3 results: Improving inertial sensor-based activity recognition in neurological populations

7.4.1. UCI-HAR datasets-M3

Table 18 presents the results of performance metrics for initial and enhanced states in UCI-HAR. In the initial state, ResNet18 architecture slightly outperformed its counterparts in all performance metrics. Moreover, the data augmentation operation provided slight improvements in the performance metrics of each architecture whereas the largest improvement was observed in GoogleNet. In the enhanced state, ResNet50 architecture provided slightly higher performances compared to other CNN architectures and reached 97% accuracy. However, comparing execution time reveals that GoogleNet classifies HAR activities faster than its counterparts. Table 19 presents the ResNet50 confusion matrix of UCI-HAR dataset in the initial and enhanced states as it outperforms other architectures in terms of all performance metrics except execution time. Here, notable improvements are observed after data augmentation especially in static activities (sitting, standing, and laying).

Table 18.HAR performance metrics in UCI HAR dataset

		Initial state					Enhanced state					
DL-CNN Epochs:5 Iteration:3750 Learning rate:0.001 Batch size: 32	Pre-trained network	Acc. (%)	Sens.	Spec.	F1	MCC	Acc. (%)	Sens.	Spec.	F1_	MCC	Training time (minutes)
	ResNet18	93.3	0.929	0.987	0.928	0.915	96.1	0.960	0.992	0.961	0.953	89.26
	ResNet50	91.8	0.914	0.984	0.911	0.897	97.0	0.970	0.994	0.970	0.964	165.38
	MobileNet-v2	90.7	0.903	0.982	0.899	0.883	96.2	0.962	0.992	0.962	0.954	143.41
	GoogleNet	81.0	0.803	0.962	0.800	0.771	91.9	0.919	0.984	0.918	0.903	75.55

Acc.: accuracy, Sens.: sensitivity, Spec.: specificity, F1: F1_score

Table 19.Confusion matrix of UCI HAR- ResNet50 (initial results-left, final results-right)

	Walking	Ascent	Descent	Sitting	Standing	Laying
Walking	106	0	0	0	0	0
Ascent	0	108	0	0	0	0
Descent	0	1	106	0	0	0
Sitting	0	0	0	89	3	12
Standing	1	1	0	14	66	11
Laying	0	0	0	2	4	76

	Walking	Ascent	Descent	Sitting	Standing	Laying
Walking	494	0	1	0	0	0
Ascent	1	547	3	0	0	0
Descent	1	0	477	0	0	0
Sitting	0	0	1	465	12	17
Standing	0	0	0	19	461	11
Laying	0	0	0	15	8	467

7.4.2. WISDM datasets-M3

Table 20 presents classification results of the four CNN architectures using the WISDM dataset in initial and enhanced states. In the initial state, ResNet50 architecture classified HAR activities better than ResNet18 and MobileNet-v2 whereas GoogleNet showed a notable poorer performance. However, this is not valid for specificity metrics which experienced similar values in all architectures. After data augmentation is implemented, significant improvements are observed in all architectures. ResNet18 reached 95.8% accuracy with the shortest training time whereas ResNet50 and MobileNet-v2 are provided slightly lower accuracies but in a much longer time (≥130min). Although GoogleNet is improved in its enhanced state, it is still the poorest in activity recognition compared to other architectures. Table 21 presents the confusion matrix for the best-enhanced state (ResNet18). Comparing activity recognition performances for each class in the initial and enhanced state reveals that the largest improvements are obtained in accurate recognition of static activities (sitting and standing).

Table 20.HAR performance metrics in WISDM dataset

		Initial state					Enhanced state					
DL-CNN Epochs:5 Iteration:3750 Learning rate:0.001 Batch size: 32	Pre-trained network	Acc. (%)	Sens.	Spec.	F1	MCC	Acc. (%)	Sens.	Spec.	F1	MCC	Training time (minutes)
	ResNet18	83.5	0.832	0.967	0.828	0.799	95.8	0.958	0.992	0.958	0.949	72.2
	ResNet50	86.0	0.854	0.972	0.854	0.827	95.4	0.953	0.991	0.953	0.944	163.49
	MobileNet-v2	82.7	0.821	0.965	0.821	0.787	95.4	0.953	0.991	0.953	0.944	129.52
	GoogleNet	71.5	0.719	0.943	0.718	0.678	89.3	0.891	0.979	0.892	0.871	80.27

Acc.: accuracy, Sens.: sensitivity, Spec.: specificity, F1: F1_score

Table 21.Confusion matrix of WISDM dataset – ResNet18 (initial results-left, final results-right)

	Jogging	Walking	Ascent	Descent	Sitting	Standing
Jogging	100	2	0	3	0	1
Walking	0	106	0	2	0	0
Ascent	3	4	85	12	0	3
Descent	3	4	8	79	5	5
Sitting	0	0	0	1	60	32
Standing	0	1	0	0	10	71

	Jogging	Walking	Ascent	Descent	Sitting	Standing
Jogging	488	3	3	1	0	0
Walking	0	546	0	5	0	0
Ascent	5	6	453	8	2	4
Descent	0	6	20	457	4	8
Sitting	0	0	3	1	468	19
Standing	0	0	4	2	21	463

7.4.3. Local datasets (HS model)-M3

Table 22 shows the initial and enhanced state results of HAR in the local dataset created from HS. In the initial state, MobileNet-v2 architecture outperforms its counterparts in terms of each performance metric whereas GoogleNet architecture performs poorly in recognition of HAR activities. Significant improvements are observed in the enhanced state where ResNet50 reaches the highest accuracy with 100%, especially GoogleNet accuracy is more than doubled in the enhanced state. Table 23 presents the confusion matrix created from ResNet50 architecture which experienced misclassification in recognition of stair activities in the initial state. After data augmentation, ResNet50 architecture better adopted stair classes and corrected the misclassifications.

Table 22.HAR performance in local HS dataset

DL-CNN Epochs:5 Iteration:190 Learning rate:0.001 Batch size: 32	Initial state						Enhanced state				
	Pre-trained network	Acc. (%)	Sens.	Spec.	F1	MCC	Acc. (%)	Sens.	Spec.	F1	MCC
	ResNet18	80.0	0.821	0.936	0.803	0.753	99.7	0.997	0.999	0.997	0.996
	ResNet50	82.5	0.827	0.942	0.822	0.765	100.0	1.000	1.000	1.000	1.000
	MobileNet-v2	85.0	0.863	0.951	0.852	0.810	97.5	0.975	0.991	0.975	0.967
	GoogleNet	42.5	0.358	0.798	0.313	0.224	95.3	0.953	0.984	0.952	0.937

Acc.: accuracy, Sens.: sensitivity, Spec.: specificity, F1: F1_score

Table 23.Confusion matrix of HS local dataset– ResNet50 (initial results-left, final results-right)

	Ascent	Descent	Walking	Standing		Ascent	Descent	Walking	Standing
Ascent	9	2	1	0	Ascent	86	0	0	0
Descent	2	5	0	0	Descent	0	95	0	0
Walking	0	2	11	0	Walking	0	0	91	0
Standing	0	0	0	8	Standing	0	0	0	87

7.4.4. Local datasets (PD model)-M3

Table 24 presents initial and enhanced results of HAR in those with PD. In the initial state, all CNN architectures experience comparable results where ResNet18 and ResNet50 outperforms other architectures. Later in the enhanced state, notable improvements were observed in all architectures but MobileNet-v2 achieved the highest performance. Table 25 presents a confusion matrix belonging to the classification result of MobileNet-v2, where misclassification in stair descent and walking activities were improved in the enhanced state.

Table 24.HAR performance metrics in local PD dataset

DL-CNN Epochs:5 Iteration:190 Learning rate:0.001 Batch size: 32	Initial state						Enhanced state				
	Pre-trained network	Acc. (%)	Sens.	Spec.	F1	MCC	Acc. (%)	Sens.	Spec.	F1	MCC
	ResNet18	94.6	0.949	0.982	0.947	0.929	98.8	0.987	0.996	0.987	0.983
	ResNet50	94.6	0.940	0.981	0.945	0.928	99.0	0.989	0.997	0.990	0.986
	MobileNet-v2	92.9	0.936	0.976	0.931	0.908	99.2	0.992	0.997	0.992	0.989
	GoogleNet	89.3	0.895	0.964	0.896	0.864	97.61	0.973	0.991	0.978	0.975

Acc.: accuracy, Sens.: sensitivity, Spec.: specificity, F1: F1_score

Table 25.Confusion matrix of PD local dataset– MobileNet-v2 (initial results-left, final results-right)

	Ascent	Descent	Walking	Standing		Ascent	Descent	Walking	Standing
Ascent	15	1	0	2	Ascent	121	1	0	2
Descent	1	10	0	0	Descent	0	99	0	0
Walking	0	0	13	0	Walking	0	0	135	0
Standing	0	0	0	14	Standing	0	0	1	145

7.4.5. Local datasets (SS model)-M3

Table 26 shows performances from initial and enhanced states in the local SS dataset. In the initial state, ResNet18, ResNet50 and MobileNet-v2 experience accuracies just above 70% whereas GoogleNet shows the poorest performance with 65.7% accuracy. In the enhanced state, all architectures except GoogleNet experience significant improvements and reach over 95% accuracy. On the other hand, GoogleNet also experience improvements but with a small margin compared to its counterparts. Table 27 present confusion matrix of ResNet50 from initial and enhanced states. In the SS group, stair ascent occurrences were mostly misclassified whereas stair descent and walking activities suffered from low recognition. In the enhanced state, notable improvements were observed, especially in stair activities.

Table 26.HAR performance in local SS dataset

		Initial state					Enhanced state				
DL-CNN Epochs:5 Iteration:190 Learning rate:0.001 Batch size: 32	Pre-trained network	Acc. (%)	Sens.	Spec.	F1	MCC	Acc. (%)	Sens.	Spec.	F1	MCC
	ResNet18	74.3	0.690	0.917	0.643	0.591	96.2	0.944	0.987	0.948	0.936
	ResNet50	71.4	0.667	0.903	0.629	0.558	98.1	0.968	0.993	0.973	0.967
	MobileNet-v2	74.3	0.690	0.913	0.650	0.590	97.4	0.960	0.992	0.960	0.952
	GoogleNet	65.7	0.500	0.874	0.563	0.516	79.8	0.655	0.927	0.656	0.647

Acc.: accuracy, Sens.: sensitivity, Spec.: specificity, F1: F1_score

Table 27.Confusion matrix of SS local dataset– ResNet50 (initial results-left, final results-right)

	Ascent	Descent	Walking	Standing		Ascent	Descent	Walking	Standing
Ascent	1	1	1	4	Ascent	36	0	0	3
Descent	0	4	0	1	Descent	1	51	0	1
Walking	0	0	12	0	Walking	0	0	120	0
Standing	1	2	0	8	Standing	0	1	0	99

7.4.6. Discussion 3: Improving inertial sensor-based activity recognition in neurological populations

The computational performance of the framework was deemed acceptable for data preparation (normalization, generally having low computational cost). Specifically, normalization of each segmented IMU window took approx. 5.4 milliseconds which was then converted into the activity image within approx. 2.1 milliseconds resulting in a total data preparation for each occurrence of about 7.5 milliseconds. However, model training was prolonged. Here, I first verify the proposed approach in benchmarking datasets and compare with reference studies. This tests whether the proposed numerical to image conversion approach is a valid and reliable approach in independent datasets. Results suggest that the proposed framework can classify activity classes in both benchmarking datasets with high accuracy, especially after the data augmentation. The pre-trained networks used in this study can achieve better or comparable classification accuracies against reference studies even when the networks are trained with a portion of the original datasets.

After promising results are obtained in benchmarking datasets, I provide an evaluation regarding the pilot studies (in HS, PD and SS) which test the proposed approach (numerical to image conversion and data augmentation) on limited local datasets. In addition, I present an analysis regarding why some CNN architectures perform better than others and recommend the necessary properties a pre-trained network needs to achieve sufficient learning.

7.4.6.1. Verification of the results in public datasets

Table 28 compares the proposed framework against several reference studies with and without data augmentation in the same public datasets. Overall, numerical to image conversion along with data augmentation significantly improves the performance of CNN architectures in HAR. This study utilized 500 occurrences/instances for each class to provide unbiased evaluation metrics as detailed in 4.1.2. Therefore, my findings should be considered in this context.

7.4.6.1.1. UCI-HAR dataset

Comparing my initial results with a reference study [369] initial results in the same dataset reveals that the proposed numerical to image conversion approach is an effective method. Here, ResNet18 architecture reaches 93.3 % accuracy which is superior to 80% accuracy [369]. In the enhanced state of UCI-HAR dataset, the methodology proposed here provides similar or better results compared to the reference studies, Table 28. Comparing the training times with a reference study [369] that uses exponential smoothing augmentation technique reveals that my approach reaches 97.0 % accuracy in 166 min training duration whereas the reference study reaches 97.9 % accuracy in 210 min. This suggests that the proposed framework can provide comparable accuracies with smaller training data with shorter durations. The difference in the training times could be attributed to the preferred data augmentation technique. For example, the exponential smoothing approach assigns exponentially decreasing

weights for older observations. However, my framework uses raw numerical data to produce activity images that are independent of the numerical values in the data stream. Producing images (e.g., activity images or spectrogram) directly from raw sensor data was proved to be effective in HAR [306, 373, 374].

7.4.6.1.2. WISDM dataset

In the initial state, my numerical to image conversion technique with ResNet50 reaches 86% accuracy that is superior to 83.4% in [369] and comparable to 86.4% in [368]. In the enhanced state, my accuracy reaches 95.8% with ResNet18 architecture that is comparable to 95.7% in [368] but poorer than 97.1% in [369]. Comparing the training time with a reference study [369] reveals that my proposed framework reaches comparable accuracies with smaller training data and shorter training duration.

Table 28.Reference studies with benchmarking datasets

Study	Method	Augmentation	Accuracy (%)	
			UCI	WISDM
Alawneh et al.**[369]**	RNN	Moving average and the exponential smoothing	97.9-80.0*	97.13-83.4*
Huang et al. **[368]**	CNN	Step detection based novel augmentation technique-not appropriate for passive activities	-	95.7-86.4*
Yen et al.**[453]**	CNN	NA	95.99	-
Jiang and Yin**[373]**	CNN	NA	97.59	-
Li and Trocan**[454]**	CNN	NA	95.75	-
Cho and Yoon**[455]**	CNN	Data sharpening	97.62	-
Proposed framework	**CNN**	**Numerical image conversion + image augmentation**	**97.0-93.3***	**95.8-86.0***

* Represents initial results where available

7.4.6.2. Verification in local datasets

I tested the proposed approach (initial state and enhanced state) on local datasets of HS, PD and SS groups. In the initial state, in terms of accuracy, CNN architectures provide higher performances in PD dataset compared to HS and SS. This could be associated with the fact that PD dataset is more balanced than SS and larger than both HS and SS. In addition, majority classes (walking and standing) are better recognized than minority classes (ascent and descent) in PD dataset. When the sizes of the datasets were artificially increased with data augmentation techniques in the enhanced state, improvements were achieved in all CNN architectures. It is important to highlight that data augmentation has no impact on the balance of a dataset because each class is enhanced at the same rate.

Figure 18 presents the average performances of all CNN architectures from Table 22, Table 24, Table 26. Sensitivity and specificity values were normalized to 0-100 to present comparable results against accuracy. Comparing initial and enhanced results considering the overall performance of all CNN architectures in the local datasets reveals that the largest improvement in terms of accuracy is observed in HS with 25.6% followed by SS with 21.4% and PD with 5.8%, as seen in Figure 18. Comparing accuracy, sensitivity, and specificity reveals that data augmentation had the largest improvement in sensitivity with 18.81% followed by accuracy with 17.62% and relatively small improvements in specificity with 5.99%. This finding could be associated with the nature of the limited and imbalanced local datasets. In the initial state, the number of true positive (TP) and true negative (TN) in the classification were relatively low. After data augmentation, models experienced better performance in predicting positive classes compared to negative classes. This resulted in a larger increase in TP compared to TN. Consequently, improvements in sensitivity were found significantly larger than specificity.

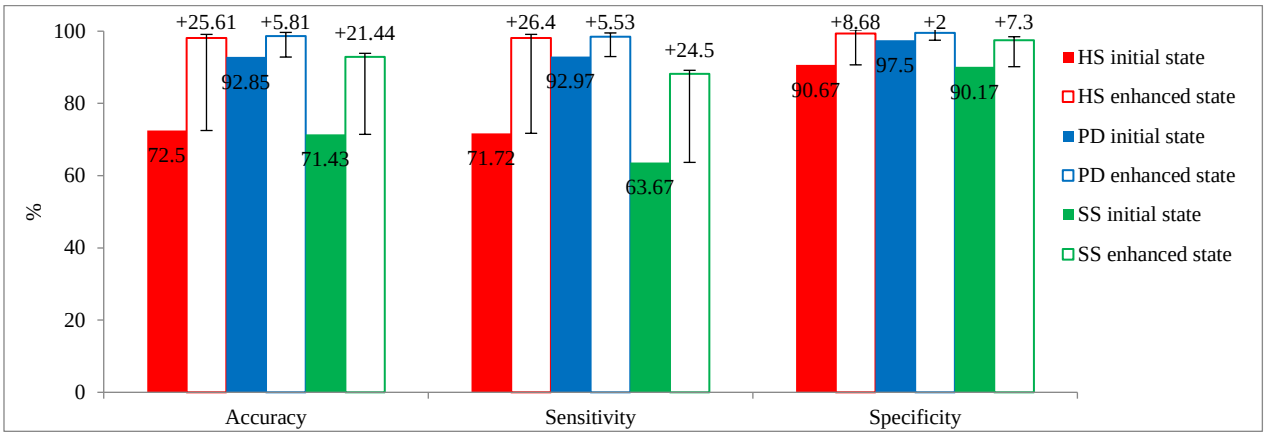

Figure 18.Comparison of performance metrices between initial and enhanced states in local dataset. Sensitivity and specificity values are normalized to 0-100 to provide comparable results with accuracy.

All four CNN architectures showed a test accuracy exceeding 90% in the enhanced state. ResNet50 outperformed all other architectures in the enhanced state whereas MobileNet-v2 achieved the best result in the initial state. Although GoogleNet architecture experienced the sharpest enhancement after data augmentation, overall performance in both initial and enhanced states is poorer than its counterparts, as shown in Figure 19. Interpreting these outcomes with the properties of pre-trained CNN architectures (Table 11) could provide useful information regarding the most suitable CNN architecture. Initially, comparing ResNet18 (18 layers) with ResNet50 and MobileNet-v2 (50 and 54 layers) reveals that higher network layer does not necessarily provide better accuracy because ResNet18 achieved comparable results, aligning with the findings of a previous study that employs the same CNN architectures[425]. This suggests that network size and the number of parameters that a network can learn also have an impact on the accuracy. Among the two architectures with the greatest number of deep layers, ResNet50 (larger size and more parameters) provides better classification than MobileNet-v2 (smaller size and fewer parameters) in the enhanced state. Alternatively, MobileNet-v2 (smaller size and fewer parameters) achieves better results than ResNet50 (larger size and more parameters) in the initial state where the dataset is limited and unbalanced. This phenomenon can also be partially observed when two architectures with the lowest number of deep layers are compared. ResNet18 (larger size and more parameters) achieves higher performance than GoogleNet (smaller size and fewer parameters) in the enhanced state. As a result, findings of enhanced state suggest that CNN architectures require approximately 22 deep layers and 7 million parameters (GoogleNet) to classify walking, standing, ascent and descent activities with more than 90% accuracy. To achieve better accuracy, the number of deep layers and/or the number of parameters needs to be increased. The maximum accuracy can be potentially achieved with approximately 50 deep layers and 25.6 million parameters (ResNet50) or approximately 54 deep layers and 3.5 million parameters (MobileNet-v2) because ResNet50 and MobileNet-v2 were found superior in HS, SS and PD datasets, respectively. On occasions when training time is considered as important as accuracy, ResNet18 architecture could be potentially a more suitable choice because this architecture has fewer deep layers and fewer parameters (fewer computation costs) than ResNet50. However, inconsistencies can occur as the previous study [416] reports that not all CNN architectures use their parameters with the same level of efficiency.

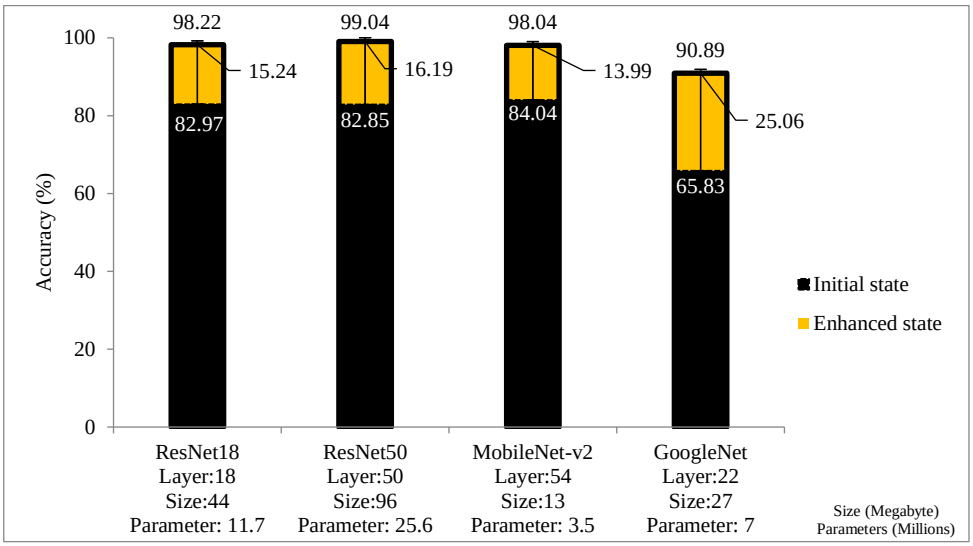

Figure 19.Comparison of CNN architectures in terms of accuracy in initial and enhanced status in the local datasets (HS-SS-PD combined)

My findings revealed that walking and standing are recognized with higher accuracy compared to stair activities, as shown in Figure 20. I also found stair ascent is the activity with the lowest recognition accuracy, aligning with many previous studies that use a single waist device [18, 368, 456]. Moreover, the figure reveals that data augmentation contributes to better detection of stair ascent and stair descent by 39.1% and 18.0%, respectively. These findings align with a similar study [368] where data augmentation was shown to be effective in recognizing stair activities. Recognition of basic daily life activities in PD and stroke populations with high accuracy has potential to provide more robust and accurate movement analysis in real life. This framework can be used to accurately classify walking bouts and assist extraction of clinically important spatiotemporal parameters during walking. Moreover, it can also provide a better picture of functional capabilities of people with PD and stroke by recognizing stair ambulation activities more accurately.

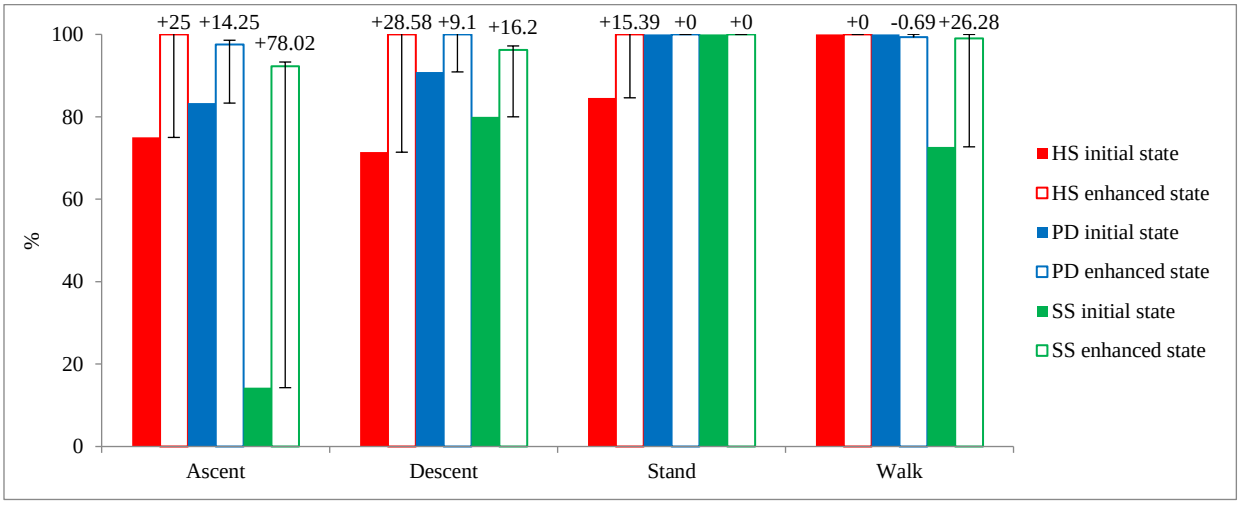

Figure 20.Recognition accuracy comparison of each activity in initial result of local dataset. This graph was derived from the architectures that provide the best performances in enhanced results.

7.4.7. Limitation and future work-M3

A limitation of the work includes total model training time. Deep learning models are structurally different from traditional machine learning models and involve significantly more training parameters, Table 11. Therefore,

deep learning-based CNN models are more complex than traditional machine learning models [457]. This computational complexity can be observed in training times in Table 18, Table 20. Although the training time reported in this study is shorter than a reference study [369], it still needs improvements.

In this chapter section, the framework was examined within the context of four basic mobility tasks only. In addition, the dataset was created in a semi-controlled environment with a scripted experimental protocol, i.e., all participants walked in the same route while wearing the same device. Future studies will aim to investigate the performances of more complex daily activities in free living environments (e.g., home). In addition, this framework can be deployed to advanced microcontrollers (Raspberry Pi 4- 1.5 GHz) to perform real-time HAR. However, this could still be slower than offline computing as a faster CPU (Core i7-7700HG-2.80 GHz) is used in this study.

7.5. Conclusion

In this chapter, a multi-layer fusion framework was initially devised, incorporating sensor data and gait characteristics, to facilitate comprehensive multimodal gait analysis. The proposed fusion approach exhibits the potential in enabling a more holistic assessment of gait across diverse indoor and outdoor terrains. The study findings demonstrate the preliminary effectiveness of this approach by revealing distinctions between indoor and outdoor experiments in terms of spatiotemporal parameters, knee joint kinematics, and muscle activities. These insights have implications for the development of individualized rehabilitation strategies, as they offer valuable information for tailoring interventions based on the specific gait characteristics observed.

Later, a feature-level sensor fusion framework was developed to combine IMU and EMG sensor data to achieve highly accurate HAR models. Here, various EMG signal processing methods were utilised to investigate how accuracy changes. Findings suggest the integration of sEMG and inertial features enhances human activity recognition (HAR) performance, particularly for activities involving stair ascent and descent. Utilising features extracted from a linear envelope of sEMG signals yields higher classification accuracy compared to features obtained from band-pass filtered sEMG signals. Furthermore, the inclusion of sEMG data from posterior leg muscles demonstrates slightly superior HAR performance compared to the inclusion of sEMG data from anterior leg muscles.

Finally, I intended to increase low AI model performance in limited HAR datasets of people with neurological conditions using data augmentation techniques. The results demonstrated substantial improvements in HAR accuracy across all activities following the artificial augmentation of the data. Furthermore, the findings highlighted the significance of developing population-specific models to achieve higher levels of accuracy for each population. The next chapter will provide reflection and possible research directions.

Chapter 8 Reflection and possible research directions

This chapter uses text from my previously published online article to fit the context and narrative of this thesis. The article appears as a book chapter (Sensor Integration for Gait Analysis), appearing in the book **Encyclopaedia of Sensors and Biosensors** published by **Elsevier** in 2023. Permission granted to freely use the whole chapter with declaration of authorisation included in Appendix 10.

(URL: https://doi.org/10.1016/B978-0-12-822548-6.00139-4)

Permission to reuse up to 6x 500- word excerpts of the published work was obtained from Elsevier on 26 May 2023 – License Number: 5556550154630. The declaration of authorisation is included in (Appendix 10).

Permission to reuse 2 figures of the published work was obtained from Elsevier on 26 May 2023 – License Number: 5556550272693. The declaration of authorisation is included in (Appendix 10).

8.1. Introduction

This chapter presents my reflection on methods I developed and presented in Chapters 6 and 7. After reflecting on these methods, I will explore potential research directions and focus on PoI4 to emphasise the utilisation of edge computing technology in the analysis of gait among individuals with neurological conditions.

8.2. Reflection

To this point, significant progress has been made in the development of multimodal gait analysis methods, which have been effectively combined with HAR techniques tailored for individuals with neurological conditions. This innovative combination enables me to conduct automated multimodal gait analysis without the need for manual gait segmentation in clinics and various environments, even over extended periods of time. The integrated framework can be summarised as follows:

The process of multimodal gait analysis commences with the collection of data using multiple wearable inertial and EMG sensors attached to the patient's body. Inertial data is sampled at a rate of 100 Hz, while EMG data is sampled at 512 Hz, following device configuration. The collected data is stored in memory cards within each sensor unit, with timestamps facilitating synchronisation across multiple wearable devices. Subsequently, the data is transferred to a computer for post-processing. The duration of data upload typically takes a few hours or more, depending on the length of data collection. Pretrained AI models are then employed to segment various activities, such as walking, stair ascent, and stair descent, utilizing the inertial data. This segmentation process involves dividing the data into 2.5-second windows (almost equivalent to two strides) and classifying each window based on the inertial data. Once all walking bouts, including stair activities, have been successfully segmented, multimodal gait analysis is conducted, considering the specific type of activity. While the developed methodologies have proved beneficial in exploring PoI1, PoI2, and PoI3 the post-processing stage remains time-consuming for researchers.

8.3. Possible research directions: Remote monitoring considerations

8.3.1. Why is innovation needed?

Since its inception in 1948, the National Health Service (NHS) in the United Kingdom has transformed and evolved to be the fifth-biggest employer globally and delivers care to over 1 million patients every 36 hours [458]. This has required the NHS and many other healthcare systems to change and adapt to new ways of working and incorporate new technological advances over the past seven decades.

By 2050, the number of people over 65's will outnumber children (under 15s) for the first time ever, driven by decreases in infant mortality [459]. Although this trend of reduced infant mortality should be celebrated, the consequence of people living longer has added a significant financial and social burden to health care in the NHS (and elsewhere). An ageing population is not the only challenge facing society, alongside is the rise in complex co-morbidities such as Dementia and Alzheimer's disease, which are now the leading cause of death in the UK [460]. The Covid-19 pandemic has also highlighted the limitations and fragility of the current volume-based healthcare system, and it is struggling to meet the expectations of society, government, staff and most importantly, patients.

8.3.2. Embracing remote monitoring with wearables

One promising opportunity to alleviate the pressure on health structures such as the NHS and deliver improved care, efficiency and outcomes for patients and society is remote assessment via medical technology (MedTech) including wearables. Defined as "products, services or solutions used to save and improve people's lives" [461], MedTech is estimated to be worth over half a trillion dollars worldwide [462] and is a significant driver of healthcare, economic growth and job creation.

Wearables can capture meaningful health data during passive tasks like walking. Walking, generally perceived as a simple and routine task, requires significant cortical processing and integration of many complex systems and has already shown considerable value in detecting impairments and disease progression [94, 463-466]. For example, slow walkers at the age of 40 were found to have more signs of accelerated aging and a variety of

neurological impairments [467, 468]. Overall, there is likely to be a wide variety of improvements and innovations in the 'anytime & anywhere' healthcare domain, central to remote monitoring. However, clinical adoption and adherence to technology will be critical in realising the benefits and contributing to personalised medicine and healthcare. Here I highlight the drivers, the type of changes that may occur in the future, and how this may be achieved.

- **Citizens, society, and patients**

Citizens and patients alike will be more involved, engaged, informed, and therefore empowered to review their health status, personal data, and management of care. Crucial to this successful implementation is ensuring patients feel involved and trust the healthcare system. Widening access to healthcare and reducing societal inequalities will drive better early diagnosis and self-management of conditions. Co-created (patient and researcher) healthcare research is important to develop trust and ensure technology is successfully integrated into the healthcare system.

- **Health System and healthcare professionals**

Digital transformation and technology can increase the effectiveness, efficiency, connectivity, and resilience of healthcare systems. Central to achieving this transformation is a requirement to upskill and improve all health professionals' digital skills/literacy to support a sustainable and learning health system. This will free up time for clinicians to offer patient-centred care and spend more time with patients, often referred to as the 'gift of time' and most importantly, compassionate care.

- **How can this be achieved?**

As technologies become more mature, embedded and mainstream, the next stage of a digital transformation will move away from a project-based implementation plan to one where data and technology are viewed as strategic assets. Empowering data-driven decisions will require a cultural shift to a digital culture that builds trust, supports a learning health system, and better connects healthcare professionals to patients. Building trust and patient engagement will be paramount. Overall, this will allow the strategic move from a traditional volume-based model of care to value-based care. Improving the ability to respond to the everchanging and increasingly volatile global health system.

The future of technology deployment and remote assessment will depend on balancing the best use of technology and data to optimise patient outcomes and safeguard patient privacy. To achieve this, the role of Government, academia, and industry in establishing the appropriate regulatory framework will be critical to ensure confidentiality and patient control over data. If this can be achieved, then the future of technology can be diverse, positive, and impactful. A summary of some of the processes outlined here to enable wearable use in clinical care is summarised in Box 1.

- Creating a culture for transparent, ethical, secure, and patient-centric data
- Moving to value-based healthcare models
- Academic and private sector (health technology) collaboration
- Diverse stakeholder leadership (patient, clinician, academic and regulator)

Box 1: Embracing remote monitoring with wearables

8.4. Conclusion

This chapter presented my reflections on automated multimodal gait analysis and its limitations such as time-consuming post-processing. From this point, I focused on mitigating problems of offline processing using edge computing, and IoT technology to enable a remote automated gait assessment tool.

The advantages of remote gait analysis are numerous. Firstly, it would eliminate the need for patients to travel to clinics, which can be particularly beneficial for individuals with limited mobility or those residing in remote areas. During times such as the COVID-19 pandemic, when individuals need to isolate themselves, remote gait analysis using wearable sensors and edge computing could become particularly valuable. Remote gait analysis also offers the potential for long-term monitoring, enabling the continuous assessment of gait patterns in natural environments. This longitudinal data can provide valuable insights into disease progression, treatment efficacy, and the impact of interventions. Moreover, remote gait analysis has the potential to revolutionize research studies

by enabling large-scale data collection. Researchers can remotely recruit participants from diverse geographic locations, resulting in more representative study populations. This approach allows for the collection of habitual gait data, minimising the influence of artificial laboratory conditions. The availability of rich, real-world gait datasets can significantly enhance the development and validation of gait analysis algorithms and models. In the next chapter, I will present a developed technology and methodology that allows automated remote gait analysis.

Chapter 9 Gait analysis on the Edge

This chapter uses text from a manuscript I prepared during my doctoral study to fit the context and narrative of this thesis.

The manuscript titled "Gait on the Edge: A Proposed Wearable for Continuous Real-Time Analysis Beyond the Lab" has been submitted to the journal Computer Methods and Programs in Biomedicine.

9.1. Introduction

In this chapter, I introduce a newly developed remote gait analysis device that utilizes cutting-edge edge computing technology. I provide a comprehensive overview of the hardware and software components incorporated into the design, delving into their functionalities and intricacies. Furthermore, I present detailed experimental results obtained from rigorous validation studies conducted to assess the device's performance and accuracy. Through this chapter, readers will gain a thorough understanding of the remote gait analysis device and its potential implications in the field of remote gait analysis.

9.2. Background

Wearable inertial devices are enabling a paradigm shift for gait assessment from the clinic to the home. Yet, capturing inertial data beyond clinics for long periods results in (very) large datasets. Previous studies that seek to examine gait in ecologically valid environments preferred data collection for multiple days (e.g., 2-7) or more. [21-23]. Those studies and others [8, 13, 469] used different sampling frequencies ranging between 32 and 128 Hz with 100 Hz usually preferred. Considering a single IMU device capable of sensing 3D acceleration and 3D angular velocity at 100 Hz, it can generate 600 data samples per second. Collecting 6 degree of freedom data (i.e., 2 × 3D, 100 Hz) for 7-days result in approx. >362 million data samples which is often stored locally on a device for post-processing. That requires big memory/storage capabilities locally on the device which may negatively impact its size. Alternatively, inertial data could be transferred to a Cloud/computer as it is being collected. However, streaming 600 data points into the Cloud every second would require very high bandwidth requirements along with introducing other challenges like data loss, latency, privacy, and power consumption. Moreover, post-processing often involves a time-consuming and labour-intensive task of downloading data from a memory card, locally processing on a computer, or uploading to a Cloud platform as analysing the large collection of data often requires high computational power. Specifically, inertial data captured over many days need labelling/categorizing as gait bouts need to be (i) detected and segmented [470] and then (ii) examined for specific sequences as defined by the gait cycle [315].

Those challenges can be mitigated by edge computing technology [25]. Edge computing refers to the decentralization of computing power from the Cloud/computer to the edge of the network, where data is collected and processed closer to the source. Such an approach enables faster and more efficient processing of data, as well as reduced latency and bandwidth [24]. Edge computing could also enhance the capabilities of gait analysis in healthcare by efficiently processing data continuously in real-time.

Improved efficiency can be explained by examining the 600 data points (as detailed above). For temporal gait analysis, researchers require initial contact (IC) and final contact (FC) moments within the gait cycle to calculate clinically important characteristics like step, stance, and swing times. In offline processing, and once data (walking bouts) has been segmented, IC and FC points are identified through a search of IMU data [159]. Typically, in normal/healthy gait there are two steps within one second [291]. Accordingly, the first phase is to identify the walking periods, then search for four data samples/moments (right foot IC and FC, as well as left foot IC and FC) within 600 data samples to calculate temporal characteristics. Subsequently, the remaining data points are considered superfluous, akin to data collected during static activities such as sitting or lying.

In this chapter, I introduce a low-cost edge device as a viable alternative to the time-consuming and computationally intensive offline instrumented gait analysis. The proposed edge device aims to address the described challenges by leveraging artificial intelligence (AI) models in conjunction with previously validated gait algorithms at the software level. Bluetooth® Low Energy (BLE) and Internet of Things (IoT) complement the device for efficient data streaming. Specifically, the proposed edge device can identify walking bouts and perform real-time gait analysis to calculate step and stride times by detecting foot IC moments. This low-cost device can operate for up to three days outside of clinical settings and requires a smartphone with Bluetooth and internet connectivity to transmit data to a Cloud platform. To assess the efficacy of the proposed edge device, validation was performed against a reference system in a lab, with statistical parameters presented to explore agreement between both systems. Additionally, a participant-specific examination (case study) was executed, wherein an

individual wore the edge device and the same reference for a day, during their customary daily activities. The results obtained from both wearable sensors were analysed and presented.

9.3. Related work

The acquisition of gait data from everyday life can offer supplementary information that can complement clinical evaluations [294]. Recent research has shifted its focus towards the utilization of devices and algorithms that can gather high-resolution and objective data to accurately reflect an individual's gait in free-living environments [294]. Consequently, innovative technologies such as smart insole devices, wearable devices, and mobile applications have been developed to support these endeavours.

9.3.1. Use of smart insole units and smartphones

Smart insoles have emerged as a promising technology for gait analysis, providing a non-invasive and portable way to collect detailed information on foot mechanics and gait patterns. Bamberg et al. introduced a wireless wearable system, which incorporated accelerometers, gyroscopes, and force sensors, to collect gait data on healthy and PD participants beyond the lab. The shoes transmit data at intervals of 13.4 milliseconds (ms) to a base station via a radio frequency transmitter for characteristics extraction such as stride length, and stride time, resulting in a net data transmission frequency of approximately 75 Hz [471]. Another study [472] proposed a lightweight smart shoe that monitors walking behaviour using an instability assessment model to produce a quantitative value, highlighting important episodes of activity. That system enables the transmission of sensor data obtained from acquisition units in the shoe to a variety of Bluetooth® enabled devices for post-processing. Schlachetzki et al. [170] developed a wearable unit that can be attached to a shoe for gait analysis different from previous studies. That system offers a high level of biomechanical resolution for gait impairment in PD. In that study, data were transmitted via Bluetooth® technology at a sampling frequency of 51.2 Hz. That system computes stride length, stride time, stance time, and inter-stride variation, and was suggested as suitable for use in both large-scale clinical studies and individual patient care. Alternatively, insoles are also used for human activity recognition. For example, SmartStep comprises insole-based and wrist-worn wearable sensors for the automatic recognition of activities of daily living. Throughout a free-living study, data were recorded at a rate of 50 Hz, and transmitted to a smartphone via BLE [473]. Some studies utilized electronic textile and fabric pressure sensor technologies to measure plantar pressure [474, 475]. Lin et al. employed a collection of electronic textile-based pressure sensors embedded within an insole to measure plantar pressure. Additionally, a low-cost IMU method was used to capture gait characteristics through the use of adaptive sampling frequencies for a tailored approach, with an upper threshold of 100 Hz [476]. Some studies did not utilize bespoke insole technology and simply attached commercial off-the-shelf IMU sensors to a shoe. For instance, a previous study [477] designed and validated a biofeedback system that functions in tandem with a mobile Android app on an LG Nexus 4 smartphone to compute step quality. Specifically, a wearable IMU was configured to transmit 6 degrees of freedom inertial data at a sampling rate of 51.2 Hz. Samples were transmitted to the feedback module via Bluetooth® in packets consisting of 16 samples.

Previous studies often transferred the raw data collected by smart insoles or IMU into a base station (e.g., computer, smartphone) for further analysis. Some studies aimed to minimize the negative impact of data transferring and developed a mobile application that utilizes sensor sets within the mobile device. For example, [478] used a smartphone as a wireless accelerometer to extract characteristics such as stride time, stance time, swing time, and cadence. The referenced study used a smartphone (attached to the user's ankle) and an application for data collection and processing.

Despite their promises, existing smart insole and IMU-based gait analysis systems with and without a complementary mobile app still face limitations. For example, many of these systems require data transmission to a base station or mobile device for post-processing, which can result in signal loss or delay, cause privacy concerns, and require a considerable amount of operating power and memory space. Additionally, while some systems can collect data wirelessly, they are often limited in terms of sampling frequency, which can reduce the accuracy of the collected data [112, 479]. Streaming raw data into a Cloud platform can also bring more limitations such as

high latency, and the need for high bandwidth. Furthermore, many systems cannot analyse data in real-time, limiting their usefulness for applications such as continuous monitoring or real-time feedback.

9.3.2. On the edge: Towards continuous gait

This research proposes edge computing technology to develop an inertial-based wearable that continuously assesses gait, with particular use beyond the lab. Edge computing has the capability to facilitate decentralized gait data processing, whereby data is collected and processed on edge devices without being transmitted to Cloud/computer or time delayed post-processing on a computer. This mitigates problems related to raw data transmission such as data loss and offers real-time feedback capabilities for users [25, 480, 481]. Furthermore, the proposed approach suggests a solution to privacy concerns, as it allows individuals and organizations to maintain a greater level of control over their data and minimize the risk of data leakage [24, 482].

The primary objective of this study is to design an edge wearable device for continuous and real-time gait analysis. The device is designed to be used easily by attaching it to the lower back (fifth lumbar vertebrae, L5) to compute step and stride times. Then, the edge device will be validated against a reference standard on a group of young adults, and it will then be used to conduct a case study for a day. Unlike most prior research, the raw data will be analysed within the edge device itself, without the need for streaming to an external base station such as a computer or mobile phone. As a result, only computed gait characteristics (e.g., step times) will be transferred to Cloud and displayed via smartphone.

The rest of this chapter is organized as follows. Section 9.4 provides detailed information regarding the hardware, electronic design, and algorithms employed in the study. Section 9.5 includes the results obtained through the validation study and case study. In Section 9.6, the proposed edge device is evaluated in terms of its accuracy, privacy, daily use, and limitations. Finally, Section 9.7 provides a conclusion that summarizes the main findings of the study and highlights potential directions for future research.

9.4. Materials and Methods

9.4.1. Hardware

The edge device consists of (i) a rechargeable lithium polymer battery (LiPo 3.7V), (ii) an Arduino Nano BLE 33 Sense module, (iii) a LiPo battery charging module, (iv) a switch, and (v) DC-DC boost converter (3.7V to 5V). Arduino Nano module was chosen due to nRF52840 (64MHz, 256 KB SRAM, 1MB flash memory) microcontroller that can run machine learning (ML) models. The module also has an embedded 2.4 GHz Bluetooth® 5 Low Energy, and LSM9DS1 IMU features a 3D accelerometer, 3D gyroscope, and 3D magnetometer. An Apple iPhone 13 smartphone (vi) was used to receive data from the edge device and send to the Cloud. The connection between the electronics components and the edge device is presented in Figure 21.

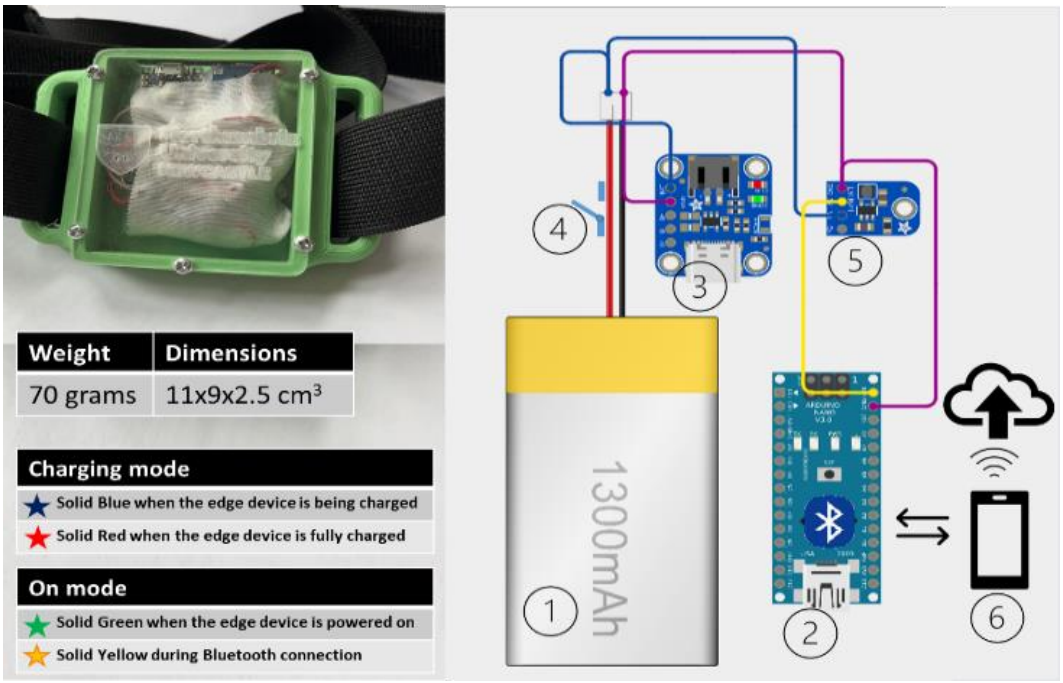

Figure 21.The edge device with black strap. Physical features along with led indicators. Electronic circuit design with connections.

9.4.2. Gait detection: Creating a ML model

Detection of gait bouts in real time plays a critical role in remote gait analysis. This eliminates the need for manual data labelling or time-consuming post-processing that was detailed in Chapter 4.

Temporal characteristics (step and stride times) from IC's can only be extracted during walking. Therefore, an AI model was trained and deployed to the microcontroller to detect walking. Data collected via embedded Arduino module IMU sensors were used on a model development platform. Edge impulse (www.edgeimpulse.com) is a Cloud-based machine learning operations (MLOps) platform for developing AI models that can be deployed to microcontrollers. It provides a user-friendly interface for data acquisition, model development/evaluation, and model deployment, rendering the platform a feasible solution. This section has two important parts model training/testing and investigating model performance. During the model training, inertial data collected from IMU placement on the lower back (fifth lumbar vertebrae, L5) were gathered from a single participant (29 years old, 90 kg, 184 cm, male) with the objective of creating a highly effective model that would incur minimal computational complexity and costs, thereby making it suitable for real-time applications. Additional participants were not included in the model development process as the model was specifically designed to differentiate between simple activities based on non-gait (more stable IMU signals) and gait (less stable IMU signals). Furthermore, solely 3D accelerometer signals were employed in the model, as the incorporation of supplementary 3D angular velocity signals would result in a twofold increase in computational complexity and costs. Two-second windows of 3D accelerometer data were used to train ML model to classify 2 different classes, (1) gait and (2) non-gait conditions (standing, lying, sitting). 2700 seconds (s) of gait and 2700s non-gait data (total of 5400s = 90 min) were collected at 100 Hz. Then 80% of this data was used for training (2160 occurrences/ 4320s) and the remaining 20% for testing (540 occurrences / 1080s). Signal pre-processing was not used as it can potentially increase the computational cost and time.

A neural network (NN) structure with 2 hidden layers (20 neurons + 10 neurons, Figure 22) was used with 100 epochs and 0.0001 learning rates. These hyperparameters were chosen considering short inferencing time and low memory usage. Model performance was investigated using accuracy and F1 score computed from a confusion matrix where TP: true positive, TN: true negative, FP: false positive and FN: false negative, Eq. 14 and 15.

$$Accuracy = \frac{TP+TN}{TP+FP+TN+FN} \quad (14)$$

$$F1-score = \frac{2xTP}{2xTP+FP+FN} \quad (15)$$

The results of the classification are illustrated in Figure 23, where it can be observed that one instance from each category was incorrectly classified by the model. Nonetheless, the NN demonstrated an accuracy and F1 score of 0.98. Moreover, the interference time on the device (Arduino Nano 33 BLE Sense, Cortex-M4F 64MHz) is 1 millisecond, enabling the device to perform gait classification in a very short time. Consequently, the model was deployed to an Arduino platform using the provided sketch file.

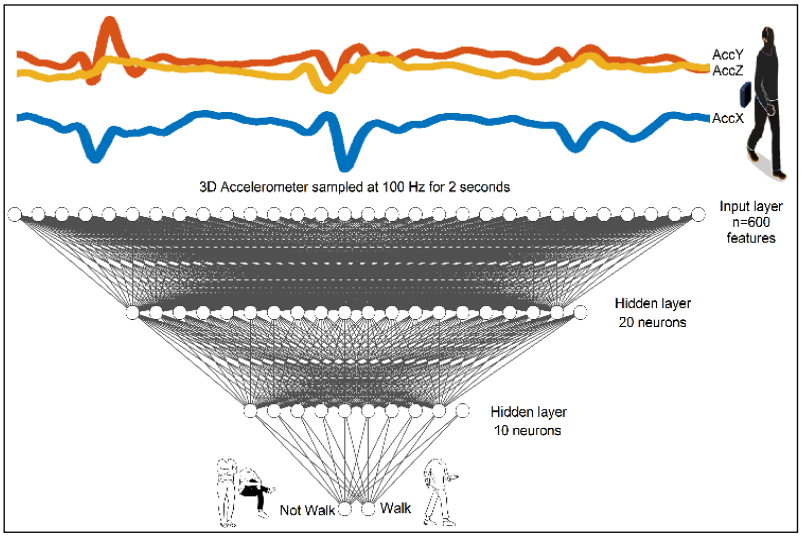

Figure 22.Data collection protocol and neural network structure used for walking (gait) activity recognition.

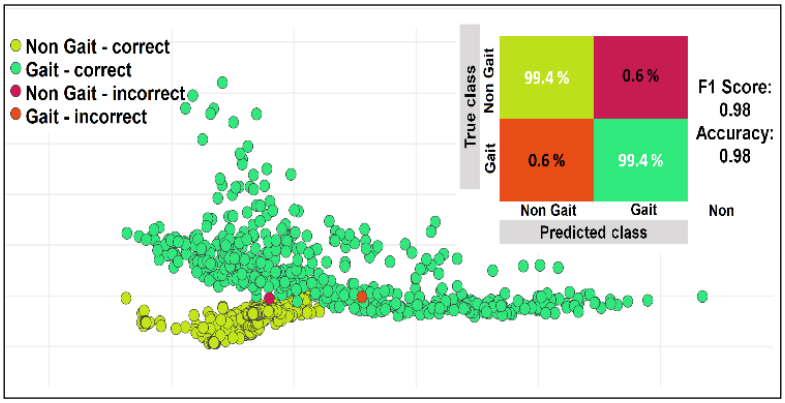

Figure 23.Classified activities by the neural network and corresponding confusion matrix

9.4.3. Calculation of temporal gait characteristics

Here, the edge device has 1MB of flash memory. Therefore, gait data (3D acceleration) is recorded for 2 minutes, then processed and deleted. The algorithms developed in this study are written in C++ language using Arduino Integrated Development Environment (IDE). The process to calculate temporal characteristics (step and stride times) is presented.

- Phase 1: When a gait bout is detected (walking starts) by the ML model, the anterior–posterior (AP) acceleration data is buffered into an array [*APacceleration*] using a serial monitor. AP acceleration data is collected at 100 Hz for 120s (2 minutes) and low pass filtered (4^{th} order Butterworth filter at 20 Hz cut-off). Therefore, the float array size is 12000. The timing was controlled by an internal timer, in an Arduino device (the *millis();* function returns milliseconds passed since the Arduino board began running the current program).

- Phase 2: Step and stride times from IC. Previously validated algorithms were used to compute IC moments from vertical [6] and AP [219] accelerations. Here, the method from AP accelerations was used due to low computational complexity. The edge device was programmed to detect peaks (IC moments) with a minimum peak distance of 0.4s (40 data points) and a minimum peak height of 1 m/s2 (Figure 24). The minimum peak distance threshold was selected considering healthy individuals walk with step times above 0.4s [13, 291].
- Phase 3: Moments (timestamps of running internal clock) of the detected peaks (IC moments) were saved in an array [*APpeakLocations*]. Each value located in this array represents right foot IC (right_IC) and left foot IC (left_IC) moments. Step times and stride times were calculated using those values with the following equations [154], where *i* represents the sequence number.

$$StepTime = APpeakLocations\ (i+1) - APpeakLocations\ (i) \quad (16)$$

$$\text{StrideTime} = \text{APpeakLocations (i + 2)} - \text{APpeakLocations (i)} \quad (17)$$

- Phase 4: Step and stride times were saved in two different arrays to be sent to the Cloud via Bluetooth®. The computed characteristics in the step and stride arrays can be transferred to the mobile app in order to optimize battery life. The mobile app can utilize a predetermined schedule, tailored to circumstances, to determine the timing of data streaming. In the event of an unavailable Bluetooth® connection, the data can be transmitted to the mobile app when the connection is re-established (Figure 25).

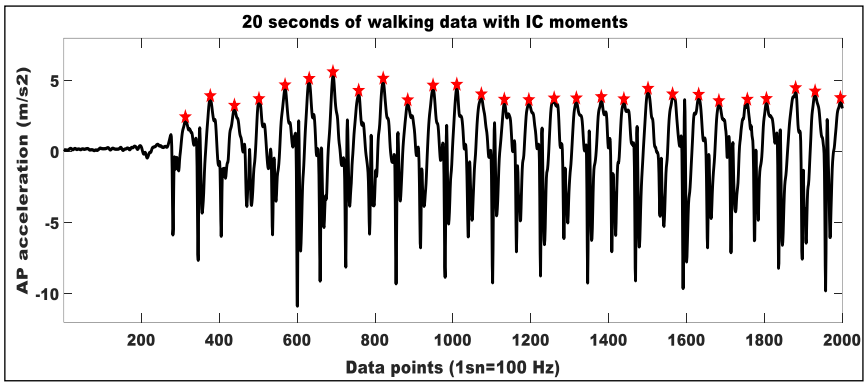

Figure 24.AP acceleration signal of lower back. Red stars represent initial contact moments.

9.4.4. Streaming calculated characteristics

Data saved in step and stride time arrays are sent to a connected Bluetooth® device with a mobile app (LightBlue®, an alternative is nRF Cloud Gateway, https://nrfcloud.com, where both applications enable users to stream data between mobile phones and Arduino Nano BLE 33 Sense). Here, an Apple iPhone 13 mobile phone, coupled with the LightBlue® app (receiver), was employed to receive data transmitted via BLE from the edge device (transmitter). The LightBlue® app also offers to transfer the received data into a connected Cloud platform as the data is being received. Here, Adafruit IO (https://io.adafruit.com), an IoT platform was used to save step and stride times characteristics as final storage. The platform enables users to view the collected data on different days and provides facilities for further data processing.

The process to stream data is as follows:

- Configuration of the edge device for the type of connection and data to be sent. Here, BLE Read and BLE Notify were used in the edge device to communicate with the mobile phone. A standard 16-bit characteristic Universal Unique Identifier (Hexadecimal, UUID:2A19) was selected.
- A mobile phone was connected to the edge device using a central address number (first connection) on the LightBlue® app. The central address number was saved in the memory of the edge device for re-connection in case of disconnection. The LightBlue® app was configured to listen to notifications that come from the central address of the edge device. In addition, Cloud connection mode was activated to transfer the values to the Cloud platform as data arrived.
- After step and stride time arrays are created, the edge device attempts to connect to the central address saved after the first connection. In the case of connection, values in step and stride arrays were sent individually. After sending all data points, the edge device returns to the gait detection mode.

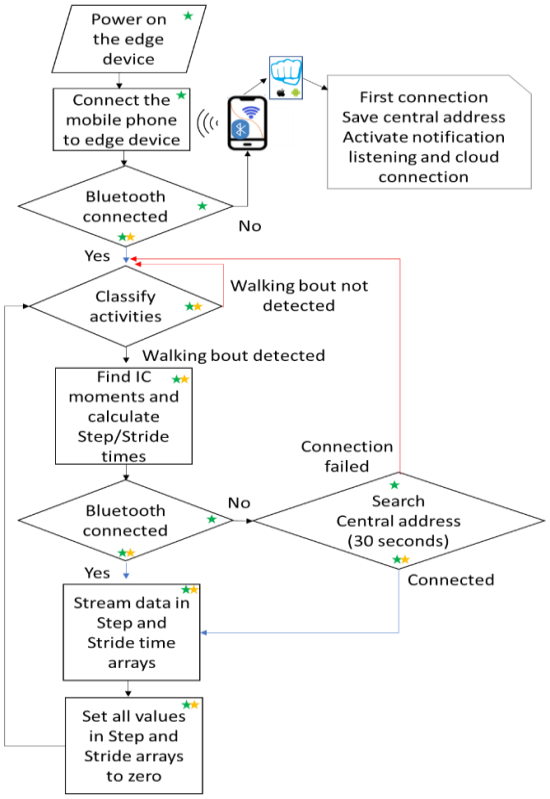

Figure 25.Flow chart of working edge-based system

9.4.5. Validation protocol

Ten healthy participants (HP's) were recruited for the main study (30.6 ± 6.4yrs, 79.2 ± 16.0kg, 176.9 ± 7.5cm, 7M:3F). Full participant demographics are presented in Appendix Table 10. Assessment and instrumentation were carried out by a physiotherapist and trained researchers, respectively. Ethical consent was granted by the Northumbria University Research Ethics Committee (REF: 21603). All participants gave informed written consent before participating in this study. Testing took place at the Clinical Gait Laboratory, Coach Lane Campus, Northumbria University, Newcastle upon Tyne. Each participant wore the edge device on L5. The edge device was configured (acceleration ±2 g, sampling rates: 100 Hz) prior to data collection. Each participant was instructed to walk (2 trials) over the ground for 2 min around a 20 m circuit at three different self-selected walking speeds (slow, preferred self-selected and fast) inside the laboratory.

The validation of the edge device was carried out using a reference technology (Mobility Lab™, APDM, Inc., Portland, OR, USA) for each of the walking speeds. Mobility Lab™, is a commercially available system that allows for IMUs to be wirelessly synchronized (Opal V1, APDM Inc., Portland, OR, USA) and software that allows for easy data collection and automatic analysis, without gait research knowledge or expert data processing [483]. Two Opal sensors were attached to feet for the purpose of this study as only steps and strides are collected. Gait characteristics obtained from the reference were compared to those obtained from the edge device.

9.4.6. Statistical analysis

I evaluated the correlation between the reference system and edge device on the temporal characteristics using Pearson's (r) and Spearman's (rho) correlation coefficients. I also investigated agreement using interclass correlation coefficients ($ICC_{2,1}$) with upper and lower bounds, which were calculated using a two-factor mixed model to assess the level of absolute agreement. I accepted that a coefficient value of 0.71 to 0.90 indicates good, while a value >0.91 indicates excellent agreement [322]. Furthermore, Bland-Altman analysis offered a straightforward and precise approach to gauging agreement, and is a valuable tool for medical professionals aiming

to compare a new measurement technique with an existing one or a benchmark standard [484]. Statistical calculations were made by IBM® SPSS® Statistics 26 and Bland-Altman plots were generated using MedCalc v20.

9.5. Results

Table 29 and Table 30 present summaries of descriptive and statistical data pertaining to validation gait characteristics, step and stride times for two different trials, acquired from the edge device and reference. The tables also provide information on the degree of correlation and agreement between both systems. Bland–Altman plots in Figure 26 and Figure 27 offer a graphical representation of the level of agreement between the two devices (trials are merged) during normal/preferred walking speed. Bland-Altman plots showing the agreement between the two devices for slow and fast walking speeds are presented in Appendix 6, Appendix Figure 4 and Appendix Figure 5.The validation study aims at investigating the agreement between step and stride times obtained from two different devices across a range of walking speeds. My findings reveal that both gait characteristics exhibited substantial to very good agreement across all speeds.For step time, strong correlations (r = 0.912, rho = 0.886) and high levels of agreement ($ICC_{2,1}$ = 0.949) were observed during slow walking. Stronger correlations (r = 0.962, rho = 0.955) and agreement ($ICC_{2,1}$ = 0.976) were obtained during preferred walking speed. The highest correlations (r = 0.964, rho = 0.980) and agreement ($ICC_{2,1}$ = 0.974) were observed during fast walking. Similarly, for stride time, I found high correlations (r=0.922, rho=0.904) and agreement ($ICC_{2,1}$ = 0.935) during slow walking, very strong correlations (r = 0.97, rho = 0.902) and agreement ($ICC_{2,1}$ = 0.971) during preferred walking speed, and the highest correlations (r = 0.975, rho = 0.959) and agreement ($ICC_{2,1}$ = 0.973) during fast walking. Results obtained from both systems during all walking speeds for each participant are presented in Appendix Table 11, Appendix Table 12, Appendix Table 13.

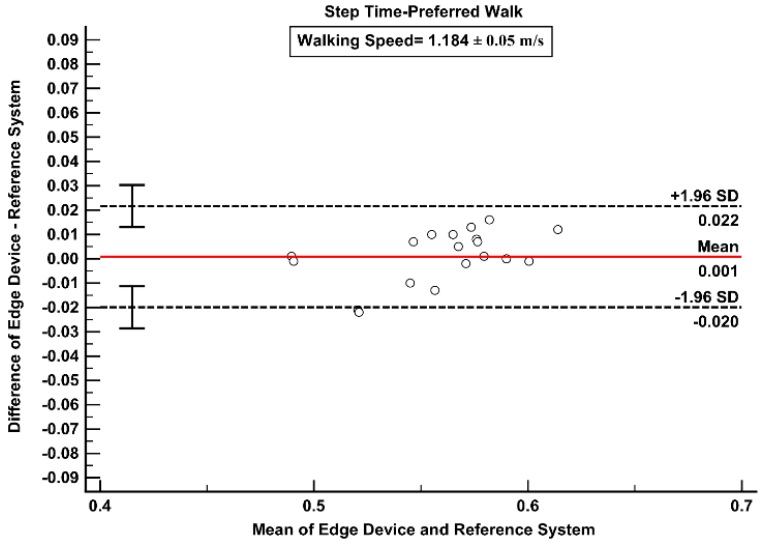

Figure 26.Bland–Altman plots demonstrating Step Time agreement between edge device and reference (preferred walking speed)

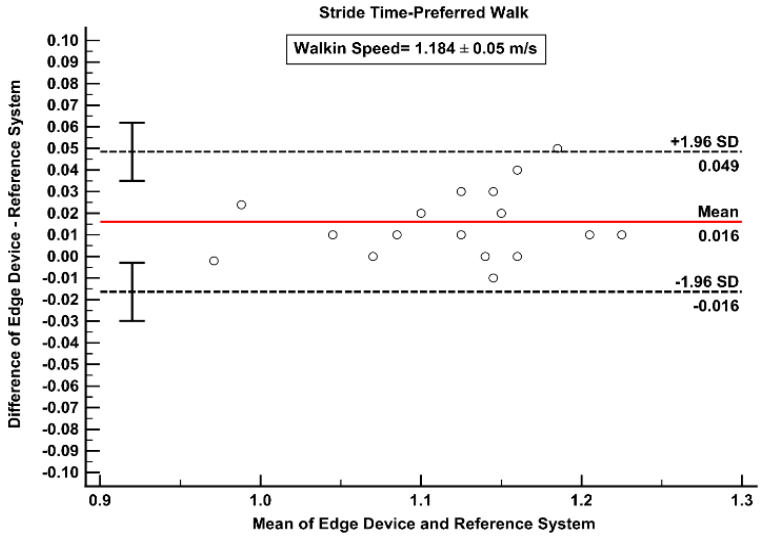

Figure 27.Bland–Altman plots demonstrating stride time agreement between Edge Device and reference (preferred walking speed)

9.5.1. Case study: Daily walking pattern monitoring

Validation results show the edge device has excellent agreement with the reference technology for all characteristics and during various walking speeds. Results indicate that the edge device can accurately collect gait characteristics in real-time and has the potential for use in continuous gait analysis beyond the controlled lab settings. The study also presents a GitHub repository (https://github.com/wearableyunus/Edge-device/wiki), containing a demonstration video, source code, and electronic and mechanical designs of the edge device, which serve to facilitate the reproducibility of the experimental results.

Subsequently, I performed a pilot study in a complex real-world scenario (e.g., walks through a city centre) to verify the feasibility of the edge device in daily life. A single participant (29 years old, 90 kg, 184 cm, male) wore the edge device on L5 for a day (6 hours), with clear instructions to walk in a routine manner. The edge device was paired with the participant's own smartphone. The smartphone battery was charged during the night and the battery level was maintained above 50% during the day as researchers observed that a low battery has an impact on BLE connection reliability. Following data collection, step times and stride times computed on the device were transmitted to the Cloud through a singular channel facilitated by a smartphone. Timestamps were included in the transmitted data, which were downloaded for analysis. A threshold was applied to distinguish between step and stride times. Specifically, data points with a duration ≤0.8s were classified as step times, whereas those >0.8s were categorized as stride times.

The commercial McRoberts wearable sensor was also placed on the lower back (above the edge device) to investigate the validity of the edge device. Data collected via McRoberts was processed offline with step and stride time characteristics extracted using the same methodology [219], after walking bouts are manually segmented. The number of steps and strides detected by the edge device were 966 and 482, respectively. Mean absolute error (MAE) and mean absolute percentage error (MAPE) were calculated using formulas presented in equation 18, where N is the number of steps and stride times, E is data computed from the edge device and M is the data computed from McRoberts.

$$MAE = \frac{\sum |M-E|}{N}, \qquad MAPE = \frac{\sum \frac{|M-E|}{M} X100}{N} \tag{18}$$

The mean absolute error (MAE) values for the step and stride times are 0.001s and 0.007s, respectively, Table 31. Alternatively, mean absolute percentage error (MAPE) values for the step and stride times are 0.203% and 0.764%, respectively. Those values indicate the level of deviation between both wearable systems. Furthermore, the mean step time and mean stride time were computed as 0.518s and 1.039s, respectively. Comparing these

results with the result of the validation study for the same participant (id:1, Appendix 6) during normal walking speeds reveals that the participant walks with slightly lower step times (faster walk) beyond the lab compared to a comfortable normal walk in the lab. Similarly, the participant walks with lower stride times (faster walk) beyond the lab compared to normal walk speed in the lab. This finding is consistent with a prior study [13] that compared laboratory-based walking with outdoor walking using different participants through offline data processing.

9.6. Discussion

This study presents a novel gait analysis system that utilizes edge computing technology. The system is capable of detecting gait in real-time and extracting clinically relevant characteristics during detected walking bouts. The validity of the edge device was established by comparing it against a reference technology for different walking speeds in young adults. Furthermore, a case study was conducted to test the edge device over a day outside of the laboratory setting.

The proposed system offers several advantages over traditional lab-based gait analysis systems. By capturing data in naturalistic settings, the system is better able to reflect real-world walking behaviour. When participants forget to wear the sensor, a researcher can detect this due to real-time analysis. This study computed clinically relevant temporal characteristics, which serve to complement a prior study [25] that focused on the extraction of spatial characteristics. In this way, a more comprehensive representation of an individual's spatiotemporal walking characteristics in uncontrolled free-living environments can be established. Additionally, the system minimizes the risks associated with data privacy as raw data is processed and deleted on the edge device, reducing the need for data transfer to Cloud-based servers. Furthermore, it reduces the need for post-processing of data, as the edge device processes the raw data as it is collected, reducing both bandwidth requirements and time-consuming post-processing.

9.6.1. Accuracy and reliability

The accuracy and reliability of wearable edge devices developed depend on several factors, including the quality of the sensor technology, algorithms used, and the placement of the sensors on the body. In general, the edge device offers a convenient and non-invasive way to gather real-time gait data in free-living environments. As a result of the validation study, both step time and stride time characteristics are more accurately detected in preferred and fast walking speeds compared to slow walking considering ICC agreement values. This finding aligns with previous studies [485, 486]. I hypothesize that the observed difference may be attributed to the smoother nature of the generated signals during slow walking, which may cause the algorithms utilized to identify peaks in IMU signals.

The accuracy of computed gait characteristics is influenced by various factors, including sensor location and the nature of sensor signals. Prior research has indicated that utilizing shank angular velocity signals results in more precise and consistent outcomes for IC and FC detection, in contrast to algorithms that rely on waist acceleration [214, 291, 305]. Differing characteristics of acceleration and angular velocity signals at various locations on the body are responsible for this discrepancy [479]. A previous study has extensively investigated the impact of IMU placement on the extraction of diverse characteristics for a neurological disorder [156].

Preferred locations for the extraction of gait characteristics are typically the waist and ankle/foot regions. Previous research has explored the use of the ankle location for real-time gait analysis through the attachment of a smartphone [478]. However, this approach may be impractical, as users would need to carry an additional mobile device during their daily activities. Another limitation is the discomfort of walking with a smartphone attached to the ankle. Furthermore, the use of a single mobile device attached to one ankle would only permit the computation of IC and foot clearance moments for a single foot, thus impeding the calculation of the step time characteristic that requires IC moments from both feet. Sensor placement on the lower back can provide gait characteristics in certain accuracies and it can allow computation of temporal and spatial characteristics by using e.g., an inverted pendulum model [215, 218].

Table 29.Validation result for step time

Step Time		Edge Device		Reference System		Pearson's	Spearman's	Agreement-95% CI Bounds			
		Average	SD	Average	SD	r	rho	$ICC_{2,1}$	Lower	Upper	p
Slow	Trial 1	0.707	0.035	0.712	0.037	**0.920****	**0.869****	**0.956**	0.833	0.989	<0.001
	Trial 2	0.715	0.096	0.7251	0.055	**0.905****	**0.863****	**0.943**	0.784	0.986	<0.001
Preferred	Trial 1	0.561	0.033	0.559	0.030	**0.967****	**0.972****	**0.982**	0.930	0.996	<0.001
	Trial 2	0.559	0.036	0.558	0.029	**0.957****	**0.939****	**0.971**	0.882	0.993	<0.001
Fast	Trial 1	0.507	0.032	0.506	0.033	**0.978****	**0.976****	**0.990**	0.960	0.997	<0.001
	Trial 2	0.499	0.027	0.497	0.036	**0.951****	**0.985****	**0.958**	0.832	0.989	<0.001

**. Correlation is significant at the 0.01 level (2-tailed).

Table 30.Validation result for stride time

Stride Time		Edge Device		Reference System		Pearson's	Spearman's	Agreement-95% CI Bounds			
		Average	SD	Average	SD	r	rho	$ICC_{2,1}$	Lower	Upper	p
Slow	Trial 1	1.39	0.062	1.411	0.073	**0.926****	**0.884****	**0.939**	0.690	0.986	<0.001
	Trial 2	1.419	0.100	1.457	0.112	**0.919****	**0.924****	**0.931**	0.595	0.984	<0.001
Preferred	Trial 1	1.131	0.069	1.114	0.062	**0.976****	**0.926****	**0.973**	0.715	0.994	<0.001
	Trial 2	1.130	0.061	1.114	0.060	**0.964****	**0.879****	**0.969**	0.758	0.993	<0.001
Fast	Trial 1	1.011	0.060	1.005	0.067	**0.983****	**0.932****	**0.988**	0.954	0.997	<0.001
	Trial 2	0.997	0.047	0.992	0.067	**0.968****	**0.985****	**0.958**	0.836	0.989	<0.001

**. Correlation is significant at the 0.01 level (2-tailed).

Table 31.Comparison results for free living

	Edge Device		McRoberts		Errors	
	Mean	SD	Mean	SD	MAE	MAPE (%)
Step Times	0.518	0.051	0.517	0.042	**0.001**	**0.203**
Stride Times	1.039	0.064	1.031	0.062	**0.007**	**0.764**

9.6.2. Limitations and improvements

Considering the sensor used in the case study, the battery life of the edge device lasts 3 days. Therefore, the edge device would need to be charged by mini-USB cable for longer assessment periods. A larger Li-Po battery cell (e.g., 2 cells with 2600 mAh) can be preferred to increase battery life. Another limitation is the inability to detect final contact moments (i.e., detecting IC moment related characteristics only (e.g., step and stride times). Future work will include adaptation of different algorithms to detect FC moments and compute other clinically important characteristics e.g., stance and swing times. Additionally, spatial characteristic step length can be potentially integrated [25]. The edge device does not differentiate true right and left steps and cannot produce asymmetry and variability outcomes. Although left/right assumptions could be made, absolute left and right could be detected by using a gyroscope sensor with an appropriate algorithm [6]. Finally, the edge device validation was performed on healthy subjects. Future studies will recruit e.g., those with PD. In this context, "cohort-specific models" refer to machine learning models that are trained on data from a specific group of people with a particular medical condition. The goal of those models is to improve the accuracy of gait recognition for individuals within the specific cohort, as previous research [18, 19] has suggested that models developed on healthy subjects may not perform as well when applied to those with different medical conditions.

9.7. Conclusion

This chapter represents the culmination of my doctoral study, serving as the final experimental work. In Chapter 6, I successfully developed and presented methodologies for extracting multimodal gait data in free-living environments. However, certain limitations, such as the time-consuming offline processing of gait data, motivated me to study the automation of HAR and parameter extraction processes. This section presents a novel wearable

edge device that automatically computes clinically important gait characteristics in real-time. Gait characteristics obtained from the device were validated against reference technology for different walking speeds in the controlled lab condition and beyond. Results indicate that the proposed edge device has high levels of accuracy, with an average ICC of 0.966 and 0.959 for step times and stride times, respectively. Findings suggest the suitability of the low-cost edge device for remote monitoring of gait and may be a pragmatic tool during rehabilitation.

The next chapter serves as the final chapter of this thesis, presenting the findings derived from the conducted studies. It will comprehensively address the PoIs listed in the previous chapters, elaborating on the methods and technologies employed. Additionally, the chapter will explore future directions and the broader impacts of utilising wearable sensor technologies in gait analysis for populations affected by Parkinson's disease (PD) and Stroke.

Chapter 10 Discussion, conclusions, and wider impact

10.1.Introduction

In this concluding chapter, I provide a summary of the knowledge acquired and the findings derived from the experimental studies conducted in my thesis. After outlining the key findings, I engage in a discussion about how I addressed the Points of Interest (PoIs) that were defined in Chapter 1. By addressing these PoIs, I then proceed to examine my hypothesis, supported by the evidence I gathered throughout my studies, and highlight my contribution to the field. Moreover, I present certain limitations that were encountered during my doctoral study and engage in a discussion regarding the broader research impact. Finally, I offer recommendations for future research endeavours in the field.

10.2. Key findings of experimental studies

Chapter 2

- Existing gait models developed to interpret gait outcomes extracted from wearable sensing technologies are limited to unimodal parameters (e.g., relying on spatiotemporal parameters only).
- A sensor fusion approach offers the essential infrastructure to combine data from multiple sensors, creating a multimodal gait tool that is both comprehensive and informative.
- There are discrepancies among the findings of previous gait studies of neurological populations due to a lack of standardisation in IMU and EMG data collection protocols such as sensor placement, configuration and algorithms used.
- Gait analysis has been shifting to free living environments that reflect daily capacity better. However, there are differences in the produced gait parameters between clinics and free living. The root causes of these differences need to be explored.
- Collecting data beyond controlled clinic settings for extended periods leads to a significant volume of unlabelled data. Manual labelling, specifically segmenting gait bouts, for gait analysis can be time-consuming and labour-intensive. Hence, the automation of this process using AI techniques can offer a faster and more efficient gait analysis tool for assessing gait in free-living conditions.

Chapter 3

- The mean temporal parameters extracted from the lower back sensor-based algorithm[6] and shank sensor-based algorithm [222] for all cohorts during treadmill, indoor, and outdoor walking show a strong correlation. However, this is not true for variability and asymmetry characteristics.
- The agreement between these algorithms is sensitive to age and neurological condition, the highest agreement is observed in young adults, then older adults then the PD group.
- The agreement between these algorithms is sensitive to the walking environment. Agreement in stride and step times is slightly higher during outdoor whereas agreement in stance and swing times is slightly higher during indoor walking.
- Overall agreement for stride and step times parameters (relies on IC only) is higher than stance and swing times parameters (relies on both IC and FC).

Chapters 5 and 6 (M1-M2-M3)

M1-HS:

- Healthy participants (HS) walked with greater *pace* and *variability* but with decreased *rhythm* during outdoor compared to indoor level walking (stride length variability characteristic did not experience any alteration)
- In terms of knee flexion angles, HS experienced slightly increased mean values (~1°) and decreased variance and asymmetry in outdoor compared to indoor level walking.
- Regardless of indoor/outdoor, the prevalence of TA muscle activation had similar patterns with RF and BF, all active around the start and end of a gait cycle during level walking. GS prevalence was observed mostly during the later stance phase before the FC moments for push off of the foot.

M1-SS:

- Stroke Survivors (SS) walked with increased pace and decreased rhythm during outdoor level walking compared to indoor. Swing time asymmetry is the only asymmetry characteristic that was found to be higher dur ing indoor compared to outdoor.

- In terms of knee flexion angle, increased mean values (~4°) and decreased variability and asymmetry were found during outdoor walking compared to indoor.
- TA, RF and BF muscle bursts were detected at the start and end of gait cycles (around IC moments). GS muscle bursts are most frequently observed in the stance phase in most SS.

M2:

- Preliminary results show the use of multimodal data (IMU and EMG) and feature-level fusion improves HAR model accuracy.
- Post-processing of sEMG data also impacts the model accuracy. Liner envelope of sEMG results with higher overall performance than the use of band pass filtered sEMG.
- Classification with features extracted from the thigh level sensor outperformed the shank level sensor.

M3:

- Augmenting data with the proposed methodology increase HAR model performance in terms of accuracy, sensitivity, and specificity in limited datasets of HS, PD and SS.
- ResNet50 outperformed all other architectures after data augmentation whereas MobileNet v2 achieved the best result before augmentation.
- Walking and standing activities are recognized with higher accuracy compared to stair ascent and descent.

10.3.Addressing research questions (PoIs)

In Chapter 2, I emphasized the numerous challenges associated with improving gait analysis in neurological populations. These challenges were initially identified through a comprehensive literature review. Also, I compared reference standard technologies and wearable technologies, assessing their usability, advantages, and disadvantages in the literature review. This comparison led me to the conclusion that wearable sensors, particularly inertial and EMG sensors, offer the potential to enhance clinical decision-making by providing rich habitual data at a minimal cost and complexity.

Expanding on the literature search, I discovered several validated algorithms developed based on IMU data, applicable to various wear locations and cohorts. This discovery led me to investigate the usability of wearable sensors in free-living conditions and the reliability and consistency of these algorithms in spatiotemporal gait analysis (PoI1). In Chapter 3, I conducted a comparative study involving 128 participants (92 HS and 36 PD) to examine the agreement between two popular wear locations and their corresponding algorithms. The results highlighted the sensitivity of these algorithms to walking environments and target cohorts, emphasizing the need for cautious interpretation by researchers and clinicians. Furthermore, I observed that most wearable sensor-based gait analysis studies tend to focus on unimodal characteristics, such as spatiotemporal parameters, attributing this limitation to both the lack of methodologies combining multiple characteristics and the technological constraints of wearable sensors (e.g., single sensor units only containing IMUs).

To address this limitation, I explored off-the-shelf wearable sensor technologies available in the market and discovered the Shimmer3 EMG unit, which incorporates both inertial and EMG sensors within a single sensor unit. This discovery prompted the development of PoI2, which aimed to investigate how the sensing capabilities of wearable sensors could be fused to obtain multimodal gait characteristics that offer more comprehensive insights than unimodal analyses. In Chapter 4, I studied various data fusion algorithms, and AI methodologies for HAR. In Chapter 6, I introduced a multilayer data fusion framework to address PoI2 on 10 HS and 3 stroke survivors (this number was planned to be 10 but I could not reach this target due to COVID-19). The output of this framework provided spatiotemporal, knee flexion angles and muscle activation characteristics of 4 different muscle groups during indoor, outdoor, and incline walking as well as stair ascent and descent. Comparing these multimodal parameters allow me to observe key differences such as SS walk with increased mean knee flexion angle values (~4°) during outdoor walking compared to indoor. In addition, muscle burst timings and durations of SS was extracted during various activities, which can potentially inform clinical gait analysis. However, during the framework's development, I encountered a significant challenge in labelling the data collected in unsupervised environments.

To mitigate this challenge, I introduced PoI3, which explored the application of AI models for human activity recognition (HAR) to accurately label data collected in unsupervised environments. Initially, I investigated classical machine learning models and employed feature-level fusion of IMU and EMG data on 10 healthy participants, achieving high accuracies in classifying basic daily activities. Features extracted from the thigh level sensor outperformed the shank level sensor. This could be useful when minimising sensing modalities in HAR systems. However, AI models require rich and diverse datasets to be able to train models effectively. Neurological cohorts often lack the diverse and rich datasets required for accurate and sensitive HAR, making it impractical to create such datasets. This is a new limitation caused by the difficulty of collecting mobility data from people with walking impairments.

This limitation led me to improve my PoI3, which explored methods to enhance the accuracy of AI models despite limited HAR datasets. To address this challenge, I developed a methodology that transformed numerical inertial data into two-dimensional activity images and employed proven data augmentation techniques to artificially increase the size of the training dataset. I tested this methodology on two different public datasets and subsequently implemented it on local datasets comprising healthy subjects (10), stroke survivors (3), and individuals with Parkinson's disease (5). The results demonstrated that data augmentation significantly improved HAR performance in terms of accuracy, sensitivity, and specificity.

By addressing PoI1-PoI3, I successfully developed an automated multimodal gait analysis tool capable of functioning in both clinical and free-living environments, accommodating various forms of walking and stair ambulation. This tool not only enhances the understanding of impaired gait but also has the potential to uncover underlying deficits associated with such impairments. However, post-processing the collected data remains time-consuming due to the need to save raw inertial and EMG data. Although the inclusion of HAR improves data labelling and subsequently reduces post-processing time, further improvements are still necessary.

To address the time-consuming post-processing challenge (PoI4), I investigated ways to improve efficiency. By leveraging edge computing technology, I developed an edge device in Chapter 9 to facilitate real-time gait analysis. At its current stage, the device is validated for 10 HS and achieved very high accuracy. However, it can generate only unimodal temporal gait characteristics in real time.

10.4.Addressing my hypothesis

I propose that exploration and a better understanding of PoIs are necessary to achieve an efficient instrumented gait analysis tool that can provide insight into various aspects of impaired gait and the discovery of underlying reasons. Thus, this leads me to the central hypothesis for my thesis:

"The use of wearable sensing technology in conjunction with advanced computing techniques may enable highly affordable, accessible, comprehensive, and objective multimodal gait analysis tools for clinical and free-living gait assessment".

From my work undertaken in this thesis, I believe my hypothesis to be valid. This thesis supports the suggested use of wearable sensing technologies as an affordable, comprehensive, and objective method to support instrumented multimodal gait analysis of people with neurological PD group and stroke survivors. The evidence for the comprehensive and objective multimodal gait analysis tools for clinical and free-living gait assessment lies in the development of the framework outlined in Chapter 6 Methodology 1 (M1). This framework utilised multimodal data fusion, effectively combining data from multiple IMU and EMG sensors to generate spatiotemporal, kinematic, and muscle activation characteristics. To improve the efficiency of this framework, I also utilised AI techniques to perform HAR in Chapter 6 Methodology 2 and 3 (M2-M3). This approach allows automatic gait bout segmentation, minimising time-consuming post-processing operations such as manual data labelling. Adopting the developed multimodal approach in both clinics and beyond may help achieve a more comprehensive gait analysis for daily monitoring of disease progression or exploring the underlying reasons for rare incidents such as falls. More work is needed to strengthen that claim as well as further investigate verification and clinical validation.

10.5. Contribution to knowledge

Through my multidisciplinary approach, I have discovered that solely focusing on unimodal characteristics, such as spatiotemporal parameters, in gait analysis of neurological populations provides limited information, whereas incorporating multimodal characteristics offers a more comprehensive and informative perspective. This becomes clear when looking at formerly developed models for gait analysis, which are employed to interpret spatiotemporal characteristics of gait. The primary elements of these models encompass postural control, pace, variability, asymmetry, and rhythm. The framework I developed within this thesis is capable of merging IMU and EMG sensors data at data level to produce additional gait characteristics. So, these characteristics related to joint kinematics and muscle activation can be integrated into these models to make them more comprehensive. Another thing that is evident in the previous gait models is that gait analysis is shifting to habitual settings to collect more habitual data that better reflect capacity of people with mobility loss. Moving beyond clinics using wearables creates large datasets (e.g., based on the number of sensors, data collection duration and sampling frequency). However, a significant amount of the data gathered in free-living scenarios can be redundant when the primary focus is on gait analysis. Data reduction is therefore crucial to alleviate the workload on researchers or other individuals performing data analysis. In most gait studies utilising wearable sensors, scripted data collection protocols are employed to conveniently label the data. An alternative method involves synchronised camera recording. Nonetheless, neither approach is ideally suited for data collection in habitual environments. Consequently, another crucial contribution of mine is the training of AI models to accurately label wearable data for data reduction purposes. Accomplishing multimodal gait analysis alongside automated gait bout recognition significantly diminishes the labour-intensive aspect of post-processing tasks in unsupervised free-living scenarios.

In a purely computing science context, my research has revealed both challenges and opportunities for further advancement. Notably, there is still scope for enhancing complex post-processing techniques and reducing their duration. To address this, I initially employed edge computing technology to create a real-time remote assessment device, enabling the extraction of unimodal gait characteristics. However, further refinements are necessary to achieve real-time remote multimodal gait analysis. Moreover, implementing verification processes, analytical methodologies, and clinical validation protocols is crucial to bolster the precision and dependability of remote monitoring instruments. This is an essential future direction for the practical application of academic research-grade tools, ensuring they find broader use in day-to-day clinical practice. It is this next step that has the potential to redefine how we approach gait analysis and neurological condition management at a clinical level.

10.6.Limitations

COVID-19 has significantly affected my PhD topic as people with neurological conditions are categorised as vulnerable in the UK. As a result, I faced challenges in recruiting participants throughout the 15-month period of my PhD. This limitation is reflected in the number of participants included in my previous studies. Despite my attempts to mitigate the impact by utilizing publicly available datasets, I only partially succeeded as my research questions necessitated a distinct dataset that was not readily accessible online.

Furthermore, my PhD thesis encountered other limitations, such as the lack of standardization in the use of wearable sensors. While there are clear guidelines for the use of surface EMG measurements provided by the European Surface Electromyography for the Non-Invasive Assessment of Muscles (http://www.seniam.org), the promotion of standardisation for wearable sensors in research remains relatively scarce.

Another limitation that emerged during my PhD project pertains to the cost associated with wearable sensor-based gait analysis endeavours. This cost encompasses expenses incurred during participant recruitment as well as the procurement of digital technologies. In Chapter 2, I highlighted the affordability and accessibility of wearable sensors, which make them suitable for a wide range of populations. However, one of my research findings suggests the importance of utilising edge computing technologies, such as processing data on the device itself, to facilitate remote gait analysis. Unfortunately, the development of such systems entails substantial costs, including the acquisition of advanced microcontrollers with high memory capacity and processing speed. Consequently, these expenses limit the feasibility of wearable sensor utilisation in gait analysis, somewhat detracting from their initial appeal.

10.7. Wider impact and future directions

I truly believe wearable sensor-based gait analysis extends beyond the realm of research and holds potential for various future directions. However, researchers and clinicians should work together to ensure the reliability of these technologies and methodologies. In Chapter 3, I conducted an experimental study to compare the temporal parameters extracted from two different sensor wear locations and algorithms, and my findings revealed the discrepancy and various levels of agreement. This could be because of the lack of standardisation in IMU data collection as I also highlighted in Chapter 2. In this context, more effort needs to be put into developing guidelines to achieve a more standardised approach. This guideline should include information about optimal wear location, sensor configuration, filters and algorithms used. Another way of ensuring the reliability of wearable technologies in gait analysis is through conducting research for clinical validation. While there have been a satisfactory number of validation studies conducted within clinical settings using reference technologies like motion capture systems or instrumented walkways, limitations arise when it comes to free-living environments. To address this, future studies should prioritize conducting validation studies in free-living conditions using alternative technologies such as foot switches or video-based systems. Additionally, validation studies should consider natural scenarios involving both single-tasking and dual-tasking situations. This could involve determining whether individuals are engaged in single or dual-tasking activities, walking alongside someone, or navigating obstacles in a busy street. Further details on these aspects can be found in Appendix 7.

The field of wearable data analysis requires advancements in the post-processing of collected data. In Chapter 6, efforts were made to address the manual, labour-intensive, and time-consuming data labelling issue associated with unsupervised data collected over extended periods, resulting in some level of improvement. However, there is still a need for further enhancements in post-processing wearable data to compute clinically relevant parameters more efficiently. As discussed in Chapter 4, the utilization of IoT technology in conjunction with Edge computing can offer significant improvements in this regard. It has the potential to enable remote and real-time gait analysis, providing valuable insights into disease progression, treatment effectiveness, and the impact of daily activities on gait in real-time. In Chapter 9, the development of an Edge device was presented, allowing real-time temporal gait analysis. Nonetheless, additional improvements are necessary to advance this approach into a multimodal tool. This includes the need for faster microcontrollers with low energy consumption and the development of robust and reliable fusion algorithms.

Overall, wearable sensor-based gait analysis has the potential to revolutionize clinical practice by providing objective and comprehensive assessment tools. This technology can facilitate personalized treatment plans and track the effectiveness of interventions, leading to improved patient outcomes. By accurately capturing gait patterns and biomechanical data, wearable sensors can guide the design and customization of prosthetics, orthotics, and exoskeletons. This can enhance mobility, stability, and overall quality of life for individuals with impaired gait. By identifying gait abnormalities and balance deficits, personalized interventions can be developed to mitigate fall risks and enhance safety.

10.8. Closing summary

It is now clear and apparent that wearable sensor technology can provide multimodal gait characteristics for extended periods regardless of the walking environment. This will initially help researchers produce more comprehensive gait models utilising multiple gait characteristics to interpret gait outcomes. Daily monitoring of impaired gait will open new research toward measuring the success of interventions and rehabilitation programs. Moreover, falls, one of the biggest fears among people with walking impairments, could potentially be further investigated using data collected in habitual environments. All these improvements and advancements in medical care will help promote healthy aging, manage neurological conditions, and improve the overall well-being of individuals.

Appendices A – Supplementary materials

Appendix 1. Full publication list

1. Moore, J.; Stuart, S.; McMeekin, P.; Walker, R.; **Celik, Y**.; Pointon, M.; Godfrey, A., Enhancing Free-Living Fall Risk Assessment: Contextualizing Mobility Based IMU Data. Sensors 2023, 23, (2), 891.

2. Das, J.; Morris, R.; Barry, G.; **Celik, Y**.; Godfrey, A.; McDonald, C.; Walker, R.; Vitorio, R.; Stuart, S., Technological solution for the assessment and rehabilitation of visuo-cognition in Parkinson's disease. In Taylor & Francis: 2023; Vol. 20, pp 253-257.

3. **Celik, Y**.; Vitorio, R.; Powell, D.; Moore, J.; Young, F.; Coulby, G.; Tung, J.; Nouredanesh, M.; Ellis, R.; Izmailova, E. S., Sensor Integration for Gait Analysis. 2023.

4. Zahid, S. A.; **Celik, Y**.; Godfrey, A.; Buckley, J. G., Use of 'wearables' to assess the up-on-the-toes test. Journal of Biomechanics 2022, 143, 111272.

5. **Celik, Y**.; Stuart, S.; Woo, W. L.; Sejdic, E.; Godfrey, A., Multi-modal gait: A wearable, algorithm and data fusion approach for clinical and free-living assessment. Information Fusion 2022, 78, 57-70.

6. **Celik, Y**.; Stuart, S.; Woo, W. L.; Pearson, L. T.; Godfrey, A. In Exploring human activity recognition using feature level fusion of inertial and electromyography data, 2022 44th Annual International Conference of the IEEE Engineering in Medicine & Biology Society (EMBC), 2022; IEEE: 2022; pp 1766-1769.

7. **Celik, Y**.; Aslan, M. F.; Sabanci, K.; Stuart, S.; Woo, W. L.; Godfrey, A., Improving Inertial Sensor-Based Activity Recognition in Neurological Populations. Sensors 2022, 22, (24), 9891.

8. Powell, D.; **Celik, Y**.; Trojaniello, D.; Young, F.; Moore, J.; Stuart, S.; Godfrey, A., Instrumenting traditional approaches to physical assessment. In Digital Health, Elsevier: 2021; pp 27-42.

9. **Celik, Y**.; Stuart, S.; Woo, W. L.; Godfrey, A., Wearable Inertial Gait Algorithms: Impact of Wear Location and Environment in Healthy and Parkinson's Populations. Sensors 2021, 21, (19), 6476.

10. **Celik, Y**.; Powell, D.; Woo, W. L.; Stuart, S.; Godfrey, A. In Developing and exploring a methodology for multi-modal indoor and outdoor gait assessment, 2021 43rd Annual International Conference of the IEEE Engineering in Medicine & Biology Society (EMBC), 2021; IEEE: 2021; pp 6759-6762.

11. **Celik, Y**.; Stuart, S.; Woo, W. L.; Godfrey, A., Extending free-living gait analysis: A pilot study towards multi-modal sensing. In Northeast Postgraduate Conference Newcastle, 2020.

12. **Celik, Y**.; Stuart, S.; Woo, W. L.; Godfrey, A., Gait analysis in neurological populations: Progression in the use of wearables. Medical Engineering & Physics 2020.

13. **Celik, Y**.; Powell, D.; Woo, W. L.; Stuart, S.; Godfrey, A. In A feasibility study towards instrumentation of the Sport Concussion Assessment Tool (iSCAT), 2020 42nd Annual International Conference of the IEEE Engineering in Medicine & Biology Society (EMBC), 2020; IEEE: 2020; pp 4624-4627.

Appendix 2. Ethics declaration, Participant information, Consent Sheet, and Debrief

Project Title: Instrumenting Gait in Neurological Disorders: Multi-Modal Approach Using Wearables

Northumbria University Ethics Reference Number: 23946

I, Yunus Celik, hereby declare that the project outlined below has received ethical approval from Northumbria University, in accordance with the established guidelines and procedures for ethical research.

Ethical Considerations:

Informed Consent: All participants involved in this study will be provided with clear and comprehensive information about the nature, purpose, and potential risks and benefits of their involvement. Their voluntary participation will be ensured through obtaining written consent prior to their participation. Confidentiality and anonymity will be maintained throughout the study, and all personal information will be securely stored.

Privacy and Data Protection: Any personal data collected during this research will be handled in accordance with relevant data protection laws and regulations. Measures will be taken to ensure that all data is stored securely and treated with the utmost confidentiality. Data will be anonymised wherever possible, and only authorized members of the research team will have access to the collected data.

Risk Assessment: A thorough risk assessment has been conducted to identify and mitigate any potential risks associated with this research project. Necessary precautions will be taken to ensure the safety and well-being of all participants involved.

Beneficence: This research aims to provide benefits to society, academia, or the participants involved. The potential positive impact of this study has been considered, and efforts will be made to maximize the benefits while minimizing any potential harm or discomfort to the participants.

Ethical Conduct: This research will be conducted in accordance with the ethical principles outlined by Northumbria University and relevant regulatory bodies. The research team will adhere to the highest standards of integrity, honesty, and professionalism throughout the project.

Ethical Review: This project has undergone a rigorous ethical review process by the Northumbria University Ethics Committee, which has granted ethical approval for its execution. Any amendments or modifications to the project will be subject to further ethical review and approval.

Instrumenting Gait in Neurological Disorders: Multi-Modal Approaches Using Wearables Participant Information Sheet

You are being invited to take part in this research study. Before you decide it is important for you to read this leaflet so you understand why the study is being carried out and what it will involve.

Reading this leaflet, discussing it with others or asking any questions you might have will help you decide whether or not you would like to take part.

INCREASED HEALTH AND SAFETY DURING COVID-19

- All research will adhere to local (university) and national (government) guidance
- We will require you to confirm you have had no: **contact with anyone testing positive or have/had symptoms of COVID-19** in the previous 14 days.
- All participants and researchers will **be required to wear a facemask at all times**. (Researchers will be wearing **appropriate PPE)**
- The laboratory including **all equipment will be cleaned** before and after each participant, with **extra tim**e given to ensure health and safety maintained and **no mixing between participants**.
- We will **maintain social distancing** at all times (1 meter plus).
- You may withdraw at any time without reason

If you need help or are worried about the virus, we can provide signposting to the appropriate services within the university –

https://www.northumbria.ac.uk/study-at-northumbria/support-for-students/counselling-and-mental-health-support/self-help

What is the Purpose of the Study

The purpose of this project is to evaluate a number of wearable technologies in laboratory and free-living (e.g. home) environments to capture accurate and useful information relating to how you move. This includes how you walk and how you look and navigate your environment. Additionally, this project helps to inform the development of new wearable technology algorithms (analytics) to detect those activities (i.e. walking, navigation) by capturing high resolution digital data that could be very helpful to aid those who may have difficulty in daily functional tasks.

Why have I been invited?

I*t is important that we assess as many people as possible and you have indicated that you are interested in taking part in this studies of this nature and that you are a healthy person aged >18 years. Additionally, you are or have been involved with a patient group or carer panel in the North East and have expressed an interest in academic-based research regarding functional activities and methods to better asses those with functional limitations.*

Do I have to take part?

No. It is up to you whether you would like to take part in the study. I am giving you this information sheet to help you make that decision. If you do decide to take part, remember that you can stop being involved in the study whenever you choose, without telling me why. You are completely free to decide whether or not to take part, or to take part and then leave the study before completion. Deciding not to take part, or leaving the study, will not affect your right to routine care.

What will happen if I take part?

E.g. *You will be asked to attend a testing session held in the Clinical Gait Laboratory at the Coach Lane campus or Biomechanics Gait Laboratory city campus of Northumbria University at a date that is convenient to you. After signing a consent form, the investigator will ask you to wear a number of sensors (noninvasive) on your person and to perform a number of functional tasks such as walking for 2 minutes during which time you will be video recorded. These non-invasive sensors will be attached with a strap and double-sided tape. In addition, disposable EMG surface electrodes (non-invasive) will be attached to pre-determined locations. A skin preparation (e.g. shaving some of the leg area) may be needed, only if the skin surface at which the electrodes have to be placed is covered with hair, to achieve a good electrode skin contact for a higher quality signal. After you have completed the aspect of the study you may be asked to wear the same sensor technologies in your home for an extended period e.g. 1 to 2 hours. This is completely voluntary and will be arranged at a date and time that suits you. The study investigator will give you a debrief sheet explaining the nature of the research, how you can find out about the results, and how you can withdraw your data if you wish. It is estimated that the total time to complete this laboratory study will be 60 minutes but additional time will be needed in your home (if you wish to undertake that component of the study).*
You will be asked to wear a face mask, gloves and keep two meters social distancing rule during the data collection for your and researchers safety.

What are the possible disadvantages of taking part?

There are no disadvantages in taking part. However, one aspect of the project is wearing many wearable technologies beyond the laboratory testing, this may cause some embarrassment depending on your personality but is mitigated by wearing of those technologies in the confines of the University and in your home only. Although the study designed in a way that both participants and researchers will be protected by face mask, gloves and social distancing, there is a reduced risk of exposure to COVID-19. But the risk amount is not more than the risk of being in social places (stores, etc.) We will maintain social distancing at all times and ensure health and safety risks are mitigated and ensure appropriate local and national COVID-19 policy is followed and adhered to.

What are the possible benefits of taking part?

By taking part in this study you will be helping researchers better understand how those with functional limitations better navigate their environment to ensure safe and effective activities of daily living and possibly reducing the incidence of falls.

Will my taking part in this study be kept confidential and anonymous?

Yes. Your name will not be written on any of the wearable data we collect; the written information you provide will have an ID number, not your name. The consent form you have signed will be stored separately from your other data. The data collected from you in this study will be confidential. The only exception to this confidentiality is if the researcher feels that you or others may be harmed if information is not shared.

How will my data be stored, and how long will it be stored for?

All paper data will be kept in locked storage. All electronic data; including the recordings from your interview, will be stored on the University U drive, which is password protected. All data will be stored in accordance with University guidelines and the Data Protection Act (2018).

All information and data gathered during this research will be stored in line with the Data Protection Act and will be destroyed 72 months following the conclusion of the study. If the research is published in a scientific journal it may be kept for longer before being destroyed. During that time the data may be used by members of the research team only for purposes appropriate to the research question, but at no point will your personal information or data be revealed. Insurance companies and employers will not be given any individual's personal information, nor any data provided by them, and nor will we allow access to the police, security services, social services, relatives or lawyers, unless forced to do so by the courts.

Personal data relating to name, age, height and general health status will be collected only. No information relating to finance, sexual orientation, religion or political views will be collected and stored.

What is the legal basis for processing personal data?

General Data Protection Regulation (GDPR) requires researchers to be transparent about the legal basis for undertaking research which will collect and process personal data. GDPR provides a number of legal bases to choose from, and for the purposes of this study relates to article 6(1e): processing is necessary for the performance of a task carried out in the public interest or in the exercise of official authority vested in the controller.

Who are the recipients or categories of recipients of personal data, if any?

The research team at Northumbria University will have access and process the data only. The team utilize a Northumbria University controlled SharePoint site which is password protected, with hierarchies of access if appropriate, and with clear onboarding and off boarding procedures to detail how researchers gain access to the system, who approves that access, and how long that access persists (e.g. until the end of the project, or just for part of the project).

No data will be transferred beyond the UK

Project Title: Instrumenting Gait in Neurological Disorders: Multi-Modal Approaches Using Wearables

	please initial where applicable
I have carefully read and understood the Participant Information Sheet.	☐
I declare that I have not knowingly been in contact with anyone displaying Covid-19 symptoms, or experienced symptoms themselves, in the 14 days before taking part in the study	☐
I agree to wear protective equipment (face-covering masks and gloves) during the study and take the risk of exposure to COVID-19	☐
I have carefully read and understand the guidance on safety issues and measures for participants and researchers safety in participant information sheets	☐
I declare that the study design is in line with government guidelines, local site policies around COVID-19 and I feel comfortable with participation	☐
I have had an opportunity to ask questions and discuss this study and I have received satisfactory answers.	☐
I understand I am free to withdraw from the study at any time, without having to give a reason for withdrawing, and without prejudice.	☐
I agree to take part in this study.	☐
I consent my leg to be shaved (if required)	☐
I also consent to the retention of these data (wearable and questionnaire) under the condition that any subsequent use also be restricted to research projects that have gained ethical approval from Northumbria University	☐
I agree to the University of Northumbria at Newcastle recording and processing this information about me. I understand that this information will be used only for the purpose(s) set out in the information sheet supplied to me, and my consent is conditional upon the University complying with its duties and obligations under the Data Protection Act 2018 which incorporates General Data Protection Regulations (GDPR).You can find out more about how we use your information here - Privacy Notices: http://www.northumbria.ac.uk/about-us/leadership-governance/vice-chancellors-office/legal-services-team/gdpr/gdpr---privacy-notices/	☐

Northumbria University NEWCASTLE

Participant code:

PARTICIPANT DEBRIEF

Name of Researcher: Yunus Celik

Name of Supervisor (if relevant): Dr Alan Godfrey 0191 227 3642

Project Title: INSTRUMENTING GAIT IN NEUROLOGICAL DISORDERS: MULTI-MODAL APPROACHES USING WEARABLES

INCREASED HEALTH AND SAFETY DURING COVID-19

- All research will adhere to local (university) and national (government) guidance
- We will require you to confirm you have had no: **contact with anyone testing positive or have/had symptoms of COVID-19** in the previous 14 days.
- All participants and researchers will **be required to wear a facemask at all times**. (Researchers will be wearing **appropriate PPE)**
- The laboratory including **all equipment will be cleaned** before and after each participant, with **extra tim**e given to ensure health and safety maintained and **no mixing between participants**.
- We will **maintain social distancing** at all times (1 meter plus).
- You may withdraw at any time without reason

If you need help or are worried about the virus, we can provide signposting to the appropriate services within the university –

https://www.northumbria.ac.uk/study-at-northumbria/support-for-students/counselling-and-mental-health-support/self-help

1. What was the purpose of the project?

The purpose of this project is to evaluate a number of wearable technologies in laboratory and free-living (home) environments to capture accurate and useful information relating to how you move. This includes how you walk and how you look around to navigate your environment. Additionally, this project helps to inform the development of new wearable technology algorithms (analytics) to detect those activities (i.e. walking, navigation) by capturing high resolution digital data that could be very helpful to aid those who may have difficulty in daily functional tasks.

Appendix 3. Chapter 2 supplementary materials

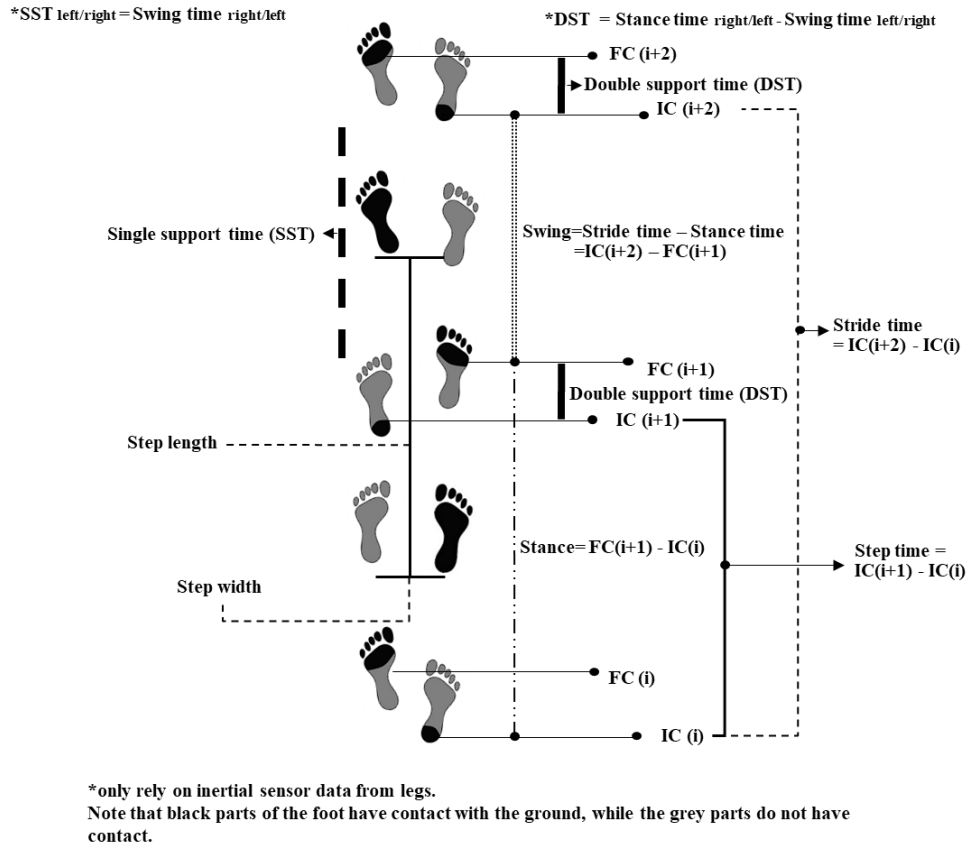

Appendix Figure 1.Temporal timings and formulae [72, 487]

Spatial measure formulae:

1.(Foot based) One way of calculating stride length is the computation of double integration of gravity correlated accelerometer signal. This approach is not widely preferred as it includes various of complex subsections like orientation estimation, gravity removal and de-drifting [225].
2.(Shank based) Trojaniello et al. proposed a more extensive method to estimate stride length using two consecutive initial contacts (ICs) of the same foot. The proposed method removes the gravity then uses Optimally Filtered Direct and Reverse Integration along with high pass filter to reduce the effect of drift in the accelerometer signal. In the final stages, AP acceleration is integrated to obtain AP velocity and AP displacement with a further integration [220].
3. (Lower trunk based) Another approach to estimating the step length is the use of inverted pendulum model; $\text{step length}=2\sqrt{2lh-h^2}$,where h is the change in the height of CoM, and l is the sensor height from the ground, detailed [215].
4. Weinberg proposed an alternative way to calculate the step length as a function of the difference between max and min vertical acceleration during steps: $\text{step length} = K\sqrt[4]{A_z,max - A_z,min}$, where K is a regression coefficient and Az represents the acceleration in vertical axis [488].

5. (Upper trunk based) In another approach, step length is calculated as a function of variance of the vertical acceleration $\text{step length} = c + d\sqrt{\text{Var}(Az)}$ where c, d and Az are regression coefficients and vertical acceleration, respectively [489].
6. (Lower trunk and lower limb based) Step width is lateral distance between two feet. Pythagorean theorem can be used to estimate step with $SW=2*\text{Step length}*\tan(\theta)$, where θ is rotational yaw angle of the IMU placed at leg in which step was executed [490].
To the best of the author's knowledge, no studies have investigated the temporal and spatial measures using wearable sensors for those with Hypoxic-Ischemic brain injury or Cervical dystonia. Therefore, to provide a guide for the reader in terms of all pathologies, Appendix Table 1 presents studies that used non-wearable technologies to investigate the spatiotemporal outcomes.

Appendix Table 1. Clinic based devices in neurological gait assessment with spatiotemporal outcomes.

Neurological Condition	Ref.	Device	Group	# subject - (Age)	Findings							Additional findings
					VEL	CAD	SPL	SDL	SW	SPT	SDT	
TBI	[253]	Motion Analysis Vicon 512-Force plate AMTI	HS	25-(27.8)	↑	↑	↑	-	-	-	-	Increased stance duration, double support and base of support in TBI
			TBI	41-(29.1)	↓	↓	↓	-	-	-	-	
HIBI FOG	[255]	Motion Analysis VICON MX-T10 Motion Analysis System, Oxford Metrics Inc., Oxford, UK	HS	15-(40.27)	↑	↑	↑	↑	-	↓	↑	Increased stance time and double support, decreased swing time and single support. Higher asymmetry in step length and time in HIBI with FOG.
			HIBI FOG	13-(37.36)	↓	↓	↓	↓	-	↑	↓	
HIBI with and without FOG	[256]	Motion Analysis VICON MX-T10 Motion Analysis System, Oxford Metrics Inc., Oxford, UK	HIBI	17-(48.88)	↑	↓	↑	↑	-	↓	↑	Increased stance time and double support, decreased swing time and single support in HIBI with FOG.
			HIBI-FOG	12-(37.83)	↓	↑	↓	↓	-	↑	↓	
CD	[262]	Walkway CIR Systems, Inc. GAITRite System	HS	10-(52.8)	↑	-	↓	-	-	↓	-	When corrected for walking speed, people with CD demonstrated higher step time variability and lower step length variability.
			CD	10-(53.9)	↓	-	↑	-	-	↑	-	

HS: Healthy subject, X: the same value, (-): not available, g=force, Fs= sampling frequency, VEL: velocity, CAD: cadence, SPL: step length SDL: stride length, SW= step with, SPT: step time, SDT: stride time

Appendix 4. Chapter 3 Supplementary Materials

Algorithm 1 (Pseudocode)

1: Filter raw vertical hip acceleration signal (The 4th order Butterworth filter with 10 Hz cut off frequency)

2: Acceleration correction to horizontal-vertical frame [33]

3: Integrated_av: Numerical integration of vertical acceleration of hip in the horizontal-vertical frame (cumtrapz)

4: IC_moments = Gaussian continuous wavelet transforms at scale 10 (Integrated_av)

5: FC_moments= Further differentiation of IC_moments

6: **for** i=1: size (IC_moments)

7: IC=find local minima in IC_moments

8: **end for**

9: **for** i=1: size (FC_moments)

10: FC=find local maxima in FC_moments

11: **end for**

12: **Return** IC and FC

Algorithm 2 (Pseudocode)

1: Wavelet decomposition (5th order coiflet, at scale 10) of shin sagittal plane angular velocity

2: Get two new approximations (a1 and a2) with appcoef function

3: ms_a1= Find peaks in a1 to locate mid swing

4: ms_a2= Find peaks in a2 to locate mid swing

4: **for** i=1: size (a1)

5: IC=find local minima in the range of [ms_a1+0.25s, ms_a1+2s]

6: **end for**

7: **for** i=1: size (a2)

8: FC=find local minima in the range of [ms_a2-2s, ms_a2-0.05s]

9: **end for**

10: **Return** IC and FC

Note: step time statistical formula is presented in Appendix Table 2 only, the same formulas are used for the remaining temporal outcomes.

Appendix Table 2. Formulas used to calculate temporal parameters along with statistical results

	Temporal parameter formula (left side only)
Algorithm 1 (A1)	Stride Time= IC(i+2) - IC(i), Stance Time= FC(i+1) - IC(i), Swing Time= IC(i+2) - FC(i+1), Step Time= IC(i+1)- IC(i)
Algorithm 2 (A2)	Stride Time= IC(j+2) - IC(j), Stance Time= FC(j+1) - IC(j), Swing Time= IC(j+2) - FC(j+1), Step Time= IC(j+1)- IC(j)
	Statistical formulas (both sides-for Step Time only)
Mean	$\left(\text{mean}(\text{Step time}_{\text{left}}) + (\text{Step time}_{\text{right}})\right)/2$
Variability	$\sqrt{\left(\text{var}\left(\text{Step time}_{\text{left}}\right) + \text{var}\left(\text{Step time}_{\text{right}}\right)\right)/2}$
Asymmetry	$\left\lvert \text{mean}\left(\text{Step time}_{\text{left}}\right) - \text{mean}\left(\text{Step time}_{\text{right}}\right) \right\rvert$

Appendix 5. Chapter 7 Supplementary Materials

Impact of changing terrain

Walking on uneven rock surface and inclined walking were excluded for stroke survivors due to safety reasons. The environments and cohorts' information for extracted parameters for the purpose of this study are presented in Appendix Table 3.

Appendix Table 3.Extracted parameters in environments/activities for healthy participants (HP) and stroke survivors (SS) for the purpose of the study.

Environment/activity	Cohort	Spatio-temporal	Knee joint angle	Muscle activity
Indoor level walking	*HP-SS*	✓	✓	✓
Outdoor level walking	*HP-SS*	✓	✓	✓
Incline walking	*HP only*	✓	✓	*X*
Walking on rock surface	*HP only*	✓	✓	*X*
Stair ascent/descent	*HP-SS*	*X*	✓	✓

Spatio-temporal outcomes

HP: Small but substantial impacts of changing terrain observed in four gait domains, Appendix Table 4. Comparing spatio-temporal characteristics of outdoor activities revealed that variability is highest in temporal characteristics during incline walking (ascent slope) compared to other activities. Additionally, higher variability observed in level walking compared to walking on a rock surface and the differences in variability found higher in spatial parameters compared to temporal. HP walks with decreased *rhythm* and increased *pace*, *variability* and *asymmetry* during incline walking compared to walking on a rock surface.

Appendix Table 4.Spatiotemporal gait characteristics of HP ground level walking in indoor and outdoor, 2min

	Indoor									
	1	2	3	4	5	6	7	8	9	10
# of strides	*104*	*105*	*103*	*76*	*95*	*104*	*124*	*103*	*100*	*82*
PACE										
Mean Stride V. (m/s)	1.361	1.11	1.291	0.943	1.204	1.27	1.273	1.205	1.077	1.015
Mean Stride L. (m)	1.569	1.242	1.493	1.073	1.406	1.438	1.161	1.349	1.371	1.223
RHYTHM										
Mean Stride Time (s)	1.150	1.118	1.158	1.134	1.165	1.131	0.912	1.117	1.270	1.206
Mean Step Time (s)	0.576	0.560	0.579	-	0.594	0.566	0.468	0.559	0.590	0.604
Mean Stance Time (s)	0.699	0.616	0.65	0.638	0.639	0.635	0.510	0.653	0.719	0.715
Mean Swing Time (s)	0.45	0.502	0.508	0.496	0.526	0.497	0.402	0.465	0.554	0.491
VARIABILITY										
Stride V. Var (m/s)	0.143	0.085	0.133	0.099	0.111	0.074	0.077	0.085	0.106	0.142
Stride L Var (m)	0.171	0.103	0.161	0.122	0.149	0.085	0.063	0.088	0.175	0.186
Step Time Var (s)	0.005	0.007	0.059	-	0.038	0.031	0.033	0.019	0.071	0.043
Stance Time Var (s)	0.005	0.002	0.022	0.027	0.007	0.005	0.008	0.022	0.033	0.011
Swing Time Var (s)	0.008	0.005	0.02	0.013	0.039	0.006	0.036	0.022	0.025	0.007
ASYMMETRY										
Stride L. Asy (m)	0.050	0.015	0.139	0.065	0.088	0.181	0.125	0.004	0.177	0.019
Step Time Asy (s)	0.029	0.039	0.044	-	0.037	0.026	0.027	0.027	0.043	0.032
Stance Time Asy (s)	0.037	0.034	0.043	0.062	0.057	0.03	0.042	0.03	0.036	0.039
Swing Time Asy (s)	0.041	0.048	0.048	0.043	0.059	0.039	0.036	0.034	0.053	0.045
	Outdoor									
	1	2	3	4	5	6	7	8	9	10
# of strides	*98*	*114*	*108*	*118*	*103*	*108*	*120*	*96*	*100*	*116*
PACE										
Mean Stride V. (m/s)	1.477	1.241	1.343	1.123	1.257	1.352	1.371	1.39	1.419	1.218
Mean Stride L. (m)	1.606	1.339	1.488	1.131	1.414	1.461	1.259	1.449	1.627	1.377

RHYTHM										
Mean Stride Time (s)	1.092	1.078	1.112	1.015	1.133	1.086	0.924	1.042	1.142	1.125
Mean Step Time (s)	0.547	0.546	0.556	0.499	0.567	0.545	0.464	0.521	-	0.566
Mean Stance Time (s)	0.648	0.589	0.622	0.557	0.6	0.604	0.51	0.588	0.622	0.636
Mean Swing Time (s)	0.444	0.489	0.490	0.452	0.533	0.481	0.413	0.455	0.519	0.488
VARIABILITY										
Stride V. Var (m/s)	0.160	0.124	0.109	0.124	0.116	0.08	0.141	0.112	-	0.159
Stride L Var (m)	0.173	0.13	0.119	0.125	0.134	0.11	0.086	0.106	-	0.185
Step Time Var (s)	0.035	0.033	0.035	0.049	0.035	0.041	0.036	0.02	-	0.071
Stance Time Var (s)	0.044	0.046	0.048	0.043	0.069	0.047	0.049	0.034	-	0.075
Swing Time Var (s)	0.043	0.043	0.044	0.042	0.051	0.046	0.042	0.034	-	0.044
ASYMMETRY										
Stride L. Asy (m)	0.126	0.143	0.125	0.019	0.057	0.248	0.024	0.056	-	0.138
Step Time Asy (s)	0.029	0.005	0.077	0.019	0.005	0.031	0.01	0.006	-	0.047
Stance Time Asy (s)	0.013	0.019	0.033	0.005	0.011	0.008	0.006	0.012	-	0.006
Swing Time Asy (s)	0.010	0.006	0.031	0.009	0.009	0.009	0.011	0.012	-	0.003

Appendix Table 5.Spatiotemporal gait characteristics of HPs during incline walking and walking on rock surface.

	Incline walking										
	1	2	3	4	5	6	7	8	9	10	
# of strides	*8*	*9*	*11*	*10*	*7*	*7*	*7*	*8*	*7*	*7*	
PACE											Average
Mean Stride V. (m/s)	1.178	1.076	1.233	1.178	1.185	1.136	1.357	1.222	1.231	1.390	1.218
Mean Stride L. (m)	1.215	1.290	1.480	1.215	1.424	1.375	1.275	1.427	1.555	1.715	1.397
RHYTHM											
Mean Stride Time (s)	1.248	1.184	1.200	1.046	1.205	1.197	0.953	1.134	1.25	1.205	1.162
Mean Step Time (s)	0.619	0.608	0.606	0.555	0.617	0.597	0.477	0.565	-	0.625	0.585
Mean Stance Time (s)	0.693	0.652	0.64	0.578	0.683	0.684	0.529	0.614	0.706	0.709	0.648
Mean Swing Time (s)	0.555	0.531	0.556	0.469	0.523	0.513	0.424	0.521	0.547	0.496	0.513
VARIABILITY											
Stride V. Var (m/s)	0.085	0.068	0.059	0.085	0.180	0.124	0.183	0.136	-	0.124	0.113
Stride L Var (m)	0.091	0.094	0.046	0.091	0.208	0.158	0.116	0.141	-	0.149	0.120
Step Time Var (s)	0.048	0.037	0.057	0.057	0.398	0.037	0.036	0.062	-	0.024	0.084
Stance Time Var (s)	0.050	0.047	0.073	0.045	0.058	0.046	0.029	0.106	-	0.074	0.058
Swing Time Var (s)	0.060	0.065	0.076	0.050	0.056	0.050	0.048	0.066	-	0.035	0.057
ASYMMETRY											
Stride L. Asy (m)	0.030	0.21	0.259	0.030	0.046	0.437	0.030	0.366	-	0.020	0.158
Step Time Asy (s)	0.000	0.025	0.051	0.029	0.269	0.047	0.004	0.002	-	0.029	0.050
Stance Time Asy (s)	0.009	0.055	0.024	0.035	0.049	0.036	0.002	0.007	-	0.049	0.029
Swing Time Asy (s)	0.010	0.007	0.010	0.017	0.022	0.048	0.015	0.015	-	0.068	0.023
	Rock surface										
	1	2	3	4	5	6	7	8	9	10	
# of strides	*6*	*6*	*8*	*3*	*6*	*6*	*5*	*4*	*8*	*7*	
PACE											Average
Mean Stride V. (m/s)	1.126	1.137	1.066	1.126	1.129	1.196	1.289	1.372	1.356	1.241	1.203
Mean Stride L. (m)	1.21	1.364	1.315	1.21	1.466	1.507	1.319	1.589	1.582	1.515	1.407
RHYTHM											
Mean Stride Time (s)	1.096	1.172	1.239	1.096	1.346	1.283	1.063	1.149	1.161	1.229	1.183
Mean Step Time (s)	0.554	0.592	0.623	0.554	0.673	0.635	0.531	0.569	-	0.623	0.594
Mean Stance Time (s)	0.607	0.64	0.717	0.607	0.775	0.734	0.585	0.641	0.652	0.705	0.666
Mean Swing Time (s)	0.489	0.532	0.522	0.489	0.571	0.549	0.478	0.508	0.509	0.524	0.517
VARIABILITY											
Stride V. Var (m/s)	0.107	0.099	0.096	0.107	0.082	0.050	0.100	0.064	-	0.101	0.084
Stride L Var (m)	0.112	0.15	0.123	0.112	0.094	0.067	0.109	0.123	-	0.136	0.108
Step Time Var (s)	0.022	0.027	0.062	0.022	0.045	0.045	0.034	0.020	-	0.054	0.036
Stance Time Var (s)	0.057	0.066	0.061	0.057	0.049	0.042	0.037	0.039	-	0.075	0.052
Swing Time Var (s)	0.033	0.033	0.033	0.033	0.059	0.037	0.063	0.046	-	0.038	0.040
ASYMMETRY											
Stride L. Asy (m)	0.211	0.190	0.032	0.211	0.167	0.307	0.100	0.006	-	0.124	0.149
Step Time Asy (s)	0.007	0.040	0.068	0.007	0.016	0.022	0.005	0.013	-	0.031	0.023
Stance Time Asy (s)	0.006	0.033	0.004	0.006	0.027	0.022	0.001	0.008	-	0.011	0.013
Swing Time Asy (s)	0.019	0.028	0.038	0.019	0.000	0.009	0.003	0.013	-	0.02	0.016

(-) parameter not available due to data collection or synchronisation error,
Stride V = stride velocity, Stride L = stride length. Var = variability, Asy = asymmetry

Appendix Table 6.Spatiotemporal gait characteristics of SS ground level walking in indoor and outdoor

	Indoor			*Outdoor*		
	1	2	3 np	1	2	3 np
# of strides	*80*	*110*	*91*	*95*	*125*	*108*
PACE						
Mean Stride V. (m/s)	0.997	0.977	1.09	1.014	0.955	1.233
Mean Stride L. (m)	1.35	1.121	1.44	1.248	1.055	1.850
RHYTHM						
Mean Stride Time (s)	1.308	1.145	1.310	1.248	1.070	1.388
Mean Step Time (s)	0.656	0.573	-	0.547	0.524	-
Mean Stance Time (s)	0.766	0.668	0.878	0.669	0.627	0.948

Mean Swing Time (s)	0.542	0.477	0.432	0.476	0.443	0.439
VARIABILITY						
Stride V. Var (m/s)	0.203	0.176	-	0.216	0.149	-
Stride L Var (m)	0.322	0.229	-	0.277	0.172	-
Step Time Var (s)	0.196	0.004	-	0.027	0.040	-
Stance Time Var (s)	0.129	0.012	-	0.072	0.077	-
Swing Time Var (s)	0.123	0.019	-	0.035	0.040	-
ASYMMETRY						
Stride L. Asy (m)	0.018	0.376	-	0.108	0.473	-
Step Time Asy (s)	0.063	0.057	-	0.164	0.041	-
Stance Time Asy (s)	0.064	0.063	-	0.134	0.042	-
Swing Time Asy (s)	0.062	0.062	-	0.103	0.031	-

(-) parameter not available due to data collection or synchronisation error, Stride V = stride velocity, Stride L = stride length. Var = variability, Asy = asymmetry,(np) non paretic side only due to failing to detect IC-FC times

Knee joint kinematics

Knee joint kinematics (HP): Increased asymmetry in knee flexion angles while walking on a rock surface was notable compared to indoor/outdoor ground-level walking. During incline walking (ascent slope), HP experienced lower mean knee flexion angles compared to indoor/outdoor ground-level walking. Increased variance and asymmetry in knee flexion angles during incline walking were other findings compared to indoor/outdoor ground-level walking. Additionally, increased mean knee flexion angles and asymmetry were found to be common during walking on rock surfaces compared to incline walking

In the stair ambulation experiment, knee flexion angles found higher during stair descent compared to stair ascent. No significant differences observed in the asymmetry of knee flexion angles.

Knee joint kinematics (SS): Increased variability and asymmetry in knee flexion angles were observed during indoor level walking compared to outdoor level walking. Similarly, SS experienced higher knee flexion angles during stair ascent compared to stair descent. Additionally, increased variance and decreased asymmetry were present during stair descent compared to the ascent.

Appendix Table 7.Kinematic knee joint angles (degree) of HPs

Indoor level walking											
	1	2	3	4	5	6	7	8	9	10	
# of strides	*104*	*105*	*103*	*76*	*95*	*104*	*124*	*103*	*100*	*82*	
											Average
Mean	62.976	51.839	63.419	62.701	59.281	64.467	62.791	66.774	64.056	67.906	62.621
Var	5.328	4.818	4.025	7.706	4.028	4.321	4.693	4.438	7.202	5.316	5.1875
Asy	3.485	3.467	1.950	0.880	0.760	2.869	1.635	0.687	0.954	1.430	1.8117
Outdoor level walking											
# of strides	*98*	*114*	*108*	*118*	*103*	*108*	*120*	*96*	*100*	*116*	
											Average
Mean	63.819	51.529	63.577	64.202	56.731	65.022	65.256	67.821	69.000	68.839	63.5796
Var	4.746	5.103	3.043	6.327	4.704	4.120	3.286	3.095	-	6.582	4.4901
Asy	0.042	2.046	2.231	3.498	0.847	1.364	1.530	2.602	-	0.175	1.592778
Incline walking											
# of strides	*8*	*9*	*11*	*10*	*7*	*7*	*7*	*8*	*7*	*7*	
											Average
Mean	59.836	49.133	57.166	59.836	48.602	64.125	62.099	70.640	59.731	62.900	59.406
Var	10.415	7.021	5.374	10.415	4.888	4.113	4.930	4.594	-	8.282	6.350
Asy	1.171	4.475	1.827	1.171	6.915	11.023	7.492	7.587	-	13.710	6.152
Rock surface											
# of strides	*6*	*6*	*8*	*3*	*6*	*6*	*5*	*4*	*8*	*7*	
											Average
Mean	65.381	56.778	54.643	65.381	52.102	69.335	62.986	70.574	70.731	67.267	63.517
Var	2.134	6.673	3.368	2.134	4.897	4.121	4.620	1.863	-	4.436	3.860
Asy	9.657	16.532	0.359	9.657	5.990	3.727	17.224	0.696	-	19.321	9.240
Stair ascent											
											Average
Mean	34.650	44.121	41.995	34.650	24.666	49.320	43.474	51.407	54.717	48.013	42.701

Var	3.264	2.369	3.942	3.264	-	4.754	3.781	2.653	-	2.491	2.989
Asy	2.901	5.516	0.337	2.901	-	0.463	7.679	4.591	-	4.758	3.643
Stair descent											
											Average
Mean	75.746	73.257	67.150	75.746	58.536	77.045	71.726	82.048	71.591	80.478	73.332
Var	8.708	7.392	3.906	8.708	-	5.847	6.227	5.500	-	7.141	6.928
Asy	0.841	1.540	4.590	0.841	-	5.807	4.293	5.964	-	1.896	3.221

(-) parameter not available due to data collection or synchronisation error

Appendix Table 8.Kinematic knee joint angles (degree) of SS

Stroke Survivors								
	Indoor level walking				*Outdoor level walking*			
	1	2	3 [np]		1	2	3 [np]	
# of strides	*80*	*110*	*91*		*95*	*125*	*108*	
				Average				Average
Mean	46.786	49.687	47.888	48.12033	50.782	53.251	52.255	52.096
Var	5.511	5.887	-	6.063667	4.682	6.002	-	5.297
Asy	17.746	26.757	-	22.2515	13.099	26.740	-	19.9195
	Stair ascent				*Stair descent*			
	1	2	3 [np]		1	2	3 [np]	
				Average				Average
Mean	32.485	40.762	36.096	36.44767	56.780	74.891	60.844	64.171
Var	5.108	5.868	-	4.712	8.003	6.999	-	7.262
Asy	14.952	2.103	-	8.5275	8.452	2.886	-	5.669

(-) parameter not available due to data collection or synchronisation error,
(np) non paretic side only due to failing to detect IC-FC times

EMG, burst timing and durations during stair ambulation

EMG, burst timing and durations (HP): The muscle activation patterns during stair ascent and descent for both groups were shown in Appendix Figure 3. Although muscle burst timing and durations slightly varied from person to person, common muscle activation patterns were revealed during stair ambulation. Findings of EMG muscle activation patterns in my participants are consistent with previous stair ambulation based EMG studies [412, 441].

In stair ascent experiments, TA found active mostly from late stance through swing phase to provide adequate foot clearance. TA muscle activation also found early stance phase in most HP. The activation at the stance phase was related to control of foot inversion-eversion, related to balance control during single limb support [441]. GS muscle bursts were detected in the stance phase (mostly mid-stance) for a short period similar to ground level walking. This finding shows good agreement with [412]. However, contradicts with [441], where GS reported being active during most stance phase. Prevalence of RF bursts was also observed in the stance phase, from early stance to midstance. BF muscle activation observed in both stance and swing phase, mostly around FC point and related to flexion of the knee for the next step over.

In stair descent experiments, TA muscle bursts were detected mostly at the initial stance phase, unlike stair ascent. This activation is potentially related to controlling foot inversion-eversion [441]. In some, TA also found active around at initial swing (FCs moments), help sustaining the foot while landing on a surface. GS muscle onset pattern observed around IC moment and lasts until stance to swing transition time. RF muscle activation were observed at the initial stance, IC moments. BF muscle burst found mostly in the opposite phase of RF. Muscle onset of BF at late stance is related to the preparation of limb loading [441].

EMG, burst timing and durations (SS): The common EMG pattern of burst timing and durations observed in HP also observed in SS group, as shown in Appendix Figure 2 - (d3-d6). Although there are differences in terms of burst timing and durations, it may not be possible to relate these differences with SS group as a result of this pilot study. Because earlier EMG based studies reported that there are other crucial parameters, such as walking velocity and age that affects muscle burst timing and durations [442]. Additionally, the number of studies for muscle activation of SS during stair ambulation is very limited, unlike level walking. Thus, future works will investigate the muscle pattern of SS during stair ambulation with a larger cohort.

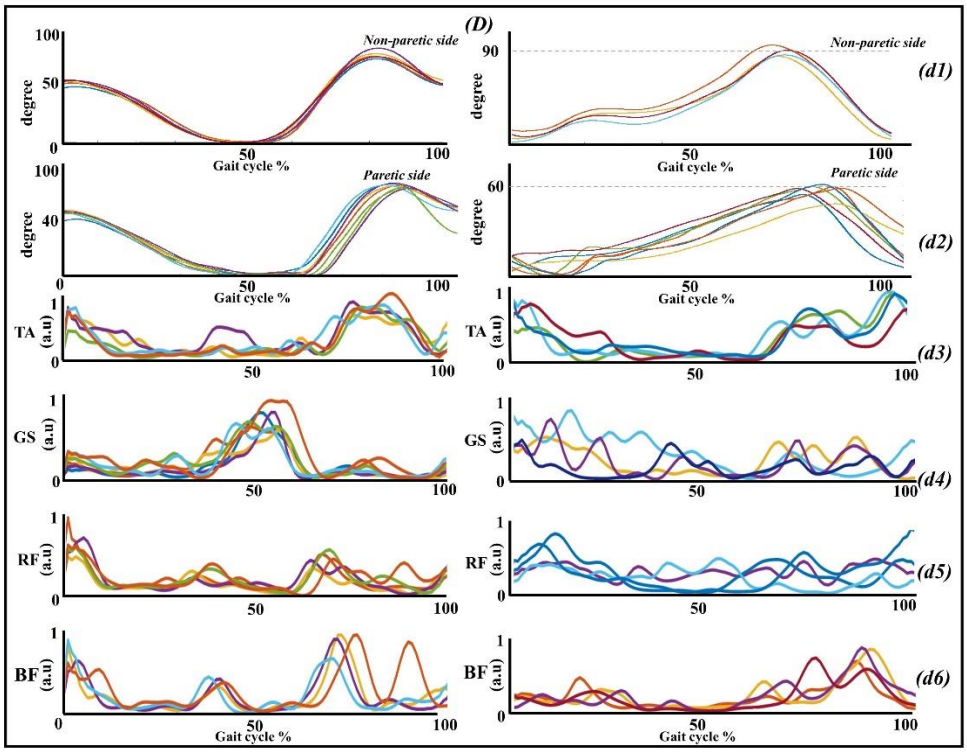

Appendix Figure 2. Stroke Gait. (D) stair ascent & descent extracted parameters from the proposed tool. (d1) left panel represents non paretic side knee flexion during stair ascent and right panel represent paretic side knee flexion during stair descent. (d2) left panel represents paretic side knee flexion during stair ascent and right panel represent non paretic side knee flexion during stair descent. Left panel of (d3-d6) presents typical lower limb muscle activations during stair ascent. Right panel of (d3-d6) presents typical lower limb muscle activations during stair descent. a.u, Arbitrary unit-peak normalised EMG

Appendix Table 9. Spatiotemporal gait characteristics of SS ground level walking in indoor and outdoor for the right and left sides. SS (#3) paretic, non-paretic data is not presented due to failing to detect paretic side IC-FC moments.

	Indoor						*Outdoor*					
	Np			*P*			*Np*			*P*		
RHYTHM	*1*	*2*	*Average*	*1*	*2*	*Average*	*1*	*2*	*Average*	*1*	*2*	*Average*
Mean Step T.ime (s)	0.558	0.57	0.564	0.754	0.575	0.6645	0.465	0.648	0.5565	0.63	0.606	0.618
Mean Stance Time (s)	0.83	0.673	0.7515	0.701	0.66	0.6805	0.736	0.427	0.5815	0.602	0.459	0.5305
Mean Swing Time (s)	0.48	0.467	0.4735	0.603	0.486	0.5445	0.425	0.503	0.464	0.528	0.545	0.5365
VARIABILITY												
Step Time Var (s)	0.004	0.004	0.004	0.003	0.002	0.0025	0.007	0.007	0.007	0.002	0.005	0.0035
Stance Time Var (s)	0.003	0.001	0.002	0.004	0.004	0.004	0.001	0.001	0.001	0.001	0.001	0.001
Swing Time Var (s)	0.004	0.004	0.004	0.003	0.003	0.003	0.001	0.001	0.001	0.001	0.001	0.001
Mean K.F.E angle (°)	55.659	63.065	59.362	37.913	36.308	37.1105	57.164	63.237	60.2005	42.576	38.311	40.4435

(K.F.E) knee flexion angle (degree), Np=non paretic side, P=paretic side
Bold indicate greater mean values comparing non paretic side to paretic side

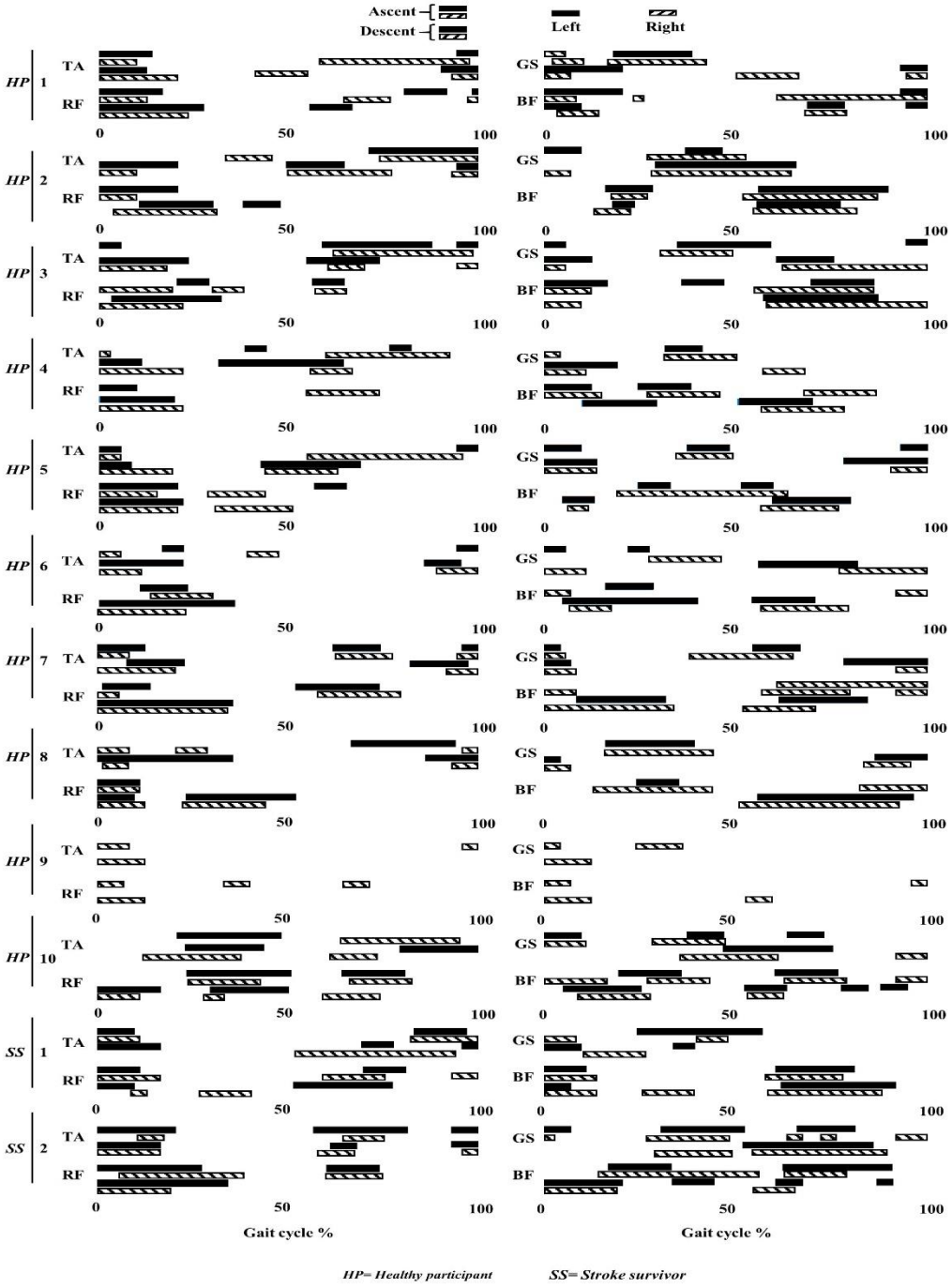

Appendix Figure 3. Muscle activity pattern for stair ambulation, healthy participants, and stroke survivors

Appendix 6. Chapter 9 Supplementary Materials

Appendix Table 10. Participants Demographics

Id	Age	Height	Weight	BMI	Id	Age	Height	Weight	BMI
1	29	184	90	26.58318	6	25	178	80	25.24934
2	26	182	78.5	23.69883	7	43	165	52	19.10009
3	39	177	78	24.89706	8	37	174	75	24.7721
4	24	186	115	33.24084	9	30	175	60	19.59184
5	24	185	78	22.79036	10	29	163	85	31.99217

Appendix Table 11.Validation results for slow walk speed

Id	Step-D1	Stride-D1	Step-R1	Stride-R1	Speed1	Step-D2	Stride-D2	Step-R2	Stride-R2	Speed2
1	0.71	1.4	0.753	1.46	0.778	0.75	1.5	0.823	1.62	0.643
2	0.7	1.34	0.707	1.39	0.934	0.7	1.38	0.707	1.49	0.889
3	0.71	1.41	0.71	1.42	0.758	0.76	1.49	0.758	1.52	0.672
4	0.67	1.34	0.682	1.34	0.887	0.69	1.38	0.706	1.39	0.852
5	0.75	1.48	0.757	1.49	0.761	0.77	1.52	0.783	1.55	0.688
6	0.72	1.4	0.72	1.43	0.785	0.73	1.45	0.73	1.5	0.739
7	0.72	1.44	0.706	1.43	0.577	0.71	1.42	0.699	1.41	0.597
8	0.63	1.25	0.637	1.25	0.774	0.59	1.15	0.608	1.19	0.889
9	0.7	1.39	0.69	1.38	0.831	0.71	1.42	0.694	1.39	0.814
10	0.76	1.45	0.766	1.52	0.663	0.74	1.48	0.743	1.51	0.656
D: edge device, R: reference system, 1: first trial, 2: second trial										

Appendix Table 12.Validation results for normal walk speed

Id	Step-D1	Stride-D1	Step-R1	Stride-R1	Speed1	Step-D2	Stride-D2	Step-R2	Stride-R2	Speed2
1	0.51	1.05	0.532	1.04	1.29	0.54	1.09	0.55	1.08	1.24
2	0.59	1.21	0.59	1.16	1.22	0.58	1.18	0.579	1.14	1.23
3	0.58	1.16	0.573	1.16	1.25	0.58	1.14	0.567	1.15	1.25
4	0.57	1.14	0.572	1.14	1.19	0.57	1.14	0.572	1.14	1.2
5	0.6	1.21	0.601	1.2	1.15	0.62	1.23	0.608	1.22	1.14
6	0.57	1.16	0.56	1.13	1.2	0.56	1.13	0.55	1.12	1.22
7	0.49	0.97	0.489	0.972	1.17	0.49	1	0.491	0.976	1.14
8	0.57	1.14	0.565	1.11	1.08	0.55	1.14	0.563	1.11	1.09
9	0.58	1.16	0.572	1.14	1.14	0.59	1.18	0.574	1.14	1.14
10	0.55	1.11	0.543	1.09	1.14	0.51	1.07	0.531	1.07	1.2
D: edge device, R: reference system, 1: first trial, 2: second trial										

Appendix Table 13.Validation results for fast walk speed

Id	Step-D1	Stride-D1	Step-R1	Stride-R1	Speed1	Step-D2	Stride-D2	Step-R2	Stride-R2	Speed2
1	0.48	0.96	0.494	0.965	1.51	0.49	0.98	0.498	0.973	1.49
2	0.54	1.04	0.539	1.05	1.46	0.53	1.06	0.539	1.06	1.45
3	0.52	1.04	0.521	1.05	1.59	0.51	1.02	0.512	1.03	1.61
4	0.51	1.04	0.51	1.01	1.52	0.5	0.99	0.504	1.01	1.5
5	0.56	1.12	0.558	1.12	1.32	0.55	1.08	0.545	1.1	1.39
6	0.51	1.01	0.5	1.01	1.48	0.49	0.99	0.49	0.99	1.52
7	0.44	0.88	0.429	0.85	1.74	0.45	0.91	0.41	0.84	1.77
8	0.53	1.05	0.527	1.04	1.34	0.51	1.02	0.514	1.01	1.38
9	0.49	0.99	0.496	0.985	1.43	0.49	0.97	0.487	0.969	1.46
10	0.49	0.98	0.486	0.973	1.45	0.47	0.95	0.471	0.94	1.52
D: edge device, R: reference system, 1: first trial, 2: second trial										

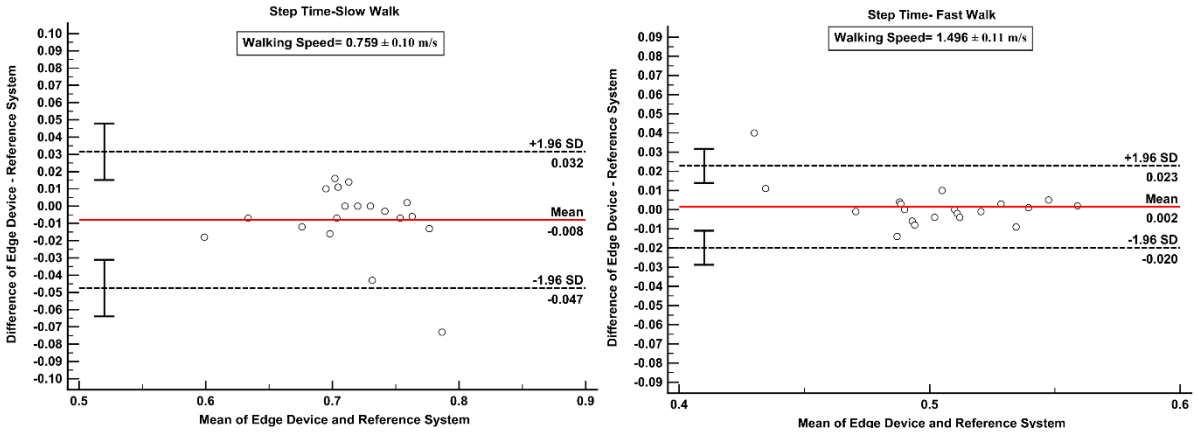

Appendix Figure 4. Bland-Altman plots for Step time during slow and fast walking speeds

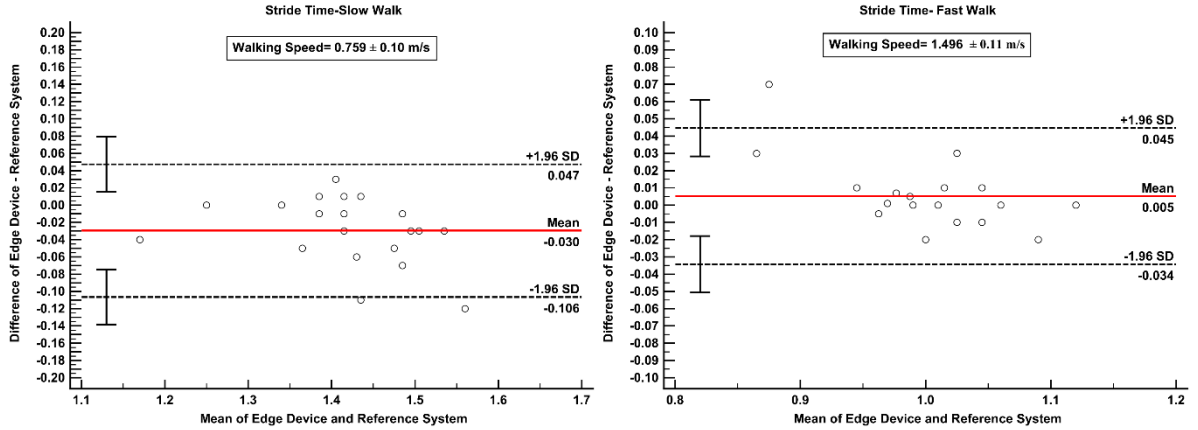

Appendix Figure 5. Bland-Altman plots for Stride time during slow and fast walking speeds

Appendix 7. Single & dual tasking

Gait assessment beyond the lab is challenging for many reasons already presented. Of focus here is the concept of single and dual tasking and how that can impact gait characteristic interpretation. As described, gait changes observed in laboratory testing are associated with, and predictive of, numerous adverse health outcomes, including neurodegenerative diseases, cognitive decline, dementia, fall risk, and mortality [491-499]. Particularly, laboratory testing allows the control and/or experimental manipulation of the environment and task complexity through well-defined protocols, which are designed to simulate different situations of daily activities. The primary idea is to stress the locomotor system out to a point where walking difficulties become clearer and the underlying mechanisms quantifiable. Although numerous laboratory-based protocols have been proposed (e.g., obstacle avoidance, fast walking, dimed lighting, etc. [500-503]), the most common protocol involves single- and dual-task walking.

The dual-task paradigm has been extensively used to investigate the contribution of executive-attentional resources to the control of walking. In such a protocol, walking and a concurrent cognitive or motor task are performed separately (single-task condition) as well as simultaneously (dual-task condition). Performance must be quantified for both tasks in single-task and dual-task conditions [504]. To avoid the influence of order effect, the two conditions must be performed in random order or counter-balanced through participants. The walking task may include bouts of walking in a straight line, walking back and forth (with 180° turns) a given distance for a fixed number of times, walking continuously over an oval or semi-rectangular circuit for a fixed time/period or treadmill walking. Regarding the concurrent task, many have been used: counting backwards, serial subtractions, number recall, reverse number recall, digit vigilance, verbal fluency, handling objects and others. These concurrent tasks target different aspects of cognitive function, such as working memory, attention, and verbal functioning. Standardized instructions to participants are recommended as they may influence task prioritization [505, 506].

The dual-task condition often yields a decrement in performance of one or both tasks compared to the single-task condition. The magnitude of the decrement, referred as “dual-task cost” or “dual-task interference”, is calculated relative to the single-task condition, in below Equation.

$$\text{Dual-task cost} = \left(\frac{\text{single-task measure} - \text{dual-task measure}}{\text{single-task measure}}\right) \times 100$$

The dual-task cost represents the interference between the two tasks that compete for resources from common brain networks, including the prefrontal cortex [503, 507-510]. Dual-task costs to walking include, but are not limited to, reduced speed, increased gait variability and poorer walking-adaptability e.g., obstacle avoidance [504, 511-513]. When movement automaticity is preserved and lower levels of executive-attentional resources are required to control walking, which is the case for healthy individuals, the dual-task cost to walking is expected to be lower [510]. In contrast, the dual-task cost is expected to be greater when single walking requires increased levels of executive-attentional control [510], which is typically the case in neurological populations as a result of impaired automaticity [511, 513]. Greater dual-task cost is also expected in individuals with limited attentional-executive resources as they may not have enough resources to deal with two simultaneous tasks. Although it is well known that dual-task walking ability declines with age [503, 514] and even more with neurological diseases [511, 513], there is still need for the development of normative data and disease-specific signatures [492, 513]. Accordingly, interpretation of gait characteristics from outdoor walking has many challenges to overcome before it can be robustly used to inform clinical practice or research trends in many clinical cohorts.

References

[1] A. Godfrey, R. Conway, D. Meagher, and G. ÓLaighin, "Direct measurement of human movement by accelerometry," *Medical engineering & physics,* vol. 30, no. 10, pp. 1364-1386, 2008.

[2] Y. Celik, S. Stuart, W. L. Woo, and A. Godfrey, "Gait analysis in neurological populations: Progression in the use of wearables," *Medical Engineering & Physics,* 2020.

[3] C. K. Taguchi, J. P. Teixeira, L. V. Alves, P. F. Oliveira, and O. F. F. Raposo, "Quality of life and gait in elderly group," *International archives of otorhinolaryngology,* vol. 20, no. 03, pp. 235-240, 2016.

[4] W. Pirker and R. Katzenschlager, "Gait disorders in adults and the elderly," *Wiener Klinische Wochenschrift,* vol. 129, no. 3-4, pp. 81-95, 2017.

[5] D. Trojaniello, A. Cereatti, and U. Della Croce, "Accuracy, sensitivity and robustness of five different methods for the estimation of gait temporal parameters using a single inertial sensor mounted on the lower trunk," *Gait & posture,* vol. 40, no. 4, pp. 487-492, 2014.

[6] J. McCamley, M. Donati, E. Grimpampi, and C. Mazza, "An enhanced estimate of initial contact and final contact instants of time using lower trunk inertial sensor data," *Gait & posture,* vol. 36, no. 2, pp. 316-318, 2012.

[7] D. Trojaniello, A. Ravaschio, J. M. Hausdorff, and A. Cereatti, "Comparative assessment of different methods for the estimation of gait temporal parameters using a single inertial sensor: application to elderly, post-stroke, Parkinson's disease and Huntington's disease subjects," *Gait & posture,* vol. 42, no. 3, pp. 310-316, 2015.

[8] L. C. Benson, C. A. Clermont, E. Bošnjak, and R. Ferber, "The use of wearable devices for walking and running gait analysis outside of the lab: A systematic review," *Gait & posture,* vol. 63, pp. 124-138, 2018.

[9] S. Lord, B. Galna, J. Verghese, S. Coleman, D. Burn, and L. Rochester, "Independent domains of gait in older adults and associated motor and nonmotor attributes: validation of a factor analysis approach," *Journals of Gerontology Series A: Biomedical Sciences and Medical Sciences,* vol. 68, no. 7, pp. 820-827, 2013.

[10] J. H. Hollman, E. M. McDade, and R. C. Petersen, "Normative spatiotemporal gait parameters in older adults," *Gait & posture,* vol. 34, no. 1, pp. 111-118, 2011.

[11] M. Roberts, D. Mongeon, and F. Prince, "Biomechanical parameters for gait analysis: a systematic review of healthy human gait," *Phys Ther Rehabil,* vol. 4, p. 6, 2017.

[12] Y. Celik *et al.*, "Sensor Integration for Gait Analysis," 2023.

[13] Y. Celik, S. Stuart, W. L. Woo, E. Sejdic, and A. Godfrey, "Multi-modal gait: A wearable, algorithm and data fusion approach for clinical and free-living assessment," *Information Fusion,* vol. 78, pp. 57-70, 2022.

[14] M. E. Issa, A. M. Helmi, M. A. Al-Qaness, A. Dahou, M. A. Elaziz, and R. Damaševičius, "Human Activity Recognition Based on Embedded Sensor Data Fusion for the Internet of Healthcare Things," in *Healthcare*, 2022, vol. 10, no. 6: Multidisciplinary Digital Publishing Institute, p. 1084.

[15] G. Şengül, E. Ozcelik, S. Misra, R. Damaševičius, and R. Maskeliūnas, "Fusion of smartphone sensor data for classification of daily user activities," *Multimedia Tools and Applications,* vol. 80, no. 24, pp. 33527-33546, 2021.

[16] S. Ramasamy Ramamurthy and N. Roy, "Recent trends in machine learning for human activity recognition—A survey," *Wiley Interdisciplinary Reviews: Data Mining and Knowledge Discovery,* vol. 8, no. 4, p. e1254, 2018.

[17] W. Sousa Lima, E. Souto, K. El-Khatib, R. Jalali, and J. Gama, "Human activity recognition using inertial sensors in a smartphone: An overview," *Sensors,* vol. 19, no. 14, p. 3213, 2019.

[18] M. K. O'Brien *et al.*, "Activity recognition for persons with stroke using mobile phone technology: toward improved performance in a home setting," *Journal of medical Internet research,* vol. 19, no. 5, p. e184, 2017.

[19] M. V. Albert, S. Toledo, M. Shapiro, and K. Koerding, "Using mobile phones for activity recognition in Parkinson's patients," *Frontiers in neurology,* vol. 3, p. 158, 2012.

[20] Y. Celik, M. F. Aslan, K. Sabanci, S. Stuart, W. L. Woo, and A. Godfrey, "Improving Inertial Sensor-Based Activity Recognition in Neurological Populations," *Sensors,* vol. 22, no. 24, p. 9891, 2022.

[21] S. Del Din *et al.*, "Analysis of free-living gait in older adults with and without Parkinson's disease and with and without a history of falls: identifying generic and disease-specific characteristics," *The Journals of Gerontology: Series A,* vol. 74, no. 4, pp. 500-506, 2019.

[22] S. Del Din, A. Godfrey, B. Galna, S. Lord, and L. Rochester, "Free-living gait characteristics in ageing and Parkinson's disease: impact of environment and ambulatory bout length," *Journal of neuroengineering and rehabilitation,* vol. 13, no. 1, p. 46, 2016.

[23] S. Del Din, A. Godfrey, C. Mazzà, S. Lord, and L. Rochester, "Free-living monitoring of Parkinson's disease: Lessons from the field," *Movement Disorders,* vol. 31, no. 9, pp. 1293-1313, 2016.
[24] X. Zeng, X. Zhang, S. Yang, Z. Shi, and C. Chi, "Gait-based implicit authentication using edge computing and deep learning for mobile devices," *Sensors,* vol. 21, no. 13, p. 4592, 2021.
[25] J. Wu *et al.*, "Real-Time Gait Phase Detection on Wearable Devices for Real-World Free-Living Gait," *IEEE Journal of Biomedical and Health Informatics,* 2022.
[26] J. Mansour and J. Pereira, "Quantitative functional anatomy of the lower limb with application to human gait," *Journal of Biomechanics,* vol. 20, no. 1, pp. 51-58, 1987.
[27] J. Verghese, A. F. Ambrose, R. B. Lipton, and C. Wang, "Neurological gait abnormalities and risk of falls in older adults," *Journal of neurology,* vol. 257, no. 3, pp. 392-398, 2010.
[28] R. Melin, K. S. Fugl-Meyer, and A. R. Fugl-Meyer, "Life satisfaction in 18-to 64-year-old Swedes: in relation to education, employment situation, health and physical activity," *Journal of rehabilitation medicine,* vol. 35, no. 2, pp. 84-90, 2003.
[29] S. Deandrea, E. Lucenteforte, F. Bravi, R. Foschi, C. La Vecchia, and E. Negri, "Risk factors for falls in community-dwelling older people:" a systematic review and meta-analysis"," *Epidemiology,* pp. 658-668, 2010.
[30] B. Homann *et al.*, "The impact of neurological disorders on the risk for falls in the community dwelling elderly: a case-controlled study," *BMJ open,* vol. 3, no. 11, p. e003367, 2013.
[31] Y. Moon, J. Sung, R. An, M. E. Hernandez, and J. J. Sosnoff, "Gait variability in people with neurological disorders: a systematic review and meta-analysis," *Human movement science,* vol. 47, pp. 197-208, 2016.
[32] R. Schniepp *et al.*, "The interrelationship between disease severity, dynamic stability, and falls in cerebellar ataxia," *Journal of neurology,* vol. 263, no. 7, pp. 1409-1417, 2016.
[33] E. Buckley, C. Mazzà, and A. McNeill, "A systematic review of the gait characteristics associated with Cerebellar Ataxia," *Gait & posture,* vol. 60, pp. 154-163, 2018.
[34] J. M. Hausdorff, "Gait dynamics in Parkinson's disease: common and distinct behavior among stride length, gait variability, and fractal-like scaling," *Chaos: An Interdisciplinary Journal of Nonlinear Science,* vol. 19, no. 2, p. 026113, 2009.
[35] M. Pistacchi *et al.*, "Gait analysis and clinical correlations in early Parkinson's disease," *Functional neurology,* vol. 32, no. 1, p. 28, 2017.
[36] S. M. Woolley, "Characteristics of gait in hemiplegia," *Topics in stroke rehabilitation,* vol. 7, no. 4, pp. 1-18, 2001.
[37] B. Balaban and F. Tok, "Gait disturbances in patients with stroke," *PM&R,* vol. 6, no. 7, pp. 635-642, 2014.
[38] J. Boudarham, N. Roche, D. Pradon, C. Bonnyaud, D. Bensmail, and R. Zory, "Variations in kinematics during clinical gait analysis in stroke patients," *PloS one,* vol. 8, no. 6, 2013.
[39] H. P. Von Schroeder, R. D. Coutts, P. D. Lyden, E. Billings, and V. L. Nickel, "Gait parameters following stroke: a practical assessment," *Journal of rehabilitation research and development,* vol. 32, pp. 25-25, 1995.
[40] K. J. Kelleher, W. Spence, S. Solomonidis, and D. Apatsidis, "The characterisation of gait patterns of people with multiple sclerosis," *Disability and Rehabilitation,* vol. 32, no. 15, pp. 1242-1250, 2010/01/01 2010, doi: 10.3109/09638280903464497.
[41] S. Guner and F. Inanici, "Yoga therapy and ambulatory multiple sclerosis assessment of gait analysis parameters, fatigue and balance," *Journal of bodywork and movement therapies,* vol. 19, no. 1, pp. 72-81, 2015.
[42] T. Egerton, D. R. Williams, and R. Iansek, "Comparison of gait in progressive supranuclear palsy, Parkinson's disease and healthy older adults," *BMC neurology,* vol. 12, no. 1, p. 116, 2012.
[43] B. Muñoz Ospina *et al.*, "Age Matters: Objective Gait Assessment in Early Parkinson's Disease Using an RGB-D Camera," *Parkinson's Disease,* vol. 2019, 2019.
[44] S. Fahn, "Members of the UPDRS development committee. Unified Parkinson's disease rating scale," *Recent developments in Parkinson's disease,* vol. 2, pp. 293-304, 1987.
[45] P. Trouillas *et al.*, "International Cooperative Ataxia Rating Scale for pharmacological assessment of the cerebellar syndrome," *Journal of the neurological sciences,* vol. 145, no. 2, pp. 205-211, 1997.
[46] R. Côté, V. Hachinski, B. Shurvell, J. Norris, and C. Wolfson, "The Canadian Neurological Scale: a preliminary study in acute stroke," *Stroke,* vol. 17, no. 4, pp. 731-737, 1986.
[47] R. C. Mohs and L. Cohen, "Alzheimer's disease assessment scale (ADAS)," *Psychopharmacol Bull,* vol. 24, no. 4, pp. 627-628, 1988.
[48] J. F. Kurtzke, "Rating neurologic impairment in multiple sclerosis: an expanded disability status scale (EDSS)," *Neurology,* vol. 33, no. 11, pp. 1444-1444, 1983.

[49] G. Williams, "High-Level Mobility Assessment Test," in *Encyclopedia of Clinical Neuropsychology*, J. S. Kreutzer, J. DeLuca, and B. Caplan Eds. New York, NY: Springer New York, 2011, pp. 1245-1247.
[50] D. M. Wrisley, M. L. Walker, J. L. Echternach, and B. Strasnick, "Reliability of the dynamic gait index in people with vestibular disorders," *Archives of physical medicine and rehabilitation,* vol. 84, no. 10, pp. 1528-1533, 2003.
[51] J. C. Schlachetzki *et al.*, "Wearable sensors objectively measure gait parameters in Parkinson's disease," *PloS one,* vol. 12, no. 10, 2017.
[52] A. Mirelman *et al.*, "Gait impairments in Parkinson's disease," *The Lancet Neurology,* 2019.
[53] J. Dicharry, "Kinematics and kinetics of gait: from lab to clinic," *Clinics in sports medicine,* vol. 29, no. 3, pp. 347-364, 2010.
[54] A. Muro-De-La-Herran, B. Garcia-Zapirain, and A. Mendez-Zorrilla, "Gait analysis methods: An overview of wearable and non-wearable systems, highlighting clinical applications," *Sensors,* vol. 14, no. 2, pp. 3362-3394, 2014.
[55] A. L. McDonough, M. Batavia, F. C. Chen, S. Kwon, and J. Ziai, "The validity and reliability of the GAITRite system's measurements: A preliminary evaluation," *Archives of physical medicine and rehabilitation,* vol. 82, no. 3, pp. 419-425, 2001.
[56] F. Wang, E. Stone, M. Skubic, J. M. Keller, C. Abbott, and M. Rantz, "Toward a passive low-cost in-home gait assessment system for older adults," *IEEE journal of biomedical and health informatics,* vol. 17, no. 2, pp. 346-355, 2013.
[57] F. Wang, M. Skubic, M. Rantz, and P. E. Cuddihy, "Quantitative gait measurement with pulse-doppler radar for passive in-home gait assessment," *IEEE Transactions on Biomedical Engineering,* vol. 61, no. 9, pp. 2434-2443, 2014.
[58] E. E. Stone and M. Skubic, "Capturing habitual, in-home gait parameter trends using an inexpensive depth camera," in *2012 Annual International Conference of the IEEE Engineering in Medicine and Biology Society*, 2012: IEEE, pp. 5106-5109.
[59] E. E. Stone and M. Skubic, "Unobtrusive, continuous, in-home gait measurement using the Microsoft Kinect," *IEEE Transactions on Biomedical Engineering,* vol. 60, no. 10, pp. 2925-2932, 2013.
[60] A. Cereatti, D. Trojaniello, and U. Della Croce, "Accurately measuring human movement using magneto-inertial sensors: techniques and challenges," in *2015 IEEE International Symposium on Inertial Sensors and Systems (ISISS) Proceedings*, 2015: IEEE, pp. 1-4.
[61] A. M. Howell, T. Kobayashi, H. A. Hayes, K. B. Foreman, and S. J. M. Bamberg, "Kinetic gait analysis using a low-cost insole," *IEEE Transactions on Biomedical Engineering,* vol. 60, no. 12, pp. 3284-3290, 2013.
[62] D. A. Jacobs and D. P. Ferris, "Estimation of ground reaction forces and ankle moment with multiple, low-cost sensors," *Journal of neuroengineering and rehabilitation,* vol. 12, no. 1, p. 90, 2015.
[63] L. Palmerini, L. Rocchi, S. Mazilu, E. Gazit, J. M. Hausdorff, and L. Chiari, "Identification of characteristic motor patterns preceding freezing of gait in Parkinson's disease using wearable sensors," *Frontiers in neurology,* vol. 8, p. 394, 2017.
[64] T. Zebin, P. Scully, and K. B. Ozanyan, "Inertial sensing for gait analysis and the scope for sensor fusion," in *2015 IEEE SENSORS*, 2015: IEEE, pp. 1-4.
[65] A. Alamdari and V. N. Krovi, "A review of computational musculoskeletal analysis of human lower extremities," in *Human Modelling for Bio-Inspired Robotics*: Elsevier, 2017, pp. 37-73.
[66] M. Iosa, P. Picerno, S. Paolucci, and G. Morone, "Wearable inertial sensors for human movement analysis," *Expert review of medical devices,* vol. 13, no. 7, pp. 641-659, 2016.
[67] R. O'Rahilly and F. Müller, *Basic human anatomy: a regional study of human structure*. WB Saunders Company, 1983.
[68] F. G. O'Connor, R. P. Wilder, and R. Nirschl, *Textbook of running medicine*. McGraw-Hill, 2001.
[69] S. Giannini, F. Catani, and M. G. Benedetti, *Gait analysis: methodologies and clinical applications*. IOS press, 1994.
[70] P. O. Riley, J. Dicharry, J. Franz, U. Della Croce, R. P. Wilder, and D. C. Kerrigan, "A kinematics and kinetic comparison of overground and treadmill running," *Medicine & Science in Sports & Exercise,* vol. 40, no. 6, pp. 1093-1100, 2008.
[71] K. Sharifmoradi and N. Farahpour, "An assessment of gait spatiotemporal and GRF of Parkinson patients," *Health Reh,* vol. 1, no. 1, pp. 1-6, 2016.
[72] S. Chen, J. Lach, B. Lo, and G.-Z. Yang, "Toward pervasive gait analysis with wearable sensors: A systematic review," *IEEE journal of biomedical and health informatics,* vol. 20, no. 6, pp. 1521-1537, 2016.

[73] P. H. Veltink, C. Liedtke, E. Droog, and H. van der Kooij, "Ambulatory measurement of ground reaction forces," *IEEE Transactions on Neural Systems and Rehabilitation Engineering,* vol. 13, no. 3, pp. 423-427, 2005.
[74] W. Xu, M.-C. Huang, N. Amini, J. J. Liu, L. He, and M. Sarrafzadeh, "Smart insole: A wearable system for gait analysis," in *Proceedings of the 5th International Conference on PErvasive Technologies Related to Assistive Environments*, 2012, pp. 1-4.
[75] J. Perry, "The contribution of dynamic electromyography to gait analysis," *J Rehabil Res Dev,* vol. 33, 1998.
[76] J. Perry and J. R. Davids, "Gait analysis: normal and pathological function," *Journal of Pediatric Orthopaedics,* vol. 12, no. 6, p. 815, 1992.
[77] W. Tao, T. Liu, R. Zheng, and H. Feng, "Gait analysis using wearable sensors," *Sensors,* vol. 12, no. 2, pp. 2255-2283, 2012.
[78] S. Hagio, M. Fukuda, and M. Kouzaki, "Identification of muscle synergies associated with gait transition in humans," *Frontiers in human neuroscience,* vol. 9, p. 48, 2015.
[79] R. E. Singh, K. Iqbal, G. White, and J. K. Holtz, "A Review of EMG Techniques for Detection of Gait Disorders," in *Machine Learning in Medicine and Biology*: IntechOpen, 2019.
[80] M. B. I. Reaz, M. S. Hussain, and F. Mohd-Yasin, "Techniques of EMG signal analysis: detection, processing, classification and applications," *Biological procedures online,* vol. 8, no. 1, pp. 11-35, 2006.
[81] W. G. Bradley, *Neurology in clinical practice: principles of diagnosis and management*. Taylor & Francis, 2004.
[82] M. Goudriaan *et al.*, "Non-neural muscle weakness has limited influence on complexity of motor control during gait," *Frontiers in human neuroscience,* vol. 12, p. 5, 2018.
[83] E. Friis, *Mechanical Testing of Orthopaedic Implants*. Woodhead Publishing, 2017.
[84] Y. Li and D. X. Dai, *Biomechanical engineering of textiles and clothing*. Woodhead Publishing, 2006.
[85] A. Elbaz *et al.*, "Patients with knee osteoarthritis demonstrate improved gait pattern and reduced pain following a non-invasive biomechanical therapy: a prospective multi-centre study on Singaporean population," *Journal of orthopaedic surgery and research,* vol. 9, no. 1, p. 1, 2014.
[86] P. Plummer-D'Amato, L. J. Altmann, A. L. Behrman, and M. Marsiske, "Interference between cognition, double-limb support, and swing during gait in community-dwelling individuals poststroke," *Neurorehabilitation and neural repair,* vol. 24, no. 6, pp. 542-549, 2010.
[87] A. Weiss, S. Sharifi, M. Plotnik, J. P. van Vugt, N. Giladi, and J. M. Hausdorff, "Toward automated, at-home assessment of mobility among patients with Parkinson disease, using a body-worn accelerometer," *Neurorehabilitation and neural repair,* vol. 25, no. 9, pp. 810-818, 2011.
[88] M. Nouredanesh, A. Godfrey, J. Howcroft, E. D. Lemaire, and J. Tung, "Fall risk assessment in the wild: A critical examination of wearable sensors use in free-living conditions," *Gait & Posture,* 2020.
[89] E. Sejdić, K. A. Lowry, J. Bellanca, M. S. Redfern, and J. S. Brach, "A comprehensive assessment of gait accelerometry signals in time, frequency and time-frequency domains," *IEEE Transactions on Neural Systems and Rehabilitation Engineering,* vol. 22, no. 3, pp. 603-612, 2013.
[90] J. Verghese, C. Wang, R. B. Lipton, R. Holtzer, and X. Xue, "Quantitative gait dysfunction and risk of cognitive decline and dementia," *Journal of Neurology, Neurosurgery & Psychiatry,* vol. 78, no. 9, pp. 929-935, 2007.
[91] R. Morris, A. Hickey, S. Del Din, A. Godfrey, S. Lord, and L. Rochester, "A model of free-living gait: a factor analysis in Parkinson's disease," *Gait & posture,* vol. 52, pp. 68-71, 2017.
[92] R. Morris *et al.*, "Cognitive associations with comprehensive gait and static balance measures in Parkinson's disease," *Parkinsonism & related disorders,* vol. 69, pp. 104-110, 2019.
[93] F. B. Horak, M. Mancini, P. Carlson-Kuhta, J. G. Nutt, and A. Salarian, "Balance and gait represent independent domains of mobility in Parkinson disease," *Physical therapy,* vol. 96, no. 9, pp. 1364-1371, 2016.
[94] S. Stuart, L. Parrington, R. Morris, D. N. Martini, P. C. Fino, and L. A. King, "Gait measurement in chronic mild traumatic brain injury: A model approach," *Human movement science,* vol. 69, p. 102557, 2020.
[95] A. Cappozzo, U. Della Croce, A. Leardini, and L. Chiari, "Human movement analysis using stereophotogrammetry: Part 1: theoretical background," *Gait & posture,* vol. 21, no. 2, pp. 186-196, 2005.
[96] P. Merriaux, Y. Dupuis, R. Boutteau, P. Vasseur, and X. Savatier, "A study of vicon system positioning performance," *Sensors,* vol. 17, no. 7, p. 1591, 2017.
[97] R. Rucco *et al.*, "Spatio-temporal and kinematic gait analysis in patients with Frontotemporal dementia and Alzheimer's disease through 3D motion capture," *Gait & posture,* vol. 52, pp. 312-317, 2017.

[98] S. L. Colyer, M. Evans, D. P. Cosker, and A. I. Salo, "A review of the evolution of vision-based motion analysis and the integration of advanced computer vision methods towards developing a markerless system," *Sports medicine-open,* vol. 4, no. 1, p. 24, 2018.
[99] E. Surer and A. Kose, "Methods and technologies for gait analysis," in *Computer Analysis of Human Behavior*: Springer, 2011, pp. 105-123.
[100] M. B. Popovic, *Biomechatronics*. Academic Press, 2019.
[101] R. G. Cutlip, C. Mancinelli, F. Huber, and J. DiPasquale, "Evaluation of an instrumented walkway for measurement of the kinematic parameters of gait," *Gait & posture,* vol. 12, no. 2, pp. 134-138, 2000.
[102] K. E. Webster, J. E. Wittwer, and J. A. Feller, "Validity of the GAITRite® walkway system for the measurement of averaged and individual step parameters of gait," *Gait & posture,* vol. 22, no. 4, pp. 317-321, 2005.
[103] B. Bilney, M. Morris, and K. Webster, "Concurrent related validity of the GAITRite® walkway system for quantification of the spatial and temporal parameters of gait," *Gait & posture,* vol. 17, no. 1, pp. 68-74, 2003.
[104] N. Mital and A. King, "Computation of rigid-body rotation in three-dimensional space from body-fixed linear acceleration measurements," 1979.
[105] D. Roetenberg, H. Luinge, and P. Slycke, "Xsens MVN: Full 6DOF human motion tracking using miniature inertial sensors," *Xsens Motion Technologies BV, Tech. Rep,* vol. 1, 2009.
[106] D. Roetenberg, *Inertial and magnetic sensing of human motion*. These de doctorat, 2006.
[107] A. M. Sabatini, "Estimating three-dimensional orientation of human body parts by inertial/magnetic sensing," *Sensors,* vol. 11, no. 2, pp. 1489-1525, 2011.
[108] M. Mathie, A. Coster, N. Lovell, and B. Celler, "Detection of daily physical activities using a triaxial accelerometer," *Medical and Biological Engineering and Computing,* vol. 41, no. 3, pp. 296-301, 2003.
[109] A. Cappozzo, "Low frequency self-generated vibration during ambulation in normal men," *Journal of Biomechanics,* vol. 15, no. 8, pp. 599-609, 1982.
[110] F. Petraglia, L. Scarcella, G. Pedrazzi, L. Brancato, R. Puers, and C. Costantino, "Inertial sensors versus standard systems in gait analysis: a systematic review and meta-analysis," *Eur. J. Phys. Rehabil. Med,* vol. 55, pp. 265-280, 2019.
[111] C. V. Bouten, K. T. Koekkoek, M. Verduin, R. Kodde, and J. D. Janssen, "A triaxial accelerometer and portable data processing unit for the assessment of daily physical activity," *IEEE transactions on biomedical engineering,* vol. 44, no. 3, pp. 136-147, 1997.
[112] A. Khan, N. Hammerla, S. Mellor, and T. Plötz, "Optimising sampling rates for accelerometer-based human activity recognition," *Pattern Recognition Letters,* vol. 73, pp. 33-40, 2016.
[113] E. K. Antonsson and R. W. Mann, "The frequency content of gait," *Journal of biomechanics,* vol. 18, no. 1, pp. 39-47, 1985.
[114] K. Aminian, P. Robert, E. Jéquier, and Y. Schutz, "Incline, speed, and distance assessment during unconstrained walking," *Medicine and science in sports and exercise,* vol. 27, no. 2, pp. 226-234, 1995.
[115] M. Sun and J. Hill, "A method for measuring mechanical work and work efficiency during human activities," *Journal of biomechanics,* vol. 26, no. 3, pp. 229-241, 1993.
[116] R. Caldas, M. Mundt, W. Potthast, F. B. de Lima Neto, and B. Markert, "A systematic review of gait analysis methods based on inertial sensors and adaptive algorithms," *Gait & posture,* vol. 57, pp. 204-210, 2017.
[117] M. J. Mathie, A. C. Coster, N. H. Lovell, and B. G. Celler, "Accelerometry: providing an integrated, practical method for long-term, ambulatory monitoring of human movement," *Physiological measurement,* vol. 25, no. 2, p. R1, 2004.
[118] A. Millecamps, K. A. Lowry, J. S. Brach, S. Perera, M. S. Redfern, and E. Sejdić, "Understanding the effects of pre-processing on extracted signal features from gait accelerometry signals," *Computers in biology and medicine,* vol. 62, pp. 164-174, 2015.
[119] D. Jarchi, J. Pope, T. K. Lee, L. Tamjidi, A. Mirzaei, and S. Sanei, "A review on accelerometry-based gait analysis and emerging clinical applications," *IEEE reviews in biomedical engineering,* vol. 11, pp. 177-194, 2018.
[120] V. Passaro, A. Cuccovillo, L. Vaiani, M. De Carlo, and C. E. Campanella, "Gyroscope technology and applications: A review in the industrial perspective," *Sensors,* vol. 17, no. 10, p. 2284, 2017.
[121] N. Barbour and G. Schmidt, "Inertial sensor technology trends," *IEEE Sensors journal,* vol. 1, no. 4, pp. 332-339, 2001.
[122] M. Kok and T. B. Schön, "Magnetometer calibration using inertial sensors," *IEEE Sensors Journal,* vol. 16, no. 14, pp. 5679-5689, 2016.

[123] S. Winiarski and A. Rutkowska-Kucharska, "Estimated ground reaction force in normal and pathological gait," *Acta of Bioengineering & Biomechanics,* vol. 11, no. 1, 2009.
[124] A. Muniz *et al.*, "Comparison among probabilistic neural network, support vector machine and logistic regression for evaluating the effect of subthalamic stimulation in Parkinson disease on ground reaction force during gait," *Journal of biomechanics,* vol. 43, no. 4, pp. 720-726, 2010.
[125] P. Aqueveque, E. Germany, R. Osorio, and F. Pastene, "Gait Segmentation Method Using a Plantar Pressure Measurement System with Custom-Made Capacitive Sensors," *Sensors,* vol. 20, no. 3, p. 656, 2020.
[126] A. Razak, A. Hadi, A. Zayegh, R. K. Begg, and Y. Wahab, "Foot plantar pressure measurement system: A review," *Sensors,* vol. 12, no. 7, pp. 9884-9912, 2012.
[127] A. Hamilton-Wright and D. W. Stashuk, "Physiologically based simulation of clinical EMG signals," *IEEE Transactions on biomedical engineering,* vol. 52, no. 2, pp. 171-183, 2005.
[128] C. Kitchin and L. Counts, *A designer's guide to instrumentation amplifiers*. Analog Devices, 2006.
[129] C. J. De Luca, L. D. Gilmore, M. Kuznetsov, and S. H. Roy, "Filtering the surface EMG signal: Movement artifact and baseline noise contamination," *Journal of biomechanics,* vol. 43, no. 8, pp. 1573-1579, 2010.
[130] A. Gupta, T. Sayed, R. Garg, and R. Shreyam, "EMG signal analysis of healthy and neuropathic individuals," in *IOP Conference Series: Materials Science and Engineering*, 2017, vol. 225, no. 1: IOP Publishing, p. 012128.
[131] V. Florimond, "Basics of surface electromyography applied to physical rehabilitation and biomechanics," *Montreal, Canada: Thought Technology Ltd,* 2009.
[132] A. Den Otter, A. Geurts, T. Mulder, and J. Duysens, "Abnormalities in the temporal patterning of lower extremity muscle activity in hemiparetic gait," *Gait & posture,* vol. 25, no. 3, pp. 342-352, 2007.
[133] K. L. Rodriguez, R. T. Roemmich, B. Cam, B. J. Fregly, and C. J. Hass, "Persons with Parkinson's disease exhibit decreased neuromuscular complexity during gait," *Clinical Neurophysiology,* vol. 124, no. 7, pp. 1390-1397, 2013.
[134] S. A. Acuña, M. E. Tyler, Y. P. Danilov, and D. G. Thelen, "Abnormal muscle activation patterns are associated with chronic gait deficits following traumatic brain injury," *Gait & posture,* vol. 62, pp. 510-517, 2018.
[135] V. Agostini, M. Ghislieri, S. Rosati, G. Balestra, and M. Knaflitz, "Surface electromyography applied to gait analysis: how to improve its impact in clinics?," *Frontiers in Neurology,* vol. 11, p. 994, 2020.
[136] L. Meng *et al.*, "Exploration of human activity recognition using a single sensor for stroke survivors and able-bodied people," *Sensors,* vol. 21, no. 3, p. 799, 2021.
[137] G. Mezzina, F. Aprigliano, S. Micera, V. Monaco, and D. De Venuto, "EEG/EMG based Architecture for the Early Detection of Slip-induced Lack of Balance," in *2019 IEEE 8th International Workshop on Advances in Sensors and Interfaces (IWASI)*, 2019: IEEE, pp. 9-14.
[138] A. Nieuwboer, R. Dom, W. De Weerdt, K. Desloovere, L. Janssens, and V. Stijn, "Electromyographic profiles of gait prior to onset of freezing episodes in patients with Parkinson's disease," *Brain,* vol. 127, no. 7, pp. 1650-1660, 2004.
[139] B. J. Thompson, E. D. Ryan, T. J. Herda, P. B. Costa, A. A. Herda, and J. T. Cramer, "Age-related changes in the rate of muscle activation and rapid force characteristics," *Age,* vol. 36, no. 2, pp. 839-849, 2014.
[140] L. A. Zukowski, J. A. Feld, C. A. Giuliani, and P. Plummer, "Relationships between gait variability and ambulatory activity post stroke," *Topics in stroke rehabilitation,* vol. 26, no. 4, pp. 255-260, 2019.
[141] N. E. Fritz, *Contribution of motor and cognitive factors to gait variability and fall risk: From clinical assessment to neural connectivity*. The Ohio State University, 2013.
[142] M. Halaki and K. Ginn, "Normalization of EMG signals: to normalize or not to normalize and what to normalize to," *Computational intelligence in electromyography analysis-a perspective on current applications and future challenges,* pp. 175-194, 2012.
[143] A. Chalard, M. Belle, E. Montané, P. Marque, D. Amarantini, and D. Gasq, "Impact of the EMG normalization method on muscle activation and the antagonist-agonist co-contraction index during active elbow extension: Practical implications for post-stroke subjects," *Journal of Electromyography and Kinesiology,* vol. 51, p. 102403, 2020.
[144] J. Van Vugt and J. Van Dijk, "A convenient method to reduce crosstalk in surface EMG," *Clinical Neurophysiology,* vol. 112, no. 4, pp. 583-592, 2001.
[145] J. C. Goldsack *et al.*, "Verification, analytical validation, and clinical validation (V3): the foundation of determining fit-for-purpose for Biometric Monitoring Technologies (BioMeTs)," *npj digital Medicine,* vol. 3, no. 1, pp. 1-15, 2020.

[146] A. Godfrey, T. Hourigan, and G. M. OLaighin, "Pendulum analysis of an integrated accelerometer to assess its suitability to measure dynamic acceleration for gait applications," in *2007 29th Annual International Conference of the IEEE Engineering in Medicine and Biology Society*, 2007: IEEE, pp. 4891-4894.
[147] T. Liu, Y. Inoue, and K. Shibata, "A wearable force plate system for the continuous measurement of triaxial ground reaction force in biomechanical applications," *Measurement Science and Technology,* vol. 21, no. 8, p. 085804, 2010.
[148] E. Dorschky, M. Nitschke, A.-K. Seifer, A. J. van den Bogert, and B. M. Eskofier, "Estimation of gait kinematics and kinetics from inertial sensor data using optimal control of musculoskeletal models," *Journal of biomechanics,* vol. 95, p. 109278, 2019.
[149] I. Poitras *et al.*, "Validity and reliability of wearable sensors for joint angle estimation: A systematic review," *Sensors,* vol. 19, no. 7, p. 1555, 2019.
[150] F. A. Storm, C. J. Buckley, and C. Mazzà, "Gait event detection in laboratory and real life settings: Accuracy of ankle and waist sensor based methods," *Gait & posture,* vol. 50, pp. 42-46, 2016.
[151] W. Teufl, M. Lorenz, M. Miezal, B. Taetz, M. Fröhlich, and G. Bleser, "Towards inertial sensor based mobile gait analysis: Event-detection and spatio-temporal parameters," *Sensors,* vol. 19, no. 1, p. 38, 2019.
[152] T. Liu, Y. Inoue, and K. Shibata, "Development of a wearable sensor system for quantitative gait analysis," *Measurement,* vol. 42, no. 7, pp. 978-988, 2009.
[153] H.-K. Lee *et al.*, "Novel algorithm for the hemiplegic gait evaluation using a single 3-axis accelerometer," in *2009 Annual International Conference of the IEEE Engineering in Medicine and Biology Society*, 2009: IEEE, pp. 3964-3966.
[154] S. Del Din, A. Godfrey, and L. Rochester, "Validation of an accelerometer to quantify a comprehensive battery of gait characteristics in healthy older adults and Parkinson's disease: toward clinical and at home use," *IEEE journal of biomedical and health informatics,* vol. 20, no. 3, pp. 838-847, 2015.
[155] J. Spörri, J. Kröll, B. Fasel, K. Aminian, and E. Müller, "The use of body worn sensors for detecting the vibrations acting on the lower back in alpine ski racing," *Frontiers in physiology,* vol. 8, p. 522, 2017.
[156] C. Caramia *et al.*, "IMU-Based Classification of Parkinson's Disease From Gait: A Sensitivity Analysis on Sensor Location and Feature Selection," *IEEE journal of biomedical and health informatics,* vol. 22, no. 6, pp. 1765-1774, 2018.
[157] S. Del Din *et al.*, "Gait analysis with wearables predicts conversion to parkinson disease," *Annals of neurology,* vol. 86, no. 3, pp. 357-367, 2019.
[158] H.-C. Chang, Y.-L. Hsu, S.-C. Yang, J.-C. Lin, and Z.-H. Wu, "A wearable inertial measurement system with complementary filter for gait analysis of patients with stroke or Parkinson's disease," *IEEE Access,* vol. 4, pp. 8442-8453, 2016.
[159] N. Lefeber, M. Degelaen, C. Truyers, I. Safin, and D. Beckwée, "Validity and reproducibility of inertial physilog sensors for spatiotemporal gait analysis in patients with stroke," *IEEE Transactions on Neural Systems and Rehabilitation Engineering,* vol. 27, no. 9, pp. 1865-1874, 2019.
[160] Y. Lou, R. Wang, J. Mai, N. Wang, and Q. Wang, "IMU-Based Gait Phase Recognition for Stroke Survivors," *Robotica,* vol. 37, no. 12, pp. 2195-2208, 2019.
[161] F. Parisi, G. Ferrari, A. Baricich, M. D'Innocenzo, C. Cisari, and A. Mauro, "Accurate gait analysis in post-stroke patients using a single inertial measurement unit," in *2016 IEEE 13th International Conference on Wearable and Implantable Body Sensor Networks (BSN)*, 2016: IEEE, pp. 335-340.
[162] S. Yang, J.-T. Zhang, A. C. Novak, B. Brouwer, and Q. Li, "Estimation of spatio-temporal parameters for post-stroke hemiparetic gait using inertial sensors," *Gait & posture,* vol. 37, no. 3, pp. 354-358, 2013.
[163] R. P.-M. Barrois *et al.*, "Observational study of 180 Turning strategies Using inertial Measurement Units and Fall risk in Poststroke hemiparetic Patients," *Frontiers in neurology,* vol. 8, p. 194, 2017.
[164] B. Dijkstra, Y. P. Kamsma, and W. Zijlstra, "Detection of gait and postures using a miniaturized triaxial accelerometer-based system: accuracy in patients with mild to moderate Parkinson's disease," *Archives of physical medicine and rehabilitation,* vol. 91, no. 8, pp. 1272-1277, 2010.
[165] M. Yoneyama, Y. Kurihara, K. Watanabe, and H. Mitoma, "Accelerometry-based gait analysis and its application to Parkinson's disease assessment—part 1: detection of stride event," *IEEE Transactions on neural systems and rehabilitation engineering,* vol. 22, no. 3, pp. 613-622, 2013.
[166] R. E. Taylor-Piliae, M. J. Mohler, B. Najafi, and B. M. Coull, "Objective fall risk detection in stroke survivors using wearable sensor technology: a feasibility study," *Topics in stroke rehabilitation,* vol. 23, no. 6, pp. 393-399, 2016.
[167] W. Zhang, M. Smuck, C. Legault, M. A. Ith, A. Muaremi, and K. Aminian, "Gait symmetry assessment with a low back 3d accelerometer in post-stroke patients," *Sensors,* vol. 18, no. 10, p. 3322, 2018.

[168] K. Oyake *et al.*, "Validity of gait asymmetry estimation by using an accelerometer in individuals with hemiparetic stroke," *Journal of Physical Therapy Science,* vol. 29, no. 2, pp. 307-311, 2017.
[169] S. A. Moore, A. Hickey, S. Lord, S. Del Din, A. Godfrey, and L. Rochester, "Comprehensive measurement of stroke gait characteristics with a single accelerometer in the laboratory and community: a feasibility, validity and reliability study," *Journal of neuroengineering and rehabilitation,* vol. 14, no. 1, p. 130, 2017.
[170] J. C. Schlachetzki *et al.*, "Wearable sensors objectively measure gait parameters in Parkinson's disease," *PloS one,* vol. 12, no. 10, p. e0183989, 2017.
[171] N. Hatanaka *et al.*, "Comparative gait analysis in progressive supranuclear palsy and Parkinson's Disease," *European neurology,* vol. 75, no. 5-6, pp. 282-289, 2016.
[172] J. Stamatakis, J. Cremers, D. Maquet, B. Macq, and G. Garraux, "Gait feature extraction in Parkinson's disease using low-cost accelerometers," in *2011 Annual International Conference of the IEEE Engineering in Medicine and Biology Society*, 2011: IEEE, pp. 7900-7903.
[173] B. Sijobert, J. Denys, C. A. Coste, and C. Geny, "IMU based detection of freezing of gait and festination in Parkinson's disease," in *2014 IEEE 19th International Functional Electrical Stimulation Society Annual Conference (IFESS)*, 2014: IEEE, pp. 1-3.
[174] M. Zago *et al.*, "Gait evaluation using inertial measurement units in subjects with Parkinson's disease," *Journal of Electromyography and Kinesiology,* vol. 42, pp. 44-48, 2018.
[175] A. Kleiner *et al.*, "The parkinsonian gait spatiotemporal parameters quantified by a single inertial sensor before and after automated mechanical peripheral stimulation treatment," *Parkinson's disease,* vol. 2015, 2015.
[176] M. H. Pham *et al.*, "Validation of a step detection algorithm during straight walking and turning in patients with Parkinson's disease and older adults using an inertial measurement unit at the lower back," *Frontiers in neurology,* vol. 8, p. 457, 2017.
[177] T. Iluz *et al.*, "Automated detection of missteps during community ambulation in patients with Parkinson's disease: a new approach for quantifying fall risk in the community setting," *Journal of neuroengineering and rehabilitation,* vol. 11, no. 1, p. 48, 2014.
[178] Y.-L. Hsu *et al.*, "Gait and balance analysis for patients with Alzheimer's disease using an inertial-sensor-based wearable instrument," *IEEE journal of biomedical and health informatics,* vol. 18, no. 6, pp. 1822-1830, 2014.
[179] P.-C. Chung, Y.-L. Hsu, C.-Y. Wang, C.-W. Lin, J.-S. Wang, and M.-C. Pai, "Gait analysis for patients with Alzheimer's disease using a triaxial accelerometer," in *2012 IEEE International Symposium on Circuits and Systems*, 2012: IEEE, pp. 1323-1326.
[180] S. Gillain *et al.*, "Gait speed or gait variability, which one to use as a marker of risk to develop Alzheimer disease? A pilot study," *Aging clinical and experimental research,* vol. 28, no. 2, pp. 249-255, 2016.
[181] W.-H. Wang *et al.*, "Alzheimer's disease classification based on gait information," in *2014 International Joint Conference on Neural Networks (IJCNN)*, 2014: IEEE, pp. 3251-3257.
[182] Y. Moon *et al.*, "Monitoring gait in multiple sclerosis with novel wearable motion sensors," *PLoS One,* vol. 12, no. 2, p. e0171346, 2017.
[183] M. Pau *et al.*, "Clinical assessment of gait in individuals with multiple sclerosis using wearable inertial sensors: Comparison with patient-based measure," *Multiple sclerosis and related disorders,* vol. 10, pp. 187-191, 2016.
[184] R. Sun *et al.*, "Assessment of postural sway in individuals with multiple sclerosis using a novel wearable inertial sensor," *Digital biomarkers,* vol. 2, no. 1, pp. 1-10, 2018.
[185] M. Psarakis, D. A. Greene, M. H. Cole, S. R. Lord, P. Hoang, and M. Brodie, "Wearable technology reveals gait compensations, unstable walking patterns and fatigue in people with multiple sclerosis," *Physiological measurement,* vol. 39, no. 7, p. 075004, 2018.
[186] R. S. McGinnis *et al.*, "A machine learning approach for gait speed estimation using skin-mounted wearable sensors: From healthy controls to individuals with multiple sclerosis," *PloS one,* vol. 12, no. 6, p. e0178366, 2017.
[187] J. M. Huisinga, M. Mancini, R. J. S. George, and F. B. Horak, "Accelerometry reveals differences in gait variability between patients with multiple sclerosis and healthy controls," *Annals of biomedical engineering,* vol. 41, no. 8, pp. 1670-1679, 2013.
[188] J. J. Craig, A. P. Bruetsch, S. G. Lynch, and J. M. Huisinga, "The relationship between trunk and foot acceleration variability during walking shows minor changes in persons with multiple sclerosis," *Clinical Biomechanics,* vol. 49, pp. 16-21, 2017.

[189] A. Matsushima, K. Yoshida, H. Genno, and S.-i. Ikeda, "Principal component analysis for ataxic gait using a triaxial accelerometer," *Journal of neuroengineering and rehabilitation,* vol. 14, no. 1, p. 37, 2017.
[190] A. Matsushima *et al.*, "Clinical assessment of standing and gait in ataxic patients using a triaxial accelerometer," *Cerebellum & ataxias,* vol. 2, no. 1, pp. 1-7, 2015.
[191] A. Hickey *et al.*, "Validity of a wearable accelerometer to quantify gait in spinocerebellar ataxia type 6," *Physiological measurement,* vol. 37, no. 11, p. N105, 2016.
[192] K. Terayama, R. Sakakibara, and A. Ogawa, "Wearable gait sensors to measure ataxia due to spinocerebellar degeneration," *Neurology and Clinical Neuroscience,* vol. 6, no. 1, pp. 9-12, 2018.
[193] W. Ilg *et al.*, "Towards ecologically valid biomarkers: real-life gait assessment in cerebellar ataxia," *bioRxiv,* p. 802918, 2019.
[194] P. Caliandro *et al.*, "Exploring risk of falls and dynamic unbalance in cerebellar ataxia by inertial sensor assessment," *Sensors,* vol. 19, no. 24, p. 5571, 2019.
[195] S. Stuart *et al.*, "Analysis of free-living mobility in people with mild traumatic brain injury and healthy controls: quality over quantity," *Journal of neurotrauma,* vol. 37, no. 1, pp. 139-145, 2020.
[196] S. L. Carey, K. Hufford, A. Martori, M. Simoes, F. Sinatra, and R. V. Dubey, "Development of a wearable motion analysis system for evaluation and rehabilitation of mild traumatic brain injury (mTBI)," in *Summer Bioengineering Conference*, 2012, vol. 44809: American Society of Mechanical Engineers, pp. 1241-1242.
[197] A. L. Martori, S. L. Carey, D. J. Lura, and R. V. Dubey, "Knee angle analysis using a wearable motion analysis system for detection and rehabilitation of mild traumatic brain injury," in *Summer Bioengineering Conference*, 2013, vol. 55607: American Society of Mechanical Engineers, p. V01AT20A032.
[198] V. Belluscio *et al.*, "Gait quality assessment in survivors from severe traumatic brain injury: an instrumented approach based on inertial sensors," *Sensors,* vol. 19, no. 23, p. 5315, 2019.
[199] M. De Vos, J. Prince, T. Buchanan, J. J. FitzGerald, and C. A. Antoniades, "Discriminating progressive supranuclear palsy from Parkinson's disease using wearable technology and machine learning," *Gait & Posture,* vol. 77, pp. 257-263, 2020.
[200] A. Dalton, H. Khalil, M. Busse, A. Rosser, R. van Deursen, and G. ÓLaighin, "Analysis of gait and balance through a single triaxial accelerometer in presymptomatic and symptomatic Huntington's disease," *Gait & posture,* vol. 37, no. 1, pp. 49-54, 2013.
[201] J. L. Adams *et al.*, "Multiple wearable sensors in Parkinson and Huntington disease individuals: a pilot study in clinic and at home," *Digital Biomarkers,* vol. 1, no. 1, pp. 52-63, 2017.
[202] K. L. Andrzejewski *et al.*, "Wearable sensors in Huntington disease: a pilot study," *Journal of Huntington's disease,* vol. 5, no. 2, pp. 199-206, 2016.
[203] M. F. Gordon *et al.*, "Quantification of Motor Function in Huntington Disease Patients Using Wearable Sensor Devices," *Digital Biomarkers,* vol. 3, no. 3, pp. 103-115, 2019.
[204] M. Barbero, R. Merletti, and A. Rainoldi, *Atlas of muscle innervation zones: understanding surface electromyography and its applications*. Springer Science & Business Media, 2012.
[205] H. J. Hermens *et al.*, "European recommendations for surface electromyography," *Roessingh research and development,* vol. 8, no. 2, pp. 13-54, 1999.
[206] E. Surface, for, the, Non-Invasive, Assessment, of, Muscles, (SENIAM), project,. "SENIAM http://www.seniam.org/, Access date: 22:09 07/07/2020." http://www.seniam.org/ (accessed 22:09 07/07/2020, 2020).
[207] H. J. Hermens, B. Freriks, C. Disselhorst-Klug, and G. Rau, "Development of recommendations for SEMG sensors and sensor placement procedures," *Journal of electromyography and Kinesiology,* vol. 10, no. 5, pp. 361-374, 2000.
[208] G. S. Kasman and S. L. Wolf, "Surface EMG made easy: a beginner's guide for rehabilitation clinicians," 2002.
[209] D. G. Lloyd and T. F. Besier, "An EMG-driven musculoskeletal model to estimate muscle forces and knee joint moments in vivo," *Journal of biomechanics,* vol. 36, no. 6, pp. 765-776, 2003.
[210] C. A. Bailey, F. Corona, M. Murgia, R. Pili, M. Pau, and J. N. Côté, "Electromyographical gait characteristics in parkinson's disease: effects of combined physical therapy and rhythmic auditory stimulation," *Frontiers in neurology,* vol. 9, p. 211, 2018.
[211] A. De Stefano, J. Burridge, V. Yule, and R. Allen, "Effect of gait cycle selection on EMG analysis during walking in adults and children with gait pathology," *Gait & posture,* vol. 20, no. 1, pp. 92-101, 2004.

[212] H. A. Cantú, J. Nantel, M. Millán, C. Paquette, and J. N. Côté, "Abnormal muscle activity and variability before, during, and after the occurrence of freezing in Parkinson's disease," *Frontiers in neurology,* vol. 10, p. 951, 2019.
[213] J. Rueterbories, E. G. Spaich, B. Larsen, and O. K. Andersen, "Methods for gait event detection and analysis in ambulatory systems," *Medical engineering & physics,* vol. 32, no. 6, pp. 545-552, 2010.
[214] G. P. Panebianco, M. C. Bisi, R. Stagni, and S. Fantozzi, "Analysis of the performance of 17 algorithms from a systematic review: Influence of sensor position, analysed variable and computational approach in gait timing estimation from IMU measurements," *Gait & posture,* vol. 66, pp. 76-82, 2018.
[215] W. Zijlstra and A. L. Hof, "Assessment of spatio-temporal gait parameters from trunk accelerations during human walking," *Gait & posture,* vol. 18, no. 2, pp. 1-10, 2003.
[216] R. C. González, A. M. López, J. Rodriguez-Uría, D. Alvarez, and J. C. Alvarez, "Real-time gait event detection for normal subjects from lower trunk accelerations," *Gait & posture,* vol. 31, no. 3, pp. 322-325, 2010.
[217] S. H. Shin and C. G. Park, "Adaptive step length estimation algorithm using optimal parameters and movement status awareness," *Medical engineering & physics,* vol. 33, no. 9, pp. 1064-1071, 2011.
[218] A. Köse, A. Cereatti, and U. Della Croce, "Bilateral step length estimation using a single inertial measurement unit attached to the pelvis," *Journal of neuroengineering and rehabilitation,* vol. 9, no. 1, p. 9, 2012.
[219] F. Bugané *et al.*, "Estimation of spatial-temporal gait parameters in level walking based on a single accelerometer: Validation on normal subjects by standard gait analysis," *Computer methods and programs in biomedicine,* vol. 108, no. 1, pp. 129-137, 2012.
[220] D. Trojaniello *et al.*, "Estimation of step-by-step spatio-temporal parameters of normal and impaired gait using shank-mounted magneto-inertial sensors: application to elderly, hemiparetic, parkinsonian and choreic gait," *Journal of neuroengineering and rehabilitation,* vol. 11, no. 1, p. 152, 2014.
[221] A. Salarian *et al.*, "Gait assessment in Parkinson's disease: toward an ambulatory system for long-term monitoring," *IEEE transactions on biomedical engineering,* vol. 51, no. 8, pp. 1434-1443, 2004.
[222] K. Aminian, B. Najafi, C. Büla, P.-F. Leyvraz, and P. Robert, "Spatio-temporal parameters of gait measured by an ambulatory system using miniature gyroscopes," *Journal of biomechanics,* vol. 35, no. 5, pp. 689-699, 2002.
[223] P. Catalfamo, S. Ghoussayni, and D. Ewins, "Gait event detection on level ground and incline walking using a rate gyroscope," *Sensors,* vol. 10, no. 6, pp. 5683-5702, 2010.
[224] S. Khandelwal and N. Wickström, "Identification of gait events using expert knowledge and continuous wavelet transform analysis," in *7th International Conference on Bio-inspired Systems and Signal Processing (BIOSIGNALS 2014), Angers, France, March 3-6, 2014*, 2014: SciTePress, pp. 197-204.
[225] A. Rampp, J. Barth, S. Schülein, K.-G. Gaßmann, J. Klucken, and B. M. Eskofier, "Inertial sensor-based stride parameter calculation from gait sequences in geriatric patients," *IEEE transactions on biomedical engineering,* vol. 62, no. 4, pp. 1089-1097, 2014.
[226] J. M. Jasiewicz *et al.*, "Gait event detection using linear accelerometers or angular velocity transducers in able-bodied and spinal-cord injured individuals," *Gait & posture,* vol. 24, no. 4, pp. 502-509, 2006.
[227] A. Pourmoghaddam, M. Dettmer, D. P. O'Connor, W. H. Paloski, and C. S. Layne, "Identification of changing lower limb neuromuscular activation in Parkinson's disease during treadmill gait with and without levodopa using a nonlinear analysis index," *Parkinson's Disease,* vol. 2015, 2015.
[228] T. D'Alessio and S. Conforto, "Extraction of the envelope from surface EMG signals," *IEEE Engineering in Medicine and Biology Magazine,* vol. 20, no. 6, pp. 55-61, 2001.
[229] S. Márquez-Figueroa, Y. S. Shmaliy, and O. Ibarra-Manzano, "Optimal extraction of EMG signal envelope and artifacts removal assuming colored measurement noise," *Biomedical Signal Processing and Control,* vol. 57, p. 101679, 2020.
[230] S. Micera, G. Vannozzi, A. Sabatini, and P. Dario, "Improving detection of muscle activation intervals," *IEEE Engineering in medicine and Biology Magazine,* vol. 20, no. 6, pp. 38-46, 2001.
[231] X. Ren, X. Hu, Z. Wang, and Z. Yan, "MUAP extraction and classification based on wavelet transform and ICA for EMG decomposition," *Medical and Biological Engineering and Computing,* vol. 44, no. 5, p. 371, 2006.
[232] R. E. Singh, K. Iqbal, G. White, and T. E. Hutchinson, "A systematic review on muscle synergies: from building blocks of motor behavior to a neurorehabilitation tool," *Applied bionics and biomechanics,* vol. 2018, 2018.
[233] R. Pilkar, A. Ramanujam, and K. J. Nolan, "Alterations in spectral attributes of surface electromyograms after utilization of a foot drop stimulator during post-stroke gait," *Frontiers in Neurology,* vol. 8, p. 449, 2017.

[234] F. Sadikoglu, C. Kavalcioglu, and B. Dagman, "Electromyogram (EMG) signal detection, classification of EMG signals and diagnosis of neuropathy muscle disease," *Procedia computer science,* vol. 120, pp. 422-429, 2017.
[235] S. A. Go, K. Coleman-Wood, and K. R. Kaufman, "Frequency analysis of lower extremity electromyography signals for the quantitative diagnosis of dystonia," *Journal of electromyography and kinesiology,* vol. 24, no. 1, pp. 31-36, 2014.
[236] R. H. Chowdhury, M. B. Reaz, M. A. B. M. Ali, A. A. Bakar, K. Chellappan, and T. G. Chang, "Surface electromyography signal processing and classification techniques," *Sensors,* vol. 13, no. 9, pp. 12431-12466, 2013.
[237] P. Kugler, C. Jaremenko, J. Schlachetzki, J. Winkler, J. Klucken, and B. Eskofier, "Automatic recognition of Parkinson's disease using surface electromyography during standardized gait tests," in *2013 35th Annual International Conference of the IEEE Engineering in Medicine and Biology Society (EMBC)*, 2013: IEEE, pp. 5781-5784.
[238] L. Roeder, T. W. Boonstra, and G. K. Kerr, "Corticomuscular control of walking in older people and people with Parkinson's disease," *Scientific reports,* vol. 10, no. 1, pp. 1-18, 2020.
[239] A. Den Otter, A. Geurts, T. Mulder, and J. Duysens, "Gait recovery is not associated with changes in the temporal patterning of muscle activity during treadmill walking in patients with post-stroke hemiparesis," *Clinical Neurophysiology,* vol. 117, no. 1, pp. 4-15, 2006.
[240] J. Jonsdottir *et al.*, "Task-oriented biofeedback to improve gait in individuals with chronic stroke: motor learning approach," *Neurorehabilitation and neural repair,* vol. 24, no. 5, pp. 478-485, 2010.
[241] G. M. Rozanski, A. H. Huntley, L. D. Crosby, A. Schinkel-Ivy, A. Mansfield, and K. K. Patterson, "Lower limb muscle activity underlying temporal gait asymmetry post-stroke," *medRxiv,* p. 19010421, 2019.
[242] G. J. Androwis, R. Pilkar, A. Ramanujam, and K. J. Nolan, "Electromyography assessment during gait in a robotic exoskeleton for acute stroke," *Frontiers in neurology,* vol. 9, p. 630, 2018.
[243] S. Srivastava, C. Patten, and S. A. Kautz, "Altered muscle activation patterns (AMAP): an analytical tool to compare muscle activity patterns of hemiparetic gait with a normative profile," *Journal of neuroengineering and rehabilitation,* vol. 16, no. 1, p. 21, 2019.
[244] N. Lodha *et al.*, "EMG synchrony to assess impaired corticomotor control of locomotion after stroke," *Journal of Electromyography and Kinesiology,* vol. 37, pp. 35-40, 2017.
[245] J. C. Kempen, C. A. Doorenbosch, D. L. Knol, V. de Groot, and H. Beckerman, "Newly identified gait patterns in patients with multiple sclerosis may be related to push-off quality," *Physical therapy,* vol. 96, no. 11, pp. 1744-1752, 2016.
[246] L. E. Cofré Lizama, A. Bastani, A. van der Walt, T. Kilpatrick, F. Khan, and M. P. Galea, "Increased ankle muscle coactivation in the early stages of multiple sclerosis," *Multiple Sclerosis Journal–Experimental, Translational and Clinical,* vol. 6, no. 1, p. 2055217320905870, 2020.
[247] L. Fiori *et al.*, "Impairment of Global Lower Limb Muscle Coactivation During Walking in Cerebellar Ataxias," *Gait & Posture,* vol. 74, p. 16, 2019.
[248] C. Conte *et al.*, "Effect of restraining the base of support on the other biomechanical features in patients with cerebellar ataxia," *The Cerebellum,* vol. 17, no. 3, pp. 264-275, 2018.
[249] M. de Tommaso, K. Ricci, A. Montemurno, E. Vecchio, and S. Invitto, "Walking-Related Dual-Task Interference in Early-to-Middle-Stage Huntington's Disease: An Auditory Event Related Potential Study," *Frontiers in psychology,* vol. 8, p. 1292, 2017.
[250] D. Kaski and A. M. Bronstein, "Treatments for neurological gait and balance disturbance: the use of noninvasive electrical brain stimulation," *Advances in Neuroscience,* vol. 2014, 2014.
[251] J. Nonnekes, R. J. Goselink, E. Růžička, A. Fasano, J. G. Nutt, and B. R. Bloem, "Neurological disorders of gait, balance and posture: a sign-based approach," *Nature Reviews Neurology,* vol. 14, no. 3, p. 183, 2018.
[252] S. Nadeau, M. Betschart, and F. Bethoux, "Gait analysis for poststroke rehabilitation: the relevance of biomechanical analysis and the impact of gait speed," *Physical Medicine and Rehabilitation Clinics,* vol. 24, no. 2, pp. 265-276, 2013.
[253] G. Williams, M. E. Morris, A. Schache, and P. R. McCrory, "Incidence of gait abnormalities after traumatic brain injury," *Archives of physical medicine and rehabilitation,* vol. 90, no. 4, pp. 587-593, 2009.
[254] S. Y. Yoon, S. C. Lee, N. Y. Kim, Y.-S. An, and Y. W. Kim, "Brain metabolism in patients with freezing of gait after hypoxic-ischemic brain injury: a pilot study," *Medicine,* vol. 96, no. 45, 2017.
[255] S. Y. Yoon, S. C. Lee, and Y. W. Kim, "Spatiotemporal Characteristics of Freezing of Gait in Patients After Hypoxic-Ischemic Brain Injury: A Pilot Study," *Medicine,* vol. 95, no. 19, 2016.

[256] S. Y. Yoon, S. C. Lee, Y.-s. An, and Y. W. Kim, "Neural correlates and gait characteristics for hypoxic-ischemic brain injury induced freezing of gait," *Clinical Neurophysiology,* vol. 131, no. 1, pp. 46-53, 2020.
[257] W. A. Rocca, "The burden of Parkinson's disease: a worldwide perspective," *The Lancet Neurology,* vol. 17, no. 11, pp. 928-929, 2018.
[258] S. Aich, P. M. Pradhan, J. Park, N. Sethi, V. S. S. Vathsa, and H.-C. Kim, "A validation study of freezing of gait (FoG) detection and machine-learning-based FoG prediction using estimated gait characteristics with a wearable accelerometer," *Sensors,* vol. 18, no. 10, p. 3287, 2018.
[259] Y. Osaki, Y. Morita, Y. Miyamoto, K. Furuta, and H. Furuya, "Freezing of gait is an early clinical feature of progressive supranuclear palsy," *Neurology and clinical neuroscience,* vol. 5, no. 3, pp. 86-90, 2017.
[260] B. Hoffland, L. Veugen, M. Janssen, J. Pasman, V. Weerdesteyn, and B. van de Warrenburg, "A gait paradigm reveals different patterns of abnormal cerebellar motor learning in primary focal dystonias," *The Cerebellum,* vol. 13, no. 6, pp. 760-766, 2014.
[261] J. Müller, G. Ebersbach, J. Wissel, C. Brenneis, L. Badry, and W. Poewe, "Disturbances of dynamic balance in phasic cervical dystonia," *Journal of Neurology, Neurosurgery & Psychiatry,* vol. 67, no. 6, pp. 807-810, 1999.
[262] C. Barr, R. Barnard, L. Edwards, S. Lennon, and L. Bradnam, "Impairments of balance, stepping reactions and gait in people with cervical dystonia," *Gait & Posture,* vol. 55, pp. 55-61, 2017.
[263] E. Mirek *et al.*, "Three-Dimensional Trunk and Lower Limbs Characteristics during Gait in Patients with Huntington's Disease," *Frontiers in neuroscience,* vol. 11, p. 566, 2017.
[264] R. Mc Ardle, S. Del Din, B. Galna, A. Thomas, and L. Rochester, "Differentiating dementia disease subtypes with gait analysis: feasibility of wearable sensors?," *Gait & Posture,* vol. 76, pp. 372-376, 2020.
[265] J. R. Merory, J. E. Wittwer, C. C. Rowe, and K. E. Webster, "Quantitative gait analysis in patients with dementia with Lewy bodies and Alzheimer's disease," *Gait & posture,* vol. 26, no. 3, pp. 414-419, 2007.
[266] N. K. Nadkarni, E. Mawji, W. E. McIlroy, and S. E. Black, "Spatial and temporal gait parameters in Alzheimer's disease and aging," *Gait & posture,* vol. 30, no. 4, pp. 452-454, 2009.
[267] A. S. Buchman and D. A. Bennett, "Loss of motor function in preclinical Alzheimer's disease," *Expert review of neurotherapeutics,* vol. 11, no. 5, pp. 665-676, 2011.
[268] B. R. Greene *et al.*, "Assessment and classification of early-stage multiple sclerosis with inertial sensors: comparison against clinical measures of disease state," *IEEE journal of biomedical and health informatics,* vol. 19, no. 4, pp. 1356-1361, 2015.
[269] P. DasMahapatra, E. Chiauzzi, R. Bhalerao, and J. Rhodes, "Free-living physical activity monitoring in adult US patients with multiple sclerosis using a consumer wearable device," *Digital Biomarkers,* vol. 2, no. 1, pp. 47-63, 2018.
[270] H. Stolze *et al.*, "Typical features of cerebellar ataxic gait," *Journal of Neurology, Neurosurgery & Psychiatry,* vol. 73, no. 3, pp. 310-312, 2002.
[271] G. Albani *et al.*, "Differences in the EMG pattern of leg muscle activation during locomotion in Parkinson's disease," *Functional neurology,* vol. 18, no. 3, pp. 165-178, 2003.
[272] U. Givon, G. Zeilig, and A. Achiron, "Gait analysis in multiple sclerosis: characterization of temporal–spatial parameters using GAITRite functional ambulation system," *Gait & posture,* vol. 29, no. 1, pp. 138-142, 2009.
[273] R. W. Motl, L. Pilutti, B. Sandroff, D. Dlugonski, J. J. Sosnoff, and J. Pula, "Accelerometry as a measure of walking behavior in multiple sclerosis," *Acta Neurologica Scandinavica,* vol. 127, no. 6, pp. 384-390, 2013.
[274] C. Caulcrick, F. Russell, S. Wilson, C. Sawade, and R. Vaidyanathan, "Unilateral Inertial and Muscle Activity Sensor Fusion for Gait Cycle Progress Estimation," in *2018 7th IEEE International Conference on Biomedical Robotics and Biomechatronics (Biorob)*, 2018: IEEE, pp. 1151-1156.
[275] A. Findlow, J. Goulermas, C. Nester, D. Howard, and L. Kenney, "Predicting lower limb joint kinematics using wearable motion sensors," *Gait & posture,* vol. 28, no. 1, pp. 120-126, 2008.
[276] F. Attal, S. Mohammed, M. Dedabrishvili, F. Chamroukhi, L. Oukhellou, and Y. Amirat, "Physical human activity recognition using wearable sensors," *Sensors,* vol. 15, no. 12, pp. 31314-31338, 2015.
[277] C.-C. Yang and Y.-L. Hsu, "A review of accelerometry-based wearable motion detectors for physical activity monitoring," *Sensors,* vol. 10, no. 8, pp. 7772-7788, 2010.
[278] H.-L. Chan, P.-K. Chao, Y.-C. Chen, and W.-J. Kao, "Wireless body area network for physical-activity classification and fall detection," in *2008 5th International Summer School and Symposium on Medical Devices and Biosensors*, 2008: IEEE, pp. 157-160.
[279] A. Bourke, J. O'brien, and G. Lyons, "Evaluation of a threshold-based tri-axial accelerometer fall detection algorithm," *Gait & posture,* vol. 26, no. 2, pp. 194-199, 2007.

[280] S. Qiu, L. Liu, H. Zhao, Z. Wang, and Y. Jiang, "MEMS inertial sensors based gait analysis for rehabilitation assessment via multi-sensor fusion," *Micromachines,* vol. 9, no. 9, p. 442, 2018.
[281] H. Zhao *et al.*, "Adaptive gait detection based on foot-mounted inertial sensors and multi-sensor fusion," *Information Fusion,* vol. 52, pp. 157-166, 2019.
[282] J. Musić, R. Kamnik, and M. Munih, "Model based inertial sensing of human body motion kinematics in sit-to-stand movement," *Simulation Modelling Practice and Theory,* vol. 16, no. 8, pp. 933-944, 2008.
[283] R. Takeda, S. Tadano, M. Todoh, M. Morikawa, M. Nakayasu, and S. Yoshinari, "Gait analysis using gravitational acceleration measured by wearable sensors," *Journal of biomechanics,* vol. 42, no. 3, pp. 223-233, 2009.
[284] R. C. King, E. Villeneuve, R. J. White, R. S. Sherratt, W. Holderbaum, and W. S. Harwin, "Application of data fusion techniques and technologies for wearable health monitoring," *Medical engineering & physics,* vol. 42, pp. 1-12, 2017.
[285] A. Godfrey, *Digital Health: Exploring Use and Integration of Wearables*. Academic Press, 2021.
[286] V. Agostini, M. Ghislieri, S. Rosati, G. Balestra, and M. Knaflitz, "Surface electromyography applied to gait analysis: How to improve its impact in clinics?," *Frontiers in Neurology,* p. 994, 2020.
[287] S. J. Lee and J. Hidler, "Biomechanics of overground vs. treadmill walking in healthy individuals," *Journal of applied physiology,* vol. 104, no. 3, pp. 747-755, 2008.
[288] G. M. Rozanski, A. H. Huntley, L. D. Crosby, A. Schinkel-Ivy, A. Mansfield, and K. K. Patterson, "Lower limb muscle activity underlying temporal gait asymmetry post-stroke," *Clinical Neurophysiology,* vol. 131, no. 8, pp. 1848-1858, 2020.
[289] M. Punt, S. M. Bruijn, H. Wittink, I. G. van de Port, and J. H. Van Dieën, "Do clinical assessments, steady-state or daily-life gait characteristics predict falls in ambulatory chronic stroke survivors?," *Journal of Rehabilitation Medicine,* vol. 49, no. 5, pp. 402-409, 2017.
[290] Y. Celik, S. Stuart, W. L. Woo, E. Sejdic, and A. Godfrey, "Multi-modal gait: A wearable, algorithm and data fusion approach for clinical and free-living assessment," *Information Fusion,* 2021.
[291] Y. Celik, S. Stuart, W. L. Woo, and A. Godfrey, "Wearable Inertial Gait Algorithms: Impact of Wear Location and Environment in Healthy and Parkinson's Populations," *Sensors,* vol. 21, no. 19, p. 6476, 2021.
[292] H. Toda, T. Maruyama, and M. Tada, "Indoor vs. Outdoor Walking: Does It Make Any Difference in Joint Angle Depending on Road Surface?," *Frontiers in Sports and Active Living,* p. 119, 2020.
[293] K. Zurales, T. K. DeMott, H. Kim, L. Allet, J. A. Ashton-Miller, and J. K. Richardson, "Gait efficiency on an uneven surface is associated with falls and injury in older subjects with a spectrum of lower limb neuromuscular function: a prospective study," *American journal of physical medicine & rehabilitation/Association of Academic Physiatrists,* vol. 95, no. 2, p. 83, 2016.
[294] E. Warmerdam *et al.*, "Long-term unsupervised mobility assessment in movement disorders," *The Lancet Neurology,* vol. 19, no. 5, pp. 462-470, 2020.
[295] F. G. Da Silva and E. Galeazzo, "Accelerometer based intelligent system for human movement recognition," in *5th IEEE International Workshop on Advances in Sensors and Interfaces IWASI*, 2013: IEEE, pp. 20-24.
[296] A. Godfrey, A. Bourke, G. Olaighin, P. Van De Ven, and J. Nelson, "Activity classification using a single chest mounted tri-axial accelerometer," *Medical engineering & physics,* vol. 33, no. 9, pp. 1127-1135, 2011.
[297] P. Gupta and T. Dallas, "Feature selection and activity recognition system using a single triaxial accelerometer," *IEEE Transactions on Biomedical Engineering,* vol. 61, no. 6, pp. 1780-1786, 2014.
[298] D. M. Karantonis, M. R. Narayanan, M. Mathie, N. H. Lovell, and B. G. Celler, "Implementation of a real-time human movement classifier using a triaxial accelerometer for ambulatory monitoring," *IEEE transactions on information technology in biomedicine,* vol. 10, no. 1, pp. 156-167, 2006.
[299] O. Steven Eyobu and D. S. Han, "Feature representation and data augmentation for human activity classification based on wearable IMU sensor data using a deep LSTM neural network," *Sensors,* vol. 18, no. 9, p. 2892, 2018.
[300] T. Zebin, P. J. Scully, and K. B. Ozanyan, "Human activity recognition with inertial sensors using a deep learning approach," in *2016 IEEE SENSORS*, 2016: IEEE, pp. 1-3.
[301] D. S. Marigold and A. E. Patla, "Age-related changes in gait for multi-surface terrain," *Gait & posture,* vol. 27, no. 4, pp. 689-696, 2008.
[302] M. Z. U. H. Hashmi, Q. Riaz, M. Hussain, and M. Shahzad, "What Lies Beneath One's Feet? Terrain Classification Using Inertial Data of Human Walk," *Applied Sciences,* vol. 9, no. 15, p. 3099, 2019.

[303] B. Hu, P. Dixon, J. Jacobs, J. Dennerlein, and J. Schiffman, "Machine learning algorithms based on signals from a single wearable inertial sensor can detect surface-and age-related differences in walking," *Journal of biomechanics,* vol. 71, pp. 37-42, 2018.
[304] H. Xu, A. Merryweather, K. B. Foreman, J. Zhao, and M. Hunt, "Dual-task interference during gait on irregular terrain in people with Parkinson's disease," *Gait & posture,* vol. 63, pp. 17-22, 2018.
[305] K. B. Mansour, N. Rezzoug, and P. Gorce, "Analysis of several methods and inertial sensors locations to assess gait parameters in able-bodied subjects," *Gait & posture,* vol. 42, no. 4, pp. 409-414, 2015.
[306] I. A. Lawal and S. Bano, "Deep human activity recognition with localisation of wearable sensors," *IEEE Access,* vol. 8, pp. 155060-155070, 2020.
[307] W. Pirker and R. Katzenschlager, "Gait disorders in adults and the elderly," *Wiener Klinische Wochenschrift,* vol. 129, no. 3, pp. 81-95, 2017.
[308] E. Navarro-Flores *et al.*, "Effect of foot health and quality of life in patients with Parkinson disease: A prospective case-control investigation," *Journal of Tissue Viability,* 2021.
[309] A. M. Jiménez-Cebrián *et al.*, "The Impact of Depression Symptoms in Patients with Parkinson's Disease: A Novel Case-Control Investigation," *International Journal of Environmental Research and Public Health,* vol. 18, no. 5, p. 2369, 2021.
[310] R. Morris, S. Stuart, G. McBarron, P. C. Fino, M. Mancini, and C. Curtze, "Validity of Mobility Lab (version 2) for gait assessment in young adults, older adults and Parkinson's disease," *Physiological measurement,* vol. 40, no. 9, p. 095003, 2019.
[311] M. Bravi *et al.*, "Validity Analysis of WalkerViewTM Instrumented Treadmill for Measuring Spatiotemporal and Kinematic Gait Parameters," *Sensors,* vol. 21, no. 14, p. 4795, 2021.
[312] N. Muthukrishnan, J. J. Abbas, and N. Krishnamurthi, "A wearable sensor system to measure step-based gait parameters for parkinson's disease rehabilitation," *Sensors,* vol. 20, no. 22, p. 6417, 2020.
[313] S. S. Yeo and G. Y. Park, "Accuracy verification of spatio-temporal and kinematic parameters for gait using inertial measurement unit system," *Sensors,* vol. 20, no. 5, p. 1343, 2020.
[314] S. Khandelwal and N. Wickström, "Evaluation of the performance of accelerometer-based gait event detection algorithms in different real-world scenarios using the MAREA gait database," *Gait & posture,* vol. 51, pp. 84-90, 2017.
[315] A. Hickey, S. Del Din, L. Rochester, and A. Godfrey, "Detecting free-living steps and walking bouts: validating an algorithm for macro gait analysis," *Physiological measurement,* vol. 38, no. 1, p. N1, 2016.
[316] S. Del Din, A. Godfrey, B. Galna, S. Lord, and L. Rochester, "Free-living gait characteristics in ageing and Parkinson's disease: impact of environment and ambulatory bout length," *Journal of neuroengineering and rehabilitation,* vol. 13, no. 1, pp. 1-12, 2016.
[317] H. Loose and J. L. Bolmgren, "GaitAnalysisDataBase–Short Overview."
[318] M. Mancini *et al.*, "The impact of freezing of gait on balance perception and mobility in community-living with Parkinson's disease," in *2018 40th Annual International Conference of the IEEE Engineering in Medicine and Biology Society (EMBC)*, 2018: IEEE, pp. 3040-3043.
[319] R. Moe-Nilssen, "A new method for evaluating motor control in gait under real-life environmental conditions. Part 1: The instrument," *Clinical biomechanics,* vol. 13, no. 4-5, pp. 320-327, 1998.
[320] T. K. Koo and M. Y. Li, "A guideline of selecting and reporting intraclass correlation coefficients for reliability research," *Journal of chiropractic medicine,* vol. 15, no. 2, pp. 155-163, 2016.
[321] P. E. Shrout and J. L. Fleiss, "Intraclass correlations: uses in assessing rater reliability," *Psychological bulletin,* vol. 86, no. 2, p. 420, 1979.
[322] G. Coulby, A. K. Clear, O. Jones, and A. Godfrey, "Low-cost, multimodal environmental monitoring based on the Internet of Things," *Building and Environment,* p. 108014, 2021.
[323] J. M. Bland and D. G. Altman, "Measuring agreement in method comparison studies," *Statistical methods in medical research,* vol. 8, no. 2, pp. 135-160, 1999.
[324] S. Del Din, A. Hickey, N. Hurwitz, J. C. Mathers, L. Rochester, and A. Godfrey, "Measuring gait with an accelerometer-based wearable: influence of device location, testing protocol and age," *Physiological measurement,* vol. 37, no. 10, p. 1785, 2016.
[325] T. R. Beijer, S. R. Lord, and M. A. Brodie, "Comparison of Handheld Video Camera and GAITRite® Measurement of Gait Impairment in People with Early Stage Parkinson's Disease: A Pilot Study," *Journal of Parkinson's disease,* vol. 3, no. 2, pp. 199-203, 2013.
[326] M. A. Brodie *et al.*, "Wearable pendant device monitoring using new wavelet-based methods shows daily life and laboratory gaits are different," *Medical & biological engineering & computing,* vol. 54, no. 4, pp. 663-674, 2016.

[327] F. M. Rast and R. Labruyère, "Systematic review on the application of wearable inertial sensors to quantify everyday life motor activity in people with mobility impairments," *Journal of NeuroEngineering and Rehabilitation,* vol. 17, no. 1, pp. 1-19, 2020.
[328] Y. Zhou *et al.*, "The detection of age groups by dynamic gait outcomes using machine learning approaches," *Scientific reports,* vol. 10, no. 1, pp. 1-12, 2020.
[329] A. Phinyomark, G. Petri, E. Ibáñez-Marcelo, S. T. Osis, and R. Ferber, "Analysis of big data in gait biomechanics: current trends and future directions," *Journal of medical and biological engineering,* vol. 38, no. 2, pp. 244-260, 2018.
[330] A. Mirelman *et al.*, "Detecting Sensitive Mobility Features for Parkinson's Disease Stages Via Machine Learning," *Movement Disorders,* 2021.
[331] S. Qiu *et al.*, "Multi-sensor information fusion based on machine learning for real applications in human activity recognition: State-of-the-art and research challenges," *Information Fusion,* vol. 80, pp. 241-265, 2022.
[332] J. Esteban, A. Starr, R. Willetts, P. Hannah, and P. Bryanston-Cross, "A review of data fusion models and architectures: towards engineering guidelines," *Neural Computing & Applications,* vol. 14, no. 4, pp. 273-281, 2005.
[333] E. Sejdić *et al.*, "Assessing interactions among multiple physiological systems during walking outside a laboratory: An android based gait monitor," *Computer methods and programs in biomedicine,* vol. 122, no. 3, pp. 450-461, 2015.
[334] D. Pan, H. Liu, D. Qu, and Z. Zhang, "Human Falling Detection Algorithm Based on Multisensor Data Fusion with SVM," *Mobile Information Systems,* vol. 2020, 2020.
[335] P. Tsinganos and A. Skodras, "On the comparison of wearable sensor data fusion to a single sensor machine learning technique in fall detection," *Sensors,* vol. 18, no. 2, p. 592, 2018.
[336] G. Koshmak, A. Loutfi, and M. Linden, "Challenges and issues in multisensor fusion approach for fall detection," *Journal of Sensors,* vol. 2016, 2016.
[337] R. Gravina, P. Alinia, H. Ghasemzadeh, and G. Fortino, "Multi-sensor fusion in body sensor networks: State-of-the-art and research challenges," *Information Fusion,* vol. 35, pp. 68-80, 2017.
[338] C. Frigo and P. Crenna, "Multichannel SEMG in clinical gait analysis: a review and state-of-the-art," *Clinical Biomechanics,* vol. 24, no. 3, pp. 236-245, 2009.
[339] X. Xi, M. Tang, and Z. Luo, "Feature-level fusion of surface electromyography for activity monitoring," *Sensors,* vol. 18, no. 2, p. 614, 2018.
[340] F. Castanedo, "A review of data fusion techniques," *The scientific world journal,* vol. 2013, 2013.
[341] F. Sun, W. Zang, R. Gravina, G. Fortino, and Y. Li, "Gait-based identification for elderly users in wearable healthcare systems," *Information Fusion,* vol. 53, pp. 134-144, 2020.
[342] M. L. Shuwandy, B. Zaidan, A. Zaidan, and A. S. Albahri, "Sensor-based mHealth authentication for real-time remote healthcare monitoring system: A multilayer systematic review," *Journal of medical systems,* vol. 43, no. 2, pp. 1-30, 2019.
[343] R. LeMoyne and T. Mastroianni, "Wearable and Wireless Systems for Healthcare I," *Gait and Reflex Response Quantification,* 2018.
[344] S. Sagiroglu and D. Sinanc, "Big data: A review," in *2013 international conference on collaboration technologies and systems (CTS)*, 2013: IEEE, pp. 42-47.
[345] S. Dash, S. K. Shakyawar, M. Sharma, and S. Kaushik, "Big data in healthcare: management, analysis and future prospects," *Journal of Big Data,* vol. 6, no. 1, pp. 1-25, 2019.
[346] T. N. Gia *et al.*, "Energy efficient wearable sensor node for IoT-based fall detection systems," *Microprocessors and Microsystems,* vol. 56, pp. 34-46, 2018.
[347] S. Greene, H. Thapliyal, and D. Carpenter, "IoT-based fall detection for smart home environments," in *2016 IEEE international symposium on nanoelectronic and information systems (iNIS)*, 2016: IEEE, pp. 23-28.
[348] C. Tunca, G. Salur, and C. Ersoy, "Deep learning for fall risk assessment with inertial sensors: Utilizing domain knowledge in spatio-temporal gait parameters," *IEEE journal of biomedical and health informatics,* vol. 24, no. 7, pp. 1994-2005, 2019.
[349] N. Shibuya *et al.*, "A real-time fall detection system using a wearable gait analysis sensor and a Support Vector Machine (SVM) classifier," in *2015 Eighth International Conference on Mobile Computing and Ubiquitous Networking (ICMU)*, 2015: IEEE, pp. 66-67.
[350] C. Buckley *et al.*, "Binary classification of running fatigue using a single inertial measurement unit," in *2017 IEEE 14th International Conference on Wearable and Implantable Body Sensor Networks (BSN)*, 2017: IEEE, pp. 197-201.

[351] M. Savadkoohi, T. Oladunni, and L. A. Thompson, "Deep neural networks for human's fall-risk prediction using force-plate time series signal," *Expert Systems with Applications,* vol. 182, p. 115220, 2021.
[352] P. Zhang, D. C. Schmidt, J. White, and G. Lenz, "Blockchain technology use cases in healthcare," in *Advances in computers*, vol. 111: Elsevier, 2018, pp. 1-41.
[353] C. Ladha *et al.*, "Toward a low-cost gait analysis system for clinical and free-living assessment," in *2016 38th Annual International Conference of the IEEE Engineering in Medicine and Biology Society (EMBC)*, 2016: IEEE, pp. 1874-1877.
[354] C. Ricciardi *et al.*, "Using gait analysis' parameters to classify Parkinsonism: A data mining approach," *Computer methods and programs in biomedicine,* vol. 180, p. 105033, 2019.
[355] M. Babar and F. Arif, "Real-time data processing scheme using big data analytics in internet of things based smart transportation environment," *Journal of Ambient Intelligence and Humanized Computing,* vol. 10, no. 10, pp. 4167-4177, 2019.
[356] M. Zeng *et al.*, "Convolutional neural networks for human activity recognition using mobile sensors," in *6th international conference on mobile computing, applications and services*, 2014: IEEE, pp. 197-205.
[357] T. Huynh and B. Schiele, "Analyzing features for activity recognition," in *Proceedings of the 2005 joint conference on Smart objects and ambient intelligence: innovative context-aware services: usages and technologies*, 2005, pp. 159-163.
[358] N. A. Capela, E. D. Lemaire, and N. Baddour, "Feature selection for wearable smartphone-based human activity recognition with able bodied, elderly, and stroke patients," *PloS one,* vol. 10, no. 4, p. e0124414, 2015.
[359] C. Catal, S. Tufekci, E. Pirmit, and G. Kocabag, "On the use of ensemble of classifiers for accelerometer-based activity recognition," *Applied Soft Computing,* vol. 37, pp. 1018-1022, 2015.
[360] M. M. H. Shuvo, N. Ahmed, K. Nouduri, and K. Palaniappan, "A Hybrid Approach for Human Activity Recognition with Support Vector Machine and 1D Convolutional Neural Network," in *2020 IEEE Applied Imagery Pattern Recognition Workshop (AIPR)*, 2020: IEEE, pp. 1-5.
[361] F. Demrozi, G. Pravadelli, A. Bihorac, and P. Rashidi, "Human activity recognition using inertial, physiological and environmental sensors: a comprehensive survey," *IEEE Access,* 2020.
[362] W. Huang, L. Zhang, Q. Teng, C. Song, and J. He, "The convolutional neural networks training with Channel-Selectivity for human activity recognition based on sensors," *IEEE Journal of Biomedical and Health Informatics,* 2021.
[363] Y. LeCun, Y. Bengio, and G. Hinton, "Deep learning," *nature,* vol. 521, no. 7553, pp. 436-444, 2015.
[364] J. Wang, Y. Chen, S. Hao, X. Peng, and L. Hu, "Deep learning for sensor-based activity recognition: A survey," *Pattern Recognition Letters,* vol. 119, pp. 3-11, 2019.
[365] F. J. Ordóñez and D. Roggen, "Deep convolutional and lstm recurrent neural networks for multimodal wearable activity recognition," *Sensors,* vol. 16, no. 1, p. 115, 2016.
[366] C. Shorten and T. M. Khoshgoftaar, "A survey on Image Data Augmentation for Deep Learning," *Journal of Big Data,* vol. 6, no. 1, p. 60, 2019/07/06 2019, doi: 10.1186/s40537-019-0197-0.
[367] L. Perez and J. Wang, "The effectiveness of data augmentation in image classification using deep learning," *arXiv preprint arXiv:1712.04621,* 2017.
[368] J. Huang, S. Lin, N. Wang, G. Dai, Y. Xie, and J. Zhou, "TSE-CNN: A two-stage end-to-end CNN for human activity recognition," *IEEE journal of biomedical and health informatics,* vol. 24, no. 1, pp. 292-299, 2019.
[369] L. Alawneh, T. Alsarhan, M. Al-Zinati, M. Al-Ayyoub, Y. Jararweh, and H. Lu, "Enhancing human activity recognition using deep learning and time series augmented data," *Journal of Ambient Intelligence and Humanized Computing,* vol. 12, no. 12, pp. 10565-10580, 2021.
[370] I. Goodfellow *et al.*, "Generative adversarial nets," *Advances in neural information processing systems,* vol. 27, 2014.
[371] R. Liu, A. A. Ramli, H. Zhang, E. Datta, E. Henricson, and X. Liu, "An Overview of Human Activity Recognition Using Wearable Sensors: Healthcare and Artificial Intelligence," *arXiv preprint arXiv:2103.15990,* 2021.
[372] N. V. Chawla, K. W. Bowyer, L. O. Hall, and W. P. Kegelmeyer, "SMOTE: synthetic minority over-sampling technique," *Journal of artificial intelligence research,* vol. 16, pp. 321-357, 2002.
[373] W. Jiang and Z. Yin, "Human activity recognition using wearable sensors by deep convolutional neural networks," in *Proceedings of the 23rd ACM international conference on Multimedia*, 2015, pp. 1307-1310.

[374] I. A. Lawal and S. Bano, "Deep human activity recognition using wearable sensors," in *Proceedings of the 12th ACM International Conference on PErvasive Technologies Related to Assistive Environments*, 2019, pp. 45-48.
[375] M. F. Aslan, K. Sabanci, and A. Durdu, "A CNN-based novel solution for determining the survival status of heart failure patients with clinical record data: numeric to image," *Biomedical Signal Processing and Control,* vol. 68, p. 102716, 2021.
[376] J. L. R. Ortiz, "Smartphone-based human activity recognition," 2015.
[377] M. Zhang and A. A. Sawchuk, "USC-HAD: a daily activity dataset for ubiquitous activity recognition using wearable sensors," in *Proceedings of the 2012 ACM conference on ubiquitous computing*, 2012, pp. 1036-1043.
[378] D. Anguita, A. Ghio, L. Oneto, X. Parra Perez, and J. L. Reyes Ortiz, "A public domain dataset for human activity recognition using smartphones," in *Proceedings of the 21th international European symposium on artificial neural networks, computational intelligence and machine learning*, 2013, pp. 437-442.
[379] M. K. O'Brien *et al.*, "Activity recognition for persons with stroke using mobile phone technology: toward improved performance in a home setting," *J Med Internet Res,* vol. 19, no. 5, p. e184, 2017.
[380] M. V. Albert, Y. Azeze, M. Courtois, and A. Jayaraman, "In-lab versus at-home activity recognition in ambulatory subjects with incomplete spinal cord injury," *Journal of neuroengineering and rehabilitation,* vol. 14, no. 1, pp. 1-6, 2017.
[381] A. O. Jimale and M. H. Mohd Noor, "Subject variability in sensor-based activity recognition," *Journal of Ambient Intelligence and Humanized Computing,* pp. 1-14, 2021.
[382] S. K. Routray and K. Sharmila, "Green initiatives in IoT," in *2017 Third International Conference on Advances in Electrical, Electronics, Information, Communication and Bio-Informatics (AEEICB)*, 2017: IEEE, pp. 454-457.
[383] S. Li, L. Da Xu, and S. Zhao, "5G Internet of Things: A survey," *Journal of Industrial Information Integration,* vol. 10, pp. 1-9, 2018.
[384] J. R. Braga, J. B. Mendes, L. A. Júnior, and A. C. Ramos, "Modeling of System Software for Computer Based Training," in *2010 Seventh International Conference on Information Technology: New Generations*, 2010: IEEE, pp. 1051-1056.
[385] P. Ray, "A survey on internet of things architectures. J King of Saud Univ Comput Inf Sci," *Elsevier,* 2018.
[386] A. Godfrey, M. Brodie, K. van Schooten, M. Nouredanesh, S. Stuart, and L. Robinson, "Inertial wearables as pragmatic tools in dementia," *Maturitas,* vol. 127, pp. 12-17, 2019.
[387] G. Coulby and F. Young, "Frameworks: integration to digital networks and beyond," in *Digital Health*: Elsevier, 2021, pp. 163-176.
[388] S. Naveen and M. R. Kounte, "Key technologies and challenges in IoT edge computing," in *2019 Third international conference on I-SMAC (IoT in social, mobile, analytics and cloud)(I-SMAC)*, 2019: IEEE, pp. 61-65.
[389] Q. Cheng, "Predictive modeling of health status using motion analysis from mobile phones," University of Illinois at Urbana-Champaign, 2017.
[390] M. Yang, H. Zheng, H. Wang, S. McClean, and N. Harris, "Assessing the utility of smart mobile phones in gait pattern analysis," *Health and Technology,* vol. 2, no. 1, pp. 81-88, 2012.
[391] A. Godfrey, V. Hetherington, H. Shum, P. Bonato, N. Lovell, and S. Stuart, "From A to Z: Wearable technology explained," *Maturitas,* vol. 113, pp. 40-47, 2018.
[392] A. Zhao *et al.*, "Multimodal Gait Recognition for Neurodegenerative Diseases," *arXiv preprint arXiv:2101.02469,* 2021.
[393] H. F. Nweke, Y. W. Teh, G. Mujtaba, and M. A. Al-Garadi, "Data fusion and multiple classifier systems for human activity detection and health monitoring: Review and open research directions," *Information Fusion,* vol. 46, pp. 147-170, 2019.
[394] C.-W. Lin, Y.-T. C. Yang, J.-S. Wang, and Y.-C. Yang, "A wearable sensor module with a neural-network-based activity classification algorithm for daily energy expenditure estimation," *IEEE Transactions on Information Technology in Biomedicine,* vol. 16, no. 5, pp. 991-998, 2012.
[395] S. H. Roy *et al.*, "A combined sEMG and accelerometer system for monitoring functional activity in stroke," *IEEE Transactions on Neural Systems and Rehabilitation Engineering,* vol. 17, no. 6, pp. 585-594, 2009.
[396] K. S. van Schooten, M. Pijnappels, S. M. Rispens, P. J. Elders, P. Lips, and J. H. van Dieën, "Ambulatory fall-risk assessment: amount and quality of daily-life gait predict falls in older adults," *Journals of Gerontology Series A: Biomedical Sciences and Medical Sciences,* vol. 70, no. 5, pp. 608-615, 2015.

[397] P. C. Formento, R. Acevedo, S. Ghoussayni, and D. Ewins, "Gait event detection during stair walking using a rate gyroscope," *Sensors,* vol. 14, no. 3, pp. 5470-5485, 2014.
[398] B. Sijobert, M. Benoussaad, J. Denys, R. Pissard-Gibollet, C. Geny, and C. A. Coste, "Implementation and validation of a stride length estimation algorithm, using a single basic inertial sensor on healthy subjects and patients suffering from Parkinson's disease," *ElectronicHealthcare,* pp. 704-714, 2015.
[399] R. Takeda, S. Tadano, A. Natorigawa, M. Todoh, and S. Yoshinari, "Gait posture estimation using wearable acceleration and gyro sensors," *Journal of biomechanics,* vol. 42, no. 15, pp. 2486-2494, 2009.
[400] K. Tong and M. H. Granat, "A practical gait analysis system using gyroscopes," *Medical engineering & physics,* vol. 21, no. 2, pp. 87-94, 1999.
[401] E. Bishop and Q. Li, "Walking speed estimation using shank-mounted accelerometers," in *2010 IEEE International Conference on Robotics and Automation*, 2010: IEEE, pp. 5096-5101.
[402] M. Brodie, A. Walmsley, and W. Page, "The static accuracy and calibration of inertial measurement units for 3D orientation," 2008.
[403] H. Dejnabadi, B. M. Jolles, and K. Aminian, "A new approach to accurate measurement of uniaxial joint angles based on a combination of accelerometers and gyroscopes," *IEEE Transactions on Biomedical Engineering,* vol. 52, no. 8, pp. 1478-1484, 2005.
[404] L. F. Nestares and R. Callupe, "Development of a wearable motion capture system to evaluate the knee joint angle during stair-climbing in hemiplegics," in *2020 IEEE XXVII International Conference on Electronics, Electrical Engineering and Computing (INTERCON)*, 2020: IEEE, pp. 1-4.
[405] C. Yi *et al.*, "Estimating three-dimensional body orientation based on an improved complementary filter for human motion tracking," *Sensors,* vol. 18, no. 11, p. 3765, 2018.
[406] D. Stegeman and H. Hermens, "Standards for surface electromyography: The European project Surface EMG for non-invasive assessment of muscles (SENIAM)," 2007.
[407] R. Blagus and L. Lusa, "SMOTE for high-dimensional class-imbalanced data," *BMC Bioinformatics,* vol. 14, no. 1, p. 106, 2013/03/22 2013, doi: 10.1186/1471-2105-14-106.
[408] Y. Wang, S. Cang, and H. Yu, "A survey on wearable sensor modality centred human activity recognition in health care," *Expert Systems with Applications,* vol. 137, pp. 167-190, 2019.
[409] W. Rose, "Electromyogram analysis," *Online course material. University of Delaware. Retrieved July,* vol. 5, p. 2016, 2011.
[410] J. Too, A. R. Abdullah, N. Mohd Saad, and W. Tee, "EMG feature selection and classification using a Pbest-guide binary particle swarm optimization," *Computation,* vol. 7, no. 1, p. 12, 2019.
[411] P. Rowe, C. Myles, C. Walker, and R. Nutton, "Knee joint kinematics in gait and other functional activities measured using flexible electrogoniometry: how much knee motion is sufficient for normal daily life?," *Gait & posture,* vol. 12, no. 2, pp. 143-155, 2000.
[412] H. Yali, S. Aiguo, G. Haitao, and Z. Songqing, "The muscle activation patterns of lower limb during stair climbing at different backpack load," *Acta of Bioengineering and Biomechanics,* vol. 17, no. 4, 2015.
[413] Y.-C. Lin, L. A. Fok, A. G. Schache, and M. G. Pandy, "Muscle coordination of support, progression and balance during stair ambulation," *Journal of biomechanics,* vol. 48, no. 2, pp. 340-347, 2015.
[414] J. Shao, K. Hu, C. Wang, X. Xue, and B. Raj, "Is normalization indispensable for training deep neural network?," *Advances in Neural Information Processing Systems,* vol. 33, 2020.
[415] O. Banos, J.-M. Galvez, M. Damas, H. Pomares, and I. Rojas, "Window size impact in human activity recognition," *Sensors,* vol. 14, no. 4, pp. 6474-6499, 2014.
[416] S. Bianco, R. Cadene, L. Celona, and P. Napoletano, "Benchmark analysis of representative deep neural network architectures," *IEEE Access,* vol. 6, pp. 64270-64277, 2018.
[417] R. Mutegeki and D. S. Han, "A CNN-LSTM approach to human activity recognition," in *2020 International Conference on Artificial Intelligence in Information and Communication (ICAIIC)*, 2020: IEEE, pp. 362-366.
[418] N. Tufek, M. Yalcin, M. Altintas, F. Kalaoglu, Y. Li, and S. K. Bahadir, "Human action recognition using deep learning methods on limited sensory data," *IEEE Sensors Journal,* vol. 20, no. 6, pp. 3101-3112, 2019.
[419] A. Canziani, A. Paszke, and E. Culurciello, "An analysis of deep neural network models for practical applications," *arXiv preprint arXiv:1605.07678,* 2016.
[420] C. Szegedy *et al.*, "Going deeper with convolutions," in *Proceedings of the IEEE conference on computer vision and pattern recognition*, 2015, pp. 1-9.
[421] K. He, X. Zhang, S. Ren, and J. Sun, "Deep residual learning for image recognition," in *Proceedings of the IEEE conference on computer vision and pattern recognition*, 2016, pp. 770-778.
[422] A. G. Howard *et al.*, "Mobilenets: Efficient convolutional neural networks for mobile vision applications," *arXiv preprint arXiv:1704.04861,* 2017.

[423] M. Sandler, A. Howard, M. Zhu, A. Zhmoginov, and L.-C. Chen, "Mobilenetv2: Inverted residuals and linear bottlenecks," in *Proceedings of the IEEE conference on computer vision and pattern recognition*, 2018, pp. 4510-4520.
[424] A. A. Ardakani, A. R. Kanafi, U. R. Acharya, N. Khadem, and A. Mohammadi, "Application of deep learning technique to manage COVID-19 in routine clinical practice using CT images: Results of 10 convolutional neural networks," *Computers in biology and medicine,* vol. 121, p. 103795, 2020.
[425] J.-E. Kim, N.-E. Nam, J.-S. Shim, Y.-H. Jung, B.-H. Cho, and J. J. Hwang, "Transfer learning via deep neural networks for implant fixture system classification using periapical radiographs," *Journal of clinical medicine,* vol. 9, no. 4, p. 1117, 2020.
[426] M. Galar, A. Fernandez, E. Barrenechea, H. Bustince, and F. Herrera, "A review on ensembles for the class imbalance problem: bagging-, boosting-, and hybrid-based approaches," *IEEE Transactions on Systems, Man, and Cybernetics, Part C (Applications and Reviews),* vol. 42, no. 4, pp. 463-484, 2011.
[427] V. López, A. Fernández, S. García, V. Palade, and F. Herrera, "An insight into classification with imbalanced data: Empirical results and current trends on using data intrinsic characteristics," *Information sciences,* vol. 250, pp. 113-141, 2013.
[428] G. Demiris, D. P. Oliver, J. Giger, M. Skubic, and M. Rantz, "Older adults' privacy considerations for vision based recognition methods of eldercare applications," *Technology and Health Care,* vol. 17, no. 1, pp. 41-48, 2009.
[429] F. Deligianni, C. Wong, B. Lo, and G.-Z. Yang, "A fusion framework to estimate plantar ground force distributions and ankle dynamics," *Information Fusion,* vol. 41, pp. 255-263, 2018.
[430] C. Cruz-Montecinos, S. Pérez-Alenda, F. Querol, M. Cerda, and H. Maas, "Changes in muscle activity patterns and joint kinematics during gait in hemophilic arthropathy," *Frontiers in physiology,* vol. 10, p. 1575, 2020.
[431] J. Li *et al.*, "Using Body Sensor Network to Measure the Effect of Rehabilitation Therapy on Improvement of Lower Limb Motor Function in Children With Spastic Diplegia," *IEEE Transactions on Instrumentation and Measurement,* vol. 69, no. 11, pp. 9215-9227, 2020.
[432] A. Middleton, S. L. Fritz, and M. Lusardi, "Walking speed: the functional vital sign," *Journal of aging and physical activity,* vol. 23, no. 2, pp. 314-322, 2015.
[433] R. Baker, "Gait analysis methods in rehabilitation," *Journal of neuroengineering and rehabilitation,* vol. 3, no. 1, pp. 1-10, 2006.
[434] M. Seiffert, F. Holstein, R. Schlosser, and J. Schiller, "Next generation cooperative wearables: Generalized activity assessment computed fully distributed within a wireless body area network," *IEEE Access,* vol. 5, pp. 16793-16807, 2017.
[435] S. Lahmiri, "Gait nonlinear patterns related to Parkinson's disease and age," *IEEE Transactions on Instrumentation and Measurement,* vol. 68, no. 7, pp. 2545-2551, 2018.
[436] A. Godfrey, S. Del Din, G. Barry, J. Mathers, and L. Rochester, "Instrumenting gait with an accelerometer: a system and algorithm examination," *Medical engineering & physics,* vol. 37, no. 4, pp. 400-407, 2015.
[437] Y. Wang *et al.*, "Gait characteristics of post-stroke hemiparetic patients with different walking speeds," *International journal of rehabilitation research. Internationale Zeitschrift fur Rehabilitationsforschung. Revue internationale de recherches de readaptation,* vol. 43, no. 1, p. 69, 2020.
[438] C. Bonnyaud, D. Pradon, N. Vuillerme, D. Bensmail, and N. Roche, "Spatiotemporal and kinematic parameters relating to oriented gait and turn performance in patients with chronic stroke," *PloS one,* vol. 10, no. 6, 2015.
[439] R. Riener, M. Rabuffetti, and C. Frigo, "Stair ascent and descent at different inclinations," *Gait & posture,* vol. 15, no. 1, pp. 32-44, 2002.
[440] S. Vallabhajosula, C. W. Tan, M. Mukherjee, A. J. Davidson, and N. Stergiou, "Biomechanical analyses of stair-climbing while dual-tasking," *Journal of biomechanics,* vol. 48, no. 6, pp. 921-929, 2015.
[441] M. G. Benedetti, V. Agostini, M. Knaflitz, and P. Bonato, "Muscle activation patterns during level walking and stair ambulation," *Applications of EMG in clinical and sports medicine,* vol. 8, no. 2, pp. 117-130, 2012.
[442] A. Schmitz, A. Silder, B. Heiderscheit, J. Mahoney, and D. G. Thelen, "Differences in lower-extremity muscular activation during walking between healthy older and young adults," *Journal of electromyography and kinesiology,* vol. 19, no. 6, pp. 1085-1091, 2009.
[443] M. Nazarahari and H. Rouhani, "40 years of sensor fusion for orientation tracking via magnetic and inertial measurement units: Methods, lessons learned, and future challenges," *Information Fusion,* vol. 68, pp. 67-84, 2021.

[444] A. Kececi, A. Yildirak, K. Ozyazici, G. Ayluctarhan, O. Agbulut, and I. Zincir, "Implementation of machine learning algorithms for gait recognition," *Engineering Science and Technology, an International Journal,* vol. 23, no. 4, pp. 931-937, 2020.
[445] O. M. Giggins, I. Clay, and L. Walsh, "Physical activity monitoring in patients with neurological disorders: a review of novel body-worn devices," *Digital Biomarkers,* vol. 1, no. 1, pp. 14-42, 2017.
[446] M. Gadaleta, G. Cisotto, M. Rossi, R. Z. U. Rehman, L. Rochester, and S. Del Din, "Deep learning techniques for improving digital gait segmentation," in *2019 41st Annual International Conference of the IEEE Engineering in Medicine and Biology Society (EMBC)*, 2019: IEEE, pp. 1834-1837.
[447] S. S. Bangaru, C. Wang, and F. Aghazadeh, "Data Quality and Reliability Assessment of Wearable EMG and IMU Sensor for Construction Activity Recognition," *Sensors,* vol. 20, no. 18, p. 5264, 2020.
[448] C. Ren, T. Fu, M. Zhou, and X. Hu, "Low-cost 3-D positioning system based on SEMG and MIMU," *IEEE Transactions on Instrumentation and Measurement,* vol. 67, no. 4, pp. 876-884, 2018.
[449] C. Gu, C. Ren, and M. Zhou, "A novel method to process surface electromyography signal for pedestrian lower limb motion pattern recognition," *Transactions of the Institute of Measurement and Control,* vol. 42, no. 13, pp. 2492-2498, 2020.
[450] J. Wang, D. Cao, J. Wang, and C. Liu, "Action Recognition of Lower Limbs Based on Surface Electromyography Weighted Feature Method," *Sensors,* vol. 21, no. 18, p. 6147, 2021.
[451] J. Cheng, X. Chen, and M. Shen, "A framework for daily activity monitoring and fall detection based on surface electromyography and accelerometer signals," *IEEE journal of biomedical and health informatics,* vol. 17, no. 1, pp. 38-45, 2012.
[452] H. Gjoreski and M. Gams, "Activity/Posture recognition using wearable sensors placed on different body locations," *Proceedings of (738) Signal and Image Processing and Applications, Crete, Greece,* vol. 2224, p. 716724, 2011.
[453] C.-T. Yen, J.-X. Liao, and Y.-K. Huang, "Human Daily Activity Recognition Performed Using Wearable Inertial Sensors Combined With Deep Learning Algorithms," *IEEE Access,* vol. 8, pp. 174105-174114, 2020.
[454] H. Li and M. Trocan, "Deep learning of smartphone sensor data for personal health assistance," *Microelectronics Journal,* vol. 88, pp. 164-172, 2019.
[455] H. Cho and S. M. Yoon, "Divide and conquer-based 1D CNN human activity recognition using test data sharpening," *Sensors,* vol. 18, no. 4, p. 1055, 2018.
[456] L. Lonini, A. Gupta, K. Kording, and A. Jayaraman, "Activity recognition in patients with lower limb impairments: do we need training data from each patient?," in *2016 38th Annual International Conference of the IEEE Engineering in Medicine and Biology Society (EMBC)*, 2016: IEEE, pp. 3265-3268.
[457] X. Hu, L. Chu, J. Pei, W. Liu, and J. Bian, "Model complexity of deep learning: A survey," *Knowledge and Information Systems,* vol. 63, no. 10, pp. 2585-2619, 2021.
[458] "The King's Fund, Activity in the NHS." https://www.kingsfund.org.uk/projects/nhs-in-a-nutshell/NHS-activity (accessed November 30, 2021.
[459] G. Andrews, "Aging and Health," 2020.
[460] D. Cornish. "Monthly mortality analysis, England and Wales - Office for National Statistics." https://www.ons.gov.uk/peoplepopulationandcommunity/birthsdeathsandmarriages/deaths/bulletins/monthlymortalityanalysisenglandandwales/march2021 (accessed November 30, 2021.
[461] "M. Europe, What is Medical Technology? ." https://www.medtecheurope.org/about-the-industry/what-is-medical-technology (accessed September 27, 2021.
[462] "Statista.com, Global total medtech revenue 2011-2024 | Statistic." https://www.statista.com/statistics/325809/worldwide-medical-technology-revenue (accessed September 27, 2021.
[463] W. Pitt, S.-H. Chen, and L.-S. Chou, "Using IMU-based kinematic markers to monitor dual-task gait balance control recovery in acutely concussed individuals," *Clinical Biomechanics,* vol. 80, p. 105145, 2020.
[464] L. A. King *et al.*, "Sensor-based balance measures outperform modified balance error scoring system in identifying acute concussion," *Annals of biomedical engineering,* vol. 45, no. 9, pp. 2135-2145, 2017.
[465] P. C. Fino *et al.*, "Detecting gait abnormalities after concussion or mild traumatic brain injury: a systematic review of single-task, dual-task, and complex gait," *Gait & Posture,* vol. 62, pp. 157-166, 2018.
[466] D. Howell, L. Osternig, and L.-S. Chou, "Monitoring recovery of gait balance control following concussion using an accelerometer," *Journal of biomechanics,* vol. 48, no. 12, pp. 3364-3368, 2015.

[467] L. J. H. Rasmussen *et al.*, "Association of neurocognitive and physical function with gait speed in midlife," *JAMA network open,* vol. 2, no. 10, pp. e1913123-e1913123, 2019.
[468] S. Fritz, "Lusardi M. White paper:“walking speed: the sixth vital sign”," *J Geriatr Phys Ther,* vol. 32, no. 2, pp. 46-9, 2009.
[469] F. Petraglia, L. Scarcella, G. Pedrazzi, L. Brancato, R. Puers, and C. Costantino, "Inertial sensors versus standard systems in gait analysis: a systematic review and meta-analysis," *European Journal of Physical and Rehabilitation Medicine,* vol. 55, no. 2, pp. 265-280, 2019.
[470] A. Atrsaei, F. Dadashi, B. Mariani, R. Gonzenbach, and K. Aminian, "Toward a remote assessment of walking bout and speed: application in patients with multiple sclerosis," *IEEE Journal of Biomedical and Health Informatics,* vol. 25, no. 11, pp. 4217-4228, 2021.
[471] S. J. M. Bamberg, A. Y. Benbasat, D. M. Scarborough, D. E. Krebs, and J. A. Paradiso, "Gait analysis using a shoe-integrated wireless sensor system," *IEEE transactions on information technology in biomedicine,* vol. 12, no. 4, pp. 413-423, 2008.
[472] H. Noshadi, F. Dabiri, S. Ahmadian, N. Amini, and M. Sarrafzadeh, "HERMES: mobile system for instability analysis and balance assessment," *ACM Transactions on Embedded Computing Systems (TECS),* vol. 12, no. 1s, pp. 1-24, 2013.
[473] N. Hegde, M. Bries, T. Swibas, E. Melanson, and E. Sazonov, "Automatic recognition of activities of daily living utilizing insole-based and wrist-worn wearable sensors," *IEEE journal of biomedical and health informatics,* vol. 22, no. 4, pp. 979-988, 2017.
[474] L. Shu, T. Hua, Y. Wang, Q. Li, D. D. Feng, and X. Tao, "In-shoe plantar pressure measurement and analysis system based on fabric pressure sensing array," *IEEE Transactions on information technology in biomedicine,* vol. 14, no. 3, pp. 767-775, 2010.
[475] A. Rezaei, M. Khoshnam, and C. Menon, "Towards user-friendly wearable platforms for monitoring unconstrained indoor and outdoor activities," *IEEE Journal of Biomedical and Health Informatics,* vol. 25, no. 3, pp. 674-684, 2020.
[476] F. Lin, A. Wang, Y. Zhuang, M. R. Tomita, and W. Xu, "Smart insole: A wearable sensor device for unobtrusive gait monitoring in daily life," *IEEE Transactions on Industrial Informatics,* vol. 12, no. 6, pp. 2281-2291, 2016.
[477] A. Vadnerkar, S. Figueiredo, N. E. Mayo, and R. E. Kearney, "Design and validation of a biofeedback device to improve heel-to-toe gait in seniors," *IEEE journal of biomedical and health informatics,* vol. 22, no. 1, pp. 140-146, 2017.
[478] N. Yodpijit, N. Tavichaiyuth, M. Jongprasithporn, C. Songwongamarit, and T. Sittiwanchai, "The use of smartphone for gait analysis," in *2017 3rd International Conference on Control, Automation and Robotics (ICCAR)*, 2017: IEEE, pp. 543-546.
[479] Y. Celik, S. Stuart, W. L. Woo, and A. Godfrey, "Gait analysis in neurological populations: Progression in the use of wearables," *Medical Engineering & Physics,* vol. 87, pp. 9-29, 2021.
[480] E. Martini *et al.*, "Real-time human pose estimation at the edge for gait analysis at a distance," in *2022 18th International Conference on Distributed Computing in Sensor Systems (DCOSS)*, 2022: IEEE, pp. 45-48.
[481] E. Martini *et al.*, "Preserving Data Privacy and Accuracy of Human Pose Estimation Software Based on CNN s for Remote Gait Analysis," in *2022 44th Annual International Conference of the IEEE Engineering in Medicine & Biology Society (EMBC)*, 2022: IEEE, pp. 3468-3471.
[482] A. A. Abdellatif, A. Mohamed, C. F. Chiasserini, M. Tlili, and A. Erbad, "Edge computing for smart health: Context-aware approaches, opportunities, and challenges," *IEEE Network,* vol. 33, no. 3, pp. 196-203, 2019.
[483] M. Mancini and F. B. Horak, "Potential of APDM mobility lab for the monitoring of the progression of Parkinson’s disease," *Expert review of medical devices,* vol. 13, no. 5, pp. 455-462, 2016.
[484] N. Ö. Doğan, "Bland-Altman analysis: A paradigm to understand correlation and agreement," *Turkish journal of emergency medicine,* vol. 18, no. 4, pp. 139-141, 2018.
[485] L. Donath, O. Faude, E. Lichtenstein, C. Nüesch, and A. Mündermann, "Validity and reliability of a portable gait analysis system for measuring spatiotemporal gait characteristics: comparison to an instrumented treadmill," *Journal of neuroengineering and rehabilitation,* vol. 13, no. 1, p. 6, 2016.
[486] E. Papi, D. Osei-Kuffour, Y.-M. A. Chen, and A. H. McGregor, "Use of wearable technology for performance assessment: A validation study," *Medical engineering & physics,* vol. 37, no. 7, pp. 698-704, 2015.
[487] S. Del Din *et al.*, "Instrumented gait assessment with a single wearable: an introductory tutorial," *F1000Research,* vol. 5, no. 2323, p. 2323, 2016.

[488] H. Weinberg, "Using the ADXL202 in pedometer and personal navigation applications," *Analog Devices AN-602 application note,* vol. 2, no. 2, pp. 1-6, 2002.
[489] E. Andersson, "Motion classification and step length estimation for gps/ins pedestrian navigation," Master's thesis, KTH Electrical Engineering, 2012.
[490] S. Díaz, S. Disdier, and M. A. Labrador, "Step Length and Step Width Estimation using Wearable Sensors," in *2018 9th IEEE Annual Ubiquitous Computing, Electronics & Mobile Communication Conference (UEMCON)*, 2018: IEEE, pp. 997-1001.
[491] J. M. Hausdorff, D. A. Rios, and H. K. Edelberg, "Gait variability and fall risk in community-living older adults: a 1-year prospective study," (in eng), *Arch Phys Med Rehabil,* vol. 82, no. 8, pp. 1050-6, Aug 2001, doi: 10.1053/apmr.2001.24893.
[492] S. W. Muir-Hunter and J. E. Wittwer, "Dual-task testing to predict falls in community-dwelling older adults: a systematic review," (in eng), *Physiotherapy,* vol. 102, no. 1, pp. 29-40, Mar 2016, doi: 10.1016/j.physio.2015.04.011.
[493] A. Weiss, A. Mirelman, A. S. Buchman, D. A. Bennett, and J. M. Hausdorff, "Using a body-fixed sensor to identify subclinical gait difficulties in older adults with IADL disability: maximizing the output of the timed up and go," (in eng), *PLoS One,* vol. 8, no. 7, p. e68885, 2013, doi: 10.1371/journal.pone.0068885.
[494] L. J. Dommershuijsen, B. M. Isik, S. K. L. Darweesh, J. N. van der Geest, M. K. Ikram, and M. A. Ikram, "Unraveling the Association Between Gait and Mortality-One Step at a Time," (in eng), *J Gerontol A Biol Sci Med Sci,* vol. 75, no. 6, pp. 1184-1190, May 22 2020, doi: 10.1093/gerona/glz282.
[495] R. Mc Ardle, S. Del Din, B. Galna, A. Thomas, and L. Rochester, "Differentiating dementia disease subtypes with gait analysis: feasibility of wearable sensors?," (in eng), *Gait Posture,* vol. 76, pp. 372-376, Feb 2020, doi: 10.1016/j.gaitpost.2019.12.028.
[496] R. Mc Ardle, B. Galna, P. Donaghy, A. Thomas, and L. Rochester, "Do Alzheimer's and Lewy body disease have discrete pathological signatures of gait?," (in eng), *Alzheimers Dement,* vol. 15, no. 10, pp. 1367-1377, Oct 2019, doi: 10.1016/j.jalz.2019.06.4953.
[497] F. Pieruccini-Faria *et al.*, "Gait variability across neurodegenerative and cognitive disorders: Results from the Canadian Consortium of Neurodegeneration in Aging (CCNA) and the Gait and Brain Study," (in eng), *Alzheimers Dement,* vol. 17, no. 8, pp. 1317-1328, Aug 2021, doi: 10.1002/alz.12298.
[498] D. K. White *et al.*, "Trajectories of gait speed predict mortality in well-functioning older adults: the Health, Aging and Body Composition study," (in eng), *J Gerontol A Biol Sci Med Sci,* vol. 68, no. 4, pp. 456-64, Apr 2013, doi: 10.1093/gerona/gls197.
[499] R. Vitório *et al.*, "Disease severity affects obstacle crossing in people with Parkinson's disease," (in eng), *Gait Posture,* vol. 40, no. 1, pp. 266-9, 2014, doi: 10.1016/j.gaitpost.2014.03.003.
[500] V. Belli *et al.*, "Prefrontal Cortical Activity During Preferred and Fast Walking in Young and Older Adults: An fNIRS Study," (in eng), *Neuroscience,* vol. 473, pp. 81-89, Oct 1 2021, doi: 10.1016/j.neuroscience.2021.08.019.
[501] R. Vitório, F. Pieruccini-Faria, F. Stella, S. Gobbi, and L. T. Gobbi, "Effects of obstacle height on obstacle crossing in mild Parkinson's disease," (in eng), *Gait Posture,* vol. 31, no. 1, pp. 143-6, Jan 2010, doi: 10.1016/j.gaitpost.2009.09.011.
[502] K. W. Li, Y. Chen, N. Li, T. Duan, and F. Zou, "Assessment of risk of tripping before and after crossing obstacles under dimmed lighting conditions," (in eng), *Work,* vol. 66, no. 3, pp. 551-559, 2020, doi: 10.3233/wor-203197.
[503] P. Nóbrega-Sousa, L. T. B. Gobbi, D. Orcioli-Silva, N. R. D. Conceição, V. S. Beretta, and R. Vitório, "Prefrontal Cortex Activity During Walking: Effects of Aging and Associations With Gait and Executive Function," (in eng), *Neurorehabil Neural Repair,* vol. 34, no. 10, pp. 915-924, Oct 2020, doi: 10.1177/1545968320953824.
[504] P. Plummer and G. Eskes, "Measuring treatment effects on dual-task performance: a framework for research and clinical practice," (in eng), *Front Hum Neurosci,* vol. 9, p. 225, 2015, doi: 10.3389/fnhum.2015.00225.
[505] V. E. Kelly, A. J. Eusterbrock, and A. Shumway-Cook, "The effects of instructions on dual-task walking and cognitive task performance in people with Parkinson's disease," (in eng), *Parkinsons Dis,* vol. 2012, p. 671261, 2012, doi: 10.1155/2012/671261.
[506] G. Yogev-Seligmann, Y. Rotem-Galili, A. Mirelman, R. Dickstein, N. Giladi, and J. M. Hausdorff, "How does explicit prioritization alter walking during dual-task performance? Effects of age and sex on gait speed and variability," (in eng), *Phys Ther,* vol. 90, no. 2, pp. 177-86, Feb 2010, doi: 10.2522/ptj.20090043.

[507] D. Orcioli-Silva *et al.*, "Levodopa Facilitates Prefrontal Cortex Activation During Dual Task Walking in Parkinson Disease," (in eng), *Neurorehabil Neural Repair,* vol. 34, no. 7, pp. 589-599, Jul 2020, doi: 10.1177/1545968320924430.

[508] A. Mirelman, I. Maidan, H. Bernad-Elazari, S. Shustack, N. Giladi, and J. M. Hausdorff, "Effects of aging on prefrontal brain activation during challenging walking conditions," (in eng), *Brain Cogn,* vol. 115, pp. 41-46, Jul 2017, doi: 10.1016/j.bandc.2017.04.002.

[509] R. Morris, S. Lord, J. Bunce, D. Burn, and L. Rochester, "Gait and cognition: Mapping the global and discrete relationships in ageing and neurodegenerative disease," (in eng), *Neuroscience and biobehavioral reviews,* vol. 64, pp. 326-45, May 2016, doi: 10.1016/j.neubiorev.2016.02.012.

[510] D. J. Clark, "Automaticity of walking: functional significance, mechanisms, measurement and rehabilitation strategies," (in eng), *Front Hum Neurosci,* vol. 9, p. 246, 2015, doi: 10.3389/fnhum.2015.00246.

[511] F. Pieruccini-Faria, J. A. Jones, and Q. J. Almeida, "Motor planning in Parkinson's disease patients experiencing freezing of gait: the influence of cognitive load when approaching obstacles," (in eng), *Brain Cogn,* vol. 87, pp. 76-85, Jun 2014, doi: 10.1016/j.bandc.2014.03.005.

[512] C. Timmermans, M. Roerdink, T. W. J. Janssen, C. G. M. Meskers, and P. J. Beek, "Dual-Task Walking in Challenging Environments in People with Stroke: Cognitive-Motor Interference and Task Prioritization," (in eng), *Stroke Res Treat,* vol. 2018, p. 7928597, 2018, doi: 10.1155/2018/7928597.

[513] R. Vitorio *et al.*, "Dual-Task Costs of Quantitative Gait Parameters While Walking and Turning in People with Parkinson's Disease: Beyond Gait Speed," (in eng), *J Parkinsons Dis,* vol. 11, no. 2, pp. 653-664, 2021, doi: 10.3233/jpd-202289.

[514] R. K. MacAulay, R. M. Brouillette, H. C. Foil, A. J. Bruce-Keller, and J. N. Keller, "A longitudinal study on dual-tasking effects on gait: cognitive change predicts gait variance in the elderly," (in eng), *PLoS One,* vol. 9, no. 6, p. e99436, 2014, doi: 10.1371/journal.pone.0099436.

Appendices B – Conference papers and copyrights

Appendix 8. A feasibility study towards instrumentation of the Sport Concussion Assessment Tool (iSCAT)

This publication appears as a conference paper "*A feasibility study towards instrumentation of the Sport Concussion Assessment Tool (iSCAT)"*, was published 42nd Annual International Conference of the IEEE Engineering in Medicine & Biology Society (EMBC) in **2020.**

(URL: https://doi.org/10.1109/EMBC44109.2020.9175656).

A feasibility study towards instrumentation of the Sport Concussion Assessment Tool (iSCAT)

Yunus Celik, Dylan Powell, Wai Lok Woo, *Senior Member, IEEE*, Samuel Stuart and Alan Godfrey, *Member, IEEE*

***Abstract*— The Sports Concussion Assessment Tool (SCAT) is a pen and paper-based evaluation tool for use by healthcare professionals in the acute evaluation of suspected concussion. Here we present a feasibility study towards instrumented SCAT (iSCAT). Traditionally, a healthcare professional subjectively counts errors according to SCAT marking criteria matrix. It is hypothesized that an instrumented version of the test will be more accurate while providing additional digital-based parameters to better inform player management. The feasibility study focuses on the SCAT physical functioning tasks only: double leg stance, single-leg stance, tandem stance and tandem gait. Amateur university rugby players underwent iSCAT testing and data were recorded with 8 inertial units attached at different anatomical locations. Video data were gathered simultaneously as reference. An iSCAT algorithm was used to detect errors and quantify additional concussion-based time and frequency domain parameters to assess participant stability during balance and gait tasks. Future work aims to instrument other SCAT features such as hand-eye coordination while deploying methods within a large concussion project.**

I. Introduction

Concussion is common in contact sports (e.g. rugby) and returning to play before sufficient recovery increases risk of more serious secondary injury. Medical staff make return-to-play decisions based on 'snapshot' post-injury subjective concussion assessment tools [1]. The 5th edition of the Sport Concussion Assessment Tool (SCAT5/SCAT) is the most recent revision/consensus of an evaluation tool for use by healthcare professionals in the acute evaluation of suspected concussion. The SCAT is a validated tool to evaluate post-concussion symptoms in athletes and includes evaluation of response to different physical tasks that inform clinical concussion diagnosis. The physical assessments performed within the SCAT include double leg stance, single-leg stance, tandem stance for balance and tandem gait/walking [2]. Athletes are assessed based on the total number of errors they make during observation of the physical tasks.

In the physical assessment stage, a healthcare professional manually counts the number of errors such as hands lifted off the iliac crest, step, stumble, fall, and lifting forefoot or heel, whilst using a stopwatch to time each task [2]. Accurately counting all errors during each test is challenging as they may occur simultaneously. This is problematic as an erroneous implementation of the test may lead to serious implications for athletes, such as failing to notice concussion in its early stages that could lead to returning to play before full recovery. That could lead to subsequent future health problems or secondary injury.

Wearable inertial measurement units (IMUs) are being used to facilitate the standardization of different physical assessments. IMUs provide objective rather than subjective assessment in addition to digital-based high resolution data not normally captured during routine clinical observation testing [3-5].

Within this study, we develop and evaluate an IMU-based algorithm, capable of counting task errors, which provides an objective assessment for SCAT. Additionally, pragmatic digital-based balance parameters (e.g. sway) are extracted which may better inform an athlete's performance before taking important return-to-play decisions [6]. The contribution of this feasibility study focuses on the investigation of an algorithm to (1) instrument SCAT physical assessment tests for objective error detection, comparing results against a manual rater, and (2) propose IMU-based parameters for a more informative concussion assessment.

II. Material and Methods

A. Participants

University-level rugby players were recruited during the academic sports season at Northumbria University. Assessment and instrumentation were carried out by a qualified physiotherapist and researcher, respectively. Ethical consent was granted by the Northumbria University Research Ethics Committee (REF: 16335/335). All players gave informed written informed consent before participating.

B. Equipment and IMU placement

Each participant wore 8 tri-axial accelerometer and tri-axial gyroscope-based IMUs (AX6, Axivity: 23x32.5x8.9 mm, 11g). IMUs recorded data at a sampling frequency of 100Hz (16-bit resolution) and at a range of ±8g. IMUs were located on the back (fifth lumbar vertebrae, L5, and seventh cervical vertebrae, C7), with the remaining 6 IMUs attached to the top of the right and left feet (RF, LF), midway on the right and left shank/legs (RL, LL) as well as right and left wrists (RW, LW).

C. SCAT: Experimental protocol, physical tasks

Assessments consisted of SCAT physical tasks, Figure 1:

(a) Double leg stance, standing balance: Participants stood (eyes closed) with their feet together with *hands-on the iliac crest*, without shoes on a flat surface for 20 seconds (s).

*Research supported by the Turkish Ministry of National Education and the Faculty of Engineering and Environment, Northumbria University.

Yunus Celik, Dylan Powell, Wai Lok Woo and Alan Godfrey are with the Computer and Information Sciences Department, Faculty of Engineering and Environment, Northumbria University, Newcastle-upon-Tyne, UK, NE1 8ST. (email: yunus.celik@northumbria.ac.uk, d.powell@northumbria.ac.uk, wailok.woo@northumbria.ac.uk and corresponding author alan.godfrey@northumbria.ac.uk phone: +0044-191-227-3642).

Samuel Stuart is with the Department of Sport, Exercise and Rehabilitation, Faculty of Health and Life Sciences, Northumbria University, Newcastle-upon-Tyne, UK. (email: sam.stuart@northumbria.ac.uk).

(b) Single leg stance, standing balance: Participants stood (eyes closed) on their non-dominant foot with dominant leg held with 30° hip flexion, 45° knee flexion for 20s. Dominant foot movements (e.g. steps) were assessed via IMUs.

(c) Tandem stance, standing balance: Participants stand heel-to-toe (i.e. non-dominant foot placed behind dominant). Participants were told to distribute their weight evenly across both feet and stand for 20s.

(d) Tandem gait: Participants stand heel-to-toe, as above. Toes of one foot touch the heel of the next at each step. Each participant performed a quick 3m tandem walk (eyes open) as accurately as possible, turning 180° and returning (total 6m).

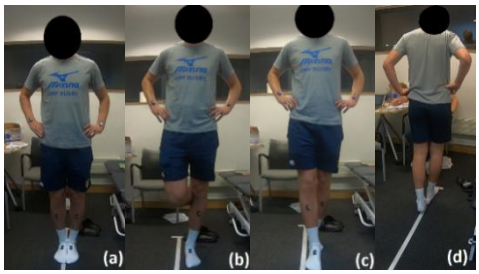

Figure 1. Test Illustrations (a) Double leg stance, (b) Single leg stance, (c) Tandem stance, (d) Tandem gait

D. iSCAT: Error detection

Error 1: Hands lifted off iliac crest. Participants stand or walk with their hands on their hips. Error detection is performed by applying a selected threshold rate and moving average filter to the sum of gyroscope signals belonging to RW and LW in Medio Lateral (ML), Antero Posterior (AP) and Vertical axes (VA). A notable change (increasing or decreasing more than 120°/s) was observed in both RW and LW and total error is calculated by counting the number of the absolute value of peaks (more than 120°/s) every 0.5s, Figure 2.

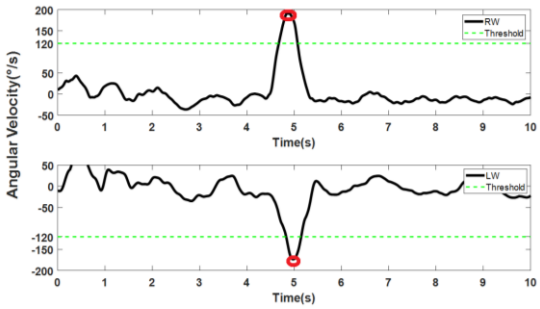

Figure 2. Detection of RW and LW hands lifted off iliac crest

Error 2: Step, stumble, or fall. Non-dominant foot and leg IMU signals must be stable during standing tasks with the dominant leg having moving tolerance in all three dimensions. Thus, steps and stumbles are detected via IMUs attached to the dominant foot and leg. The number of errors are calculated by counting dominant foot strikes on the ground.

Accordingly, accelerometer signals from RL in AP axis and RF in the VA axis represent the same directions because of the attachment locations, are added for a better detection where non-dominant foot is LF in the following example. Peak detection algorithm was used to detect two step-stumble errors (>4 m/s^2), Figure 3.

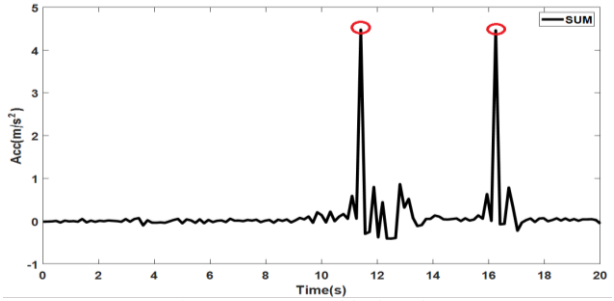

Figure 3. Step-stumble detection

Error 3: Moving hip into >30° abductions. In standing balance tasks (a) to (c), participants move their hips in ML and AP directions. Accelerometer and gyroscope data from L5 are used to estimate body tilt using the equation of complementary filter [7] given in the following:

$$angle(i) = 0.98*(angle(i-1) + gyro*dt) + 0.02(acc) \quad (1)$$

The initial angle was set to 90° for a clear understanding of arrow plotting, *dt* and *i* represent the derivation and sample number, whereas *gyro* and *acc* represent gyroscope and accelerometer data, respectively. Boundaries (green) were set to 60° and 120° to count the number of 30° abductions. The angles >120° and <60° are illustrated with black arrows using [20]. The participant here, experienced two abduction errors (10° and 2°) as illustrated with black arrows/lines, Figure 4.

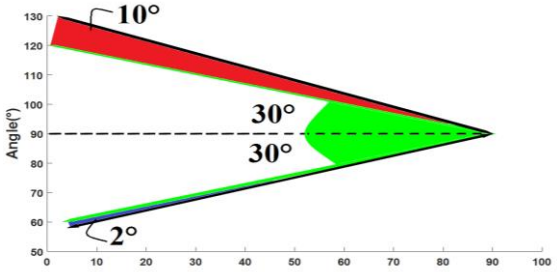

Figure 4. 30 ° abduction detection for a single participant

Error 4: Lift forefoot or heel. Detected using RF and LF accelerometer and gyroscope data in AP-ML axes. Angles between foot and ground calculated using a complementary filter. During the stable balance tasks, computed RF and LF angles must be <5°, determined by manual observation via video. In this example, the initial foot angle is set to 90° and angles >95° and <85° are extracted for arrow illustration, Figure 5, where 5 forefoot-heel lifting errors detected (black arrows/lines).

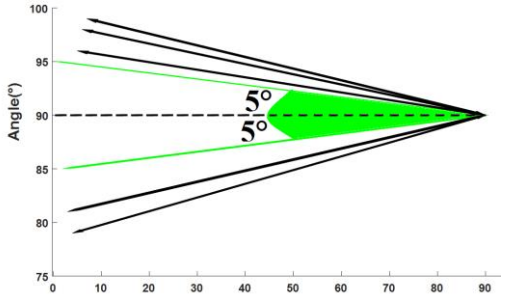

Figure 5. Lifted forefoot – heel detection

Error 5: Out of test position for >5s: Detected when there is no significant change considering determined threshold rates and angles in all IMUs for >5s.

E. IMU Algorithms and parameter extraction

Currently, raw IMU data are manually segmented for each task in MATLAB®. Pre-processing for parameter extraction was implemented by a 4th order Butterworth low-pass filter, 5Hz cut-off frequency. The following describes the aforementioned algorithms used to quantify the parameters.

Standing balance: Accelerometer derivation (Jerk), Root Mean Square (RMS) and other standing balance parameters are listed in Table I. Additionally, accelerometer sway path is calculated, where the signal is represented with the a_x, a_y and a_z in the corresponding axes, and D is the height of the sensor attached to L5 in the z-axis. Sway area is calculated according to the convex hull of the data points [8, 9].

Tandem gait: Symmetry assessed according to peak points and step times using RL and LL IMU data. Tandem steps detected by setting a threshold (100°/s) in the ML axis. Then, step time calculated by extracting time between each set of steps. RL and LL step peaks during tandem gait are shown with red and blue circles, respectively (Figure 6).

TABLE I. SUMMARY OF EXTRACTED MEASURES

Abbreviation	Domain	Description	
RMS (m/s^2)	Time	Root mean square of signal	$RMS = \sqrt{\frac{1}{n}(a^2_{M1} + \ldots . a^2_{Mn})}$
Jerk (m^2/s^5)	Time	First derivative of acceleration signal	$JERK = \frac{1}{2}\int_0^t \left(\frac{da_{PA}}{dt}\right)^2 + \left(\frac{da_{ML}}{dt}\right)^2$
Range (m/s^2)	Time	Maximum distance between any two points of data	
PWR (m^2/s^4)	Frequency	Total power of the spectrum of the acceleration	
CF (Hz)	Frequency	Centroid frequency	
MA (m/s^2)	Time	Mean acceleration	
SP (-)	Time	Sway path of accelerometer	$A = \sqrt{a_x^2 + a_y^2 + a_z^2}$ $\alpha = \cos^{-1}(\frac{a_x}{A})$ $\beta = \cos^{-1}(\frac{a_y}{A})$ $\gamma = \cos^{-1}(\frac{a_z}{A})$ $d_x = D * \cos\alpha$ $d_y = D * \cos\beta$
PL (m/s^2)	Time	Path length of accelerometer	
SA (mm^2/s^5)	Time	Sway area of accelerometer	

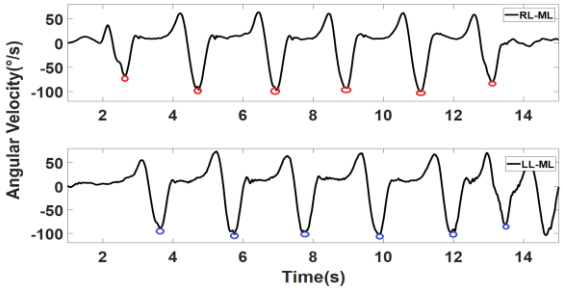

Figure 6. Step track of tandem gait in ML axis, RL and LL are presented with red and blue, respectively.

III. RESULTS

Four male rugby players (aged 19-22years) were recruited for SCAT assessment where physical tasks were conducted immediately after questions. The entire SCAT assessment took approximately 15 minutes/participant.

A. Manual recording compared to iSCAT

Table II shows good error agreements between manual recording and iSCAT for *hands lifted off iliac crest* and *step-stumble* errors. However, upon examining video recordings, discrepancies were attributed to manual errors for *hip abduction* and *lifting forefoot-heel* errors since they are difficult to detect from manual observation during testing. In manual recording and iSCAT, a single leg stance (b) was the most challenging task for participants while double leg stance (a) was the easiest, based on the number of errors.

TABLE II. NUMBER OF ERRORS

	Manual		iSCAT	
Participant Number	Task (a)-(b)-(c)	Total Errors	Task (a)-(b)-(c)	Total Errors
1	1-5-3	9	0-7-3	10
2	0-4-0	4	0-4-1	5
3	0-6-3	9	0-13-0	13
4	0-10-4	14	0-13-3	16

B. iSCAT plus: Standing balance parameters

To investigate preliminary iSCAT parameter to best inform balance, we analysed L5 and C7 data and extracted parameters in AP and ML directions for each task. Jerk, Range and total power of signal parameters indicate that task (b) was more unstable and challenging compared to tasks (a) and (c) for all participants while task (a) parameters were slightly more stable than (c). The mean parameter values of participants are presented with standard deviations for each task, Table III.

TABLE III. EXTRACTED STANDING BALANCE PARAMETERS

		TASK	AP	SD	ML	SD
TIME DOMAIN	RMS	a	0.928	0.105	0.071	0.051
		b	0.912	0.121	0.106	0.043
		c	0.909	0.126	0.091	0.044
	JERK	a	0.172	0.023	0.175	0.128
		b	1.619	1.613	1.168	1.080
		c	0.460	0.527	0.279	0.149
	MV	a	0.928	0.105	0.070	0.051
		b	0.910	0.121	0.089	0.042
		c	0.908	0.126	0.089	0.045
	RANGE	a	0.297	0.085	-	-
		b	1.160	0.660	-	-
		c	0.504	0.119	-	-
FREQ	PWR	a	2.411	0.790	-	-
		b	3.717	3.188	-	-
		c	2.128	0.903	-	-
	CF	a	0.885	0.117	-	-
		b	0.899	0.126	-	-
		c	0.906	0.129	-	-
		TASK	**AREA**	**SD**	-	-
SWAY	SWAY PATH LENGTH	a	2.434	0.571	-	-
		b	2.036	0.504	-	-
		c	1.992	0.477	-	-
	SWAY AREA	a	0.073	0.088	-	-
		b	0.897	0.581	-	-
		c	0.204	0.136	-	-

C. *iSCAT plus : Tandem gait*

Symmetry is evaluated considering step time and peak values. It was found that each participant performed a higher standard deviation of the peak, portraying asymmetry characteristics. Furthermore, the time taken to complete the tandem gait was extracted for each participant and could be used clinically as well as error rates.

TABLE IV. SYMMETRY PARAMETERS FOR TANDEM GAIT

Participant Number	Tandem Walking Time (s)	RL-LL	Step Time	Peaks (SD)
1	22.05	RL	1.65	35.94
		LL	1.73	11.44
2	17.77	RL	1.85	20.80
		LL	1.78	20.05
3	32.70	RL	2.43	17.93
		LL	2.45	7.76
4	23.69	RL	2.11	23.38
		LL	2.09	7.78

IV. DISCUSSION

iSCAT is capable of facilitating objective and better informed concussion assessment, providing useful information such as error count but also symmetry and time to complete a tandem gait test. This could improve diagnostic processes [6]. Preliminary results showed that manual observation aligned with preliminary iSCAT methods for most error scoring, e.g. hands lifted from iliac crest. Although there were some differences, this was during very subtle movements relating to the heel rise and knee flexion errors. These are more challenging for a single physiotherapist to spot during live testing and so iSCAT showcased its potential use as a complete monitoring tool to aid player assessment. Indeed, we may see greater iSCAT accuracy in future work where we plan to use multiple physiotherapists for manual observations. iSCAT parameters showed similarity to previous IMU work in concussion, health controls [10-12] and other groups [4, 13]. Yet, iSCAT encountered a few limitations such as not counting errors during very slow movements and so had difficultly discriminating when an error was made. For example, one player had his dominant foot very near the ground so any step error resulted in a movement that was small and not exceeding any iSCAT threshold.

Previously [14-16], IMUs were used to assess gait and balance, including those with neurological conditions [13, 17, 18]. Results here show similarity in terms of mean error and medium similarity for tandem gait waking time [19]. Our feasibility study supports the growing evidence that IMU data could be useful to improve current clinical assessments [11]. Time and frequency domain parameters were extracted during tasks. Jerk, Range, Power of signal were sensitive and informative for each. In the iSCAT, balance measures for each task validated the accuracy of the number of errors calculated by the algorithm. More errors were detected in less stable (i.e. more challenging) tasks, i.e. single leg stance with greater errors observed.

V. CONCLUSION

Physical assessment tasks of the SCAT were instrumented using eight IMUs and novel algorithms. The latter has been able to automatically calculate errors during the physical tasks and has good agreement with standard reference of clinical observation. The proposed methodology has good potential for practical utility in sports related assessments but future work will aim to automate and streamline IMU data streams while instrumenting additional SCAT features.

REFERENCES

[1] J. Rafferty *et al.*, "On average, a professional rugby union player is more likely than not to sustain a concussion after 25 matches," *British journal of sports medicine,* vol. 53, no. 15, pp. 969-973, 2019.

[2] R. J. Echemendia *et al.*, "The sport concussion assessment tool 5th edition (SCAT5): background and rationale," *Br J Sports Med,* vol. 51, no. 11, pp. 848-850, 2017.

[3] A. Godfrey *et al.*, "iCap: Instrumented assessment of physical capability," *Maturitas,* vol. 82, no. 1, pp. 116-122, 2015.

[4] M. Mancini *et al.*, "ISway: a sensitive, valid and reliable measure of postural control," *JNER,* vol. 9, no. 1, p. 59, 2012.

[5] A. Salarian, et al, "iTUG, a sensitive and reliable measure of mobility," *IEEE Transactions on Neural Systems and Rehabilitation Engineering,* vol. 18, no. 3, pp. 303-310, 2010.

[6] G. Fuller, et al, "The performance of the World Rugby Head Injury Assessment Screening Tool: a diagnostic accuracy study," *Sports Medicine-Open,* vol. 6, no. 1, p. 2, 2020.

[7] S. Colton and F. Mentor, "The balance filter," *Presentation, Massachusetts Institute of Technology,* 2007.

[8] C. Seimetz, et al, "A comparison between methods of measuring postrual stability: force plates versus accelerometers," *Biomedical sciences instrumentation,* vol. 48, p. 386, 2012.

[9] T. Wollseifen, "Different methods of calculating body sway area," *Pharmaceutical Programming,* vol. 4, no. 1-2, pp. 91-106, 2011.

[10] J.-H. Park, et al, "Quantifying effects of age on balance and gait with inertial sensors in community-dwelling healthy adults," *Experimental gerontology,* vol. 85, pp. 48-58, 2016.

[11] L. A. King *et al.*, "Sensor-based balance measures outperform modified balance error scoring system in identifying acute concussion," *A of biomed eng,* vol. 45, no. 9, pp. 2135-2145, 2017.

[12] A. Rouis, et al, "Validity of a low-cost wearable device for body sway parameter evaluation," *Computer methods in biomechanics and biomedical engineering,* vol. 17, no. sup1, pp. 182-183, 2014.

[13] T. Chen *et al.*, "Postural sway in patients with early Parkinson's disease performing cognitive tasks while standing," *Neurological research,* vol. 40, no. 6, pp. 491-498, 2018.

[14] S. Hacker, et al, "Gait Analysis with IMU," in *Proceedings of the International Joint Conference on Biomedical Engineering Systems and Technologies-Volume 1*, 2014: SCITEPRESS-Science and Technology Publications, Lda, pp. 127-133.

[15] R. E. Mayagoitia, J. C. Lötters, P. H. Veltink, and H. Hermens, "Standing balance evaluation using a triaxial accelerometer," *G&P,* vol. 16, no. 1, pp. 55-59, 2002.

[16] R. Moe-Nilssen and J. L. Helbostad, "Trunk accelerometry as a measure of balance control during quiet standing," *G&P,* vol. 16, no. 1, pp. 60-68, 2002.

[17] J. J. Craig, A. P. Bruetsch, S. G. Lynch, F. B. Horak, and J. M. Huisinga, "Instrumented balance and walking assessments in persons with multiple sclerosis show strong test-retest reliability," *Journal of neuroengineering and rehabilitation,* vol. 14, no. 1, p. 43, 2017.

[18] A. J. Solomon, et al, "Detection of postural sway abnormalities by wireless inertial sensors in minimally disabled patients with multiple sclerosis: a case–control study," *Journal of neuroengineering and rehabilitation,* vol. 12, no. 1, p. 74, 2015.

[19] G. W. Fuller, et al, "Sport concussion assessment tool—Third edition normative reference values for professional Rugby Union players," *J of science and medicine in sport,* vol. 21, no. 4, pp. 347-351, 2018.

[20] Johnson(2020).https://www.mathworks.com/matlabcentral/file exchange/278-arrow, MATLAB Central File Exchange. Retrieved January 15, 2020. (Accessed:15/01/2020)

Appendix 9. Developing and exploring a methodology for multi-modal indoor and outdoor gait assessment

This publication appears as a conference paper "*Developing and exploring a methodology for multi-modal indoor and outdoor gait assessment"*, was published 43rd Annual International Conference of the IEEE Engineering in Medicine & Biology Society (EMBC) in **2021.**

(URL: https://doi.org/10.1109/EMBC44109.2020.9175656).

2021 43rd Annual International Conference of the
IEEE Engineering in Medicine & Biology Society (EMBC)
Oct 31 - Nov 4, 2021. Virtual Conference

2021 43rd Annual International Conference of the IEEE Engineering in Medicine & Biology Society (EMBC) | 978-1-7281-1179-7/21/$31.00 ©2021 IEEE | DOI: 10.1109/EMBC46164.2021.9629502

Developing and exploring a methodology for multi-modal indoor and outdoor gait assessment

Yunus Celik, Dylan Powell, Wai Lok Woo, *Senior Member, IEEE*, Samuel Stuart and Alan Godfrey, *Senior Member, IEEE*

***Abstract*— Gait assessment is emerging as a prominent way to understand impaired mobility and underlying neurological deficits. Various technologies have been used to assess gait inside and outside of laboratory settings, but wearables are the preferred option due to their cost-effective and practical use in both. There are robust conceptual gait models developed to ease the interpretation of gait parameters during indoor and outdoor environments. However, these models examine uni-modal gait characteristics (e.g., spatio-temporal parameters) only. Previous studies reported that understanding the underlying reason for impaired gait requires multi-modal gait assessment. Therefore, this study aims to develop a multi-modal approach using a synchronized inertial and electromyography (EMG) signals. Firstly, initial contact (IC), final contact (FC) moments and corresponding time stamps were identified from inertial data, producing temporal outcomes e.g., step time. Secondly, IC/FC time stamps were used to segment EMG data and define onset and offset times of muscle activities within the gait cycle and its subphases. For investigation purposes, we observed notable differences in temporal characteristics as well as muscle onset/offset timings and amplitudes between indoor and outdoor walking of three stroke survivors. Our preliminary analysis suggests a multi-modal approach may be important to augment and improve current inertial conceptual gait models by providing additional quantitative EMG data.**

I. Introduction

Alterations in gait characteristics such as reduced step velocity, increased asymmetry in temporal parameters are common post-stroke, negatively impacting mobility and cause falls [1]. Following a stroke, 37% are able to walk independently, 12% can walk with assistance while 50% of patients have severe mobility impairment [2], such as asymmetrical gait. Therefore, regaining community-based ambulation has been identified as a major rehabilitation goal in clinics and rehabilitation centres. And gait assessment is commonly used to support rehabilitation programs by providing insight into postural stability, balance, and different aspects of impaired gait (e.g., muscle characteristics) [3].

Various technologies such as motion capture systems, instrumented treadmills, walkways, force platforms, EMG have been used as a gold/reference system to monitor different aspects of human movement in clinics. However, the use of more than one reference/gold standard gait system brings complexities (e.g., synchronization) when needing to collect diverse but complementary outcomes[4]. Thus, the number of studies investigating more than one physiological outcome remains limited. Consequently, failing to use multiple sensing modalities in gait studies is a limitation in the field, though studies have found clinically useful characteristics in EMG gait patterns for specific populations [5].

Contemporary wearables overcome the limitations of reference/gold standard systems by enabling multiple sensing modalities. Wearables also provide a cost-effective assessment of multiple gait characteristics for use during controlled environments (e.g., clinic/lab) and uncontrolled outdoor environments (e.g., home, garden). Previous studies developed free-living (outdoor) conceptual gait models using wearables to better understand the complexities in neurological gait and underlying mechanisms [6, 7]. Those models detail gait domains (e.g. pace) with subcategories of spatial and temporal characteristics (e.g., step velocity/time) [8]. Wearables offering numerous sensing modalities within a single wearable enables new opportunities to be taken, augmenting existing spatial and temporal gait models with additional data for more informed gait assessment.

Within this developmental pilot study, we propose a methodology using IMU and EMG data within a single wearable. Here, we (i) develop the methodology in a small group of older stroke survivors and (ii) broadly examine use of the methodology to provide additional insight for indoor (laboratory) and outdoor (free-living) gait. Specifically, the harmonised approach can identify initial and final contacts (ICs/FCs), and subsequently, the onset/offset times and amplitudes of the muscle activities within the gait cycle sub-phases. The main aim of this study is to provide a multi-modal outdoor gait assessment tool using the latest technology which overcome unimodal approaches of previous studies. Additionally, this pilot study contributes to preliminary investigation of muscle activity in the lower limb of those with stroke, by evaluating the relationship between temporal characteristics (e.g., swing times) and muscle characteristics (e.g., on/off set timing, amplitude) in indoor and outdoor environments.

II. Methods and Measurements

A. Subjects and Design

This pilot study recruited three male stroke survivors (72.3 ± 3.1yrs, 78.5 ± 12.1kg, 176 ± 8.2cm). Assessment and

Yunus Celik is supported by the Turkish Ministry of National Education and Faculty of Engineering and Environment, Northumbria University. Work was supported by the Private Physiotherapy Education Fund (RPJ03732). Dr Sam Stuart is supported by a Parkinson's Foundation post-doctoral fellowship and clinical research award (PF-FBS-1898, PF-CRA-2073).

Yunus Celik, Dylan Powell, Wai Lok Woo and Alan Godfrey are with the Computer and Information Sciences Department, Faculty of Engineering and Environment, Northumbria University, Newcastle-upon-Tyne, UK, NE1 8ST. (email: yunus.celik@northumbria.ac.uk, d.powell@northumbria.ac.uk, wailok.woo@northumbria.ac.uk and corresponding author alan.godfrey@northumbria.ac.uk phone: +0044-191-227-3642).

Samuel Stuart is with the Department of Sport, Exercise and Rehabilitation, Faculty of Health and Life Sciences, Northumbria University, Newcastle-upon-Tyne, UK. (email: sam.stuart@northumbria.ac.uk).

instrumentation were carried out by a physiotherapist and researcher, respectively. Ethical consent was granted by the Northumbria University Research Ethics Committee (REF: 21603). All participants gave informed written consent before participating in this study.

B. Data collection and physical task procedures

Each participant wore a single Shimmer3 EMG wearable (24.276 cm^3, 23.6g) with a strap on the shank level of the less affected side (left for all). Skin preparation was performed with alcohol swabs to achieve better skin-electrode contact. Disposable surface electrodes (circular - Ag/AgCI, silver/silver chloride) were placed bilaterally (inter-electrode spacing ≈ 30mm) on clean skin according to SENIAM recommendations and locations: tibialis anterior (TA) and gastrocnemius (GS), with a reference electrode around the ankle (fibula) [9].

The Shimmer3 wearable allows multi-modal capture of IMU and EMG data simultaneously. Signals were recorded at a sampling frequency of 512Hz, and the IMU was configured (16-bit resolution, ±8g, ±500°/s) prior to data collection. Here, participants were asked to perform (i) 2-minutes walking around a 20m circuit at their preferred self-selected speed inside the laboratory (ii) 20-minute scripted outdoor walking (free-living) with the same wearables. The free-living route consisted of a pre-defined route indoor and outdoor route, walking on different surfaces (e.g., laminate, asphalt). Data recorded during indoor and outdoor walking were analysed.

III. DATA PROCESSING AND ANALYSIS

IMU and EMG data were transferred to a workstation (Windows 10) from the Shimmer3 via proprietary software (Consensys). Custom programs (MATLAB®, R2018b; Mathworks, Natick, USA) analysed raw (sample level) IMU and EMG data.

A. IC and FC detection: Temporal gait

A previously validated method [10] was used, whereby shank sagittal plane angular velocity was used to identify IC (i.e. heel strike) and FC (i.e. toe-off) and corresponding time stamps. In brief, wavelet decomposition (5th order *coiflet* with ten scales) was used to split the signal into low (approximation) and high frequency (details) components.

Subsequently, drift and high-frequency movement artefacts were removed with an initial approximation. Then, two new approximations were obtained to enhance IC and FC events. For each approximation, the time corresponding to the global maximum (t_{ms}, mid-swing) of the signals were detected. Finally, IC/FC events were searched (local minima) in predetermined intervals [IC (t_{ms}+0.25s, t_{ms}+2s), FC (t_{ms}-2s, t_{ms}-0.05s)]. Temporal gait parameters were estimated according to identified IC/FC events in the following equations where i is the number of the gait cycle (or stride).

$$\text{Stride time} = \text{IC}(i+1) - \text{IC}(i) \quad (1)$$

$$\text{Stance time} = \text{FC}(i) - \text{IC}(i) \quad (2)$$

$$\text{Swing time} = \text{IC}(i+1) - \text{FC}(i) \quad (3)$$

B. Electromyography processing: Segmentation

Extracted IC and FC time stamps information were used to identify the sub-phases of the gait cycle (stance and swing phases). As Shimmer3 EMG provides synchronised IMU and EMG data, muscle activation characteristics were segmented for stance and swing phases using timestamp information. Once EMG data is segmented, appropriate filtering must be performed to ensure signals are physiological related and not corrupted by noise. Thus, all EMG data were bandpass filtered (zero-lag 4th-order Butterworth filter) with cut off frequencies of 20 Hz and 250 Hz, followed by full-wave rectification, and low-pass filtering (10 Hz, zero-lag 4th-order Butterworth) to achieve a smoother signal to identify muscle onset/offset. All EMG values for each subject underwent time normalisation (gait cycle %) and amplitude normalisation to the highest EMG value (Root Mean Square, RMS).

C. EMG time domain features

(i). Muscle activity/inactivity timing

Detection of muscle onset/offset and overall level of activity in a muscle at any time is relatively identifiable from the linear envelope of raw EMG signals. There are various methods to extract the linear envelope of EMG signal such RMS, mean of moving window, and use of a set of filters along with rectification [4]. Once the linear envelope is extracted, muscle onset/offset can be detected via a predetermined threshold, manual observation, or clustering algorithms [11]. The latter finds resemblances between data points and groups these according to their similarities.

Here, the filters introduced in Section III.B and full-wave rectification were used to extract the linear envelope of the EMG signal, while k-means clustering was used to search muscle bursts (onset). The reason for using k-means is that it does not require *a priori* setting of thresholds and has shown the ability to differentiate bursts (onset), even when bursts are short or have spike-like characters [12]. Similar to [13], each data point in the EMG linear envelopes are clustered into subsets of data using k-means. Then, EMG signals are dichotomized into periods of onset/offset according to the amplitude of each data point. Here, the numbers of centroids (clusters), which influence sensitivity was set to five after visual inspection for all EMG signals analysed [14]. Muscle offset is identified for the lowest two clusters whereas the remaining three clusters are accepted as muscle onset.

(ii). Muscle activity amplitude analysis

Root mean square (RMS) of an EMG signal represents the average power of muscle activation for a given period. RMS is used to extract the linear envelope and analyse variations in the amount of information between the abduction and adduction movements [15]. A linear relationship between the contraction force and the RMS value of the EMG signal was reported in previous studies [16]. Thus, normalized RMS values can be a useful parameter in terms of understanding physiological activity during contraction of lower limb muscles in gait assessment.

$$RMS = \sqrt{\frac{1}{N}\sum_{k=1}^{N} x_k^2} \quad (4)$$

where N is the number of samples and x_k is the k-sample.

IV. RESULTS

A. Temporal characteristics

Temporal characteristics extracted in the laboratory and scripted outdoor are presented in Table 1. Participant 1 and 3 experienced a decrease in temporal parameters (stride, stance,

and swing time) during scripted outdoor compared to laboratory. Contrarily, Participant 2 experienced increased temporal parameters in outdoor compared to laboratory. Also, overall standard deviation in temporal parameters found higher during indoor walking compared to outdoor walking.

TABLE 1. INDOOR AND OUTDOOR TEMPORAL CHARACTERISTICS

	Subjects	Total Strides	Stride T. Mean (SD)	Stance T. Mean (SD)	Swing T. Mean (SD)
Indoor	1	60	1.33 (0.22)	0.84 (0.22)	0.49 (0.06)
	2	76	1.25 (0.09)	0.82 (0.1)	0.42 (0.08)
	3	110	1.09 (0.04)	0.63 (0.04)	0.45 (0.05)
Outdoor	1	245	1.11 (0.05)	0.67 (0.07)	0.43 (0.04)
	2	246	1.34 (0.06)	0.87 (0.07)	0.46 (0.06)
	3	247	1.03 (0.04)	0.60 (0.05)	0.43 (0.05)

T.= Time (seconds)

B. EMG on/off set timing

From IC/FC events, corresponding muscle activities of TA and GS are extracted during gait cycle sub-phases. Muscle onset is shaded using raw EMG signals in Fig. 1(a). Onset and offset detection are performed by using k-means clustering algorithm after the linear envelope is extracted, Fig. 1(b).

Muscle activity timing is extracted as percentage (%) of gait cycle (stride), stance and swing timings. Average of extracted time parameters are illustrated in Fig. 2 (a). Average muscle on time durations is longer during lab for all subjects and both muscle groups compared to outdoor. TA muscle on-time duration was found higher than GS across gait cycles for all stroke survivors. GS muscle was found more active during the stance phase, whereas TA muscle was more active during the swing phase. Also, the difference between the indoor and outdoor overall on-time duration of TA is minor, whereas the differences are noticeable for GS muscle.

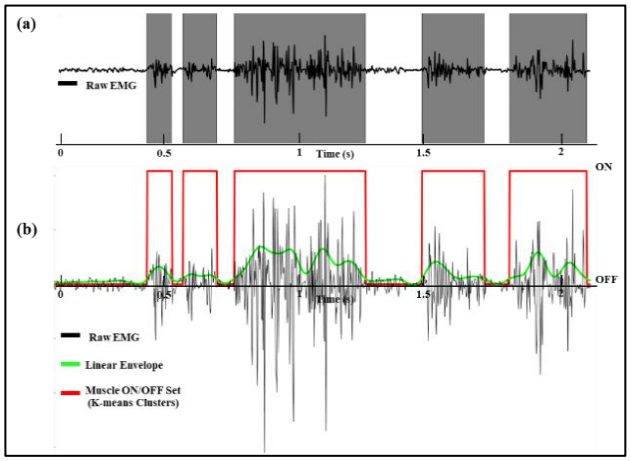

Fig 1. (a) On periods of raw EMG signal (shaded), (b) Detection of the on/off periods of muscle activity

C. EMG-RMS parameters

Intensity of muscle activities are normalized to peak RMS value in corresponding gait cycle and average RMS values are presented in Figure 2 (b). Amplitude (RMS) of GS is higher than TA in stance phase in both indoor and outdoor as expected [17]. All participant experienced increased RMS values in outdoor compared to lab assessment. Also, the RMS values of TA were found higher in swing phase compared to the stance phase.

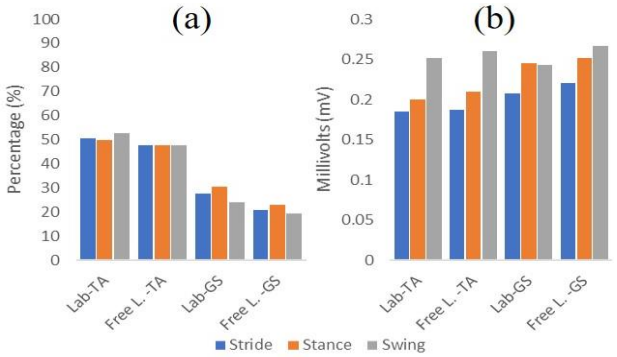

Fig 2. (a) Average-Stride-Stance-Swing (%) of muscle activity timing for TA and GS. (b) Average-Stride-Stance-Swing (mV) of peak muscle activity amplitude (RMS) for TA and GS

V. DISCUSSION

A multi-modal methodology is presented (Fig. 3) where raw IMU data helps identify the gait cycle and its sub phases by means of detecting IC/FC events which further segments synchronised EMG data. Our preliminary investigation (pilot study) shows that there are variances in the stride, stance, and swing times along with muscle characteristics in terms of temporal organisation of muscle onset/offset between indoor and outdoor. These differences may account for specific impairments and compensations in the lower limbs that contribute to poor gait quality [5].

Underlying reasons for differences in temporal parameters include, environmental factors (e.g., walking terrain) on the generated IMU signals [18] and instability of the developed algorithm are possible dominant factors [19]. This could also be due to the fact that stroke survivors may change the way they walk (e.g., increased speed) while under observation in controlled lab environment [20].

Muscle onset timings found shorter but more powerful for both muscle groups in all participants during outdoor compared to indoor. Changes in the temporal parameters, walking velocity and age may be associated with the variations in muscle activities during indoor walking [21]. However, the number of studies that investigate muscle activation level during outdoor is very limited [4] and so more research is needed to provide further insights.

The developed methodology can contribute to the field by investigating how muscle characteristics change during outdoor walking. Investigation of muscle characteristics in gait sub-phases may help clinicians to better understand an individual's muscle characteristics such as muscle onset-offset timing and RMS during outdoor walking. Conceptual gait models have been developed for ease of interpretation of gait assessment due to the redundancy of parameters and covariance amongst characteristics. The proposed models are developed based on spatiotemporal outcomes and do not include kinematic, kinetic or muscle activation characteristics, which could prove beneficial[4]. Previous limitations are complexity of design/instrumentation that is used to collect synchronized multiple gait characteristics in the indoor and outdoor. Therefore, the proposed multimodal approach here may contribute to the advancement of existing gait models by the integration of muscle characteristics.

This study has certain limitations, primarily the population size. However, this study is designed as a pilot aiming not only to provide a less complex design with a single wearable compared to previous studies but also to provide highly useful

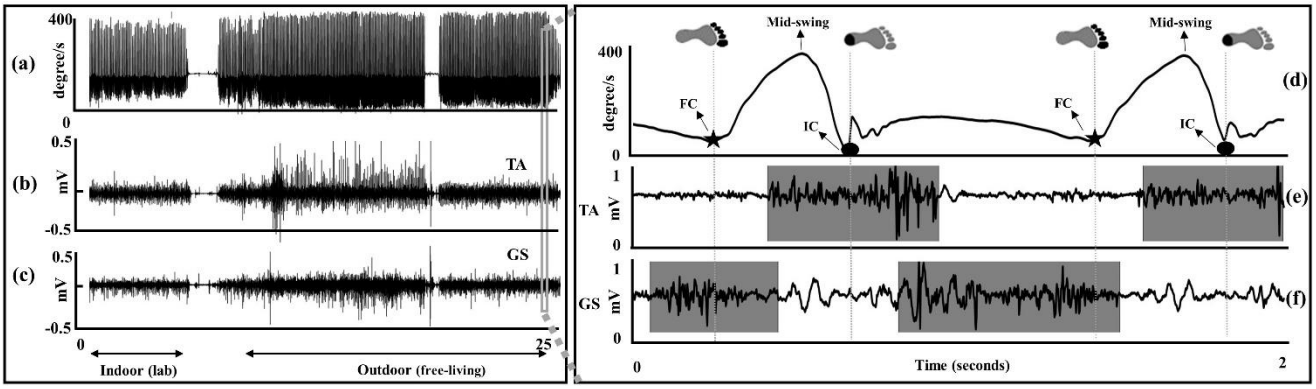

Fig. 3. Developed methodology; (a) IMU data (angular velocity), (b) Calibrated raw TA-EMG signals, (c) Calibrated raw GS-EMG signals, (d) angular velocity signal with identified initial contact (dot) and final contact (star) in the zoomed time interval, (e, f) Segmented EMG signals and onset/offset of TA and GS in the zoomed time interval, respectively

quantitative multiple gait characteristics in indoor and outdoor environments. Future studies will aim to increase the population size and implement the methodology on various cohorts (e.g., Parkinson's Disease).

VI. Conclusion

The methodology had promising potential for practical utility in multi-modal indoor and outdoor gait assessment. Integration of muscle characteristics into existing gait models can be more comprehensive and informative as muscle activity of the lower extremities during gait need to be well-coordinated to provide dynamic balance, propulsion, and foot clearance. Investigation of the validity on various cohorts with larger population size can contribute to field.

References

[1] S. A. Moore, A. Hickey, S. Lord, S. Del Din, A. Godfrey, and L. Rochester, "Comprehensive measurement of stroke gait characteristics with a single accelerometer in the laboratory and community: a feasibility, validity and reliability study," *Journal of neuroengineering and rehabilitation,* vol. 14, no. 1, p. 130, 2017.

[2] B. Balaban and F. Tok, "Gait disturbances in patients with stroke," *PM&R,* vol. 6, no. 7, pp. 635-642, 2014.

[3] A. Godfrey, R. Conway, D. Meagher, and G. ÓLaighin, "Direct measurement of human movement by accelerometry," *Medical engineering & physics,* vol. 30, no. 10, pp. 1364-1386, 2008.

[4] Y. Celik, S. Stuart, W. L. Woo, and A. Godfrey, "Gait analysis in neurological populations: Progression in the use of wearables," *Medical Engineering & Physics,* 2020.

[5] G. M. Rozanski, A. H. Huntley, L. D. Crosby, A. Schinkel-Ivy, A. Mansfield, and K. K. Patterson, "Lower limb muscle activity underlying temporal gait asymmetry post-stroke," *medRxiv,* p. 19010421, 2019.

[6] S. Del Din *et al.*, "Analysis of free-living gait in older adults with and without Parkinson's disease and with and without a history of falls: identifying generic and disease-specific characteristics," *The Journals of Gerontology: Series A,* vol. 74, no. 4, pp. 500-506, 2019.

[7] S. Lord, B. Galna, and L. Rochester, "Moving forward on gait measurement: toward a more refined approach," *Movement Disorders,* vol. 28, no. 11, pp. 1534-1543, 2013.

[8] R. Morris, A. Hickey, S. Del Din, A. Godfrey, S. Lord, and L. Rochester, "A model of free-living gait: A factor analysis in Parkinson's disease," *Gait & posture,* vol. 52, pp. 68-71, 2017.

[9] H. J. Hermens, B. Freriks, C. Disselhorst-Klug, and G. Rau, "Development of recommendations for SEMG sensors and sensor placement procedures," *Journal of electromyography and Kinesiology,* vol. 10, no. 5, pp. 361-374, 2000.

[10] K. Aminian, B. Najafi, C. Büla, P.-F. Leyvraz, and P. Robert, "Spatio-temporal parameters of gait measured by an ambulatory system using miniature gyroscopes," *Journal of biomechanics,* vol. 35, no. 5, pp. 689-699, 2002.

[11] G. Staude, C. Flachenecker, M. Daumer, and W. Wolf, "Onset detection in surface electromyographic signals: a systematic comparison of methods," *EURASIP Journal on Advances in Signal Processing,* vol. 2001, no. 2, p. 867853, 2001.

[12] S. Srivastava, C. Patten, and S. A. Kautz, "Altered muscle activation patterns (AMAP): an analytical tool to compare muscle activity patterns of hemiparetic gait with a normative profile," *Journal of neuroengineering and rehabilitation,* vol. 16, no. 1, p. 21, 2019.

[13] A. Den Otter, A. Geurts, T. Mulder, and J. Duysens, "Gait recovery is not associated with changes in the temporal patterning of muscle activity during treadmill walking in patients with post-stroke hemiparesis," *Clinical Neurophysiology,* vol. 117, no. 1, pp. 4-15, 2006.

[14] A. Den Otter, A. Geurts, T. Mulder, and J. Duysens, "Abnormalities in the temporal patterning of lower extremity muscle activity in hemiparetic gait," *Gait & posture,* vol. 25, no. 3, pp. 342-352, 2007.

[15] F. D. Farfán, J. C. Politti, and C. J. Felice, "Evaluation of EMG processing techniques using information theory," *Biomedical engineering online,* vol. 9, no. 1, p. 72, 2010.

[16] T. Y. Fukuda *et al.*, "Root mean square value of the electromyographic signal in the isometric torque of the quadriceps, hamstrings and brachial biceps muscles in female subjects," *J Appl Res,* vol. 10, no. 1, pp. 32-39, 2010.

[17] C. Cruz-Montecinos, S. Pérez-Alenda, F. Querol, M. Cerda, and H. Maas, "Changes in muscle activity patterns and joint kinematics during gait in hemophilic arthropathy," *Frontiers in physiology,* vol. 10, p. 1575, 2020.

[18] F. A. Storm, C. J. Buckley, and C. Mazzà, "Gait event detection in laboratory and real life settings: Accuracy of ankle and waist sensor based methods," *Gait & posture,* vol. 50, pp. 42-46, 2016.

[19] G. P. Panebianco, M. C. Bisi, R. Stagni, and S. Fantozzi, "Analysis of the performance of 17 algorithms from a systematic review: Influence of sensor position, analysed variable and computational approach in gait timing estimation from IMU measurements," *Gait & posture,* vol. 66, pp. 76-82, 2018.

[20] S. Del Din, A. Godfrey, B. Galna, S. Lord, and L. Rochester, "Free-living gait characteristics in ageing and Parkinson's disease: impact of environment and ambulatory bout length," *Journal of neuroengineering and rehabilitation,* vol. 13, no. 1, pp. 1-12, 2016.

[21] A. Schmitz, A. Silder, B. Heiderscheit, J. Mahoney, and D. G. Thelen, "Differences in lower-extremity muscular activation during walking between healthy older and young adults," *Journal of electromyography and kinesiology,* vol. 19, no. 6, pp. 1085-1091, 2009.

Appendix 10. Creative Commons 4.0 license

Creative Commons Legal Code

Attribution 4.0 International

Official translations of this license are available in other languages.
Creative Commons Corporation (“Creative Commons”) is not a law firm and does not provide legal services or legal advice. Distribution of Creative Commons public licenses does not create a lawyer-client or other relationship. Creative Commons makes its licenses and related information available on an “as-is” basis. Creative Commons gives no warranties regarding its licenses, any material licensed under their terms and conditions, or any related information. Creative Commons disclaims all liability for damages resulting from their use to the fullest extent possible.

Using Creative Commons Public Licenses

Creative Commons public licenses provide a standard set of terms and conditions that creators and other rights holders may use to share original works of authorship and other material subject to copyright and certain other rights specified in the public license below. The following considerations are for informational purposes only, are not exhaustive, and do not form part of our licenses.

Considerations for licensors: Our public licenses are intended for use by those authorized to give the public permission to use material in ways otherwise restricted by copyright and certain other rights. Our licenses are irrevocable. Licensors should read and understand the terms and conditions of the license they choose before applying it. Licensors should also secure all rights necessary before applying our licenses so that the public can reuse the material as expected. Licensors should clearly mark any material not subject to the license. This includes other CC-licensed material, or material used under an exception or limitation to copyright.

Considerations for the public: By using one of our public licenses, a licensor grants the public permission to use the licensed material under specified terms and conditions. If the licensor’s permission is not necessary for any reason–for example, because of any applicable exception or limitation to copyright–then that use is not regulated by the license. Our licenses grant only permissions under copyright and certain other rights that a licensor has authority to grant. Use of the licensed material may still be restricted for other reasons, including because others have copyright or other rights in the material. A licensor may make special requests, such as asking that all changes be marked or described. Although not required by our licenses, you are encouraged to respect those requests where reasonable.

Creative Commons Attribution 4.0 International Public License

By exercising the Licensed Rights (defined below), You accept and agree to be bound by the terms and conditions of this Creative Commons Attribution 4.0 International Public License ("Public License"). To the extent this Public License may be interpreted as a contract, You are granted the Licensed Rights in consideration of Your acceptance of these terms and conditions, and the Licensor grants You such rights in consideration of benefits the Licensor receives from making the Licensed Material available under these terms and conditions.

Section 1 – Definitions.

a. **Adapted Material** means material subject to Copyright and Similar Rights that is derived from or based upon the Licensed Material and in which the Licensed Material is translated, altered, arranged, transformed, or otherwise modified in a manner requiring permission under the Copyright and Similar Rights held by the Licensor. For purposes of this Public License, where the Licensed Material is a musical work, performance, or sound recording, Adapted Material is always produced where the Licensed Material is synched in timed relation with a moving image.
b. **Adapter's License** means the license You apply to Your Copyright and Similar Rights in Your contributions to Adapted Material in accordance with the terms and conditions of this Public License.
c. **Copyright and Similar Rights** means copyright and/or similar rights closely related to copyright including, without limitation, performance, broadcast, sound recording, and Sui Generis Database Rights, without regard to how the rights are labeled or categorized. For purposes of this Public License, the rights specified in Section 2(b)(1)-(2) are not Copyright and Similar Rights.
d. **Effective Technological Measures** means those measures that, in the absence of proper authority, may not be circumvented under laws fulfilling obligations under Article 11 of the WIPO Copyright Treaty adopted on December 20, 1996, and/or similar international agreements.
e. **Exceptions and Limitations** means fair use, fair dealing, and/or any other exception or limitation to Copyright and Similar Rights that applies to Your use of the Licensed Material.
f. **Licensed Material** means the artistic or literary work, database, or other material to which the Licensor applied this Public License.
g. **Licensed Rights** means the rights granted to You subject to the terms and conditions of this Public License, which are limited to all Copyright and Similar Rights that apply to Your use of the Licensed Material and that the Licensor has authority to license.
h. **Licensor** means the individual(s) or entity(ies) granting rights under this Public License.
i. **Share** means to provide material to the public by any means or process that requires permission under the Licensed Rights, such as reproduction, public display, public performance, distribution, dissemination, communication, or importation, and to make material available to the public including in ways that members of the public may access the material from a place and at a time individually chosen by them.
j. **Sui Generis Database Rights** means rights other than copyright resulting from Directive 96/9/EC of the European Parliament and of the Council of 11 March 1996 on the legal protection of databases, as amended and/or succeeded, as well as other essentially equivalent rights anywhere in the world.
k. **You** means the individual or entity exercising the Licensed Rights under this Public License. **Your** has a corresponding meaning.

Section 2 – Scope.

a. **License grant**.
   1. Subject to the terms and conditions of this Public License, the Licensor hereby grants You a worldwide, royalty-free, non-sublicensable, non-exclusive, irrevocable license to exercise the Licensed Rights in the Licensed Material to:
      A. reproduce and Share the Licensed Material, in whole or in part; and
      B. produce, reproduce, and Share Adapted Material.

2. Exceptions and Limitations. For the avoidance of doubt, where Exceptions and Limitations apply to Your use, this Public License does not apply, and You do not need to comply with its terms and conditions.
3. Term. The term of this Public License is specified in Section 6(a).
4. Media and formats; technical modifications allowed. The Licensor authorizes You to exercise the Licensed Rights in all media and formats whether now known or hereafter created, and to make technical modifications necessary to do so. The Licensor waives and/or agrees not to assert any right or authority to forbid You from making technical modifications necessary to exercise the Licensed Rights, including technical modifications necessary to circumvent Effective Technological Measures. For purposes of this Public License, simply making modifications authorized by this Section 2(a)(4) never produces Adapted Material.
5. Downstream recipients.
   A. Offer from the Licensor – Licensed Material. Every recipient of the Licensed Material automatically receives an offer from the Licensor to exercise the Licensed Rights under the terms and conditions of this Public License.
   B. No downstream restrictions. You may not offer or impose any additional or different terms or conditions on, or apply any Effective Technological Measures to, the Licensed Material if doing so restricts exercise of the Licensed Rights by any recipient of the Licensed Material.
6. No endorsement. Nothing in this Public License constitutes or may be construed as permission to assert or imply that You are, or that Your use of the Licensed Material is, connected with, or sponsored, endorsed, or granted official status by, the Licensor or others designated to receive attribution as provided in Section 3(a)(1)(A)(i).

b. **Other rights**.

1. Moral rights, such as the right of integrity, are not licensed under this Public License, nor are publicity, privacy, and/or other similar personality rights; however, to the extent possible, the Licensor waives and/or agrees not to assert any such rights held by the Licensor to the limited extent necessary to allow You to exercise the Licensed Rights, but not otherwise.
2. Patent and trademark rights are not licensed under this Public License.
3. To the extent possible, the Licensor waives any right to collect royalties from You for the exercise of the Licensed Rights, whether directly or through a collecting society under any voluntary or waivable statutory or compulsory licensing scheme. In all other cases the Licensor expressly reserves any right to collect such royalties.

Section 3 – License Conditions.

Your exercise of the Licensed Rights is expressly made subject to the following conditions.

a. **Attribution**.

1. If You Share the Licensed Material (including in modified form), You must:

   A. retain the following if it is supplied by the Licensor with the Licensed Material:
      i. identification of the creator(s) of the Licensed Material and any others designated to receive attribution, in any reasonable manner requested by the Licensor (including by pseudonym if designated);
      ii. a copyright notice;
      iii. a notice that refers to this Public License;
      iv. a notice that refers to the disclaimer of warranties;
      v. a URI or hyperlink to the Licensed Material to the extent reasonably practicable;
   B. indicate if You modified the Licensed Material and retain an indication of any previous modifications; and
   C. indicate the Licensed Material is licensed under this Public License, and include the text of, or the URI or hyperlink to, this Public License.
2. You may satisfy the conditions in Section 3(a)(1) in any reasonable manner based on the medium, means, and context in which You Share the Licensed Material. For example, it may be reasonable to satisfy the conditions by providing a URI or hyperlink to a resource that includes the required information.
3. If requested by the Licensor, You must remove any of the information required by Section 3(a)(1)(A) to the extent reasonably practicable.
4. If You Share Adapted Material You produce, the Adapter's License You apply must not prevent recipients of the Adapted Material from complying with this Public License.

Section 4 – Sui Generis Database Rights.

Where the Licensed Rights include Sui Generis Database Rights that apply to Your use of the Licensed Material:

a. for the avoidance of doubt, Section 2(a)(1) grants You the right to extract, reuse, reproduce, and Share all or a substantial portion of the contents of the database;
b. if You include all or a substantial portion of the database contents in a database in which You have Sui Generis Database Rights, then the database in which You have Sui Generis Database Rights (but not its individual contents) is Adapted Material; and
c. You must comply with the conditions in Section 3(a) if You Share all or a substantial portion of the contents of the database.

For the avoidance of doubt, this Section 4 supplements and does not replace Your obligations under this Public License where the Licensed Rights include other Copyright and Similar Rights.

Section 5 – Disclaimer of Warranties and Limitation of Liability.

a. Unless otherwise separately undertaken by the Licensor, to the extent possible, the Licensor offers the Licensed Material as-is and as-available, and makes no representations or warranties of any kind concerning the Licensed Material, whether express, implied, statutory, or other. This includes, without limitation, warranties of title, merchantability, fitness for a particular purpose, non-infringement, absence of latent or other defects, accuracy, or the presence or absence of errors, whether or not known or discoverable. Where disclaimers of warranties are not allowed in full or in part, this disclaimer may not apply to You.

b. To the extent possible, in no event will the Licensor be liable to You on any legal theory (including, without limitation, negligence) or otherwise for any direct, special, indirect, incidental, consequential, punitive, exemplary, or other losses, costs, expenses, or damages arising out of this Public License or use of the Licensed Material, even if the Licensor has been advised of the possibility of such losses, costs, expenses, or damages. Where a limitation of liability is not allowed in full or in part, this limitation may not apply to You.

c. The disclaimer of warranties and limitation of liability provided above shall be interpreted in a manner that, to the extent possible, most closely approximates an absolute disclaimer and waiver of all liability.

Section 6 – Term and Termination.

a. This Public License applies for the term of the Copyright and Similar Rights licensed here. However, if You fail to comply with this Public License, then Your rights under this Public License terminate automatically.
b. Where Your right to use the Licensed Material has terminated under Section 6(a), it reinstates:

   1. automatically as of the date the violation is cured, provided it is cured within 30 days of Your discovery of the violation; or
   2. upon express reinstatement by the Licensor.

   For the avoidance of doubt, this Section 6(b) does not affect any right the Licensor may have to seek remedies for Your violations of this Public License.
c. For the avoidance of doubt, the Licensor may also offer the Licensed Material under separate terms or conditions or stop distributing the Licensed Material at any time; however, doing so will not terminate this Public License.
d. Sections 1, 5, 6, 7, and 8 survive termination of this Public License.

Section 7 – Other Terms and Conditions.

a. The Licensor shall not be bound by any additional or different terms or conditions communicated by You unless expressly agreed.
b. Any arrangements, understandings, or agreements regarding the Licensed Material not stated herein are separate from and independent of the terms and conditions of this Public License.

Section 8 – Interpretation.

a. For the avoidance of doubt, this Public License does not, and shall not be interpreted to, reduce, limit, restrict, or impose conditions on any use of the Licensed Material that could lawfully be made without permission under this Public License.
b. To the extent possible, if any provision of this Public License is deemed unenforceable, it shall be automatically reformed to the minimum extent necessary to make it enforceable. If the provision cannot be reformed, it shall be severed from this Public License without affecting the enforceability of the remaining terms and conditions.
c. No term or condition of this Public License will be waived and no failure to comply consented to unless expressly agreed to by the Licensor.
d. Nothing in this Public License constitutes or may be interpreted as a limitation upon, or waiver of, any privileges and immunities that apply to the Licensor or You, including from the legal processes of any jurisdiction or authority.

Appendix 11. Statement of Authorisation for Encyclopedia of Sensors and Biosensors Chapter

ELSEVIER LICENSE
TERMS AND CONDITIONS

May 26, 2023

This Agreement between Mr. Yunus Celik ("You") and Elsevier ("Elsevier") consists of your license details and the terms and conditions provided by Elsevier and Copyright Clearance Center.

License Number	5556541043665
License date	May 26, 2023
Licensed Content Publisher	Elsevier
Licensed Content Publication	Elsevier Books
Licensed Content Title	Encyclopedia of Sensors and Biosensors
Licensed Content Author	Yunus Celik,Rodrigo Vitorio,Dylan Powell,Jason Moore,Fraser Young,Graham Coulby,James Tung,Mina Nouredanesh,Robert Ellis,Elena S. Izmailova,Sam Stuart,Alan Godfrey
Licensed Content Date	Jan 1, 2023
Licensed Content Pages	21
Start Page	263
End Page	283
Type of Use	reuse in a thesis/dissertation
I am an academic or government institution with a full-text subscription to this journal and the audience of the material consists of students and/or employees of this institute?	No

Portion	excerpt
Number of excerpts	8
Format	both print and electronic
Are you the author of this Elsevier chapter?	Yes
How many pages did you author in this Elsevier book?	20
Will you be translating?	No
Title	INSTRUMENTING GAIT IN NEUROLOGICAL DISORDERS: MULTI-MODAL APPROACH USING WEARABLES
Institution name	Northumbria University
Expected presentation date	Aug 2023
Portions	page 2-20
Requestor Location	Mr. Yunus Celik Brandon Grove 28, Newcastle Upon Tyne Newcastle upon tyne, Northumberland NE21PA United Kingdom Attn: Northumbria University
Publisher Tax ID	GB 494 6272 12
Total	0.00 USD
Terms and Conditions	

INTRODUCTION

1. The publisher for this copyrighted material is Elsevier. By clicking "accept" in connection with completing this licensing transaction, you agree that the following terms and conditions apply to this transaction (along with the Billing and Payment terms and conditions

established by Copyright Clearance Center, Inc. ("CCC"), at the time that you opened your Rightslink account and that are available at any time at http://myaccount.copyright.com).

GENERAL TERMS

2. Elsevier hereby grants you permission to reproduce the aforementioned material subject to the terms and conditions indicated.

3. Acknowledgement: If any part of the material to be used (for example, figures) has appeared in our publication with credit or acknowledgement to another source, permission must also be sought from that source. If such permission is not obtained then that material may not be included in your publication/copies. Suitable acknowledgement to the source must be made, either as a footnote or in a reference list at the end of your publication, as follows:

"Reprinted from Publication title, Vol /edition number, Author(s), Title of article / title of chapter, Pages No., Copyright (Year), with permission from Elsevier [OR APPLICABLE SOCIETY COPYRIGHT OWNER]." Also Lancet special credit - "Reprinted from The Lancet, Vol. number, Author(s), Title of article, Pages No., Copyright (Year), with permission from Elsevier."

4. Reproduction of this material is confined to the purpose and/or media for which permission is hereby given.

5. Altering/Modifying Material: Not Permitted. However figures and illustrations may be altered/adapted minimally to serve your work. Any other abbreviations, additions, deletions and/or any other alterations shall be made only with prior written authorization of Elsevier Ltd. (Please contact Elsevier's permissions helpdesk here). No modifications can be made to any Lancet figures/tables and they must be reproduced in full.

6. If the permission fee for the requested use of our material is waived in this instance, please be advised that your future requests for Elsevier materials may attract a fee.

7. Reservation of Rights: Publisher reserves all rights not specifically granted in the combination of (i) the license details provided by you and accepted in the course of this licensing transaction, (ii) these terms and conditions and (iii) CCC's Billing and Payment terms and conditions.

8. License Contingent Upon Payment: While you may exercise the rights licensed immediately upon issuance of the license at the end of the licensing process for the transaction, provided that you have disclosed complete and accurate details of your proposed use, no license is finally effective unless and until full payment is received from you (either by publisher or by CCC) as provided in CCC's Billing and Payment terms and conditions. If full payment is not received on a timely basis, then any license preliminarily granted shall be deemed automatically revoked and shall be void as if never granted. Further, in the event that you breach any of these terms and conditions or any of CCC's Billing and Payment terms and conditions, the license is automatically revoked and shall be void as if never granted. Use of materials as described in a revoked license, as well as any use of the materials beyond the scope of an unrevoked license, may constitute copyright infringement and publisher reserves the right to take any and all action to protect its copyright in the materials.

9. Warranties: Publisher makes no representations or warranties with respect to the licensed material.

10. Indemnity: You hereby indemnify and agree to hold harmless publisher and CCC, and their respective officers, directors, employees and agents, from and against any and all claims arising out of your use of the licensed material other than as specifically authorized pursuant to this license.

11. No Transfer of License: This license is personal to you and may not be sublicensed, assigned, or transferred by you to any other person without publisher's written permission.

12. No Amendment Except in Writing: This license may not be amended except in a writing signed by both parties (or, in the case of publisher, by CCC on publisher's behalf).

13. Objection to Contrary Terms: Publisher hereby objects to any terms contained in any purchase order, acknowledgment, check endorsement or other writing prepared by you, which terms are inconsistent with these terms and conditions or CCC's Billing and Payment terms and conditions. These terms and conditions, together with CCC's Billing and Payment terms and conditions (which are incorporated herein), comprise the entire agreement between you and publisher (and CCC) concerning this licensing transaction. In the event of any conflict between your obligations established by these terms and conditions and those established by CCC's Billing and Payment terms and conditions, these terms and conditions shall control.

14. Revocation: Elsevier or Copyright Clearance Center may deny the permissions described in this License at their sole discretion, for any reason or no reason, with a full refund payable to you. Notice of such denial will be made using the contact information provided by you. Failure to receive such notice will not alter or invalidate the denial. In no event will Elsevier or Copyright Clearance Center be responsible or liable for any costs, expenses or damage incurred by you as a result of a denial of your permission request, other than a refund of the amount(s) paid by you to Elsevier and/or Copyright Clearance Center for denied permissions.

LIMITED LICENSE

The following terms and conditions apply only to specific license types:

15. **Translation**: This permission is granted for non-exclusive world **English** rights only unless your license was granted for translation rights. If you licensed translation rights you may only translate this content into the languages you requested. A professional translator must perform all translations and reproduce the content word for word preserving the integrity of the article.

16. **Posting licensed content on any Website**: The following terms and conditions apply as follows: Licensing material from an Elsevier journal: All content posted to the web site must maintain the copyright information line on the bottom of each image; A hyper-text must be included to the Homepage of the journal from which you are licensing at http://www.sciencedirect.com/science/journal/xxxxx or the Elsevier homepage for books at http://www.elsevier.com; Central Storage: This license does not include permission for a scanned version of the material to be stored in a central repository such as that provided by Heron/XanEdu.

Licensing material from an Elsevier book: A hyper-text link must be included to the Elsevier homepage at http://www.elsevier.com . All content posted to the web site must maintain the copyright information line on the bottom of each image.

Posting licensed content on Electronic reserve: In addition to the above the following clauses are applicable: The web site must be password-protected and made available only to bona fide students registered on a relevant course. This permission is granted for 1 year only. You may obtain a new license for future website posting.

17. **For journal authors:** the following clauses are applicable in addition to the above:

Preprints:

A preprint is an author's own write-up of research results and analysis, it has not been peer-reviewed, nor has it had any other value added to it by a publisher (such as formatting, copyright, technical enhancement etc.).

Authors can share their preprints anywhere at any time. Preprints should not be added to or enhanced in any way in order to appear more like, or to substitute for, the final versions of articles however authors can update their preprints on arXiv or RePEc with their Accepted Author Manuscript (see below).

If accepted for publication, we encourage authors to link from the preprint to their formal publication via its DOI. Millions of researchers have access to the formal publications on ScienceDirect, and so links will help users to find, access, cite and use the best available version. Please note that Cell Press, The Lancet and some society-owned have different preprint policies. Information on these policies is available on the journal homepage.

Accepted Author Manuscripts: An accepted author manuscript is the manuscript of an article that has been accepted for publication and which typically includes author-incorporated changes suggested during submission, peer review and editor-author communications.

Authors can share their accepted author manuscript:

- immediately
    - via their non-commercial person homepage or blog
    - by updating a preprint in arXiv or RePEc with the accepted manuscript
    - via their research institute or institutional repository for internal institutional uses or as part of an invitation-only research collaboration work-group
    - directly by providing copies to their students or to research collaborators for their personal use
    - for private scholarly sharing as part of an invitation-only work group on commercial sites with which Elsevier has an agreement
- After the embargo period
    - via non-commercial hosting platforms such as their institutional repository
    - via commercial sites with which Elsevier has an agreement

In all cases accepted manuscripts should:

- link to the formal publication via its DOI
- bear a CC-BY-NC-ND license - this is easy to do
- if aggregated with other manuscripts, for example in a repository or other site, be shared in alignment with our hosting policy not be added to or enhanced in any way to appear more like, or to substitute for, the published journal article.

Published journal article (JPA): A published journal article (PJA) is the definitive final record of published research that appears or will appear in the journal and embodies all value-adding publishing activities including peer review co-ordination, copy-editing, formatting, (if relevant) pagination and online enrichment.

Policies for sharing publishing journal articles differ for subscription and gold open access articles:

Subscription Articles: If you are an author, please share a link to your article rather than the full-text. Millions of researchers have access to the formal publications on ScienceDirect, and so links will help your users to find, access, cite, and use the best available version.

Theses and dissertations which contain embedded PJAs as part of the formal submission can be posted publicly by the awarding institution with DOI links back to the formal publications on ScienceDirect.

If you are affiliated with a library that subscribes to ScienceDirect you have additional private sharing rights for others' research accessed under that agreement. This includes use for classroom teaching and internal training at the institution (including use in course packs and courseware programs), and inclusion of the article for grant funding purposes.

Gold Open Access Articles: May be shared according to the author-selected end-user license and should contain a CrossMark logo, the end user license, and a DOI link to the formal publication on ScienceDirect.

Please refer to Elsevier's posting policy for further information.

18. **For book authors** the following clauses are applicable in addition to the above: Authors are permitted to place a brief summary of their work online only. You are not allowed to download and post the published electronic version of your chapter, nor may you scan the printed edition to create an electronic version. **Posting to a repository:** Authors are permitted to post a summary of their chapter only in their institution's repository.

19. **Thesis/Dissertation**: If your license is for use in a thesis/dissertation your thesis may be submitted to your institution in either print or electronic form. Should your thesis be published commercially, please reapply for permission. These requirements include permission for the Library and Archives of Canada to supply single copies, on demand, of the complete thesis and include permission for Proquest/UMI to supply single copies, on demand, of the complete thesis. Should your thesis be published commercially, please reapply for permission. Theses and dissertations which contain embedded PJAs as part of the formal submission can be posted publicly by the awarding institution with DOI links back to the formal publications on ScienceDirect.

Elsevier Open Access Terms and Conditions

You can publish open access with Elsevier in hundreds of open access journals or in nearly 2000 established subscription journals that support open access publishing. Permitted third party re-use of these open access articles is defined by the author's choice of Creative Commons user license. See our open access license policy for more information.

Terms & Conditions applicable to all Open Access articles published with Elsevier:

Any reuse of the article must not represent the author as endorsing the adaptation of the article nor should the article be modified in such a way as to damage the author's honour or reputation. If any changes have been made, such changes must be clearly indicated.

The author(s) must be appropriately credited and we ask that you include the end user license and a DOI link to the formal publication on ScienceDirect.

If any part of the material to be used (for example, figures) has appeared in our publication with credit or acknowledgement to another source it is the responsibility of the user to ensure their reuse complies with the terms and conditions determined by the rights holder.

Additional Terms & Conditions applicable to each Creative Commons user license:

CC BY: The CC-BY license allows users to copy, to create extracts, abstracts and new works from the Article, to alter and revise the Article and to make commercial use of the Article (including reuse and/or resale of the Article by commercial entities), provided the user gives appropriate credit (with a link to the formal publication through the relevant DOI), provides a link to the license, indicates if changes were made and the licensor is not represented as endorsing the use made of the work. The full details of the license are available at http://creativecommons.org/licenses/by/4.0.

CC BY NC SA: The CC BY-NC-SA license allows users to copy, to create extracts, abstracts and new works from the Article, to alter and revise the Article, provided this is not done for commercial purposes, and that the user gives appropriate credit (with a link to the formal publication through the relevant DOI), provides a link to the license, indicates if changes were made and the licensor is not represented as endorsing the use made of the work. Further, any new works must be made available on the same conditions. The full details of the license are available at http://creativecommons.org/licenses/by-nc-sa/4.0.

CC BY NC ND: The CC BY-NC-ND license allows users to copy and distribute the Article, provided this is not done for commercial purposes and further does not permit distribution of the Article if it is changed or edited in any way, and provided the user gives appropriate credit (with a link to the formal publication through the relevant DOI), provides a link to the license, and that the licensor is not represented as endorsing the use made of the work. The full details of the license are available at http://creativecommons.org/licenses/by-nc-nd/4.0. Any commercial reuse of Open Access articles published with a CC BY NC SA or CC BY NC ND license requires permission from Elsevier and will be subject to a fee.

Commercial reuse includes:

- Associating advertising with the full text of the Article
- Charging fees for document delivery or access
- Article aggregation
- Systematic distribution via e-mail lists or share buttons

Posting or linking by commercial companies for use by customers of those companies.

20. **Other Conditions**:

v1.10

Questions? customercare@copyright.com.

ELSEVIER LICENSE
TERMS AND CONDITIONS

May 26, 2023

This Agreement between Mr. Yunus Celik ("You") and Elsevier ("Elsevier") consists of your license details and the terms and conditions provided by Elsevier and Copyright Clearance Center.

License Number	5556541290238
License date	May 26, 2023
Licensed Content Publisher	Elsevier
Licensed Content Publication	Elsevier Books
Licensed Content Title	Encyclopedia of Sensors and Biosensors
Licensed Content Author	Yunus Celik,Rodrigo Vitorio,Dylan Powell,Jason Moore,Fraser Young,Graham Coulby,James Tung,Mina Nouredanesh,Robert Ellis,Elena S. Izmailova,Sam Stuart,Alan Godfrey
Licensed Content Date	Jan 1, 2023
Licensed Content Pages	21
Start Page	263
End Page	283
Type of Use	reuse in a thesis/dissertation
Portion	figures/tables/illustrations
Number of figures/tables/illustrations	2

Format	both print and electronic
Are you the author of this Elsevier chapter?	Yes
How many pages did you author in this Elsevier book?	20
Will you be translating?	No
Title	INSTRUMENTING GAIT IN NEUROLOGICAL DISORDERS: MULTI-MODAL APPROACH USING WEARABLES
Institution name	Northumbria University
Expected presentation date	Aug 2023
Portions	Fig6 and Fig 7 in the chapter
Requestor Location	Mr. Yunus Celik Brandon Grove 28, Newcastle Upon Tyne Newcastle upon tyne, Northumberland NE21PA United Kingdom Attn: Northumbria University
Publisher Tax ID	GB 494 6272 12
Total	0.00 USD
Terms and Conditions	

INTRODUCTION

1. The publisher for this copyrighted material is Elsevier. By clicking "accept" in connection with completing this licensing transaction, you agree that the following terms and conditions apply to this transaction (along with the Billing and Payment terms and conditions established by Copyright Clearance Center, Inc. ("CCC"), at the time that you opened your Rightslink account and that are available at any time at http://myaccount.copyright.com).

GENERAL TERMS

2. Elsevier hereby grants you permission to reproduce the aforementioned material subject to the terms and conditions indicated.

3. Acknowledgement: If any part of the material to be used (for example, figures) has appeared in our publication with credit or acknowledgement to another source, permission must also be sought from that source. If such permission is not obtained then that material may not be included in your publication/copies. Suitable acknowledgement to the source must be made, either as a footnote or in a reference list at the end of your publication, as follows:

"Reprinted from Publication title, Vol /edition number, Author(s), Title of article / title of chapter, Pages No., Copyright (Year), with permission from Elsevier [OR APPLICABLE SOCIETY COPYRIGHT OWNER]." Also Lancet special credit - "Reprinted from The Lancet, Vol. number, Author(s), Title of article, Pages No., Copyright (Year), with permission from Elsevier."

4. Reproduction of this material is confined to the purpose and/or media for which permission is hereby given.

5. Altering/Modifying Material: Not Permitted. However figures and illustrations may be altered/adapted minimally to serve your work. Any other abbreviations, additions, deletions and/or any other alterations shall be made only with prior written authorization of Elsevier Ltd. (Please contact Elsevier's permissions helpdesk here). No modifications can be made to any Lancet figures/tables and they must be reproduced in full.

6. If the permission fee for the requested use of our material is waived in this instance, please be advised that your future requests for Elsevier materials may attract a fee.

7. Reservation of Rights: Publisher reserves all rights not specifically granted in the combination of (i) the license details provided by you and accepted in the course of this licensing transaction, (ii) these terms and conditions and (iii) CCC's Billing and Payment terms and conditions.

8. License Contingent Upon Payment: While you may exercise the rights licensed immediately upon issuance of the license at the end of the licensing process for the transaction, provided that you have disclosed complete and accurate details of your proposed use, no license is finally effective unless and until full payment is received from you (either by publisher or by CCC) as provided in CCC's Billing and Payment terms and conditions. If full payment is not received on a timely basis, then any license preliminarily granted shall be deemed automatically revoked and shall be void as if never granted. Further, in the event that you breach any of these terms and conditions or any of CCC's Billing and Payment terms and conditions, the license is automatically revoked and shall be void as if never granted. Use of materials as described in a revoked license, as well as any use of the materials beyond the scope of an unrevoked license, may constitute copyright infringement and publisher reserves the right to take any and all action to protect its copyright in the materials.

9. Warranties: Publisher makes no representations or warranties with respect to the licensed material.

10. Indemnity: You hereby indemnify and agree to hold harmless publisher and CCC, and their respective officers, directors, employees and agents, from and against any and all claims arising out of your use of the licensed material other than as specifically authorized pursuant to this license.

11. No Transfer of License: This license is personal to you and may not be sublicensed, assigned, or transferred by you to any other person without publisher's written permission.

12. No Amendment Except in Writing: This license may not be amended except in a writing signed by both parties (or, in the case of publisher, by CCC on publisher's behalf).

13. Objection to Contrary Terms: Publisher hereby objects to any terms contained in any purchase order, acknowledgment, check endorsement or other writing prepared by you, which terms are inconsistent with these terms and conditions or CCC's Billing and Payment terms and conditions. These terms and conditions, together with CCC's Billing and Payment terms and conditions (which are incorporated herein), comprise the entire agreement between you and publisher (and CCC) concerning this licensing transaction. In the event of any conflict between your obligations established by these terms and conditions and those established by CCC's Billing and Payment terms and conditions, these terms and conditions shall control.

14. Revocation: Elsevier or Copyright Clearance Center may deny the permissions described in this License at their sole discretion, for any reason or no reason, with a full refund payable to you. Notice of such denial will be made using the contact information provided by you. Failure to receive such notice will not alter or invalidate the denial. In no event will Elsevier or Copyright Clearance Center be responsible or liable for any costs, expenses or damage incurred by you as a result of a denial of your permission request, other than a refund of the amount(s) paid by you to Elsevier and/or Copyright Clearance Center for denied permissions.

LIMITED LICENSE

The following terms and conditions apply only to specific license types:

15. **Translation**: This permission is granted for non-exclusive world **English** rights only unless your license was granted for translation rights. If you licensed translation rights you may only translate this content into the languages you requested. A professional translator must perform all translations and reproduce the content word for word preserving the integrity of the article.

16. **Posting licensed content on any Website**: The following terms and conditions apply as follows: Licensing material from an Elsevier journal: All content posted to the web site must maintain the copyright information line on the bottom of each image; A hyper-text must be included to the Homepage of the journal from which you are licensing at http://www.sciencedirect.com/science/journal/xxxxx or the Elsevier homepage for books at http://www.elsevier.com; Central Storage: This license does not include permission for a scanned version of the material to be stored in a central repository such as that provided by Heron/XanEdu.

Licensing material from an Elsevier book: A hyper-text link must be included to the Elsevier homepage at http://www.elsevier.com . All content posted to the web site must maintain the copyright information line on the bottom of each image.

Posting licensed content on Electronic reserve: In addition to the above the following clauses are applicable: The web site must be password-protected and made available only to bona fide students registered on a relevant course. This permission is granted for 1 year only. You may obtain a new license for future website posting.

17. **For journal authors:** the following clauses are applicable in addition to the above:

Preprints:

A preprint is an author's own write-up of research results and analysis, it has not been peer-reviewed, nor has it had any other value added to it by a publisher (such as formatting, copyright, technical enhancement etc.).

Authors can share their preprints anywhere at any time. Preprints should not be added to or enhanced in any way in order to appear more like, or to substitute for, the final versions of articles however authors can update their preprints on arXiv or RePEc with their Accepted Author Manuscript (see below).

If accepted for publication, we encourage authors to link from the preprint to their formal publication via its DOI. Millions of researchers have access to the formal publications on ScienceDirect, and so links will help users to find, access, cite and use the best available version. Please note that Cell Press, The Lancet and some society-owned have different preprint policies. Information on these policies is available on the journal homepage.

Accepted Author Manuscripts: An accepted author manuscript is the manuscript of an article that has been accepted for publication and which typically includes author-incorporated changes suggested during submission, peer review and editor-author communications.

Authors can share their accepted author manuscript:

- immediately
    - via their non-commercial person homepage or blog
    - by updating a preprint in arXiv or RePEc with the accepted manuscript
    - via their research institute or institutional repository for internal institutional uses or as part of an invitation-only research collaboration work-group
    - directly by providing copies to their students or to research collaborators for their personal use
    - for private scholarly sharing as part of an invitation-only work group on commercial sites with which Elsevier has an agreement
- After the embargo period
    - via non-commercial hosting platforms such as their institutional repository
    - via commercial sites with which Elsevier has an agreement

In all cases accepted manuscripts should:

- link to the formal publication via its DOI
- bear a CC-BY-NC-ND license - this is easy to do
- if aggregated with other manuscripts, for example in a repository or other site, be shared in alignment with our hosting policy not be added to or enhanced in any way to appear more like, or to substitute for, the published journal article.

Published journal article (JPA): A published journal article (PJA) is the definitive final record of published research that appears or will appear in the journal and embodies all value-adding publishing activities including peer review co-ordination, copy-editing, formatting, (if relevant) pagination and online enrichment.

Policies for sharing publishing journal articles differ for subscription and gold open access articles:

Subscription Articles: If you are an author, please share a link to your article rather than the full-text. Millions of researchers have access to the formal publications on ScienceDirect, and so links will help your users to find, access, cite, and use the best available version.

Theses and dissertations which contain embedded PJAs as part of the formal submission can be posted publicly by the awarding institution with DOI links back to the formal publications on ScienceDirect.

If you are affiliated with a library that subscribes to ScienceDirect you have additional private sharing rights for others' research accessed under that agreement. This includes use for classroom teaching and internal training at the institution (including use in course packs and courseware programs), and inclusion of the article for grant funding purposes.

Gold Open Access Articles: May be shared according to the author-selected end-user license and should contain a CrossMark logo, the end user license, and a DOI link to the formal publication on ScienceDirect.

Please refer to Elsevier's posting policy for further information.

18. **For book authors** the following clauses are applicable in addition to the above: Authors are permitted to place a brief summary of their work online only. You are not allowed to download and post the published electronic version of your chapter, nor may you scan the printed edition to create an electronic version. **Posting to a repository:** Authors are permitted to post a summary of their chapter only in their institution's repository.

19. **Thesis/Dissertation**: If your license is for use in a thesis/dissertation your thesis may be submitted to your institution in either print or electronic form. Should your thesis be published commercially, please reapply for permission. These requirements include permission for the Library and Archives of Canada to supply single copies, on demand, of the complete thesis and include permission for Proquest/UMI to supply single copies, on demand, of the complete thesis. Should your thesis be published commercially, please reapply for permission. Theses and dissertations which contain embedded PJAs as part of the formal submission can be posted publicly by the awarding institution with DOI links back to the formal publications on ScienceDirect.

Elsevier Open Access Terms and Conditions

You can publish open access with Elsevier in hundreds of open access journals or in nearly 2000 established subscription journals that support open access publishing. Permitted third party re-use of these open access articles is defined by the author's choice of Creative Commons user license. See our open access license policy for more information.

Terms & Conditions applicable to all Open Access articles published with Elsevier:

Any reuse of the article must not represent the author as endorsing the adaptation of the article nor should the article be modified in such a way as to damage the author's honour or reputation. If any changes have been made, such changes must be clearly indicated.

The author(s) must be appropriately credited and we ask that you include the end user license and a DOI link to the formal publication on ScienceDirect.

If any part of the material to be used (for example, figures) has appeared in our publication with credit or acknowledgement to another source it is the responsibility of the user to ensure their reuse complies with the terms and conditions determined by the rights holder.

Additional Terms & Conditions applicable to each Creative Commons user license:

CC BY: The CC-BY license allows users to copy, to create extracts, abstracts and new works from the Article, to alter and revise the Article and to make commercial use of the Article (including reuse and/or resale of the Article by commercial entities), provided the user gives appropriate credit (with a link to the formal publication through the relevant DOI), provides a link to the license, indicates if changes were made and the licensor is not represented as endorsing the use made of the work. The full details of the license are available at http://creativecommons.org/licenses/by/4.0.

CC BY NC SA: The CC BY-NC-SA license allows users to copy, to create extracts, abstracts and new works from the Article, to alter and revise the Article, provided this is not done for commercial purposes, and that the user gives appropriate credit (with a link to the formal publication through the relevant DOI), provides a link to the license, indicates if changes were made and the licensor is not represented as endorsing the use made of the

work. Further, any new works must be made available on the same conditions. The full details of the license are available at http://creativecommons.org/licenses/by-nc-sa/4.0.

CC BY NC ND: The CC BY-NC-ND license allows users to copy and distribute the Article, provided this is not done for commercial purposes and further does not permit distribution of the Article if it is changed or edited in any way, and provided the user gives appropriate credit (with a link to the formal publication through the relevant DOI), provides a link to the license, and that the licensor is not represented as endorsing the use made of the work. The full details of the license are available at http://creativecommons.org/licenses/by-nc-nd/4.0. Any commercial reuse of Open Access articles published with a CC BY NC SA or CC BY NC ND license requires permission from Elsevier and will be subject to a fee.

Commercial reuse includes:

- Associating advertising with the full text of the Article
- Charging fees for document delivery or access
- Article aggregation
- Systematic distribution via e-mail lists or share buttons

Posting or linking by commercial companies for use by customers of those companies.

20. **Other Conditions**:

v1.10

Questions? customercare@copyright.com.

ELSEVIER LICENSE
TERMS AND CONDITIONS

May 26, 2023

This Agreement between Mr. Yunus Celik ("You") and Elsevier ("Elsevier") consists of your license details and the terms and conditions provided by Elsevier and Copyright Clearance Center.

License Number	5556550154630
License date	May 26, 2023
Licensed Content Publisher	Elsevier
Licensed Content Publication	Elsevier Books
Licensed Content Title	Encyclopedia of Sensors and Biosensors
Licensed Content Author	Yunus Celik,Rodrigo Vitorio,Dylan Powell,Jason Moore,Fraser Young,Graham Coulby,James Tung,Mina Nouredanesh,Robert Ellis,Elena S. Izmailova,Sam Stuart,Alan Godfrey
Licensed Content Date	Jan 1, 2023
Licensed Content Pages	21
Start Page	263
End Page	283
Type of Use	reuse in a thesis/dissertation
Portion	excerpt
Number of excerpts	6

Format	both print and electronic
Are you the author of this Elsevier chapter?	Yes
How many pages did you author in this Elsevier book?	20
Will you be translating?	No
Title	INSTRUMENTING GAIT IN NEUROLOGICAL DISORDERS: MULTI-MODAL APPROACH USING WEARABLES
Institution name	Northumbria University
Expected presentation date	Aug 2023
Portions	pages 2-20
Requestor Location	Mr. Yunus Celik Brandon Grove 28, Newcastle Upon Tyne Newcastle upon tyne, Northumberland NE21PA United Kingdom Attn: Northumbria University
Publisher Tax ID	GB 494 6272 12
Total	0.00 USD
Terms and Conditions	

INTRODUCTION

1. The publisher for this copyrighted material is Elsevier. By clicking "accept" in connection with completing this licensing transaction, you agree that the following terms and conditions apply to this transaction (along with the Billing and Payment terms and conditions established by Copyright Clearance Center, Inc. ("CCC"), at the time that you opened your Rightslink account and that are available at any time at http://myaccount.copyright.com).

GENERAL TERMS

2. Elsevier hereby grants you permission to reproduce the aforementioned material subject to the terms and conditions indicated.

3. Acknowledgement: If any part of the material to be used (for example, figures) has appeared in our publication with credit or acknowledgement to another source, permission must also be sought from that source. If such permission is not obtained then that material may not be included in your publication/copies. Suitable acknowledgement to the source must be made, either as a footnote or in a reference list at the end of your publication, as follows:

"Reprinted from Publication title, Vol /edition number, Author(s), Title of article / title of chapter, Pages No., Copyright (Year), with permission from Elsevier [OR APPLICABLE SOCIETY COPYRIGHT OWNER]." Also Lancet special credit - "Reprinted from The Lancet, Vol. number, Author(s), Title of article, Pages No., Copyright (Year), with permission from Elsevier."

4. Reproduction of this material is confined to the purpose and/or media for which permission is hereby given.

5. Altering/Modifying Material: Not Permitted. However figures and illustrations may be altered/adapted minimally to serve your work. Any other abbreviations, additions, deletions and/or any other alterations shall be made only with prior written authorization of Elsevier Ltd. (Please contact Elsevier's permissions helpdesk here). No modifications can be made to any Lancet figures/tables and they must be reproduced in full.

6. If the permission fee for the requested use of our material is waived in this instance, please be advised that your future requests for Elsevier materials may attract a fee.

7. Reservation of Rights: Publisher reserves all rights not specifically granted in the combination of (i) the license details provided by you and accepted in the course of this licensing transaction, (ii) these terms and conditions and (iii) CCC's Billing and Payment terms and conditions.

8. License Contingent Upon Payment: While you may exercise the rights licensed immediately upon issuance of the license at the end of the licensing process for the transaction, provided that you have disclosed complete and accurate details of your proposed use, no license is finally effective unless and until full payment is received from you (either by publisher or by CCC) as provided in CCC's Billing and Payment terms and conditions. If full payment is not received on a timely basis, then any license preliminarily granted shall be deemed automatically revoked and shall be void as if never granted. Further, in the event that you breach any of these terms and conditions or any of CCC's Billing and Payment terms and conditions, the license is automatically revoked and shall be void as if never granted. Use of materials as described in a revoked license, as well as any use of the materials beyond the scope of an unrevoked license, may constitute copyright infringement and publisher reserves the right to take any and all action to protect its copyright in the materials.

9. Warranties: Publisher makes no representations or warranties with respect to the licensed material.

10. Indemnity: You hereby indemnify and agree to hold harmless publisher and CCC, and their respective officers, directors, employees and agents, from and against any and all claims arising out of your use of the licensed material other than as specifically authorized pursuant to this license.

11. No Transfer of License: This license is personal to you and may not be sublicensed, assigned, or transferred by you to any other person without publisher's written permission.

12. No Amendment Except in Writing: This license may not be amended except in a writing signed by both parties (or, in the case of publisher, by CCC on publisher's behalf).

13. Objection to Contrary Terms: Publisher hereby objects to any terms contained in any purchase order, acknowledgment, check endorsement or other writing prepared by you, which terms are inconsistent with these terms and conditions or CCC's Billing and Payment terms and conditions. These terms and conditions, together with CCC's Billing and Payment terms and conditions (which are incorporated herein), comprise the entire agreement between you and publisher (and CCC) concerning this licensing transaction. In the event of any conflict between your obligations established by these terms and conditions and those established by CCC's Billing and Payment terms and conditions, these terms and conditions shall control.

14. Revocation: Elsevier or Copyright Clearance Center may deny the permissions described in this License at their sole discretion, for any reason or no reason, with a full refund payable to you. Notice of such denial will be made using the contact information provided by you. Failure to receive such notice will not alter or invalidate the denial. In no event will Elsevier or Copyright Clearance Center be responsible or liable for any costs, expenses or damage incurred by you as a result of a denial of your permission request, other than a refund of the amount(s) paid by you to Elsevier and/or Copyright Clearance Center for denied permissions.

LIMITED LICENSE

The following terms and conditions apply only to specific license types:

15. **Translation**: This permission is granted for non-exclusive world **English** rights only unless your license was granted for translation rights. If you licensed translation rights you may only translate this content into the languages you requested. A professional translator must perform all translations and reproduce the content word for word preserving the integrity of the article.

16. **Posting licensed content on any Website**: The following terms and conditions apply as follows: Licensing material from an Elsevier journal: All content posted to the web site must maintain the copyright information line on the bottom of each image; A hyper-text must be included to the Homepage of the journal from which you are licensing at http://www.sciencedirect.com/science/journal/xxxxx or the Elsevier homepage for books at http://www.elsevier.com; Central Storage: This license does not include permission for a scanned version of the material to be stored in a central repository such as that provided by Heron/XanEdu.

Licensing material from an Elsevier book: A hyper-text link must be included to the Elsevier homepage at http://www.elsevier.com . All content posted to the web site must maintain the copyright information line on the bottom of each image.

Posting licensed content on Electronic reserve: In addition to the above the following clauses are applicable: The web site must be password-protected and made available only to bona fide students registered on a relevant course. This permission is granted for 1 year only. You may obtain a new license for future website posting.

17. **For journal authors:** the following clauses are applicable in addition to the above:

Preprints:

A preprint is an author's own write-up of research results and analysis, it has not been peer-reviewed, nor has it had any other value added to it by a publisher (such as formatting, copyright, technical enhancement etc.).

Authors can share their preprints anywhere at any time. Preprints should not be added to or enhanced in any way in order to appear more like, or to substitute for, the final versions of articles however authors can update their preprints on arXiv or RePEc with their Accepted Author Manuscript (see below).

If accepted for publication, we encourage authors to link from the preprint to their formal publication via its DOI. Millions of researchers have access to the formal publications on ScienceDirect, and so links will help users to find, access, cite and use the best available version. Please note that Cell Press, The Lancet and some society-owned have different preprint policies. Information on these policies is available on the journal homepage.

Accepted Author Manuscripts: An accepted author manuscript is the manuscript of an article that has been accepted for publication and which typically includes author-incorporated changes suggested during submission, peer review and editor-author communications.

Authors can share their accepted author manuscript:

- immediately
    - via their non-commercial person homepage or blog
    - by updating a preprint in arXiv or RePEc with the accepted manuscript
    - via their research institute or institutional repository for internal institutional uses or as part of an invitation-only research collaboration work-group
    - directly by providing copies to their students or to research collaborators for their personal use
    - for private scholarly sharing as part of an invitation-only work group on commercial sites with which Elsevier has an agreement
- After the embargo period
    - via non-commercial hosting platforms such as their institutional repository
    - via commercial sites with which Elsevier has an agreement

In all cases accepted manuscripts should:

- link to the formal publication via its DOI
- bear a CC-BY-NC-ND license - this is easy to do
- if aggregated with other manuscripts, for example in a repository or other site, be shared in alignment with our hosting policy not be added to or enhanced in any way to appear more like, or to substitute for, the published journal article.

Published journal article (JPA): A published journal article (PJA) is the definitive final record of published research that appears or will appear in the journal and embodies all value-adding publishing activities including peer review co-ordination, copy-editing, formatting, (if relevant) pagination and online enrichment.

Policies for sharing publishing journal articles differ for subscription and gold open access articles:

Subscription Articles: If you are an author, please share a link to your article rather than the full-text. Millions of researchers have access to the formal publications on ScienceDirect, and so links will help your users to find, access, cite, and use the best available version.

Theses and dissertations which contain embedded PJAs as part of the formal submission can be posted publicly by the awarding institution with DOI links back to the formal publications on ScienceDirect.

If you are affiliated with a library that subscribes to ScienceDirect you have additional private sharing rights for others' research accessed under that agreement. This includes use for classroom teaching and internal training at the institution (including use in course packs and courseware programs), and inclusion of the article for grant funding purposes.

Gold Open Access Articles: May be shared according to the author-selected end-user license and should contain a CrossMark logo, the end user license, and a DOI link to the formal publication on ScienceDirect.

Please refer to Elsevier's posting policy for further information.

18. **For book authors** the following clauses are applicable in addition to the above: Authors are permitted to place a brief summary of their work online only. You are not allowed to download and post the published electronic version of your chapter, nor may you scan the printed edition to create an electronic version. **Posting to a repository:** Authors are permitted to post a summary of their chapter only in their institution's repository.

19. **Thesis/Dissertation**: If your license is for use in a thesis/dissertation your thesis may be submitted to your institution in either print or electronic form. Should your thesis be published commercially, please reapply for permission. These requirements include permission for the Library and Archives of Canada to supply single copies, on demand, of the complete thesis and include permission for Proquest/UMI to supply single copies, on demand, of the complete thesis. Should your thesis be published commercially, please reapply for permission. Theses and dissertations which contain embedded PJAs as part of the formal submission can be posted publicly by the awarding institution with DOI links back to the formal publications on ScienceDirect.

Elsevier Open Access Terms and Conditions

You can publish open access with Elsevier in hundreds of open access journals or in nearly 2000 established subscription journals that support open access publishing. Permitted third party re-use of these open access articles is defined by the author's choice of Creative Commons user license. See our open access license policy for more information.

Terms & Conditions applicable to all Open Access articles published with Elsevier:

Any reuse of the article must not represent the author as endorsing the adaptation of the article nor should the article be modified in such a way as to damage the author's honour or reputation. If any changes have been made, such changes must be clearly indicated.

The author(s) must be appropriately credited and we ask that you include the end user license and a DOI link to the formal publication on ScienceDirect.

If any part of the material to be used (for example, figures) has appeared in our publication with credit or acknowledgement to another source it is the responsibility of the user to ensure their reuse complies with the terms and conditions determined by the rights holder.

Additional Terms & Conditions applicable to each Creative Commons user license:

CC BY: The CC-BY license allows users to copy, to create extracts, abstracts and new works from the Article, to alter and revise the Article and to make commercial use of the Article (including reuse and/or resale of the Article by commercial entities), provided the user gives appropriate credit (with a link to the formal publication through the relevant DOI), provides a link to the license, indicates if changes were made and the licensor is not represented as endorsing the use made of the work. The full details of the license are available at http://creativecommons.org/licenses/by/4.0.

CC BY NC SA: The CC BY-NC-SA license allows users to copy, to create extracts, abstracts and new works from the Article, to alter and revise the Article, provided this is not done for commercial purposes, and that the user gives appropriate credit (with a link to the formal publication through the relevant DOI), provides a link to the license, indicates if changes were made and the licensor is not represented as endorsing the use made of the

work. Further, any new works must be made available on the same conditions. The full details of the license are available at http://creativecommons.org/licenses/by-nc-sa/4.0.

CC BY NC ND: The CC BY-NC-ND license allows users to copy and distribute the Article, provided this is not done for commercial purposes and further does not permit distribution of the Article if it is changed or edited in any way, and provided the user gives appropriate credit (with a link to the formal publication through the relevant DOI), provides a link to the license, and that the licensor is not represented as endorsing the use made of the work. The full details of the license are available at http://creativecommons.org/licenses/by-nc-nd/4.0. Any commercial reuse of Open Access articles published with a CC BY NC SA or CC BY NC ND license requires permission from Elsevier and will be subject to a fee.

Commercial reuse includes:

- Associating advertising with the full text of the Article
- Charging fees for document delivery or access
- Article aggregation
- Systematic distribution via e-mail lists or share buttons

Posting or linking by commercial companies for use by customers of those companies.

20. **Other Conditions**:

v1.10

Questions? customercare@copyright.com.

ELSEVIER LICENSE
TERMS AND CONDITIONS

May 26, 2023

This Agreement between Mr. Yunus Celik ("You") and Elsevier ("Elsevier") consists of your license details and the terms and conditions provided by Elsevier and Copyright Clearance Center.

License Number	5556550272693
License date	May 26, 2023
Licensed Content Publisher	Elsevier
Licensed Content Publication	Elsevier Books
Licensed Content Title	Encyclopedia of Sensors and Biosensors
Licensed Content Author	Yunus Celik,Rodrigo Vitorio,Dylan Powell,Jason Moore,Fraser Young,Graham Coulby,James Tung,Mina Nouredanesh,Robert Ellis,Elena S. Izmailova,Sam Stuart,Alan Godfrey
Licensed Content Date	Jan 1, 2023
Licensed Content Pages	21
Start Page	263
End Page	283
Type of Use	reuse in a thesis/dissertation
Portion	figures/tables/illustrations
Number of figures/tables/illustrations	2

Format	both print and electronic
Are you the author of this Elsevier chapter?	Yes
How many pages did you author in this Elsevier book?	20
Will you be translating?	No
Title	INSTRUMENTING GAIT IN NEUROLOGICAL DISORDERS: MULTI-MODAL APPROACH USING WEARABLES
Institution name	Northumbria University
Expected presentation date	Aug 2023
Portions	Figure 8 and Box 1 in the chapter
Requestor Location	Mr. Yunus Celik Brandon Grove 28, Newcastle Upon Tyne Newcastle upon tyne, Northumberland NE21PA United Kingdom Attn: Northumbria University
Publisher Tax ID	GB 494 6272 12
Total	0.00 USD
Terms and Conditions	

INTRODUCTION

1. The publisher for this copyrighted material is Elsevier. By clicking "accept" in connection with completing this licensing transaction, you agree that the following terms and conditions apply to this transaction (along with the Billing and Payment terms and conditions established by Copyright Clearance Center, Inc. ("CCC"), at the time that you opened your Rightslink account and that are available at any time at http://myaccount.copyright.com).

GENERAL TERMS

2. Elsevier hereby grants you permission to reproduce the aforementioned material subject to the terms and conditions indicated.

3. Acknowledgement: If any part of the material to be used (for example, figures) has appeared in our publication with credit or acknowledgement to another source, permission must also be sought from that source. If such permission is not obtained then that material may not be included in your publication/copies. Suitable acknowledgement to the source must be made, either as a footnote or in a reference list at the end of your publication, as follows:

"Reprinted from Publication title, Vol /edition number, Author(s), Title of article / title of chapter, Pages No., Copyright (Year), with permission from Elsevier [OR APPLICABLE SOCIETY COPYRIGHT OWNER]." Also Lancet special credit - "Reprinted from The Lancet, Vol. number, Author(s), Title of article, Pages No., Copyright (Year), with permission from Elsevier."

4. Reproduction of this material is confined to the purpose and/or media for which permission is hereby given.

5. Altering/Modifying Material: Not Permitted. However figures and illustrations may be altered/adapted minimally to serve your work. Any other abbreviations, additions, deletions and/or any other alterations shall be made only with prior written authorization of Elsevier Ltd. (Please contact Elsevier's permissions helpdesk here). No modifications can be made to any Lancet figures/tables and they must be reproduced in full.

6. If the permission fee for the requested use of our material is waived in this instance, please be advised that your future requests for Elsevier materials may attract a fee.

7. Reservation of Rights: Publisher reserves all rights not specifically granted in the combination of (i) the license details provided by you and accepted in the course of this licensing transaction, (ii) these terms and conditions and (iii) CCC's Billing and Payment terms and conditions.

8. License Contingent Upon Payment: While you may exercise the rights licensed immediately upon issuance of the license at the end of the licensing process for the transaction, provided that you have disclosed complete and accurate details of your proposed use, no license is finally effective unless and until full payment is received from you (either by publisher or by CCC) as provided in CCC's Billing and Payment terms and conditions. If full payment is not received on a timely basis, then any license preliminarily granted shall be deemed automatically revoked and shall be void as if never granted. Further, in the event that you breach any of these terms and conditions or any of CCC's Billing and Payment terms and conditions, the license is automatically revoked and shall be void as if never granted. Use of materials as described in a revoked license, as well as any use of the materials beyond the scope of an unrevoked license, may constitute copyright infringement and publisher reserves the right to take any and all action to protect its copyright in the materials.

9. Warranties: Publisher makes no representations or warranties with respect to the licensed material.

10. Indemnity: You hereby indemnify and agree to hold harmless publisher and CCC, and their respective officers, directors, employees and agents, from and against any and all claims arising out of your use of the licensed material other than as specifically authorized pursuant to this license.

11. No Transfer of License: This license is personal to you and may not be sublicensed, assigned, or transferred by you to any other person without publisher's written permission.

12. No Amendment Except in Writing: This license may not be amended except in a writing signed by both parties (or, in the case of publisher, by CCC on publisher's behalf).

13. Objection to Contrary Terms: Publisher hereby objects to any terms contained in any purchase order, acknowledgment, check endorsement or other writing prepared by you, which terms are inconsistent with these terms and conditions or CCC's Billing and Payment terms and conditions. These terms and conditions, together with CCC's Billing and Payment terms and conditions (which are incorporated herein), comprise the entire agreement between you and publisher (and CCC) concerning this licensing transaction. In the event of any conflict between your obligations established by these terms and conditions and those established by CCC's Billing and Payment terms and conditions, these terms and conditions shall control.

14. Revocation: Elsevier or Copyright Clearance Center may deny the permissions described in this License at their sole discretion, for any reason or no reason, with a full refund payable to you. Notice of such denial will be made using the contact information provided by you. Failure to receive such notice will not alter or invalidate the denial. In no event will Elsevier or Copyright Clearance Center be responsible or liable for any costs, expenses or damage incurred by you as a result of a denial of your permission request, other than a refund of the amount(s) paid by you to Elsevier and/or Copyright Clearance Center for denied permissions.

LIMITED LICENSE

The following terms and conditions apply only to specific license types:

15. **Translation**: This permission is granted for non-exclusive world **English** rights only unless your license was granted for translation rights. If you licensed translation rights you may only translate this content into the languages you requested. A professional translator must perform all translations and reproduce the content word for word preserving the integrity of the article.

16. **Posting licensed content on any Website**: The following terms and conditions apply as follows: Licensing material from an Elsevier journal: All content posted to the web site must maintain the copyright information line on the bottom of each image; A hyper-text must be included to the Homepage of the journal from which you are licensing at http://www.sciencedirect.com/science/journal/xxxxx or the Elsevier homepage for books at http://www.elsevier.com; Central Storage: This license does not include permission for a scanned version of the material to be stored in a central repository such as that provided by Heron/XanEdu.

Licensing material from an Elsevier book: A hyper-text link must be included to the Elsevier homepage at http://www.elsevier.com . All content posted to the web site must maintain the copyright information line on the bottom of each image.

Posting licensed content on Electronic reserve: In addition to the above the following clauses are applicable: The web site must be password-protected and made available only to bona fide students registered on a relevant course. This permission is granted for 1 year only. You may obtain a new license for future website posting.

17. **For journal authors:** the following clauses are applicable in addition to the above:

Preprints:

A preprint is an author's own write-up of research results and analysis, it has not been peer-reviewed, nor has it had any other value added to it by a publisher (such as formatting, copyright, technical enhancement etc.).

Authors can share their preprints anywhere at any time. Preprints should not be added to or enhanced in any way in order to appear more like, or to substitute for, the final versions of articles however authors can update their preprints on arXiv or RePEc with their Accepted Author Manuscript (see below).

If accepted for publication, we encourage authors to link from the preprint to their formal publication via its DOI. Millions of researchers have access to the formal publications on ScienceDirect, and so links will help users to find, access, cite and use the best available version. Please note that Cell Press, The Lancet and some society-owned have different preprint policies. Information on these policies is available on the journal homepage.

Accepted Author Manuscripts: An accepted author manuscript is the manuscript of an article that has been accepted for publication and which typically includes author-incorporated changes suggested during submission, peer review and editor-author communications.

Authors can share their accepted author manuscript:

- immediately
    - via their non-commercial person homepage or blog
    - by updating a preprint in arXiv or RePEc with the accepted manuscript
    - via their research institute or institutional repository for internal institutional uses or as part of an invitation-only research collaboration work-group
    - directly by providing copies to their students or to research collaborators for their personal use
    - for private scholarly sharing as part of an invitation-only work group on commercial sites with which Elsevier has an agreement
- After the embargo period
    - via non-commercial hosting platforms such as their institutional repository
    - via commercial sites with which Elsevier has an agreement

In all cases accepted manuscripts should:

- link to the formal publication via its DOI
- bear a CC-BY-NC-ND license - this is easy to do
- if aggregated with other manuscripts, for example in a repository or other site, be shared in alignment with our hosting policy not be added to or enhanced in any way to appear more like, or to substitute for, the published journal article.

Published journal article (JPA): A published journal article (PJA) is the definitive final record of published research that appears or will appear in the journal and embodies all value-adding publishing activities including peer review co-ordination, copy-editing, formatting, (if relevant) pagination and online enrichment.

Policies for sharing publishing journal articles differ for subscription and gold open access articles:

Subscription Articles: If you are an author, please share a link to your article rather than the full-text. Millions of researchers have access to the formal publications on ScienceDirect, and so links will help your users to find, access, cite, and use the best available version.

Theses and dissertations which contain embedded PJAs as part of the formal submission can be posted publicly by the awarding institution with DOI links back to the formal publications on ScienceDirect.

If you are affiliated with a library that subscribes to ScienceDirect you have additional private sharing rights for others' research accessed under that agreement. This includes use for classroom teaching and internal training at the institution (including use in course packs and courseware programs), and inclusion of the article for grant funding purposes.

Gold Open Access Articles: May be shared according to the author-selected end-user license and should contain a CrossMark logo, the end user license, and a DOI link to the formal publication on ScienceDirect.

Please refer to Elsevier's posting policy for further information.

18. **For book authors** the following clauses are applicable in addition to the above: Authors are permitted to place a brief summary of their work online only. You are not allowed to download and post the published electronic version of your chapter, nor may you scan the printed edition to create an electronic version. **Posting to a repository:** Authors are permitted to post a summary of their chapter only in their institution's repository.

19. **Thesis/Dissertation**: If your license is for use in a thesis/dissertation your thesis may be submitted to your institution in either print or electronic form. Should your thesis be published commercially, please reapply for permission. These requirements include permission for the Library and Archives of Canada to supply single copies, on demand, of the complete thesis and include permission for Proquest/UMI to supply single copies, on demand, of the complete thesis. Should your thesis be published commercially, please reapply for permission. Theses and dissertations which contain embedded PJAs as part of the formal submission can be posted publicly by the awarding institution with DOI links back to the formal publications on ScienceDirect.

Elsevier Open Access Terms and Conditions

You can publish open access with Elsevier in hundreds of open access journals or in nearly 2000 established subscription journals that support open access publishing. Permitted third party re-use of these open access articles is defined by the author's choice of Creative Commons user license. See our open access license policy for more information.

Terms & Conditions applicable to all Open Access articles published with Elsevier:

Any reuse of the article must not represent the author as endorsing the adaptation of the article nor should the article be modified in such a way as to damage the author's honour or reputation. If any changes have been made, such changes must be clearly indicated.

The author(s) must be appropriately credited and we ask that you include the end user license and a DOI link to the formal publication on ScienceDirect.

If any part of the material to be used (for example, figures) has appeared in our publication with credit or acknowledgement to another source it is the responsibility of the user to ensure their reuse complies with the terms and conditions determined by the rights holder.

Additional Terms & Conditions applicable to each Creative Commons user license:

CC BY: The CC-BY license allows users to copy, to create extracts, abstracts and new works from the Article, to alter and revise the Article and to make commercial use of the Article (including reuse and/or resale of the Article by commercial entities), provided the user gives appropriate credit (with a link to the formal publication through the relevant DOI), provides a link to the license, indicates if changes were made and the licensor is not represented as endorsing the use made of the work. The full details of the license are available at http://creativecommons.org/licenses/by/4.0.

CC BY NC SA: The CC BY-NC-SA license allows users to copy, to create extracts, abstracts and new works from the Article, to alter and revise the Article, provided this is not done for commercial purposes, and that the user gives appropriate credit (with a link to the formal publication through the relevant DOI), provides a link to the license, indicates if changes were made and the licensor is not represented as endorsing the use made of the

work. Further, any new works must be made available on the same conditions. The full details of the license are available at http://creativecommons.org/licenses/by-nc-sa/4.0.

CC BY NC ND: The CC BY-NC-ND license allows users to copy and distribute the Article, provided this is not done for commercial purposes and further does not permit distribution of the Article if it is changed or edited in any way, and provided the user gives appropriate credit (with a link to the formal publication through the relevant DOI), provides a link to the license, and that the licensor is not represented as endorsing the use made of the work. The full details of the license are available at http://creativecommons.org/licenses/by-nc-nd/4.0. Any commercial reuse of Open Access articles published with a CC BY NC SA or CC BY NC ND license requires permission from Elsevier and will be subject to a fee.

Commercial reuse includes:

- Associating advertising with the full text of the Article
- Charging fees for document delivery or access
- Article aggregation
- Systematic distribution via e-mail lists or share buttons

Posting or linking by commercial companies for use by customers of those companies.

20. **Other Conditions**:

v1.10

Questions? customercare@copyright.com.

Appendix 12. Statement of Authorisation for IEEE Material

A feasibility study towards instrumentation of the Sport Concussion Assessment Tool (iSCAT)

Conference Proceedings:
2020 42nd Annual International Conference of the IEEE Engineering in Medicine & Biology Society (EMBC)

Author: Yunus Celik; Dylan Powell; Wai Lok Woo; Samuel Stuart; Alan Godfrey

Publisher: IEEE

Date: 20-24 July 2020

Thesis / Dissertation Reuse

The IEEE does not require individuals working on a thesis to obtain a formal reuse license, however, you may print out this statement to be used as a permission grant:

Requirements to be followed when using any portion (e.g., figure, graph, table, or textual material) of an IEEE copyrighted paper in a thesis:

1) In the case of textual material (e.g., using short quotes or referring to the work within these papers) users must give full credit to the original source (author, paper, publication) followed by the IEEE copyright line © 2011 IEEE.
2) In the case of illustrations or tabular material, we require that the copyright line © [Year of original publication] IEEE appear prominently with each reprinted figure and/or table.
3) If a substantial portion of the original paper is to be used, and if you are not the senior author, also obtain the senior author's approval.

Requirements to be followed when using an entire IEEE copyrighted paper in a thesis:

1) The following IEEE copyright/ credit notice should be placed prominently in the references: © [year of original publication] IEEE. Reprinted, with permission, from [author names, paper title, IEEE publication title, and month/year of publication]
2) Only the accepted version of an IEEE copyrighted paper can be used when posting the paper or your thesis on-line.
3) In placing the thesis on the author's university website, please display the following message in a prominent place on the website: In reference to IEEE copyrighted material which is used with permission in this thesis, the IEEE does not endorse any of [university/educational entity's name goes here]'s products or services. Internal or personal use of this material is permitted. If interested in reprinting/republishing IEEE copyrighted material for advertising or promotional purposes or for creating new collective works for resale or redistribution, please go to http://www.ieee.org/publications_standards/publications/rights/rights_link.html to learn how to obtain a License from RightsLink.

If applicable, University Microfilms and/or ProQuest Library, or the Archives of Canada may supply single copies of the dissertation.

BACK CLOSE WINDOW

Developing and exploring a methodology for multi-modal indoor and outdoor gait assessment

Conference Proceedings:
2021 43rd Annual International Conference of the IEEE Engineering in Medicine & Biology Society (EMBC)

Author: Yunus Celik; Dylan Powell; Wai Lok Woo; Samuel Stuart; Alan Godfrey

Publisher: IEEE

Date: 1-5 Nov. 2021

Thesis / Dissertation Reuse

The IEEE does not require individuals working on a thesis to obtain a formal reuse license, however, you may print out this statement to be used as a permission grant:

Requirements to be followed when using any portion (e.g., figure, graph, table, or textual material) of an IEEE copyrighted paper in a thesis:

1) In the case of textual material (e.g., using short quotes or referring to the work within these papers) users must give full credit to the original source (author, paper, publication) followed by the IEEE copyright line © 2011 IEEE.
2) In the case of illustrations or tabular material, we require that the copyright line © [Year of original publication] IEEE appear prominently with each reprinted figure and/or table.
3) If a substantial portion of the original paper is to be used, and if you are not the senior author, also obtain the senior author's approval.

Requirements to be followed when using an entire IEEE copyrighted paper in a thesis:

1) The following IEEE copyright/ credit notice should be placed prominently in the references: © [year of original publication] IEEE. Reprinted, with permission, from [author names, paper title, IEEE publication title, and month/year of publication]
2) Only the accepted version of an IEEE copyrighted paper can be used when posting the paper or your thesis on-line.
3) In placing the thesis on the author's university website, please display the following message in a prominent place on the website: In reference to IEEE copyrighted material which is used with permission in this thesis, the IEEE does not endorse any of [university/educational entity's name goes here]'s products or services. Internal or personal use of this material is permitted. If interested in reprinting/republishing IEEE copyrighted material for advertising or promotional purposes or for creating new collective works for resale or redistribution, please go to http://www.ieee.org/publications_standards/publications/rights/rights_link.html to learn how to obtain a License from RightsLink.

If applicable, University Microfilms and/or ProQuest Library, or the Archives of Canada may supply single copies of the dissertation.

BACK CLOSE WINDOW

Exploring human activity recognition using feature level fusion of inertial and electromyography data

Conference Proceedings:
2022 44th Annual International Conference of the IEEE Engineering in Medicine & Biology Society (EMBC)

Author: Yunus Celik; Samuel Stuart; Wai Lok Woo; Liam T. Pearson; Alan Godfrey

Publisher: IEEE

Date: 11-15 July 2022

Thesis / Dissertation Reuse

The IEEE does not require individuals working on a thesis to obtain a formal reuse license, however, you may print out this statement to be used as a permission grant:

Requirements to be followed when using any portion (e.g., figure, graph, table, or textual material) of an IEEE copyrighted paper in a thesis:

1) In the case of textual material (e.g., using short quotes or referring to the work within these papers) users must give full credit to the original source (author, paper, publication) followed by the IEEE copyright line © 2011 IEEE.
2) In the case of illustrations or tabular material, we require that the copyright line © [Year of original publication] IEEE appear prominently with each reprinted figure and/or table.
3) If a substantial portion of the original paper is to be used, and if you are not the senior author, also obtain the senior author's approval.

Requirements to be followed when using an entire IEEE copyrighted paper in a thesis:

1) The following IEEE copyright/ credit notice should be placed prominently in the references: © [year of original publication] IEEE. Reprinted, with permission, from [author names, paper title, IEEE publication title, and month/year of publication]
2) Only the accepted version of an IEEE copyrighted paper can be used when posting the paper or your thesis on-line.
3) In placing the thesis on the author's university website, please display the following message in a prominent place on the website: In reference to IEEE copyrighted material which is used with permission in this thesis, the IEEE does not endorse any of [university/educational entity's name goes here]'s products or services. Internal or personal use of this material is permitted. If interested in reprinting/republishing IEEE copyrighted material for advertising or promotional purposes or for creating new collective works for resale or redistribution, please go to http://www.ieee.org/publications_standards/publications/rights/rights_link.html to learn how to obtain a License from RightsLink.

If applicable, University Microfilms and/or ProQuest Library, or the Archives of Canada may supply single copies of the dissertation.

BACK CLOSE WINDOW